STUTZMAN

NATIONAL ACADEMIES OF SCIENCE AND ENGINEERING

NATIONAL RESEARCH COUNCIL

of the

UNITED STATES OF AMERICA

UNITED STATES NATIONAL COMMITTEE

International Union of Radio Science

National Radio Science Meeting

3-5 January 1990

Sponsored by USNC/URSI
in cooperation with
Institute of Electrical and Electronics Engineers

University of Colorado
Boulder, Colorado
U.S.A.

National Radio Science Meeting
3-5 January 1990
Condensed Technical Program

TUESDAY, 2 JANUARY

2000-2400
USNC-URSI Meeting — Broker Inn

WEDNESDAY, 3 JANUARY

0855-1200

AE-1	EMI MEASUREMENTS	CR1-42
B-1	EM THEORY I	CR2-28
B-2	RANDOM AND ROUGH SURFACES	CR1-46
D-1	HIGH FREQUENCY AND HIGH SPEED INTEGRATED CIRCUITS	CR1-40
F-1	RADAR BACKSCATTER, ATTENUATION, AND DROPSIZE DISTRIBUTIONS	CR1-9
G-1	IONOSPHERIC MODELING	CR2-6
H-1	RADIO EMISSIONS	CR0-30
J-1	CENTIMETER-WAVE RADIO ASTRONOMY	CR2-26

1335-1700

G-2	CEDAR TECHNIQUES	CR2-6
H-2	COMMON AND UNCOMMON WAVE PHENOMENA IN SPACE AND IONOSPHERIC PLASMAS	CR0-30
J-1	CENTIMETER-WAVE RADIO ASTRONOMY	CR2-26

1355-1540

F-2	TROPOSPHERIC WIND, WAVES, AND ATTENUATION	CR1-46

1355-1700

A-1	ANTENNAS AND FIELDS MEASUREMENTS	CR1-42
B-3	SCATTERING	CR2-28
E-1	HIGH POWER ELECTROMAGNETICS IV	CR1-9

1415-1700

D-2	ADVANCED DEVICES	CR1-40

1600-1700

F-3	OCEAN AND TERRAIN EFFECTS	CR1-46

1700-1800

Commission A Business Meeting	CR1-42
Commission D Business Meeting	CR1-40
Commission E Business Meeting	CR1-9
Commission F Business Meeting	CR1-46
Commission H Business Meeting	CR0-30
Commission J Business Meeting	CR2-26

THURSDAY, 4 JANUARY

0830-1200
PLENARY SESSION — Muenzinger Psychology E050 (Auditorium)

1335-1440

J-2	GENERAL SESSION: SOLAR RADIO ASTRONOMY DURING MAX 91	CR2-26

United States National Committee

INTERNATIONAL UNION OF RADIO SCIENCE

PROGRAM AND ABSTRACTS

National Radio Science Meeting
3-5 January 1990

Sponsored by USNC/URSI in cooperation
with IEEE groups and societies:

Antennas and Propagation
Circuits and Systems
Communications
Electromagnetic Compatibility
Geoscience Electronics
Information Theory
Instrumentation and Measurement
Microwave Theory and Techniques
Nuclear and Plasma Sciences
Quantum Electronics and Applications

To copy

136
59 Mijass and reference
68
99
94
36
143
146
147
148
268
271

Com F International URSI
Chair R.C. Crane
VC G. Brussaard

NOTE:

Programs and Abstracts of the USNC/URSI Meetings are available from:

USNC/URSI
National Academy of Sciences
2101 Constitution Avenue, N.W.
Washington, DC 20418

at $2 for meetings prior to 1970, $3 for 1971-1975, and $5 for 1976-1990 meetings.

The full papers are not published in any collected format; requests for them should be addressed to the authors who may have them published on their own initiative. Please note that these meetings are national. They are not organized by the International Union, nor are the programs available from the International Secretariat.

MEMBERSHIP

United States National Committee
INTERNATIONAL UNION OF RADIO SCIENCE

Chairman:	Sidney A. Bowhill*
Vice Chairman:	Chalmers M. Butler*
Secretary:	David C. Chang*
Immediate Past Chairman:	Robert K. Crane*

Members Representing Societies, Groups, and Institutes:

American Geophysical Union	Dr. George W. Reed
American Astronomical Society	Dr. William J. Welch
IEEE Antennas & Propagation Society	Dr. W. Ross Stone
IEEE Microwave Theory and Techniques Society	Dr. A. A. Oliner
American Meterological Society	Dr. Richard Hahlgren

Members-at-Large:

Dr. Julius Goldhirsh
Dr. James W. Mink
Dr. Kenneth Davies (90)
Dr. Lewis Duncan
Dr. Irene Peden (90)
Dr. David J. Thompson
~~Dr. Gary Brown (93)~~

Liaison Representatives from Government Agencies:

National Telecommunications & Information Administration	Dr. Hans Liebe
National Science Foundation	Dr. Laura P. Bautz
Federal Communications Commission	Mr. William A. Daniel
Department of Defense	Mr. William J. Cook
Department of the Army	Mr. Earl J. Holliman
Department of the Air Force	Dr. Allan C. Schell

Chairmen of the USNC/URSI Commissions:

Commission A	Dr. Edmund K. Miller
Commission B	Dr. Robert S. Elliott
Commission C	Dr. Aaron D. Wyner
Commission D	Dr. Tatsuo Itoh
Commission E	Dr. Emil Soderberg (acting chair)
Commission F	Dr. Calvin T. Swift VC; Hans Richter
Commission G	Dr. Charles M. Rush incoming VC; Goldhirsh
Commission H	Dr. Mario Grossi
Commission J	Dr. J. Richard Fisher

* Member of USNC/URSI Executive Committee

Chairmen and Vice Chairmen of Commissions of URSI resident in the United States:	
Chairman of Commission B	Prof. Thomas B.A. Senior
Chairman of Commission F	Dr. Robert K. Crane
Foreign Secretary of the U.S. National Academy of Sciences	Dr. William E. Gordon
Chairman, National Research Council, Commission on Physical Sciences, Mathematics, and Resources	Dr. Norman Hackerman
Chairman, National Research Council, Board on Physics and Astronomy	Prof. Norman F. Ramsey
Honorary Members	Dr. Harold H. Beverage Dr. Ernst Weber
NRC Staff Director	Mr. Donald C. Shapero
NRC Program Officer	Dr. Robert L. Riemer
NRC Administrative Associate	Ms. Susan M. Wyatt

DESCRIPTION OF THE INTERNATIONAL UNION OF RADIO SCIENCE

The International Union of Radio Science is one of 18 world scientific unions organized under the International Council of Scientific Unions (ICSU). It is commonly designated as URSI (from its French name, Union Radio Scientifique Internationale). Its aims are (1) to promote the scientific study of radio communications, (2) to aid and organize radio research requiring cooperation on an international scale and to encourage the discussion and publication of the results, (3) to facilitate agreement upon common methods of measurement and the standardization of measuring instruments, and (4) to stimulate and to coordinate studies of the scientific aspects of telecommunications using electromagnetic waves, guided and unguided. The International Union itself is an organizational framework to aid in promoting these objectives. The actual technical work is largely done by the National Committee in the various countries.

The officers of the International Union are:

President:	Prof. A.L. Cullen (U.K.)
Past President:	Dr. A.P. Mitra (India)
Vice Presidents:	Dr. Ing. H.J. Albrecht (F.R.G.) R.L. Dowden (New Zealand) E.D. Jull (Canada) Prof. V. Zima (Czechoslovakia)
Secretary-General	J. Van Bladel (Belgium)
Honorary Presidents:	G. Beynon (U.K.) W. Dieminger (West Germany) W. Christiansen (Australia)

The Secretary-General's office and the headquarters of the organization are located at Avenue Albert Lancaster, 32, B-1180 Brussels, Belgium. The Union is supported by contributions (dues) from 38 member countries. Additional funds for symposia and other scientific activities of the Union are provided by ICSU from contributions received for this purpose from UNESCO.

The International Union, as of the XXth General Assembly held in Washington, DC in August 1981, has nine bodies called Commissions for centralizing studies in the principal technical fields.

Every three years the International Union holds a meeting called the General Assembly. The next is the XXIIIrd, to be held in 1990. The Secretariat prepares and distributes the Proceedings of the General Assemblies. The

International Union arranges international symposia on specific subjects pertaining to the work of one or several Commissions and also cooperates with other Unions in international symposia on subjects of joint interest.

Radio is unique among the fields of scientific work in having a specific adaptability to large-scale international research programs, since many of the phenomena that must be studied are worldwide in extent and yet are in a measure subject to control by experimenters. Exploration of space and the extension of scientific observations to the space environment are dependent on radio for their research. One branch, radio astronomy, involves cosmic phenomena. URSI thus has a distinct field of usefulness in furnishing a meeting ground for the numerous workers in the manifold aspects of radio research; its meetings and committee activities furnish valuable means of promoting research through exchange of ideas.

Steering Committee:

S.W. Maley, Chairman (303) 492-7004
D.C. Chang
D.S. Cook
P.L. Jensen
M.G. Kindgren

Technical Program Committee:

D.C. Chang, Chairman
R.S. Elliott
L. Fedor
J.R. Fisher
M.D. Grossi
T. Itoh
M. Kanda
S.W. Maley
C.M. Rush
L.L. Scharf
E.K. Smith
E. Soderberg
C.T. Swift
D.J. Thompson

Wednesday Morning, 3 January, 0855-1200

Session AE-1 0855-Weds. CR1-42
EMI MEASUREMENTS
Chairman: J.W. Adams, Electromagnetic Fields Division,
National Institute of Standards and Technology, Boulder, CO 80303

AE1-1
0900

LARGE-SYSTEM EMC TESTING USING TIME-DOMAIN TECHNIQUES

J.W. Adams, A.R. Ondrejka, K.H. Cavcey, J.E. Cruz
Electromagnetic Fields Division
National Institute of Standards and Technology
Boulder, CO 80303

Improved techniques for determining critical resonant frequencies and the current response of internal wiring due to external fields for large structures (whole systems) are discussed. The measurement method is based on using a periodic sequence of low-level, radiated impulses. Their level is so low that they do not disturb other spectrum users. A fiber-optic trigger system permits coherent detection of these test impulses and rejection of other signals. Therefore other spectrum users do not significantly disturb these measurements. The field-strength levels are low, a distinct advantage from both cost and personnel hazard standpoints. There are several problems that must be addressed before the full potential of this technique can be realized. One of these is to establish an upper bound of induced current that will not be exceeded for any orientation between a radiating source and test object. Another is to establish conditions for which bulk current injection is valid in order to allow conducted electromagnetic susceptibility testing that is equivalent to radiated susceptibility testing.

AE1-2
0920

TRANSIENT WAVEFORM MEASUREMENT EXTRAPOLATION ISSUES

M.A. Dinallo
BDM International
1801 Randolph Road, SE
Albuquerque, New Mexico 87106

Recent measurements of surface currents on the EMP Test Aircraft (EMPTAC) at the TRESTLE and HPD simulation facilities have been analyzed and extrapolated (forthcoming as an AFSC/WL-BDM Technical report). Thus far the derived extrapolation functions are in agreement with previously published results (D.E. Merewether et.al., "Characterization of Errors in the Extrapolation of Data from an EMP Simulator to an EMP Criterion," Sensor and Simulation Notes, Note 232, October 25, 1977, Kirtland AFB, NM) However, noncausality of the extrapolated waveform raises the question of implementation of a commonly used 3B technique (C.E. Baum, "Extrapolation Techniques for Interpreting the Results of Test in EMP Simulators in Terms of EMP Criteria," Sensor and Simulation Notes, Note 222, March 20, 1977, Kirtland AFB, NM). Since 3B extrapolation requires "knowing" the criterion current response, scale model measurements from the University of Michigan (UM) anechoic chamber will be discussed (V.V. Liepa and J.F. Huang, "Exterior Electromagnetic Response of EMPTAC Aircraft," Internal Application Memo, Memo 43, April 1987, Kirtland AFB, NM) along with convolving incident field spectrums for both in-flight and ground mode interaction configurations. It will be shown that point-to-point comparisons with the criteria data produces causal results. However, implementing the 3B extrapolation method produces non-causal temporal waveforms. Some criteria for performing causal convolution of waveforms will be discussed.

AE1-3 Similarity of Non-stationary Time Limited Signals
0940

D.S. Friday
Electromagnetic Fields Division
National Institute of Standards and Metrology
325 Broadway
Boulder, Colorado 80303

This problem is motivated by NIST efforts to develop time domain methods for EMI/EMC evaluation of large operational systems (See for example, Adams Ondrejka, Cavcey, and Cruz - this conference). The system is excited with a series of pulsed electromagnetic fields, and the response is observed. The response is either the reflection from the system at a particular point in space or a measurement of an induced current at some critical point in the system. The direction of the incident radiation is an experimental factor that affects the results. A grid of points in some subspace surrounding the system under test must be determined that extracts all relevant information from the test, yet is not unnecessarily redundant. Information of interest may be resonant frequencies, for example. The different and complex geometries of the systems under test make a detailed EM theory based evaluation impractical, except possibly for rough approximations. The problem addressed, is to develop another criteria for determining the spacial sampling design, that is based on minimal prior assumptions. The approach is based on empirical observations of response waveforms at various spacings. The usual measures of similarity for stationary processes, such as cross-correlation, are not directly applicable. We explore alternative measures of response similarity, upon which practical decisions on spacial sampling intervals may be based.

AE1-4
1000

A TEM DRIVEN MODE-STIRRED CHAMBER
A SINGLE FACILITY FOR RADIATED EMC TESTING, 10 kHz - 40 GHz

M.L. Crawford
Electromagnetics Fields Division
National Institute of Standards and Technology
Boulder, CO 80303

Fundamental to ensuring the electromagnetic compatibility (EMC) of electronic equipment and systems within their operating environment is the ability to accurately measure and simulate these environments for test purposes. In recent years the NIST, 723.03, has been developing improved methods and facilities for EMC testing. Two methods are the transverse electromagnetic (TEM) cell and the reverberating or mode-stirred chamber. Each approach has its advantages and limitations. The TEM cell, though very useful, is limited to frequencies below a few hundred MHz, depending upon the size of the equipment under test (EUT). This limitation is due to the requirement that only the fundmental TEM mode exist in the cell at frequencies for which tests are to be made. The mode-stirred chamber technique has significant advantages for testing large EUT's efficiently and cost effectively. But this method is restricted to frequencies above a few hundred MHz, depending upon the size of the test chamber. This limitation is a consequence of requiring the chamber to be electrically large so that sufficient modes will exist to ensure adequate mode mixing and hence, spatial uniformity in the fields generated for testing. It may be possible to combine these two measurement concepts into a common facility that can be used for EMC testing over the combined frequency range of the TEM cell and the mode-stirred chamber (10 kHz - 40 GHz). If this can be achieved, significant cost and time savings (approximately 10/1) with a possible improvement in measurement accuracy may be realized in performing essential EMC tests. This presentation will describe work in progress at NIST to develop a single, integrated facility using a large shielded enclosure configured as a TEM transmission line driven mode-stirred chamber. TEM test fields are generated at frequencies below multimode cutoff, and mode-stirred test fields are generated at frequencies above multimode cutoff. The discussion will include the proposed facility design, advantages and limitations, and theoretical basis for the work and the proposed experimental approach for evaluating a 1/10 scale model of a large enclosure having a test volume of 8m x 16m x 30m.

AE1-5 1040 ELECTROMAGNETIC INTERFERENCE PRODUCES ERRONEOUS DATA IN LIGHTNING LOCATION SYSTEM: D.N. March, Montana State University

The U.S. Bureau of Land Management has a lightning location system made by the Lightning Location and Protection Company that covers the Western United States. The system uses crossed-loop direction finders located throughout the area to triangulate to locations of cloud-to-ground discharges. While processing data from the system, several anomalies were noted. Lightning activity was repeatedly reported present near one city when no storms were present and the area near the city had the highest lightning activity in a wide area. Further analysis of the data using peak current isodensity maps showed that the lightning near the city had low peak currents. Examination of the data showed that the majority of events (supposedly discharges) recorded at certain storm times had very low peak currents. Further, these events were located by triangulation of radiants from the city in question and one of several nearby direction finders. An on-site measurement of electromagnetic interference within the pass-band of the direction finder located at the city with abnormally high activity showed a significant amount of interference present but only intermittently. The noise source was identified. How the system made errors when noise was present at only one site was determined.

Two other direction finder sites with high electromagnetic interference were found using polar plots showing what percent of events (supposedly discharges) were detected by the direction finder that were detected by the system. One direction finder had a low probability of detecting discharges within its reasonable service area. On-site measurements confirmed the presence of a high amplitude continuous interfering signal. The polar plots of performance of another direction finder showed apparent performance far exceeding that of other direction finders. The performance of the site was corrupted by locally generated interference. Again on-site measurements identified the source of interference. Electromagnetic interference measurements were also made at direction finder sites where no performance degradation was observed. In those cases the interference levels were low.

Conclusions based on data from the BLM lightning location system must take into account system problems caused by electromagnetic noise.

AE1-6
1100

A WIDEBAND MODEL FOR ELECTROMAGNETIC INTERFERENCE FROM CORONA ON MULTICONDUCTOR POWER LINES

R.G. Olsen and M. Wu
Electrical and Computer Engineering Department
Washington State University
Pullman, WA 99164-2752

Recently, a wideband method has been developed to predict the interference fields from a distribution of corona on a single conductor power line which is located above a lossy earth (R.G. Olsen and M. Wu, Radio Sci, 24, 340-350, 1989). The method has been validated for frequencies up to 30 MHz and can also be shown to reduce to the existing quasi-static solution for frequencies below 1 MHz. In this paper, the method is extended to the multiconductor case. Results based on the method will be shown and compared to results from an empirical method developed by the Bonneville Power Administration.

AE1-7 1120 FIELDS RADIATED BY ELECTROSTATIC DISCHARGES AS INTERFERENCE SOURCES, M.T. Ma, National Institute of Standards and Technology, U.S. Department of Commerce, Boulder, Colorado

Electrostatic discharge (ESD) is a common phenomenon with a potential to seriously upset electronic equipment. Considerable effort has gone into the study of the ESD currents in order to develop simulators for simplifying and standardizing ESD testing. The fields radiated by ESD may also be considered as a special form of electromagnetic interference to the nearby device. The ESD spark is modeled theoretically as an electrically short, time dependent, linear dipole situated above an infinite ground plane. Experimental data of the electric fields radiated by ESDs, obtained by measurements with a specially designed broadband time-domain antenna, are compared with the computed results.

Session B-1 0855-Weds. CR2-28
EM THEORY I
Chairman: D.G. Dudley, Electromagnetics Laboratory, Univ. of Arizona, Tucson, AZ 85721

B1-1
0900 UNIFORM ASYMPTOTIC EVALUATION OF KIRCHOFF INTEGRALS FOR ONE-DIMENSIONAL APERTURES EMPLOYING THE PAULI-CLEMMOW METHOD

R. A. Whitaker and L. W. Pearson
McDonnell Douglas Research Laboratories
P.O. Box 516
St. Louis, MO 63166

Kirchoff integrals arise in the estimation of radiation and diffraction effects from electrically large apertures. For one dimensional apertures, the integrals are readily treated asymptotically using Fourier methods. The evaluation is complicated by diffraction effects at the edges of the aperture. Specifically, we must resort to so-called "uniform" methods for observation angles such that the saddle point of the integrand approaches a pole--i.e. near a geometrical optics shadow or reflection boundary. The method of van der Waerden is most commonly used (e. g. Felsen and Marcuvitz, Radiation and Scattering of Waves, Prentice-Hall,1971, p. 399 ff.).

Boersma and Rahmat-Samii have compared van der Waerden's asymptotic method with the less frequently employed Pauli-Clemmow method in the context of the Geometrical Theory of Diffraction (GTD). They have shown that the former method leads to the uniform asymptotic theory (UAT) results of Aluwalia, Lewis, and Boersma while the latter leads to the uniform theory of diffraction (UTD) of Kouyoumjian and Pathak. The preponderance of workers now employ the UTD in preference to the UAT. The focus of the present paper is the Pauli-Clemmow evaluation of one-dimensional Kirchoff integrals, which yields a uniform result that is compatible with the UTD format.

The error estimates established by Clemmow (Quart. Journ. Mech. and Applied Math, Vol. III, Pt. 2, 241-256, 1950) are heuristic. We have established that the terms of the Pauli-Clemmow asymptotic series arising in our application form an asymptotic scale and that the series is a generalized Poincare asymptotic expansion.

The one-dimensional Kirchoff integral contains a multivalued integrand and part of the multivalued character of the integrand survives the mapping to the angular spectrum plane. This contrasts to the exact half-plane diffraction problem that Boersma and Rahmat-Samii considered. The multivaluedness must be dealt with carefully, and consequently, the present treatment is somewhat more general than that of Boersma and Rahmat-Samii.

B1-2
0920

VALIDATION OF HOMOGENIZATION THEORY FOR CALCULATING THE ELECTRICAL CONSTANTS OF COMPOSITE MATERIALS

R.G. Olsen and B.A. Vanhoff
Department of Electrical and Computer Engineering
Washington State University
Pullman, WA 99164-2752

It is known that periodically inhomogeneous materials can be replaced with equivalent homogeneous but anisotropic materials if the period is electrically small. To find the tensor elements for the equivalent material requires that a quasi-electrostatic and/or a quasi-magnetostatic problem be solved within a cell of dimensions equal to the period under certain periodic boundary conditions.

In this work, homogenization theory is applied to inhomogeneous material which is periodic in two dimensions and uniform in the third. Within the period cell, the cross-section may have arbitrary dielectric, magnetic and loss properties provided that it remains electrically small. In particular a computer program, into which techniques for accelerating the solution have been incorporated has been written using a finite difference technique to solve the quasi-electrostatic/quasi-magnetostatic problem. This program has been used to examine the usefulness of variational bounds for the tensor elements and to compare with the results of experiments on simple composite materials.

B1-3
0940

INTEGRAL EQUATIONS FOR ELECTROMAGNETIC SCATTERING FROM AN INDENTED SCREEN

J. S. Asvestas, M/S A02-26, Corporate Research Center
Grumman Corporation
Bethpage, NY 11714-3580
R. E. Kleinman, Department of Mathematical Sciences
University of Delaware
Newark, DE 19716

Systems of boundary integral equations are derived for the three-dimensional problem of scattering of a time harmonic electromagnetic wave by an indentation on an infinite, planar, perfectly conducting screen.

Depending on the formulation, these systems fall into three categories. The first consists of equations defined on the boundary of the indentation only, where the unknown function is the total electric current density, and the remaining two consist of equations defined on the indentation and its projection onto the plane of the screen, with the unknown functions being, in one case, the electric current density on the indentation boundary and the tangential magnetic field on the projection, while in the last case an additional unknown, the tangential electric field on the projection, is involved. The degree of complexity of these systems increases as the number of unknowns is reduced.

The geometry of the indentation is quite general and the Green functions are defined only in terms of the free space scalar Green function for the Helmholtz equation and its image about the infinite plane. Both these functions are independent of the geometry of the indentation.

B1-4 1000 **INTEGRAL REPRESENTATIONS FOR ELECTROMAGNETIC SCATTERING**

E. L. Roetman*, G. L. Hower** R. P. Kochlar*
*Boing Advanced Systems, 9725 E. Marginal Way So. Seattle, WA 98108
**Washington State University, ECE Dept., Pullman WA. 99164-2752

Integral equation expressions are widely used in obtaining approximate (numerical) solutions for electromagnetic scattering problems. The usual derivation of these expressions (J. A. Stratton, Electromagnetic Theory, McGraw-Hill, New York, 1941) proceeds from the vector Green's theorem which places restrictions on the continuity of the fields and their derivatives.

The paper presents a matrix formulation of the necessary integral equations which follows from the first order Maxwell equations alone. The approach yields expressions for the fields involving a 6 x 6 Green's Tensor, $\underline{G}$, whose components have a simple and direct physical interpretation. The field representation which results is given by

$$\mathbf{F} = -\int_V \underline{G}\mathbf{J}\, dv - \int_S \underline{G}\mathbf{J}_s\, ds$$

where F is a six-component vector giving both the electric (E) and magnetic (H) fields at points in region V bounded by surface S, **J** is a vector of the electric and magnetic volume current components and $\mathbf{J}_s$ similarly represents the surface currents. Specifically,

$$\mathbf{F} = \begin{bmatrix} \mathbf{E} \\ \mathbf{H} \end{bmatrix}, \qquad \mathbf{J} = \begin{bmatrix} \mathbf{J}_e \\ \mathbf{J}_m \end{bmatrix}, \qquad \mathbf{J}_s = \begin{bmatrix} -\mathbf{n}\times\mathbf{H} \\ \mathbf{n}\times\mathbf{E} \end{bmatrix}$$

where $\mathbf{J}_e$ and $\mathbf{J}_m$ are the electric and magnetic volume current densities respectively, and **n** is the outward normal on S.

Features of the results include: 1) a relaxation of restrictions on continuity since only the first order Maxwell equations are invoked in the derivation, 2) a development which requires the use of the system adjoint to the equations of Maxwell and careful analysis of the singularities, and 3) an expression of the usual Stratton-Chu integral equations but with the automatic inclusion of necessary line sources (F. Kottler, Ann. Phys, 71, 457-508, 1923) in cases where the surface S consists of different zones separated by a closed contour C.

The paper will discuss details of the above formulation and its application to obtaining equations for scattering in terms of equivalent volume polarization currents or in terms of equivalent surface sources.

B1-5
1020

EXACT AND APPROXIMATE SOLUTIONS OF THE (HELMHOLTZ) WEYL COMPOSITION EQUATION IN ELECTROMAGNETICS

Louis Fishman
Center for Wave Phenomena
Department of Mathematics
Colorado School of Mines
Golden, Colorado 80401

Phase space and path integral methods have been applied to both mathematical and computational forward and inverse wave propagation modeling at the level of the scalar one-way Helmholtz equation. These methods are particularly appropriate for extended, strongly inhomogeneous, multidimensional channeling environments. Operator symbols play a pivotal role in the analytical constructions and numerical algorithms. The construction of the operator symbol requires the exact (or approximate) solution of the (Helmholtz) Weyl composition equation in the Weyl pseudo-differential operator calculus. The exact symbols for several model refractive index profiles are constructed and briefly analyzed. The symbols exactly corresponding to a family of operator rational approximations are also derived for the same model profiles. The exactly solved profiles model wells with trapped modes and sharp gradient effects. The results are used to illustrate several points pertinent to wide-angle propagation modeling and the refractive index profile reconstruction problem.

B1-6
1040

DERIVATION AND APPLICATIONS OF THE MAGNETIC FIELD OF POINT CURRENT SOURCES IN SPECIFIC VOLUME CONDUCTORS

A. Stewart Ferguson and Dominique Durand
Applied Neural Control Laboratory
Department of Biomedical Engineering
Case Western Reserve University
Cleveland, OH 44106, U.S.A.

Theory is presented for the magnetic fields generated by point sources of current located in two volume conductor shapes. The equations are derived for the magnetic field both interior and exterior to a semi-infinite conducting volume, and exterior to a conducting spherical volume. In both volumes, the magnetic field generated by a point source is shown to be identical to the magnetic field of a line current with the same value of current.

For the semi-infinite volume conductor, the magnetic field exterior to the conducting region is equivalent to that of a semi-infinite line current, starting at the position of the point source, oriented perpendicular to the surface of the conducting volume, and flowing towards infinity. Within the conducting semi-infinite volume, the field is equivalent to that of a semi-infinite line current, oriented perpendicular to the surface and flowing from infinity to the position of the "mirror-image" of the point source. The field exterior to a conducting sphere is equivalent to that generated by a finite-length line current flowing from the position of thepoint source to the center of the sphere.

The relationship between these results and earlier results for the volume ("return") currents of dipoles in the same volume conductors are developed. The implications of working with point sources in lieu of dipoles current sources to reduce source modelling errors and to better understand the effects of volume currents are discussed. In particular, models of biological systems such as closely-packed neurons can be modelled more accurately and the difficulty in detecting the magnetic fields of deeply located neurons can now be explained. Applications of these results in both the forward and inverse magnetic mapping problem are discussed.

B1-7
1100

A CONVERGENT BORN SERIES FOR LARGE REFRACTIVE INDICES

R. E. Kleinman
Center for the Mathematics of Waves
Department of Mathematical Sciences
University of Delaware
Newark, DE 19716, U.S.A.

G. F. Roach
Department of Mathematics
University of Strathclyde
Glasgow G1 1XH, Scotland

P. M. van den Berg
Laboratory for Electromagnetic Research
Department of Electrical Engineering
Delft University of Technology
Delft, The Netherlands

Abstract

It is shown that a generalized over–relaxation method applied to the domain integral equation arising in scattering by penetrable objects results in a convergent iterative solution. This modified Born series converges when the original Born series diverges for a wide range of indices of refraction and scatterer size. Moreover the modified series converges more rapidly than the original Born series in those cases where the original series converges. Numerical examples demonstrating the effectiveness of this method are presented in 1, 2, and 3 dimensions.

B1-8
1120

AN IMPROVEMENT TO THE BORN APPROXIMATION

A. Q. Howard, Jr., W.C. Chew (†),
and M.C. Moldoveanu
Schlumberger Well Services
Houston, Texas 77252-2175
†University of Illinois at Champaign-Urbana

A correction to the well-known Born approximation for the apparent conductivity (induced voltage) in a layered medium is derived. Unlike previous corrections, which rely primarily on adjusting the background conductivity artificially to fit the data, the correction comes naturally out of the physics of the problem. The correction involves a single constant α, and is nonlinear in conductivity. Traditionally, the Born approximation is corrected by allowing the background conductivity to vary slowly with the logging coordinate in the logging formation, in such a way as to offset the nonlinear deviation of the apparent conductivity from the (linear) Born approximation. Adjusting the background conductivity to match prescribed data, while computationally efficient, is not justified by physics because, by definition, the background conductivity is a constant.

When the background conductivity is zero, the Born approximation reduces to Doll's geometric factor theory for induction (H. G. Doll, *J. of Petroleum Technology*, **1**, 148–162, 1949). The utility of working with a response function, which results from the Born approximation, is particularly useful in the inverse problem (A. Q. Howard, Jr. *Geophysics*, **52**, No. 2, 186–193, 1987). The Born approximation in induction logging is usually adequate when conductivity contrasts are no more than 10, and when peak conductivities are less than 0.1 S/m. Actual conductivities encountered in logging have dynamic range in excess of 1000, and salt saturated brine can have conductivity on the order of 10 S/m. Thus, the Born approximation cannot by itself cover the conductivity range. The proposed correction allows the conductivity contrast to increase from 10 to perhaps 100. Higher contrasts require a full nonlinear conductivity solution and are beyond the scope of this paper. The new α correction to the Born approximation is based upon a rigorous inhomogeneous Greens' function formulation. It results in a simple nonlinear correction to the explicit conductivity dependence in the integral formulation for the scattered field. The correction compensates for the tendency of the Born approximation to overestimate the apparent conductivity of a formation at large conductivity contrast. The correction is accurate in example 100:1 conductivity contrast situations.

B1-9
1140

WHY UNIFORMLY ACCELERATED CHARGES DON'T RADIATE

Alan Rolf Mickelson
Dept. of Electrical and Computer Engineering
University of Colorado, Campus Box 425
Boulder, CO 80309

Rather surprisingly, simple calculations show that charges in a uniform state of acceleration do not emit radiation. These calculations are shown not to be in disagreement with results calculated from Lienart-Wiechart potentials. As it turns out, the conditions for the derivation of the Lienart-Wiechart potentials to be valid are violated for a uniformly accelerated charge, and the uniformly accelerated case must therefore be treated by alternate means. In the derivation of the Lienart-Wiechart potentials it is, in fact, tacitly assumed that the charge must be at rest before some time t_i and return to rest following some time t_f. For the uniformly accelerated charge, it is exactly the motion before t_i and after t_f that allow the charge's field lines to keep from kinking and therefore omitting a $1/r$ field.

Although the author sees no broad area of applications for his results, the results do shed some light on some fundamental points in electromagnetics. A singularly confounding question has always been, if deceleration causes charges to radiate, then why is radiation reaction proportional to the derivative of the acceleration, and not the acceleration itself? That uniformly accelerated charges don't radiate helps to clear up this point, if not to explain the run-away solutions of Dirac's equation of motion for a charged particle. A second issue is that of the principle of equivalence. If one can transform away a uniform acceleration,then how can a charge know if it is uniformly accelerated? Indeed, if a uniformly accelerated charge doesn't radiate, then it probably doesn't know it is being accelerated either and therefore the principle of equivalence applies to electromagnetic quantities equally well as to mechanical ones.

In conclusion, although it seems paradoxical that a uniformly accelerated charge should not radiate, the seeming paradox has to do with the definition of uniform. When one understands this uniform to mean throughout all time, then it is seen that the no-radiation result is actually simply a consequence of principles we already know.

B1-10
1200

ELECTRON OSCILLATIONS AND DOUBLE-SLIT PARADOX

By Petr Beckmann, Professor Emer. Electr. Eng., Univ. of Colo., Galilean Electrodynamics, Box 251, Boulder, CO 80306.

It is shown directly from the Maxwell equations that the velocity of an electron with average v will oscillate about that value, giving rise to a non-radiating electromagnetic wave in the neighborhood of the electron. The oscillations are characterized by the de Broglie relation, which is normally simply postulated. Applying the result, the wave-particle paradox of electron diffraction by a double slit is resolved: the electron goes through only one aperture, but the wave surrounding it is diffracted by both of them. In the neighborhood of the electron the group velocity of the diffracted field is slowed to that of the electron, giving rise to the observed diffraction pattern.

The reason why the electron undergoes natural oscillations is essentialy the same as in the case of a tuned circuit, for a moving electron exhibits self-inductance and stores its electrical energy in space rather than a man-made capacitor. The inductance comes about as follows: as the electron accelerates (from its original rest position, for example), a magnetic field builds up, which by Faraday's Law induces an electric field opposed to the change and eventually decelerating the electron. This decreases the magnetic field and induces a Faraday field accelerating the electron again. Thus the instantaneous velocity oscillates about a mean velocity. No energy is lost in these oscillations, for the energy of the oscillating field simply moves between the magnetic and electric field surrounding the electron; since the two are 90° out of phase, the direction of the Poynting vector oscillates back and forth rather than being constant as it is in the case of radiation.

The electric field in Maxwell's equations is the sum of two fields, the irrotational Coulomb field and the Faraday field whose curl is proportional to the rate of change of the magnetic field, $\mathbf{E} = \mathbf{E}_c + \boldsymbol{\psi}$, where the Faraday field, in terms of the static potential ϕ and the vector potential $\mathbf{A}$, is $\boldsymbol{\psi} = -\partial\mathbf{A}/\partial t = -(\phi/c^2)\partial\mathbf{v}/\partial t \approx -(\phi/c^2)d\mathbf{v}/d\dot{t}$. Since the velocity of a charge does not change the energy of its Coulomb field, we need not concern ourselves with the Faraday field.

The magnetic energy density of the moving electron is found from $\mathbf{B} = \mathbf{v} \times \mathbf{E}_c/c^2$, so that the Poynting-Heaviside Theorem reads

$$\iint (\boldsymbol{\psi} \times \mathbf{H}) \cdot d\mathbf{S} + \iiint \mathbf{J} \cdot \boldsymbol{\psi} dV = -\frac{\partial}{\partial t} \iiint \left[\tfrac{1}{2}\epsilon\psi^2 + \frac{{E_c}^2 \sin^2\theta}{2c^4} v^2 \right] dV$$

where the integration is performed over all space outside a small sphere surrounding the electron in a coordinate system moving with the average position of the electron, and v is the electron's velocity with respect to that system. The right side of (6) is the change in total energy within the volume V. If this is to be conserved, the right side must vanish. On substituting (3) and (5) in the non-negative integrand, it follows that $\partial(C_1\dot{v}^2 + C_2 v^2)/\partial t = 0$, where the constants C_1 and C_2 are by (3) and (5) positive. Performing the differentiation, canceling by $2\dot{v}$ and setting the positive ratio $C2/C1 = \omega^2$, we have $\ddot{v} + \omega^2 v = 0$, which is the equation of a velocity oscillating about a mean v_0 (when transformed to the laboratory system).

This has far-reaching consequences casting doubt on Einstein's interpretation of the Relativity Principle and leading directly to results that hitherto had to be postulated (P. Beckmann, *Einstein Plus Two*, Golem Press, Boulder, Colo., 1987).

A further such result is the resolution of the double-slit paradox which will here be explained.

Session B-2 0855-Weds. CR1-46
RANDOM AND ROUGH SURFACES
Chairman: A. Ishimaru, Dept. of Electrical Engineering,
Univ. of Washington, Seattle, WA 98195

B2-1 0900 ELECTROMAGNETIC FIELDS SCATTERED BY RANDOM SURFACES

Samya Louza and N. F. Audeh
Electrical and Computer Engineering Department
University of Alabama in Huntsville
Huntsville, AL 35899

Abstract:

Electromagnetic fields scattered by rough surfaces has been of interest for a long time due to its applications in radar and communications. In previous works, these surfaces were considered as particular models of periodic roughness, e.g. sinusoidal, saw–tooth, etc. In some cases however, one can hardly assume periodicity and, for all practical purposes, it is not always possible to express the exact shape of the surfaces analytically. From this it follows that one convenient method is to calculate the scattered field by rough surfaces which are described statistically.

In this work a model of a rough surface consisting of linearlized plane segments or facets of random slopes has been postulated. Each segment is considered as a perfectly smooth surface and the scattered field is calculated. The surface roughness is in one dimension and the facets horizontal projections are variable. Two assumptions are made: the incident beam is reflected by each element according to the Fresnel reflection coefficient in the locally specular direction, and the elementary fields which are reflected in the same direction are summed to form one resultant field in that direction. Such a rough surface is described by Markov chain from which a wide class of surfaces is generated with the same statistical properties by using a suitable choice of a stochastic matrix. We also generated a number of Gaussian distributions with the same statistical properties as those constructed by Markov chain.

The line connecting the points obtained by each Gaussian distribution is considered as a profile of a rough surface. Thus, there are two sets of rough surfaces, one according to Markov chain and the other follows Gaussian distribution. Using ray tracing and the assumptions mentioned above, the scattered fields by these surfaces are calculated and compared.

B2-2
0920

ROUGH SURFACE SCATTERING

John A. DeSanto and Richard J. Wombell
Department of Mathematics
Colorado School of Mines
Golden, Colorado 80401

Rigorous analytical methods in rough surface scattering lead to integral equations. These can be of three types depending on whether we evaluate/integrate over coordinate or spectral variables. Three different examples of such equations will be discussed: the coordinate-coordinate approach (the usual coordinate-space integral equation), the spectral-spectral approach (the diagrammatic method in transform space), and a mixed version called the spectral-coordinate (SC) method. The advantages and disadvantages of each method will be discussed. Since all methods involve integral equations, they express the full multiple scattering and must be treated numerically. We compare and contrast numerical and approximation methods for treating these equations. We illustrate our results with numerical results using the SC method.

B2-3
0940

WAVE PROPAGATION IN RANDOM MEDIA: WIENER-HERMITE EXPANSION APPROACH

Cornel Eftimiu

McDonnell Douglas Research Laboratories
St. Louis, MO 63166

An approach to the problem of wave propagation in random media, based on the Wiener-Hermite functional expansion of the Green's function, is presented. The hierarchy of coupled integral equations which is established must be closed by truncation. The expressions for the first two statistical moments of the Green's function contain, for any nontrivial truncation, contributions from all orders of the perturbation theory expansion. The results are compared to those obtained by using the so-called weak fluctuation approximation and the nonlinear approximation.

B2-4
1000

A DISTORTED WAVE BORN APPROXIMATION FOR HIGH FREQUENCY SCATTERING FROM A ROUGH CONDUCTING SURFACE

Gary S. Brown
Bradley Department of Electrical Engineering
Virginia Polytechnic Institute & State University
Blacksburg, Virginia 24061-0111

The distorted wave Born approximation is very useful when the unknown function under study can be expressed as the sum of a known term and an unknown term with the former being strongly dominant. In the case of low frequency scattering from a randomly rough conducting surface, the dominant term is the coherent or average scattered field while the small (or perturbation) term is the zero mean fluctuating field. In this limit, the distorted wave Born approximation (DWBA) yields a result for the fluctuating field that is identical to that produced by first order smoothing. This result is superior to the Rice first order boundary perturbation theory because it permits arbitrary slopes.

In the high frequency limit, methods such as smoothing and boundary perturbation fail and what remains is the rather crude physical optics approximation; crude because it is little better than the ray optics limit. The purpose of this paper is to show how one can develop an improved approximation based upon the DWBA. The result that is obtained is very similar to a first order iteration of the integral equation for the current induced on the surface by the incident field. It differs in that the current that is iterated is the exact optical limit result and not just the Kirchhoff term. Thus, one must include both incidence shadowing and any multiple ray bounces that occur in the ray optic limit if this result is to be an appreciable improvement over the standard first order Born iteration. The net effect of including these factors is a partial summation of iterative terms that is exact in the ray optic limit. The analysis also shows that one should evaluate the integral in the iteration process exactly since an asymptotic evaluation would only reproduce the known result. In essence, the application of the DWBA in this limit has the effect of using the ray optic limit as a starting point to recover some degree of frequency dependent diffraction effects.

B2-5
1020

ELECTROMAGNETIC SCATTERING AND DEPOLARIZATION ACROSS ROUGH SURFACES--FULL WAVE SOLUTIONS

Ezekiel Bahar and Guorong Huang
Department of Electrical Engineering
University of Nebraska-Lincoln
Lincoln, NE 68588-0511

Full wave solutions are derived for the vertically and horizontally polarized waves scattered across a two dimensionally rough interface separating two different propagating media. Since the normal to the rough surface is not restricted to the reference plane of incidence, the waves are depolarized upon scattering and the single scattered radiation fields are expressed as integrals of a surface element transmission scattering matrix that also account for coupling between the vertically and horizontally polarized waves. The integrations are over the rough surface area as well as the complete two dimensional wave spectrum of the radiation fields. The full wave solutions satisfy the duality and reciprocity relationships in electromagnetic theory and they are invariant to coordinate transformations. It is shown that in the high frequency limit the full wave solutions reduce to the physical optics solutions, while in the low frequency limit (for very small mean square height and negligible slopes) the full wave solutions reduce to Rice's small perturbation solutions. Thus the full wave solution accounts for specular point scattering as well as diffuse, Bragg type scattering in a unified self-consistent manner. It is therefore not necessary to use hybrid perturbed - physical optics solutions based on two scale models of composite surfaces with large and small roughness scales.

B2-6
1040

EFFECTIVE ELECTROMAGNETIC PROPERTIES OF ROUGH SURFACES: DERIVED FROM THE METHOD OF HOMOGENIZATION

Christopher L. Holloway and Edward F. Kuester
MIMICAD CENTER
Dept. of Electrical and Computer Engineering
Campus Box 425
University of Colorado, Boulder 80309

The problem of describing theoretically the interaction of electromagnetic waves with a rough surface is an old one, with the first attempts dating back at least as far as those of Lord Rayleigh. Scattering from ocean waves or from rough terrain are but a few of the applications to which such a model might be applied. More recently, there has been interest in modeling accurately the effect of surface roughness of finitely conducting metal on the losses produced in microwave structures. However, in microwave circles, these results are generally used as a qualitative description of the roughness effects rather than as a quantitative modeling tool for use in precise designs.

There are, in fact, a number of theoretical approaches that have been taken to analyze electromagnetic (and the mathematically similar acoustic) field problems in the vicinity of rough surfaces. Most recently, a method known as ***homogenization*** has been used to solve problems of this type when the period of the surface roughness is small compared to the wavelength. Only a few results are published that are applicable to electromagnetic problems.

Homogenization is based on the method of multiple-scales in which information about both the microscopic and macroscopic structure of the problem of interest is accounted for. In this technique an asymptotic expansion of the fields as a function of δ (the period of the structure) is obtained, providing both fine-scale and gross variations of the field. Since in most problems, only the averaged fields are of interest, it is possible to examine them as solutions of Maxwell's equations, and to obtain appropriate boundray conditions for them.

In this paper both two-dimensionally and three-dimensionally rough perfectly and non-perfectly conducting surfaces are analyzed. For all these cases, the boundary conditions for the average fields are given and numerically computed values for the parameters entering into them are presented. Comparisons will be made with results found in the literature.

B2-7
1100

MMW BACKSCATTERING ENHANCEMENT BY VERY ROUGH ONE-DIMENSIONAL SURFACES

Yasuo Kuga

The Radiation Laboratory
Department of Electrical Engineering and Computer Science
University of Michigan
Ann Arbor, Michigan, 48109

Stephen M. King, Akira Ishimaru, and Jei-Shuan Chen

Department of Electrical Engineering
University of Washington
Seattle, Washington, 98195

In recent years backscattering enhancement by random media has attracted considerable interest and its importance in remote sensing has been recognized. Although the existence of backscattering enhancement from a rough surface in the optical region has been reported in the past, the backscattering enhancement effect in the millimeter wave (MMW) and microwave regions has not been verified experimentally.

In this paper we will present experimental evidence of the MMW backscattering enhancement by very rough one-dimensional surfaces. One-dimensional surface profiles with the surface characteristics of $\sigma=l=3$ mm (rms slope=$\sqrt{2}$) are generated using the Gaussian correlation function. The 50 cm by 50 cm rough surface is constructed with fast drying cement and the surface is painted with conducting paint. The MMW system is based on the HP8510 NWA operating in the 75 to 100 GHz frequency range. The transmitting antenna is a rectangular horn antenna and the receiving antenna is a scalar horn antenna connected to the orthmode coupler to detect both polarizations. The receiving antenna is mounted on a computer controlled rotational stage to obtain the bistatic scattering characteristics. The sample surface is mounted on a translational stage and the measurement is conducted on 21 locations on the surface, each separated by 15 mm over 300 mm total length. We measured the same surface at the incident angle of 0, 10, 20, 30 and 40 degrees. After taking the spatial and frequency averages, we detected the clear evidence of the backscattering enhancement effect in all cases. The experimental results are compared with the Monte-Carlo numerical simulation.

B2-8
1120

SCATTERING OF LIGHT FROM HIGH SLOPED ONE- AND TWO-DIMENSIONAL RANDOM ROUGH SURFACES

M.-J. Kim, K.A. O'Donnell and M. E. Knotts
School of Physics
Georgia Institute of Technology
Atlanta, GA 30332-0430

The scattering of acoustic and electromagnetic waves from random rough surfaces is a subject of wide interest and great practical importance. It is also a subject of considerable theoretical as well as experimental difficulty, and many questions have remained unanswered over the years. The particular problem that will be discussed here is the scattering of light from conductive surfaces which have steep slopes. We present an experimental study of scattering from such surfaces to facilitate a better understanding of the scattering phenomena.

Firstly, two dimensional random rough surfaces are considered. These surfaces are fabricated in photoresist and may or may not have gaussian statistics, depending on the fabrication procedure. In the previous experimental study of the scattering of light from such surfaces, whose surface features were somewhat larger than the incident wavelength, enhanced backscatter peaks and large cross-polarized components were observed in the scatter envelope (K.A. O'Donnell and E.R. Mendez, J.Opt.Soc.Am. A, 4, 1194-1205, 1987). Enhancement peaks have been attributed to multiple scattering, though there is still an active debate over the mechanisms which are responsible for such effects. By showing experimentally how incoherent and coherent components of scattered light depend on the ratio of the surface parameters to the incident wavelength, we will investigate the physical origin of these anomalous effects. The wavelengths which we have available lie between the ultraviolet and the infrared, and allow considerable variation in the ratio of the surface structure size to illumination wavelength.

We have also fabricated essentially one-dimensional (or corrugated) rough surfaces. These have been made in photoresist using both speckle-exposing and new direct-writing techniques. These are of interest because the corresponding theoretical problem can be somewhat less difficult, and we will present experimental results for such surfaces following gaussian and nongaussian statistics.

B2-9
1140

SCATTERING BY THIN RANDOMLY IRREGULAR CRACKS IN CONDUCTING PLANES

Cornel Eftimiu

McDonnell Douglas Research Laboratories
St. Louis, MO 63166

Scattering of plane electromagnetic waves by gaps or cracks in conducting planes is considered in the case when the constant width of the crack is much smaller than the wavelength and the randomly irregular crack is a straight line on the average. The randomness is treated in second order of perturbation theory. The domain of validity of perturbation thery is extended by using Padé approximants.

B2-10 1200 SCATTERING BY THIN RANDOMLY IRREGULAR CRACKS IN CONDUCTING PLANES

II. METHOD OF MOMENTS APPROACH

Cornel Eftimiu and P. L. Huddleston

McDonnell Douglas Research Laboratories

St. Louis, MO 63166

The average field scattered by a gap or crack in a conducting plane, in the case when the width is constant and the average of the random shape is a straight line, is calculated by using the method of moments. The surface current is represented by a whole domain expansion in functions which explicitly depend on the random shape, which is treated as a realization of a stochastic process. The coefficients of the expansion are assumed to be deterministic. The results are compared with those obtained by using perturbation theory for purposes of mutual validation.

D1-1
0900

Millimeter Wave Integrated Circuit Technology

Chente Chao
TRW

ABSTRACT - This paper presents the status of millimeter wave integrated circuit technology development at TRW. Significant progress in both monolithic and hybrid integrated circuit techniques has been achieved. The combination of these techniques has made feasible many system applications. Highlights of the development include the following:

Characterization and Modeling Technique - Systematic modeling of both active and passive components is being conducted. Emphasis has been placed on improving the model accuracy with better theoretical analysis and measurement technique. The characterization of device by optical technique in millimeter wave frequencies is being developed.

Circuit Technique Development - Recently, many circuit components have been proven in the microstrip circuit. For millimeter wave frequencies, the advantage of coplaner waveguide (CPW) circuit technique is being exploited. Monolithic circuits utilizing both microstrip and CPW techniques are being developed.

Computer-Aided Design Methodology - Knowledge-based CAD technique for the design of microwave monolithic integrated circuit has been developed. An example of MUSIC (Microwave Universal Structured Integrated Circuit) technique will be presented.

Circuit Integration Technique - An advanced technique for the integration of microwave and millimeter wave monolithic and hybrid circuit components has been derived. This utilizes multi-layer circuit board with thin film technique to achieve compact and reliable integration.

Millimeter Wave IC Applications - The availability of high performance monolithic integrated circuits based on GaAs MESFET and AlGaAs HEMT devices has made possible many system applications. Examples in sensor, seeker and phased array applications will be presented.

D1-2
0940 GaAs BASED MILLIMETER WAVE ICs: TECHNOLOGY CHOICES AND CIRCUIT PERFORMANCE, J. Geddes, S. Swirhun, J. Mondal, and V. Sokolov

GaAs based MMICs are expected to provide circuit building blocks for the next generation of millimeter wave systems in a number of applications such as FMCW radars for remote sensing, satellite to satellite secure communication and phased array radar for communication and target identification. Basic circuit functions in such applications are low noise amplifiers, power amplifiers and phase shifters. The rapid advance in GaAs based device technology has provided a number of choices for implementation of these functions including ion implanted metal semiconductor field-effect transistors (MESFETs), epitaxial MESFETs, and several varieties of high electron mobility transistors (HEMTs). The choice of technology for a given application depends on many factors including performance requirments, manufacturability, frequency, circuit function and the desireability of integrating multiple device types on a single IC. This paper will discuss choices available for millimeter wave ICs and their relationship to circuit performance and manufacturability.

D1-3
1040 DESIGN AND PERFORMANCE OF A 32-BIT GaAs MICROPROCESSOR FABRICATED WITH JFET TECHNOLOGY, R. Zulug and W.A. Geideman, McDonnell Douglas Electronic Systems Company, Huntington Beach, CA 92647

The design, architecture (RISC) and performance of a GaAs 32-bit microprocessor will be presented. This circuit is part of a projected single board GaAs computer operating at a 200 MHz clock rate with 100 MIPS average throughput.

D1-4
1100

GaAs and InP HBT Technologies for Ultra-High Speed ICs

Nitin J. Shah

AT&T Bell Laboratories

Murray Hill, New Jersey 07974

The needs of wide bandwidth data- and tele-communication and super-fast signal processing and computing have pushed the clock-rate of high-speed digital circuits well into the gigahertz range with sub-nanosecond gate delays.

The results from Si BJT circuits, BiCMOS, as well as GaAs and InP based HFETs are reported in the several GHz range. These results are reviewed, from the viewpoint of ultra-high speed MSI circuit requirements.

The technology of GaAs and InP heterojunction bipolar transistors is described. Device results on these transistors and their application to circuits will be reviewed, in the context of the performance, speed-power trade-off and the scale of integration.

D1-5
1120

AN EXPERIMENTAL METHOD FOR LARGE SIGNAL CHARACTERIZATION OF SOLID STATE NEGATIVE RESISTANCE DEVICES, A. Mortazawi and T. Itoh, Department of Electrical and Computer Engineering, The University of Texas at Austin, Austin, Texas 78712

For an accurate solid state oscillator design, the large signal impedance of the negative resistance device should be determined. To satisfy the steady state condition for oscillation, the impedance of the passive circuit seen from the active device's port should be equal to negative of the large signal impedance of device. Therefore, by measuring the impedance of the circuit seen by the active device the large signal impedance of the device at the frequency of oscillation can be determined. To measure the large signal impedance, a single Gunn diode is connected to a half wave microstrip line resonator. The output of this structure is connected to a triple stub tuner. After biasing the circuit, the stub tuner is adjusted to obtain the maximum power from the oscillator. Then we disconnect the diode and insert a coaxial cable in its place without disabling the rest of the circuit. The impednace at the far end of the coax is measured; afterward, the plane of the reference is moved to the diode end of the coax.. The large signal impedance of the Gunn diode is the negative of the impedance measured. Using this large signal impedance measurement and assuming that the equivalent circuit of the diode consists of a negative resistance in parallel with a capacitance, the values of the negative resistance and the shunt capacitance can be determined. It should be remembered that this equivalent circuit is valid only at the oscillation frequency.

By using the large signal impedance of the active device obtained by the above method, an X band Gunn oscillator was designed. In order not to alter the operating condition of the Gunn diode, the diode was connected to exactly the same microstrip resonator as the one used in the measurement. The capacitive part of the large signal impedance of the diode was compensated using a shorted stub and a quarter wave transformer was used to match the diode's impedance to a 50 ohm load. The Gunn diode oscillator designed in this manner operated at the same frequency and produced the same amount of power as in the measurement case. This method of measurement of the large signal impedance is also expandable for characterization of three port active devices.

D1-6
1140

LOSS MEASUREMENTS WITH AU-ON-GAAS MICROSTRIP RESONATORS

Todd Nichols
Department of Electrical and Computer Engineering
University of Colorado at Boulder
Boulder, CO 80309-0425

Losses in planar conductors are in general due to conductor loss, dielectric loss, and radiation loss. When low-loss dielectrics and proper shielding are used, loss is principly due to the conductors. Contributions to planar conductor loss include finite conductivity, edge shape, and surface roughness. In this talk will be presented some recent results of loss measurements using Au-on-GaAs microstrip linear resonators.

Issues pertinent to the measurement of attenuation in these microstrips include fabrication, wafer-probe transition, calibration, actual calculation of losses from the measured data, and sources of error. Several gap-coupled two-port resonators with vertical edges were fabricated this past summer at the Avionics Laboratory at Wright-Patterson Air Force Base in Dayton, OH. The resonators were probed with a Cascade Microtech wafer-probing station and an HP8510 VNA. Williams and Miers (MTT, pp. 1219-1223, July 1988) detailed a coplanar-to-microstrip transition without via holes; this device was used to facilitate probing. The 8510 was calibrated using on-wafer standards and the LRL procedure. Losses were calculated from the curves and compared with various theoretical predictions.

Ongoing work at the University of Colorado combines moment-method calculations of the attenuation constants of various lossy conductors on an infinite perfect dielectric above an infinite perfect ground plane, and experimental measurements of attenuation constants in Au-on-GaAs microstrip resonators with different edge shapes and groove patterns.

Session F-1 0855-Weds. CR1-9
RADAR BACKSCATTER, ATTENUATION, AND DROPSIZE DISTRIBUTIONS
Chairman: S.A. Frisch, NOAA/ERL Wave Propagation Laboratory, Boulder, CO 80303

F1-1
0900 PARTICLE-SHAPE DISTRIBUTION IN THE MELTING LAYER OF THE ATMOSPHERE

David A.de Wolf
Bradley Dept.of Electrical Engineering
Virginia Polytechnic Inst. and State U.
Blacksburg, VA 24060
H.W.J. Russchenberg, L.P. Ligthart
Department of Electrical Engineering,
TU Delft
The Netherlands

Analysis of radiowave propagation through (and scattering from) the layer in which ice particles melt and become raindrops requires a model for the distribution of particle shapes, as well as for the effective permittivity and sizes. The present study models the irregularly-shaped melting particles as a collection of spheroids of various shape and orientation.

A mathematical model for the shape distribution (i.e. for the dependence upon the depolarization parameters) is used to show: (a) that the shape of the distribution density does not need to be known accurately for modelling co- and cross-polarized signal statistics ; (b) that these are also not sensitive to the width parameter; (c) that the center of the distribution is crucial; (d) that plausible physical assumptions do show that the particle distribution is weighted more towards oblateness.

F1-2 0920 EVOLUTION OF CLOUD DROPSIZE DISTRIBUTIONS OBSERVED BY GROUND-BASED DOPPLER RADAR

E.E. Gossard, Cooperative Institute for Research in Environmental Sciences (CIRES), University of Colorado/NOAA, Boulder, CO 80309; and R.G. Strauch, NOAA/ERL/Wave Propagation Laboratory, Boulder, CO 80303

A technique is described for using ground-based Doppler radars to monitor the development of the dropsize spectra of number density, cloud liquid water density and liquid flux, in time and height. It is shown how such observations reveal the height-time location of rapid growth and how dropsize growth rates can be remotely sensed in an important subrange of the number-density spectrum. The observations show that significant spectral broadening can occur as a result of microphysical-kinematic processes not taken into account in the usual microphysical considerations.

Jan 1990 Nat. Radio Sci. Meet.

F1-3
0940

RAIN INDUCED ATTENUATION AT MILLIMETER WAVE FREQUENCIES: THEORY AND EXPERIMENT

A.D. Sarma and R.J. Hill
NOAA/ERL/Wave Propagation Laboratory
325 Broadway, Boulder, CO 80303

Measurements of rain induced attenuation at 230 GHz and 142 GHz have been made at Flatville, IL during 1985. Rain rate was measured by using three independent methods: Weighing bucket, ground-based precipitation probe and laser rain gages. The laser rain gages measure the rain drop size distribution averaged over a 50 m path.

The experimental drop size distribution results due to drizzle, widespread and thunderstorm are compared with the familiar drop size distributions due to Laws and Parsons (LP), Marshall and Palmer, Joss et al., and log-normal distributions. It is found that the experimental results closely follow the thunderstorm distribution of Joss et al. (JT). For all of these drop size distributions, the rain-induced attenuation at 230 GHz and 142 GHz is estimated using Mie theory and compared with the experimental results taken during light to moderate precipitation. These qualitative experimental results closely agree with the attenuation values due to JT distribution.

The LP distribution currently recommended by the International Radio Consultative Committee (CCIR) overestimates the attenuation. The applicability of the JT distribution is to be checked more thoroughly both at low and high rainfall rates in climatical regions similar to that of Flatville, IL. If our findings are confirmed then the LP distribution will be totally inappropriate for frequencies above 30 GHz. Similar findings are reported elsewhere in Europe. These results have important implications in the millimeter wave systems design.

F1-4
1000

USE OF POLARIMETRIC MEASURABLES TO DISCRIMINATE LARGE HAIL

D.S. Zrnic
National Severe Storms Laboratory
1313 Halley Circle
Norman, OK 73069

N. Balakrishnan
Deptartment of Aerospace Engineering
Indian Institute of Science
Bangalore 560 012
India

We examine the utility of the correlation coefficient between linear orthogonally polarized echoes, the differential reflectivity and reflectivity factor to discriminate large hail.

Calculations with a model of wet, dry and spongy hail allow us to make inferences concerning polarimetric signatures from hail producing storms. Both model and data suggest that a drop in the correlation coefficient is greater when larger hail is mixed with rain. We have observed that differential reflectivity in the storm with large hail was negative throughout the core. Above the melting layer the valuer were about -0.5 dB and below about -1 dB. Hailstones modeled as oblate spheroids with axis ratios between 0.6 and 0.8, and minor axis in the horizontal plane reproduce essential features of our measurements. Other investigators have noticed negative differential reflectivity in storms with hail larger than 2 cm. Thus we believe that differential reflectivity values lower than -1 dB and reflectivity factors above 60 dBZ signify presence of hailstones larger than 2 cm in diameter.

F1-5 THE KENNAUGH TARGET CHARACTERISTIC POLARIZATION STATES FOR BISTATIC CASE
1040 Amit P. Agrawal
Department of Electrical Engineering
Northern Illinois University
Dekalb, IL 60115

The Kennaugh target characteristic polarization state theory for bistatic case is developed. The six target characteristic polarization states as obtained for the monostatic case (Agrawal and Boerner, IEEE Transc. Geoscience and Remote Sensing, Jan. 1989) are investigated in the bistatic case. The characteristic polarization states are displayed on the Poincare sphere, and on the polarization power and phase plots. Several simple bistatic target cases are considered for demonstrating this useful concept to radar target classification and identification.

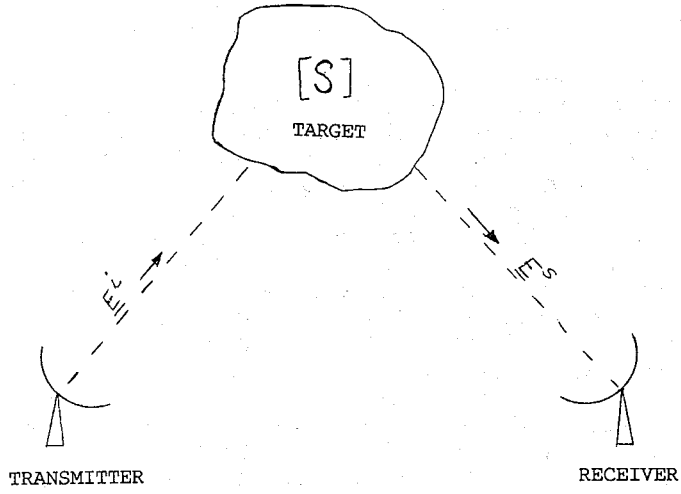

F1-6
1100

SENSITIVITY OF OPTIMAL POLARIZATIONS TO RAIN BACKSCATTER PARAMETERS

Amit P. Agrawal
Department of Electrical Engineering
Northern Illinois University
Dekalb, IL 60115, USA

In radar meteorology, the optimal polarizations play an important role in determining the characteristic parameters of hydrometeors such as rain. In this paper, the optimal polarizations (A.P. Agrawal and W.M. Boerner, IEEE Trans. Geoscience and Remote Sensing, Jan. 1989) for a single dielectric spheroidal raindrop are determined, and the relation of the optimal polarizations to the raindrop parameters are discussed on the Poincare sphere. It has been found that the crosspol nulls are sensitive to the canting angle and the copol nulls are sensitive to the drop size and shape of a spheroidal raindrop.

An ensemble of spheroidal raindrops is considered with exponential type size distribution and the gaussian type canting angle distribution, and the optimal polarizations are computed. It is found that by the measurement of optimal polarizations, these raindrop distribution parameters such as mean and variance of the canting angle distribution and the amplitude and the median of the drop size distribution can be determined.

F1-7
1120

ATTENUATION OF CO- AND CROSS-POLARIZED LINE-OF-SIGHT SIGNALS THROUGH A LAYER OF DIELECTRIC SPHEROIDS

David A.de Wolf
Bradley Dept.of Electrical Engineering
Virginia Polytechnic Inst. and State U.
Blacksburg, VA 24060
H.W.J. Russchenberg, L.P. Ligthart
Department of Electrical Engineering,
TU Delft
The Netherlands

This study is prompted by a desire to understand the differences in attenuation of essentially harmonic plane waves that propagate through the melting layer. The latter is considered as a stochastic collection of dielectric spheroids with effective real permittivities between 20 and 80 and concomitant imaginary parts at about 10% of these values (a previous study shows that more precise values do not affect the signal-scattering calculations).

The interaction is modelled as if the particles are much smaller than the wavelength. Although they are not at 20-30 GHz, this does not appear to be a serious flaw for forward-scattering attenuation calculations. A coherent-field calculation is employed for both co- and cross-polar reception. The co-polar ratio of received to transmitted power in dB (CPD), and the concomitant cross-polar quantity (XPD) are plotted as functions of permittivity, elevation angle, polarization angle for vertically-oriented spheroids. The effects of shape averaging around highly prolate or oblate averages are shown. A problem with the phase difference is noted.

Session G-1 0855-Weds. CR2-6
IONOSPHERIC MODELING
Chairman: K. Davies, NOAA/SEL, 325 Broadway, Boulder, CO 80303

G1-1
0900 A HIGH LATITUDE IONOSPHERIC SPECIFICATION MODEL (HLISM)

David N. Anderson, James A. Whalen & Santimay Basu
Ionospheric Physics Division (LIM)
Geophysics Laboratory (AFSC)
Hanscom AFB, MA 01731

Robert E. Daniell, Jr., Lincoln D. Brown, and William G. Whartenby

Jan J. Sojka and Robert W. Schunk

We have developed a semi-empirical model of the high latitude ionospheric model (HLISM) intended to be driven by real-time data so that it can provide real-time specification of the trough, auroral oval, and polar cap regions. It is intended to be incorporated into a global version of the Ionospheric Conductivity and Electron Density (GLOBAL ICED) model being developed for the U.S. Air Force Air Weather Service for use at the new Space Forecast Center. HLISM consists of a set of semi-empirical regional models (trough, auroral oval, and polar cap) coupled with a parameterized version of the Utah State University ionospheric model. Besides the usual solar and geomagnetic indices, the model accepts as input both ground-based and satellite based data and performs a least squares adjustment of its parameters to fit that data. This model is described briefly and examples of parameterized ion and electron density distributions are presented. In addition, validation of HLISM using ground-based and satellite data for two, four-day periods in December 1981 and February 1982 is discussed in detail.

G1-2
0920

GLOBAL MEASUREMENTS OF THE SLAB THICKNESS OF THE IONOSPHERE

by

X. M. Liu and K. Davies
Space Environment Laboratory, NOAA, Boulder, CO

ABSTRACT

Slab thickness of the ionosphere, obtained from Faraday contents and maximum electron densities at 18 locations around the world, shows diurnal, seasonal, and solar cycle variations. At sunspot minimum, the nighttime thickness is about 260 km, essentially independent of season, and the noon values vary from around 210 in winter to around 320 km in summer. At sunspot maximum, the nighttime thickness is around 300 km, and the noon values vary between 260 km and 340 km. There is an early-morning peak in slab thickness. On average, the global slab thickness T increases with the 10.7 cm solar noise flux F as:

$$\text{Equinox } T = 192 + 0.741\,F$$

$$\text{Winter } T = 183 + 0.863\,F$$

$$\text{Summer } T = 225 + 0.655\,F$$

G1-3
0940

Estimating F-region Peak Parameters

Adolf K. Paul
Naval Ocean Systems Center,Code 542
Ocean and Atmospheric Sciences Division
San Diego,California 92152-5000

When accurate virtual heights and frequencies are available in the vicinity of the F-region maximum, an accurate estimate of the ordinary and extraordinary critical frequency can be obtained from the linear decrease of the divided differences DF(f)=df/dh' with frequency, under the assumption of a parabolic peak (Paul, A. K. and D. L. Mackison, J.A.T.P., 43, 221 -223, 1981). The slope of the function DF(f) is inversely proportional to the half thickness ym. Estimates of the height of the maximum can then be obtained for each frequency by multiplying ym by the corresponding parabolic coefficient and subtracting those values from the observed virtual heights. Such residuals can be adjusted to an approximately constant value by small changes of the critical frequencies in an iterative process. The method will be presented and the effects of underlying ionozation will be discussed.

G1-4
1000

IONOGRAM INVERSION FOR A TILTED IONOSPHERE

J. W. WRIGHT
British Antarctic Survey, Cambridge, U. K.
(now at 1915 Spruce Avenue, Longmont Colo. 80501)

Digital ionosondes such as the Dynasonde disclose that the ionosphere is seldom horizontal even when it is plane-stratified to a good approximation. The local magnetic dip does not then determine correctly the radiowave propagation angle for inversion of the ionogram to a plasma density profile. The measured echo direction of arrival can be used together with the known dip for an improved propagation angle. The effects are small for simple one-parameter laminae, but become important when differential (ordinary, extraordinary) retardations are used to aid correction for 'valley' and 'starting' ambiguities. The resulting profile describes the plasma distribution along the direction of propagation, rather than the vertical; it thus conveys information about horizontal gradients. Observations suggest that advances in inversion methods may be practicable for application to modern ionosonde recordings, by which local lateral structure can be described in greater detail.

G1-5 1040

HF/VHF PROPAGATION RESOURCE DEVELOPMENT

D. P. Roesler
Collins Defense Communications
Rockwell International Corporation
350 Collins Road NE MS 137-138
Cedar Rapids, IA 52498
(319) 395-1551

Ionospheric dependent propagation in the HF/VHF spectrum is very complex for real-time skywave communications systems. Understanding and coping with these complexities is part of an on-going independent research and development project at Collins Defense Communications of Rockwell International Corporation.

This paper will describe the various resources used to enhance HF propagation management. This will include the types of solar geophysical data that has been used from the Space Environment Services Center (SESC) satellite broadcasts and the Space Environment Laboratory Data Acquisition and Display Services (SELDADS) computer bulletin board.

This project continuously collects and stores several HF data bases in parallel with the collection of the SESC and SELDADS data. Several useful characteristics were found by comparing operational HF conditions/reports with the SESC and SELDADS reports. The HF data consist of internal Communications Central operators' observations, Advanced Link Quality Analyzer (ALQA) step-sounding measurements between Cedar Rapids and Dallas, and SELSCAN™ LQA observations.

The Communications Central operators log abnormal propagation conditions (noise bursts, blackouts) while handling twenty-four hour world-wide traffic. These logs are compared to solar geophysical activity as reported by the SESC and SELDADS.

Another HF data base is the continuously sounded 2- to 30-MHz channel between Cedar Rapids, Iowa and Dallas, Texas using the ALQA as the test signal. The primary characteristics used from the ALQA data base is the time, frequency, signal-to-noise ratio density and the RMS multipath spread. These data consist of a sounding every minute. Frequencies between 2-30 MHz are sampled/sounded every thirty minutes.

By monitoring the SESC GOES6 and/or GOES7 x-ray level in the 1-8 angstrom channel and other measurements, it was found that up to several minutes of advanced warning can be gained for HF black-outs for propagation paths in the sun-lit midlatitudes. Some examples will be shown on the timing, impact and duration of certain flares with HF data observations.

G1-6
1100

DEVELOPMENT OF A NEW FIELD STRENGTH MODEL FOR PROPHET

D.B.Sailors *, J.R.Gnessin **, and D.L.Lucas ***
* Ocean and Atmospheric Sciences Division
Naval Ocean Systems Center
San Diego,CA 92152-5000
** Systems Exploration,Inc.
4141 Jutland Drive
San Diego,CA 92117
***2900 Valmont Rd,Suite H
Boulder,CO 80301

A new field strength model was developed for PROPHET which was a significant departure from prior versions. Until recently, the model was based on that developed by the Deutsche Bundespost(Damboldt,T., NATO AGARD Conference Proc.-No. 173,1975). In the new model, the Deutsche Bundespost model was replaced for paths shorter than 7000 km by a model relying on propagation via the regular E-layer and the F2-layer. The routine finds a lower order mode for the E-layer, F2-layer, and a mixed E-layer and F2-layer. Only one E-layer hop is considered in the mixed mode. The MUF model used is the MINIMUF-85 model(Sailors et al., NOSC TR 1121, July 1986). The E-layer MUF is calculated as in IONOCAP.

The ionospheric absorption equation is the one used in IONOCAP with the near specular reflection losses calculated for E-layer modes at low frequencies. The over-the-MUF losses are calculated using the Phillips (Wheeler,J.L,Radio Sci.,1,1303-1308,1966) method for values of frequency/MUF ratio up to about 1.5 MHz depending on ground distance and with values greater being considered in the "scatter" region. The losses above these values are estimated as in IONOCAP. The value of the absorption index I at night has a value which is a function of solar activity (Wakii,N.,J.Radio Res. Labs,Japan,18,191-208,May 1971). All the losses calculated are a function of geomagnetic latitude, length of path, time of day and season since the excess system loss tables of IONOCAP are used in the module along with the distribution of the MUFs.

Using CCIR Data Base C, the new model's bias and rms error for frequencies less than the MUF were 1.1dB high and 13.5dB, respectively, and for frequencies above the MUF the bias and rms error were 2.7dB low and 15.8dB,respectively. The most pronounced improvement seems to be in the over-the-MUF loss which show a much lower average residual from the previous method of about one-fifth and an rms residual of less than one-half.

G1-7
1120

IONOSPHERIC PROFILES FOR NIGHTTIME PROPAGATION

Jerry A. Ferguson
Ocean and Atmospheric Sciences Division
Naval Ocean Systems Center
San Diego, CA 92152-5000
Richard P. Buckner
Telecommunications Sciences
Richardson, TX 75080-4650

The long wavelength propagation model used by the Naval Ocean Systems Center requires specification of the ionosphere. The accuracy of the calculations this model therefore depend directly on the accuracy of this specification. Comparisons of the calculations from this model with measurements allow evaluation of it. Signal strength measurments were made aboard a merchant ship travelling between the United States and Europe. The daytime portions of these data have previously been used to evaluate the parameters of the daytime ionosphere. Those comparisons showed the the calculations were generally within 3 dB of the measurements. The present paper evaluates calculations for the nighttime measurements using that same model.

G1-8
1140

TRANSIENT ELECTROMAGNETIC DETECTION AND IDENTIFICATION

R. K. Bahr, D. W. Brandt, and D. G. Dudley
Electromagnetics Laboratory
Department of Electrical and Computer Engineering
University of Arizona
Tucson, AZ 85721, USA

Numerous researchers have analyzed specific aspects of an ionospheric communications channel. However, surprisingly little has been done towards integration of these individual components into a complete model. A complete model might include signal and signal source modelling, ionospheric propagation effects, signal reception in the presence of noise, and the detection/estimation of the signal/signal parameters.

In this paper we discuss modelling of an ionospheric communications channel designed to study the detection of earth-based transient electromagnetic pulses via a satellite-based receiver. We begin with an analysis of the desired transient based upon the known generating mechanism. The signal present at the satellite receiver consists of noise plus the transient pulse modified by ionospheric propagation, followed by free-space loss. Ionospheric propagation effects are modelled by a WKB approximation. Noise contributions include atmospheric noise, human-made coherent and non-coherent noises, and lightning. We complete the channel model description by examining the optimal maximum *a posteriori* (MAP) technique of estimating the pulse arrival times. The pulse occurence times are assumed to be described by a Poisson point process.

Session H-1 0855-Weds. CR0-30
RADIO EMISSIONS
R.F. Benson, NASA Goddard Space Flight Center, Greenbelt, MD 20771

H1-1 0900 IMPULSIVE VLF WAVES OBSERVED ON THE DE 1 SATELLITE, V.S. Sonwalkar, R.A. Helliwell, and U.S. Inan, Space Telecommunications and Radioscience Lab, Stanford University, Stanford, CA 94305

We report observations of wideband impulsive VLF waves received on the DE 1 satellite. The observations are based on the measurements of electric and magnetic fields in the frequency range of 0.650 Hz to 16.0 kHz. These wave are impulsive in nature and endure for a relatively short time ($\sim$1 s or less). They are typically found for L > 4 over a wide range of latitudes including the geomagmetic equator. They are often accompanied by discrete emissions or a hiss band. At times, these waves trigger emissions with rising frequency. Some features of these waves are consistent with the previous observations of electrostatic impulsive plasma waves (Ondoh et al. J. Com. Res. Lab., 36, No. 147, 1-12, 1989; Reinleitner et al., J. Geophys. Res., 88, 3079-3039, 1983). Observations of some of these waves with the magnetic antenna, however, indicates that they are electromagnetic in nature, a result that has not been reported before. In one case, 08 Jan 1987, the measured broad band electric field was $\sim$5 μV/m, and magnetic field was$\sim$0.5 pT. This implies a refractive index of $\sim$30 consistent with whistler-mode propagation. We discuss possible generation and propagation mechanisms for these waves.

H1-2
0920

INTENSE AURORAL KILOMETRIC RADIATION OBSERVED AT LARGE DISTANCES FROM THE EARTH BY ISEE-3

R.F. Benson and J. Fainberg, Code 692
NASA Goddard Space Flight Center
Greenbelt, MD 20771

Using a new data selection criterion, and a new analysis of antenna spin modulated signals received by ISEE-3, it has been possible to extend the upper limit of the auroral kilometric radiation (AKR) power flux density observed by distant satellites by more than a factor of 10. The AKR observed by ISEE-3 during one event when the spacecraft was at the orbital distance of the moon, and on the morning side of the earth, corresponded to a power flux density of 2×10^{-13} W/m^2/Hz normalized to a radial distance of 25 R_E assuming that the power falls off as $1/r^2$. Data were selected during near-earth "swing-bys" of ISEE-3 prior to its escape trajectory to Comet Giacobini-Zinner. Intense AKR events accompanied by 2 MHz signals were singled out for special study. An analysis of the received signal intensity as a function of antenna spin was performed to determine that the 2 MHz signals, as well as some of the lower frequency channels, were caused by a nonlinear receiver response to intense AKR at 250 kHz. This conclusion was based on the observed departure of the signal variations from a cos Ø dependence where Ø is the angle designating the instantaneous antenna orientation in the antenna spin plane. An analysis of the depth of signal modulation, as a function of cos Ø, was used to infer AKR signal intensities that caused receiver saturation even when the spacecraft was at lunar orbital distances. Such intense signals are attributed to an extended AKR source since a $1/r^2$ extrapolation assuming a point source yields intensities equivalent to the largest source region values (obtained by ISIS 1 and Viking) at a source-to-observer distance greater than 1 R_E. In addition, the present observations indicate that great care must be used when interpreting signals as AKR harmonics when **intense** fundamental AKR is present.

H1-3
0940

LOWER HYBRID WAVES EXCITED BY WHISTLER MODE WAVES THROUGH LINEAR MODE COUPLING IN THE IONOSPHERE AND MAGNETOSPHERE,
T.F. Bell and H.D. Ngo, Space Telecommunications and Radioscience Lab, Stanford University, Stanford, CA 94305

Lower hybrid waves are an important plasma wave mode in a number of diverse fields of plasma physics. They have been proposed as a means of plasma heating in fusion devices, as a means of heating ions and creating ion conics in the auroral region and as a means of thermalizing the incoming energetic ions at the bow shock. They are also apparently involved in ionospheric modification experiments, and in the ion heating recently observed over powerful VLF transmitters. Although lower hybrid waves have been studied extensively in the last decade, their origin is still unclear. However, it has become evident from recent satellite data that high amplitude lower hybrid waves are commonly stimulated throughout large regions of the ionosphere and magnetosphere by ordinary electromagnetic VLF whistler-mode waves, such as whistlers and signals from VLF transmitters, as they propagate through regions where small scale magnetic-field-aligned plasma density irregularities exist. In this phenomenon the amplitude of the excited lower hybrid waves can exceed that of the input electromagnetic waves by as much as 30 dB.

Although other explanations have been proposed, it is believed that the lower hybrid waves are excited by a passive linear mode coupling mechanism as the EM waves are scattered by the small scale irregularities. The lower hybrid waves are a type of quasi-electrostatic whistler-mode wave whose wave vector lies close to the resonance cone direction. In the present paper we show how the linear mode coupling theory of lower hybrid wave excitation provides an explanation for lower hybrid waves observed on spacecraft both within the magnetosphere and at the bow shock. We also show how this phenomenon affects the propagation of whistler mode waves in the magnetosphere.

H1-4
1000

ACTIVE EXPERIMENTS WITH SATELLITE-BORNE VLF TRANSMITTER

M.C. Lee
Plasma Fusion Center
Massachusetts Institute of Technology
Cambridge, Massachusetts 02139

Space experiments with mother-daughter satellites are proposed for the study of nonlinear VLF wave interactions with the ionospheric plasmas. Stimulated ionospheric plasma processes triggered by powerful VLF waves, which are injected from a satellite-borne transmitter, will be investigated. These processes may contribute to the better understanding of several outstanding phenomena, such as the spectral broadening of VLF waves, the puzzling explosive spread F, lightning-induced lower hybrid waves, and the possible particle precipitation from the ionosphere. In-situ measurements of VLF wave-induced plasma turbulence and scattered VLF waves will be made by the diagnostic instruments carried by the daughter satellite, while the mother satellite is primarily used to conduct the transmission of VLF pump waves. In addition, ground-based diagnoses with radars, all-sky imager, and VLF receivers will be arranged for the remote sensing of the VLF wave-stimulated ionospheric plasma processes.

H1-5
1040

PROPAGATION OF VLF ELECTROMAGNETIC WAVEPACKETS IN A MAGNETO-PLASMA

J. S. Xu and K. C. Yeh
Department of Electrical and Computer Engineering
University of Illinois at Urbana-Champaign
1406 W. Green St.
Urbana, IL 61801 - 2991

The propagation of a VLF electromagnetic wave packet in a magneo-plasma is studied. The wave packet is constructed by superposing a group of characteristic waves of variable amplitudes across the spectrum. The dispersion relation and the characteristic vector are solved from Maxwell's equation and the material relation for a medium under the condition of QL approximation. Accurate to the second order, a set of analytic expressions of the field vectors for a Guassian packet has been obtained. Some numerical results showing the polarization of wave fields and the variation of the envelope of the wave packet as a function of time are given.

It is found that the polarization of a Guassian packet gradually varies from the right - hand circular to the elliptical when the angle between geomagnetic field and wave vector increases. On the other hand, the polarization parameters are only weakly affected by changes in the carrier frequency of the wave packet.

Additionally, the effect of dispersion on wave envelope is also investigated. When the wave packet moves with the group velocity, the relative strength of its center gradually diminishes with an average rate of about 8 dB per 100 periods (for carrier frequency of 5 kHz). The higher is the carrier frequency, the faster is the attenuation. Besides, the Guassian envelope is found to spread three dimensionally, and two of the three axes of the ellipsoid rotate around the $\mathbf{V_g} \times \mathbf{k}$ as it propagates. The rotation of the pulse ellipsoid tends toward a stable direction after a propagation of about 250 periods.

H1-6
1100

COMPUTER SIMULATION STUDIES OF PLASMA WAVES, DYNAMICS, AND TURBULENCE IN THE HIGH LATITUDE IONOSPHERE WITH MAGNETOSPHERIC COUPLING*

M.J. Keskinen, S.T. Zalesak, J.A. Fedder, and J.D. Huba
Space Plasma Branch
Plasma Physics Division
Naval Research Laboratory
Washington, DC 20375-5000

H.G. Mitchell and P. Satyanarayana
Science Applications International Corp.
McLean, VA 22102

The nonlinear evolution of plasma interchange and Kelvin-Helmholtz instabilities in the high latitude F-region ionosphere with scale-size-dependent magnetospheric coupling and in the presence of an E-region and associated Hall conductivity effects has been studied using numerical simulation techniques. The spectrum of density and electric field fluctuations has been computed from the simulations and found to be in agreement with observations. Applications to plasma structure and turbulence in and near convecting patches, blobs, and arcs in the high latitude ionosphere are made.

*Work supported by DNA and ONR.

H1-7 SOURCE OF RADIO EMISSIONS FROM THE DAYSIDE OF URANUS
1120

J. D. Menietti, D. B. Curran, and H. K. Wong
Southwest Research Institute
Department of Space Sciences
P.O. Drawer 28510
San Antonio, TX 78228-0510

During the inbound trajectory toward Uranus the Planetary Radio Astronomy Instrument on board the Voyager 2 spacecraft observed narrowband smooth (n-smooth) emission at frequencies centered near 60 kHz and O-mode emission (the "dayside source") in a frequency range narrowly confined around 160 kHz. By assuming empirical models of the plasma density for the dayside magnetosphere of Uranus, and using cold plasma theory together with stringent observational constraints we have performed ray tracing calculations to determine the source location of both the n-smooth and O-mode emission.

The "dayside source" appears to originate along magnetic field lines with a footprint near the north magnetic pole. Sources of nightside, high frequency, broadband smooth (b-smooth) emission observed by Voyager after encounter are believed to exist near the conjugate footprint of these same field lines. Kaiser et al. (M. L. Kaiser, M. D. Desch, and J. E. P. Connerney, J. Geophys. Res., 94, 2399, 1989) have previously determined that the n-smooth emission is X-mode fundamental gyroemission with a source near the magnetic equator. Our results for the n-smooth emission are consistent with the source being X-mode second harmonic gyroemission but not O-mode. These findings are discussed in the context of the most recent developments in the theory of the cyclotron maser instability.

H1-8
1140

COLLECTIVE EMISSION OF AKR FROM GYROPHASE-BUNCHED ELECTRON BEAMS

Joseph E. Borovsky

Space Plasma Physics Group, SST-8

Los Alamos National Laboratory

Los Alamos, New Mexico 87545

A model for the emission of Auroral Kilometric Radiation is presented. Narrow-band electromagnetic waves above and below the electron cyclotron frequency are emitted by beams of energetic electrons that are spatially gyrophase bunched. When such beams are temporally modulated, the resulting temporal current pattern acts as an antenna to produce electromagnetic waves. Such beams may exist below strong plasma double layers on the magnetic field lines that are connected to discrete auroral arcs. For the auroral zone, the properties of the emission are described, including bandwidths, frequency drifts, polarizations, wave vectors, and power levels. Suggestions for critical measurements for future satellites will be made.

Session J-1 0855-Weds. CR2-26
CENTIMETER-WAVE RADIO ASTRONOMY
Chairman: R. Lacasse, NRAO, P.O. Box 2, Green Bank, WV 24944

J1-1
0900

70-METER DEEP SPACE NETWORK ANTENNA MICROWAVE PERFORMANCE

Somebody else gave paper Mark Gatti?

Dan D. A. Bathker
Telecommunications Science and Engineering Division
Jet Propulsion Laboratory
California Institute of Technology
Pasadena, California, USA 91109

The NASA Deep Space Network 64-m tracking antennas constructed in 1965 (Goldstone, California) and 1971-72 (Madrid, Spain and Canberra, Australia) have been substantially modified for improved microwave performance. The original quadric-profile Cassegrains have been extended to 70 m with shaped dual-reflector profiles for uniform illumination, and improved manufacturing and setting accuracies were achieved for the new reflecting surfaces. Aperture blocking by the quadripod feed support was reduced, and the main reflector structure was stiffened. The original moderate-offset Cassegrain feeds, termed "tricone", as well as the rotatable asymmetric (now shaped) subreflector were retained as a successful (although space-limited) means of rapidly changing operating frequency bands. Fieldwork began in late 1986 and was completed by late 1988. The long wavelength aperture efficiency for these very-low-noise antennas is now 0.765. At DSN spacecraft communication frequencies, aperture efficiencies are 0.76 at S-band (2.3 GHz) and 0.69 at X-band (8.4 GHz). Limited Goldstone testing at 13 mm (22 GHz) and 9.4 mm (32 GHz) shows peak aperture efficiencies of 0.50 and 0.35, respectively. At 9.4 mm the beam is measured as 32 arc sec, at half power.

All measured efficiencies are consistent with expectations based on a surface tolerance of 0.65 mm rms (surface normal measure), as determined by use of 12 GHz microwave holography near 45-degree elevation angle. Data provided by holographic imaging allowed for very rapid setting adjustments of the 1300 individual reflecting panels on each antenna to achieve an initial 0.7-mm goal consistent with excellent X-band operations. Analysis of holographic images following rapid setting indicates a theoretical potential for refinement to 0.3 mm, with an estimated 0.4 mm achievable in practice. The holographic imaging also provided data on uniformity of the aperture illumination, blockage and diffraction phenomena, the alignment of the rotatable tricone subreflector, and structural gravity loading.

This accomplishment is the result of significant contributions to the design, implementation and characterization of the antennas by many colleagues at the Jet Propulsion Laboratory, a number of skilled contractors, the aforementioned DSN stations and NASA. Eikontech, Ltd., Sheffield, England provided invaluable holographic imaging services. The remarkable success of this major and highly time-constrained effort has been dramatically demonstrated during the recent Voyager 2 encounter with Neptune.

The research described in this report was conducted or supported by the Jet Propulsion Laboratory, California Institute of Technology, under an agreement with the National Aeronautics and Space Administration. 10/89.

J1-2
0920

RADIO SOURCE MEASUREMENTS WITH A DSN 70-M ANTENNA OPERATING AT 32 GHZ

Michael J. Klein, Mark S. Gatti and Thomas B. H. Kuiper
Jet Propulsion Laboratory
4800 Oak Grove Drive
Pasadena, CA 91109

A 32 GHz receiver has been installed on NASA's Deep Space Network 70-meter antenna located at Goldstone, California. The primary Purpose of the Installation was to measure the high frequency performance of the antenna after it was upgraded and enlarged from 64-m to 70-m. System calibrations were performed and several radio sources were measured between March and July 1989. The measurements were highly repeatable, which suggests that the precision of the data is about 2.5 percent. The peak of the aperture efficiency function at 32 GHz is 0.35 +/- .05 centered around 45 degrees elevation. The estimated error (2 sigma) of the efficiency number is dominated by the uncertainty in the absolute flux density calibration.

A secondary objective of this work was to initiate a study of the absolute calibration of radio source flux densities at short centimeter wavelengths. Our preliminary analysis of the 70-m data has uncovered an inconsistency between the flux densities our primary flux density calibration source, Virgo A (3C 274), and the planet Venus. The implications of this discrepancy are being investigated and plans for a new series of measurements are being developed. The new measurements will be made with two receiving systems. One will be a cooled High Electron Mobility Transistor (HEMT) amplifier operating on a 1.5-m clear aperture antenna; the other is a 32 GHz maser amplifier operating on a 5-m aperture antenna. The status of these systems will be reported and the experimental plans will be discussed.

Jan 1990 Nat. Radio Sci. Meet.

J1-3
0940

DESIGN AND PERFORMANCE ANALYSIS OF THE NEW NASA BEAMWAVEGUIDE ANTENNA

T. Veruttipong, W. Imbriale, and D. A. Bathker
Telecommunications Science and Engineering Division
Jet Propulsion Laboratory,
California Institute of Technology
Pasadena, California, USA 91109

The NASA Deep Space Network (DSN) is constructing a new 34 meter research and development antenna as a precursor to introducing beamwaveguide antennas and Ka-band frequencies into the operational network.

A primary requirement of the DSN is to provide optimal reception of very low signal levels. Low overall system noise levels of 16–20 K are achieved by using cryogenically cooled amplifiers closely coupled with an appropriately balanced antenna gain/spillover design. Additionally, high power transmitters (up to 400 kW CW) are required for spacecraft emergency command and planetary radar experiments. The frequency bands allocated for deep space telemetry are narrow bands near 2.1 and 2.3 GHz (S-band), 7.1 and 8.4 GHz (X-band), and 32 and 34.5 GHz (Ka-band). However, for radio astronomy use it would be desirable to be able to operate over a majority of the frequency band from 1 to 43 GHz.

Feeding a large low-noise, ground-based antenna via a beamwaveguide system has several advantages over directly placing the feed at the focal point of a dual-shaped antenna. For example, significant simplifications are possible in the design of high-power, water-cooled transmitters and low-noise cyrogenic amplifiers, since these systems do not have to rotate as in a normally fed dual reflector. Furthermore, these systems and other components can be placed in a more accessible location, leading to improved service and availability. Also, the losses associated with rain on the feedhorn radome are eliminated because the feedhorn can be sheltered from weather.

The design of the beamwaveguide is based upon a Geometrical Optics (GO) criteria introduced by Mizusawa and Kitsuregawa in 1973 which guarantees a perfect image from a reflector pair. Since it is desirable to retrofit existing antennas with beamwaveguides as well as construct new antennas, there are actually two independent designs built into the R&D antenna. The first, termed a bypass design, places the beamwaveguide outside the existing elevation bearing on the rotating azimuth platform. The second, a center design, places the beamwaveguide through the center of the dish, inside the elevation bearing and through the azimuth axis into a pedestal room located below the antenna. The bypass design uses a single pair of paraboloids and two flat mirrors whereas the center design uses the same four-mirror design (although not the same four mirrors) above the ground and a flat plate and beam magnifier ellipse in the pedestal room. A beam magnifier is required since the pair of paraboloids requires a 29-dB gain horn to feed it whereas at the lower frequencies a 29-dB gain horn would be too large to fit in the pedestal room. The ellipse design allows the use of a smaller 22-dB gain horn in the pedestal room.

The performance was analyzed using an appropriate combination of Physical Optics (PO) and Geometrical Theory of Diffraction (GTD) software. The initial operation (Phase 1) of the project is for independent X- and Ka-band receive modes and performance predictions for these frequencies will be given. A preliminary design of Phase 2, which will consist of simultaneous S-X transmit and receive and simultaneous X-Ka receive, will also be presented.

The research described in this report was conducted by the Jet Propulsion Laboratory, California Institute of Technology, under an agreement with the National Aeronautics and Space Administration.

Under construction

J1-4
1000

AN ELEVEN FREQUENCY, SHAPED REFLECTOR FEED SYSTEM FOR THE VLBA

P. J. Napier
National Radio Astronomy Observatory
Socorro, New Mexico, USA.

The Very Long Baseline Array (VLBA) comprises ten 25m diameter reflector antennas. The antennas use a Cassegrain geometry in which the primary and secondary reflectors are shaped to provide high efficiency. The secondary focus is offset from the axis of the primary reflector allowing a number of secondary focus feed horns to be permanently mounted in a circle around the axis of the primary. Different feeds can then be selected by rotating the secondary around the axis of the primary so that the secondary focal point coincides with the desired feed. Locations for nine feeds covering frequency bands between 1.5 GHz and 86 GHz are provided. Additionally, a dual frequency crossed dipole feed for 300 MHz and 600 MHz is permanently located at the center of the secondary. This feed can be used when the subreflector is moved up so that the dipole is close to the best fit prime focus of the primary reflector. All movements of the subreflector needed to change between the eleven possible frequency bands can be accomplished in a few seconds using an automated mechanism.

The secondary focus feed horns are corrugated horns. The 1.5 GHz horn, because of its large size, is constructed from sheet metal and fiberglass using a novel fabrication technique. A dual frequency capability for the 2.3 GHz and 8.4 GHz bands is provided quasi-optically using a dichroic reflector over the 2.3 GHz feed and an ellipsoid over the 8.4 GHz feed.

Design considerations for the system will be reviewed and predicted and measured performance parameters will be discussed.

J1-5
1040

GREGORIAN SUBREFLECTORS FOR THE ARECIBO TELESCOPE

Michael M. Davis
National Astronomy & Ionosphere Center
P.O. Box 995
Arecibo, Puerto Rico 00613

I. Performance Measurements of the Mini-Gregorian

The predicted and measured performance of an off-axis dual subreflector feed installed on the Arecibo 1000-foot diameter spherical telescope are in excellent agreement. The 16 foot secondary and eight foot tertiary illuminate a 350 foot aperture on the main reflector, offset fifty feet uphill from the optical axis. Sensitivity at 5 GHz is 1.5 K/Jy at high zenith angles, dropping slightly as the illuminated area is blocked by the support platform. System temperature is 40 K, somewhat better than expected given the scattering off the support structure. Beam shape, sidelobe level and beam squint are in agreement with the predicted performance.

II. Performance Goals of the Full Gregorian

The Arecibo Gregorian Upgrading program will replace the present narrowband line feeds with a 65-foot secondary and 35-foot tertiary subreflector system. A set of standard scalar horns will be used to illuminate a 700 by 850 foot aperture and to provide continuous, wideband frequency coverage from 300 MHz to at least 8 GHz. The zenith sensitivity of 12 K/Jy will drop less than 1 db at the highest zenith angle because of a fifty foot downhill offset of the illuminated region. A 60-foot screen around the edge of the primary combined with this offset eliminates any increase in system temperature at high zenith angles. A new ground-referenced pointing system will provide 5" rms pointing. The S-Band cw transmitter power will be doubled to 1 MW. Combined with the other improvements, this will increase the planetary radar capabilities by a factor of ten to forty, depending on the declination of the target.

J1-6
1100

ACTIVE THERMAL COMPENSATION OF TELESCOPE SURFACE

R. P. Ingalls, Associate Director
Haystack Observatory
Westford, MA 01886

Active thermal compensation is used on a solid aluminum area of the Haystack Radio Telescope surface to force its temperature to track the much less thermally massive honeycomb surface panels. This technique eliminated a serious loss in aperture efficiency that occurred during rapid temperature change due to differential expansion of portions of the surface. In the future, this technique will be used to compensate for a major component of gravitational distortion by introducing programmed temperature offsets as a function of elevation angle.

Thermoelectric heat pump elements, driven by bipolar power supplies under closed loop computer control, accomplish bi-directional temperature tracking by the solid aluminum area of the surface. A self compensating water loop system exchanges the pumped heat energy to the radome air, avoiding the need for complex heater-chiller equipment.

Examples of the improvement in telescope performance through the use of this thermal control technique are illustrated.

J1-7
1120

ELECTROMAGNETIC DESIGN CONSIDERATIONS FOR A NEW, LARGE RADIO TELESCOPE

Roger D. Norrod
National Radio Astronomy Observatory
P. O. Box 2
Green Bank, West Virginia 24944

A project is underway to construct a new, large radio telescope at NRAO's Green Bank facility. The goal is to advance the state-of-the-art in large single-dishes on several fronts. During the last fifteen years, many researchers have made advances in our understanding of antenna performance, especially clear aperture designs. This paper will discuss how NRAO plans to take advantage of these advances and how the proposed design will affect future users.

J1-8
1140

A PROPOSAL TO EXPAND THE VLA AND VLBA

R. A. Perley
National Radio Astronomy Observatory
Socorro, N.M. 87801

The Very Large Array is the most productive and powerful radio telescope ever built. It has been fully subscribed since its completion in 1980, and there is no indication that its productivity will decrease in the future. But the VLA was designed and built with the technology of the 1970s, and great enhancement of its capabilities is now feasible using currently available technology. Use of this technology could provide increases in sensitivity by factors of 3 to 20, depending on the observing band. A considerable body of scientific investigation, currently beyond the VLA's reach, would then become possible.

The NRAO is building the Very Long Baseline Array (VLBA), with completion slated for the end of 1992. This new instrument will provide a resolution more than two orders of magnitude greater than that of the VLA. But the VLBA is notably insensitive to angular scales 1 to 10 times the VLA's maximum resolution. This 'blind spot' can be rectified by expansion of the VLA to include the two closest VLBA antennas plus addition of four new antennas situated in New Mexico and eastern Arizona.

The NRAO thus proposes to enhance the capabilities of the VLA/VLBA by modernization of the VLA's receivers and IF transmission system to allow 1 GHz bandwidth with reduced system temperatures at all bands, construction of a 33-antenna FX correlator with enhanced spectral capability, fiber-optic links with the Los Alamos and Pie Town VLBA antennas, and construction of four further antennas which would also be connected by fiber-optic links to the new correlator. This 33-antenna array would operate as a connected-element array when the VLA is in it 'A'-configuration. During other configurations, the four new antennas would join the VLBA, greatly improving its sensitivity and beam-forming performance.

This proposal thus greatly enhances both the VLA and VLBA, and greatly improves the linking of both instruments into a unified array. The increases in resolution, sensitivity and array performance are such that this VLA/VLBA array should be considered a new, general-purpose radio telescope for the 1990s and beyond.

Wednesday Afternoon, 3 January, 1355-1700

Session A-1 1355-Weds. CR1-42
ANTENNAS AND FIELDS MEASUREMENTS
Chairman: M. Kanda, Electromagnetic Fields Division, National Bureau of Standards and Technology, Boulder, CO 80303

A1-1
1400

A MEASURE OF COUPLING EFFICIENCY FOR ANTENNA PENETRATIONS

D.G. Dudley
Electromagnetics Laboratory
ECE, Building 104
University of Arizona
Tucson, AZ 85721, USA

K.F. Casey
JAYCOR
39650 Liberty Street, Suite 320
Fremont, CA 94538, USA

We consider the electromagnetic penetration into a shielded enclosure through an antenna feeding the region inside the shield. We use reciprocity to relate the far-zone fields to the short circuit current in the transmission line. Using a Norton equivalent circuit, we derive a measure of coupling efficiency, relating the electric field incident on the antenna to the current incident on the receiver. We demonstrate that the coupling efficiency can be determined by standard measurements at a terminal plane located on the transmission line together with a measurement of the radiated field in transmit mode.

We consider two examples. We first analyze coupling to an open-ended coaxial waveguide. We then consider the EMP-induced currents in the receiver when coupled through a transmission line to a center-fed dipole antenna. For the case of the dipole, we include results for different receiver bandwidths and transmission line lengths.

A1-2
1420

OPTICAL SENSING OF E AND H FIELDS IN A LOOP ANTENNA WITH DOUBLE GAPS

K.D. Masterson and M. Kanda
Electromagnetic Fields Division
National Institute of Standards and Technology
Boulder, CO 80303

Detection of electric and magnetic fields using a Loop Antenna with Double Gaps (LADG) has been reported previously (L.D. Driver and M. Kanda, IEEE Trans. Electro-magn. Compat., 30, no. 4, 495-503, Nov. 1988 and M. Kanda, IEEE Trans. Electro-magn. Compat., 26. no. 3, pp. 102-110, 1984). We are using photonic sensors to directly detect the voltages across each gap of the antenna. The optical signals are transmitted along a fiber to a detection and processing unit where they can be combined in a variety of ways to give either the gap voltages directly or their sum and difference. The latter are directly proportional to the electric and magnetic fields respectively. We describe the photonic sensor requirements and various processing options, and we report on the progress and current results of an application to a 10 cm diameter loop.

A1-3
1440

STATISTICAL ANALYSIS OF IMPEDANCE MISMATCH MEASUREMENTS AND COMPARISON WITH COUPLING INTO A 50 OHM PROBE†

G. E. Sieger and R. J. King*
Lawerence Livermore National Laboratory
P.O. Box 808, L-l56
Livermore, California 94550

The receiving cross section of a component or subsystem depends on both the gain of the couping object and the impedance mismatch between the coupling object and the load. The mismatch factor can be calculated from measurements of the load impedance and the self-impedance of the coupling object, from which the receiving gain can be obtained from a measurement of the receiving cross section. Also, from a knowledge of the gain and the self-impedance of a coupling object, the power that would be coupled into any load component can be inferred.

To investigate the statistical nature of the mismatch factor, we have made impedance measurements over a range of microwave frequencies for variety of cases. For any one combination of coupling object and load, the mismatch factor is typically a highly structured function of frequency, which can vary by an order of magnitude over a small frequency change. However, the average mismatch factor is a fairly smoothly varying function of frequency, in which fluctuations due to individual impedance resonances are not very significant. This average mismatch factor shows some systematic dependance on frequency, which may be an indication of typical circuit-board construction or geometry, or of typical component characteristics. Our measurements show that the average insertion loss due to an impedance mismatch is generally not very great. It varies from about 5 dB for frequencies below 2 GH_Z to l-2 db for frequencies about 5 GH_Z. For individual cases, the uncertainties of these values range from about 3-4 dB below 2 GH_Z to about l dB above 5 GH_Z.

For comparison, the mismatch factor corresponding to a 50 Ohm load, averaged over couping objects, was also calculated. That insertion loss is generally less than that for realistic load components, but not by more than 3 dB. Also for comparison, the mismatch factor for a 50 Ohm probe, which would result from connecting the probe in parallel with the load impedance, was calculated for each combination of load and couping-object impedances. Based on our results, the average power that would be coupled into a 50 Ohm probe is slightly greater below about 4 GH_Z, and less by 3-4 dB above 4 GH_Z, than the power coupled into a typical load.

In summary, it appears that although there can be an uncertainty of several dB in predicting the mismatch factor of a particular component at one frequency, the average mismatch factor for a variety of receiving systems can be predicted with more accuracy. Finally, the power that would be coupled into a 50 Ohm load or into a 50 Ohm probe in parallel with a load would not differ greatly from the power coupled into a typical load component.

1990 Nat. Rad Sci Meet

A-1 We-PM

A1-4
1520

DESIGN AND OPERATION OF THE NIST ULTRA-BROADBAND ANTENNA

A.R. Ondrejka, J.M. Ladbury, and H.W. Medley
Electromagnetic Fields Division
National Institute of Standards and Technology
Boulder, CO 80303

A relatively portable active antenna with a frequency response of 1 kHz to 1 GHz is described. The antenna is designed to be used for Time Domain EM field analysis, and therefore to have both constant amplitude and phase characteristics at all frequencies. The combination guarantees a good impulse response, and therefore, an output which is a high fidelity reproduction of the fields which illuminate it.

Below 120 MHz, this antenna functions as a high impedance electric field sensor. At higher frequencies the antenna becomes a terminated TEM horn. The unique "woofer - tweeter" combination produces an antenna factor of 22 dB, plus or minus 3 dB, over most of its frequency range. It degrades to 36 dB at 1 kHz, and 30 dB at 1 GHz. A switchable broadband amplifier provides an additional 20 dB gain for very low level signals.

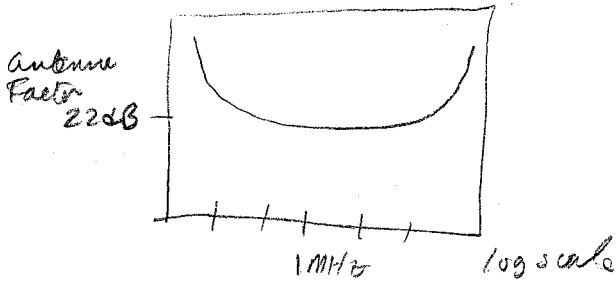

A1-5
1540

INFRARED DETECTION OF ELECTROMAGNETIC PENETRATION THROUGH NARROW SLOTS IN A PLANAR CONDUCTING SURFACE

Mark Smith, Ron Sega, John Norgard
Electromagnetics Laboratory
College of Engineering and Applied Science
University of Colorado
Colorado Springs, CO 80933–7150

Microwave field detection is generally performed using probes that transform the field value at discrete locations into electrical signals. These signals are then interpreted and yield information on the magnitude of the field at various locations.

Another method of field measurement is pursued in this paper and involves detecting the field through microwave heating of a conducting medium. The medium used is a resistive paper. Conduction currents are formed in the paper from the impinging tangential component of the electric field. These currents create local Joule heating of the paper and are detected using an infrared camera.

The infrared imaging technique is applied to the detection of the field generated by a narrow slot in a ground plane (Reed, Butler, & King, "Electromagnetic Penetration through Narrow Slots in Screens," 1988 URSI Meeting, Syracuse, University, June 1988). The slot is illuminated by an incident electric field and measurements are performed on the shadow side, cf. Figure 1. A two dimensional picture of the aperture E–field is created by piecing together the infrared images taken at numerous discrete positions.

1 to 10 GHz

8 mhos/m on paper 80 μ thick

Saturates at 10 mw/cm²

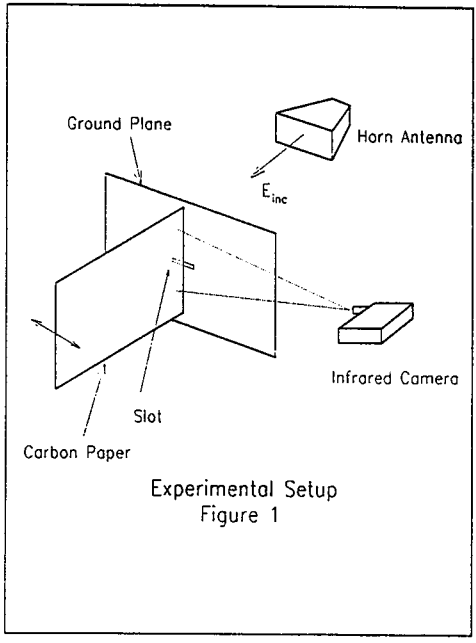

Experimental Setup
Figure 1

23' X 20' anechoic chamber at CU, SPS.

A1-6 1600 OPTIMIZATION OF ELECTRODE SHAPE FOR UNIFORM SURFACE CURRENT DENSITY

David A. Ksienski
Electrical Engineering and Applied Physics
Case Western Reserve University
Cleveland, Ohio 44106

Small electrodes for use in implantation within the human body must often sustain high current densities. These high current densities usually peak near the edges of the electrodes and can produce corrosion which limits the usefulness of the electrode. A numerical model of an electrode with no current peaks will be presented. The model includes an electrode and an insulating base on which the electrode is mounted and the conducting fluid which surrounds both. The problem is formulated via the boundary element method which is used to determine the current flow and potential on the electrode and the insulating base. The shape of this corrosion resistant electrode is obtained through iterative extrapolation from near field calculations.

Session B-3 1355-Weds. CR2-28
SCATTERING
Chairman: S.M. Rao, Dept. of Electrical Engineering, Auburn Univ., Auburn, AL 36193

B3-1 1400 **SCATTERING BY AN INHOMOGENEOUS PENETRABLE CYLINDER OF ARBITRARY SHAPE USING RAY TRACING**

Hyeongdong Kim and Hao Ling
Department of Electrical and Computer Engineering
The University of Texas at Austin
Austin,TX 78712-1084

ABSTRACT

For penetrable objects of arbitray shape, the volume integral equation approach and surface integral approach are used widely. However, these methods require large computer storage and computation time and hence limit the maximum body size which may be tractable. In this study, ray tracing technique is applied to the scattering of large inhomogeneous penetrable bodies. Using geometrical optics, the ray trajectories as well as the associated phase, amplitude, and polarization of the ray field along the ray are calculated numerically. Once the geometrical optics field at the boundary of the scatterer is obtained, Huygen's principle is used to formulate the scattered field from the equivalent Huygen sources $\vec{J}_s = \hat{n}\times\vec{H}$ and $\vec{M}_s = \vec{E}\times\hat{n}$ on the boundary radiating in free space. For the scattered field calculation, a ray tube integration scheme is used. In order to validate the ray results, they are compared with the formal exact solution to a class of inhomogeneous cylinders. For more general comparisons, the exact solution to the multi-layered cylinder is also implemented and compared against the ray results. For each case, good agreement is obtained in the high frequency regime. As expected in geometrical optics calculations, the variation of permittivity and permeability inside the scatterer and on the boundary should be smooth such that ray optics is a valid approximation to Maxwell's equations. In contrast to moment method solutions of integral equations, this ray tracing method is best suited for bodies that are arbitrary large in terms of the wavelength, and it is expected to complement the low-frequency moment method technique.

B3-2
1420

ELECTROMAGNETIC SCATTERING FROM MULTIPLE CYLINDERS USING THE BYMOMENT METHOD

R. Lee
A.C. Cangellaris
Electromagnetics Laboratory
ECE, Building 104
University of Arizona
Tucson, AZ 85721, USA

Electromagnetic scattering from multiple objects has been a subject of interest for at least the past 37 years (Twersky, J. Acoust. Soc. Am.,24, 42-46, 1952). Unfortunately, because of the complexity of the problem, the majority of the literature involves simple geometries such as perfectly conducting circular cylinders or infinitely thin strips.

The finite-element method is ideally suited for handling complicated geometries. However, for open region problems, it is necessary to truncate the mesh at some finite distance from the scatterer. We use a technique which we call the bymoment method to accurately handle this boundary truncation. This method uses Green's theorem to couple the finite-element solution inside and around each of the cylinders to the exterior region. This method allows us to enclose each cylinder by its own individual mesh, resulting in an enormous computational and memory savings. A description of the method is given along with comparisons to numerical results available in the literature.

B3-3
1440

ELECTROMAGNETIC SCATTERING FROM ARBITRARY SHAPED THREE DIMENSIONAL CONDUCTING BODIES BURIED INSIDE LOSSY DIELECTRIC MATERIALS OF ARBITRARY THICKNESS

Sadasiva M. Rao, Dept. of Elect. Engg., Auburn University, Auburn, AL 36849

In this work, we consider the problem of determining the electromagnetic scattering from general shaped three dimensional conducting objects buried inside lossy dielectric materials of arbitrary thickness as shown in the fig. The problem is formulated in terms of a set of coupled integral equations involving equivalent electric and magnetic surface currents radiating in unbounded media. The conducting structures and the dielectric material surfaces are modeled by planar triangular patches and the method of moments is used to solve the integral equations. Numerical results comparing with other available data for scattering cross section of certain canonical shapes will be presented.

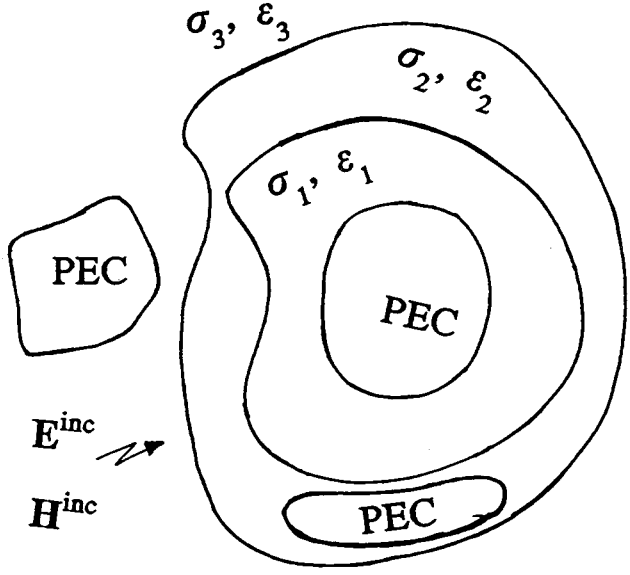

B3-4 1520 SCATTERING FROM CYLINDER COATED BY LAYERED CHIRAL MATERIALS AND JUMP-IMMITTANCE SHEETS

Roberto D. Graglia
CESPA - c/o Dip. Elettronica
Politecnico di Torino, Italy

Piergiorgio L.E. Uslenghi
Dept. of Electrical Engineering & Computer Science
University of Illinois at Chicago
Chicago, IL 60680

C. Long Yu
Pacific Missile Test Center
Point Mugu, CA 93042

The scattering of an arbitrarily polarized plane wave normally incident on a metallic cylinder coated by layered chiral materials is considered. Any two adjacent layers are separated by anisotropic jump-immittance sheets. A chain-matrix algorithm is employed in which inverses of matrices are evaluated analytically; the related computer code is tested on a variety of structures.

A procedure is developed to analyze the radar cross-section of the structure for various geometric and electromagnetic parameters, as was previously done for anisotropic Jaumann absorbers (R.D. Graglia and P.L.E. Uslenghi, Electromagnetics, vol. 7, no. 2, pp. 117-127, 1987). Numerical results based on this analysis are presented and discussed.

B3-5
1540

HIGHER-ORDER HARMONICS IN ELECTROMAGNETIC SCATTERING FROM A NONLINEAR ANISOTROPIC CYLINDER

M.A. Hasan
GE Aerospace
Government Electronic Systems Division
Moorestown, NJ 08057

P.L.E. Uslenghi
Dept. of Electrical Engineering & Computer Science
University of Illinois at Chicago
Chicago, IL 60680

The determination of the electromagnetic field scattered by a nonlinear anisotropic cylinder under obliquely incident plane wave excitation has been considered previously by the authors (National Radio Science Meeting, Boulder, CO, January 1988; also: IEEE Trans. Antennas Propagat., to appear), for the fundamental frequency components of the scattered field.

In the present work, second and third harmonics of the scattered field are studied, when the material of the scatterer is characterized by Volterra-type integrals for the electric and magnetic flux density vectors. A perturbation technique is employed, and several numerical results are presented and discussed.

B3-6
1600

SCATTERING FROM A CAVITY-BACKED CIRCULAR APERTURE PENETRATED BY A WIRE: THE EXTERIOR REGION

D.B. Wright
R. Lee
D.G. Dudley
Electromagnetics Laboratory
ECE, Building 104
University of Arizona
Tucson, AZ 85721, USA

The problem considered is that of a wire penetrating a circular aperture in an infinite conducting screen and entering a circular cylindrical cavity. Results for the transient current propagating along the wire outside the cavity are presented. The current is evaluated in the frequency domain by the method of moments. An approximate method for evaluating the exterior current at an observation point far from the aperture is discussed. To obtain the transient response, a numerical inverse Fourier transform is used. The current response is examined as a function of different aperture and cavity dimensions. Results obtained with the approximate method are compared to the method of moments solution.

In addition, an approximate method is presented for evaluating the fields outside the cavity at observation points located far from the aperture. Frequency domain results are presented which compare this far-field approximation to the method of moments solution. The presence of interior resonance features in the exterior fields is discussed.

B3-7
1620

A FINITE DIFFERENCE APPROXIMATION IN THE K-SPACE APPROACH

Saila Ponnapalli
Tapan K. Sarkar
Department of Electrical Engineering
Syracuse University
Syracuse, New York 13244-1240

Jack Nachamkin
Lockheed Corporation
Organization 91-60
Building 256
3251 Hanover St.
Palo Alto, CA 94304-1191

ABSTRACT

An accurate method of utilizing a finite difference approximation in the integro-differential operator equation arising in scattering problems from arbitrarily shaped, homogeneous or inhomogeneous, lossy or lossless obstacles is presented. The k-space approach is used to solve the operator equation, and the finite difference approximation is carried out in the frequency domain as a simple trigonometric multiplication. The use of this approximation alleviates the necessity for considering principle value integrals which arise when the order of differential and integral operations are interchanged in the operator equation, and consideraby simplifies the solution procedure. Results are compared for an infinitely long circular cylinder of diameter 2λ and several permitivities. The bistatic scattering cross sections obtained with and without the finite difference approximation are in excellent agreement.

B3-8
1640

AN ITERATIVE TECHNIQUE BASED ON THE METHOD OF LEAST SQUARES APPLIED TO SCATTERING PROBLEMS USING THE K-SPACE APPROACH

Saila Ponnapalli
Tapan K. Sarkar
Department of Electrical Engineering
Syracuse University
Syracuse, New York 13244-1240

Jack Nachamkin
Lockheed Corporation
Organization 91-60
Building 256
3251 Hanover St.
Palo Alto, CA 94304-1191

ABSTRACT

An iterative technique based on the method of least squares and utilizing variational trial functions is presented. It is applied in the solution of scattering problems involving arbitrarily shaped homogeneous or inhomogeneous penetrable obstacles, utilizing a volume formulation and the k-space approach. The method has the advantage that it guarantees strong convergence of the residuals and also solution convergence when the problem is well posed. Numerical results are presented for infinitely long homogeneous circular cylinders with TE plane wave excitation. A comparison of the performance of the iterative technique with the conjugate gradient method is made. Modifications of the iterative method which involve increasing the number of trial functions are discussed and numerical results are presented which demonstrate the effects of the modifications.

Session D-2 1415-Weds. CR1-40
ADVANCED DEVICES
Chairman: C. Chao, TRW, Redondo Beach, CA

D2-1
1420

GAAS SCHOTTKY BARRIER DIODES FOR MILLIMETER AND SUBMILLIMETER WAVELENGTH APPLICATIONS

T.W. Crowe
Semiconductor Device Laboratory
Department of Electrical Engineering
University of Virginia
Charlottesville, VA 22903-2442

GaAs Schottky barrier diodes are used in a variety of applications in the millimeter and submillimeter wavelength range, including mixer elements for heterodyne receivers, varactor multipliers for submillimeter LO sources, and sideband generators for tunable power sources in the THz frequency range. Although SIS junctions currently offer better noise performance at millimeter and long submillimeter wavelengths, the demand for Schottky mixer elements continues to grow. This is due to their excellent noise performance, high frequency response and relatively simple and reliable implementation into receivers. The recent interest in atmospheric chemistry promises to spur further developments in Schottky technology. For these applications the goal will be compact, reliable (hopefully, all-solid-state) receivers for airborne and satellite applications well into the THz frequency range. This talk will discuss recent developments that are beginning to make such receiver systems realizable, as well as future work that remains to be done.

D2-2
1440

RF PERFORMANCE OF A SURFACE - CHANNEL SCHOTTKY BARRIER MIXER STRUCTURE

R. J. Mattauch, W. L Bishop, and D. G. Garfield*
Semiconductor Device Laboratory
Department of Electrical Engineering
University of Virginia
Thornton Hall
Charlottesville, VA 22903-2442

The Schottky barrier diode is the mixer element of choice for heterodyne radiometers operating at frequencies in excess of 100 GHz and above superconducting transition temperatures. Applications requiring the greatest sensitivity, such as radio astronomy, utilized whisker contacted devices due to the low parasitic shunt capacitance of such structures. The whisker contacted device, however, can suffer from mechanical instability and is difficult to incorporate into integrated microwave circuitry. Whiskerless structures, for the most part, have exhibited prohibitively high values of shunt capacitance. This talk will discuss design, fabrication, and RF performance of a whiskerless "surface-channel" structure designed to minimize shunt capacitance while maintaining excellent current-voltage characteristics. Diode fabrication techniques will be discussed and results compared with those obtained with photolithographically fabricated "air-bridge" structures. Mixer mount and required diode mounting techniques will be presented. Special attention will be paid to the RF characterization circuitry and its calibration. Device DC excited noise temperature at the LO along with mixer conversion loss and noise temperature in the 100 GHz range will be presented.

*Stanford Telecommunications, Reston, VA 22090

D2-3 1520 **Short channel effects in self-aligned AlGaAs/GaAs HFETs studied by Monte Carlo technique**

by
Geir U. Jensen
Univ. of Minnesota, Univ. of Virginia and Minnesota Supercomputer Institute
Tor A. Fjeldly
Norwegian Institute of Technology and Minnesota Supercomputer Institute
Michael Shur
Univ. of Virginia and Minnesota Supercomputer Institute

Using supercomputer self-consistent Monte Carlo simulation, we studied planar-doped, self-aligned AlGaAs/GaAs Heterostructure Field-Effect Transistors (HFETs) with gate lengths in the range 0.1 to 1.0 μm, and varying depth of the implanted contacts. Our simulations clearly show that overshoot effects, leading to electron velocities far in excess of long-channel values, and non-ideal effects such as electron real space transfer into the AlGaAs layer and electron injection in the substrate are very important for all the devices. The real space transfer leads to the decrease of transconductances at high gate voltages (transconductance compression) in agreement with numerous experimental data. The increase in electron energy at high drain bias and a commensurate increase in the electron transfer due to the hot electron effects leads to a negative differential resistance at high gate bias (decrease in the drain current and increase in the gate current). Short channel effects SCE) in the form of high output conductance in the saturation region, a negative threshold voltage shift, and an increase of the subthreshold current levels become extremely important in the devices with smaller gate lengths. Electron distributions within the device with different gate lengths generated by the Monte Carlo program show that dominant mechanism leading to SCE is the injection of electrons from the contacts into the GaAs buffer beneath the two-dimensional channel. This is also consistent with the output drain conductance and the threshold voltage shift being approximately inversely proportional to the square of the gate length. An increase in the contact depth from 0.05 μm to 0.28 μm results in an increase in the output conductance from 37 to 134 mS/mm.

The SCE begin to become overwhelming when the contact depth is on the order of the separation between the n^+ source and drain contact regions. In order to minimize the SCE the contact regions should be made as shallow as possible, or the separation between these regions could be increased by using T-gates or side walls to reduce implant straggle under the gate or by using non-self-aligned structures. We also suggest that SCE can be drastically reduced by increasing the degree of electron confinement in the channel. This can be achieved by increasing the p-type doping density of the substrate, or by abandoning the AlGaAs/GaAs device structure for quantum well structures, where there is an abrupt energy barrier between channel and substrate, as for example in pseudomorphic AlGaAs/InGaAs/GaAs HFETs.

D2-4
1540

HIGH TRANSCONDUCTANCE ß-SiC BURIED-GATE JFET's

Galina Kelner
Naval Research Laboratory
Washington, DC 20375-5000

Abstract

An improved performance buried-gate SiC junction field effect transistor (JFET) has been fabricated and evaluated. This structure employs an n-type ß-SiC film epitaxially grown by chemical vapor deposition on the Si(0001) face of a p-type 6H α-SiC single crystal. The current in the n-type channel was modulated using the p-type α-SiC layer as a gate. Electron-beam evaporated Ti/Au was utilized as an ohmic contact to the n-type ß-SiC layer and thermally evaporated Al was used to contact the p-type gate. The maximum dc transconductance of 20 mS/mm was obtained, which is the highest reported for a ß-SiC FET structure. The experimental data are analyzed using a charge control model. This analysis shows that the effective field-effect mobility (565 $cm^2/V-s$) is close to the measured Hall mobility (470 $cm^2/V-s$). Calculated drain current versus drain voltage characteristics for a buried-gate JFET are in good agreement with experimental data. This modeling also shows that the device performance may be improved by scaling down the channel length and optimizing the device design.

D2-5 PANEL ON FUTURE TRENDS OF HIGH FREQUENCY DEVICES AND CIRCUITS
1600

Session E-1 1355-Weds. CR1-9
HIGH POWER ELECTROMAGNETICS IV
Organizer and Chairman: J.P. Castillo, R&D Associates, P.O. Box 9377, Albuquerque, NM 87119

E1-1
1400

RECENT ADVANCES IN HIGH POWER ELECTROMAGNETICS

Maj. R. L. Gardner, USAFR
Weapons Laboratory (AFSC), Kirtland AFB, NM 87117

Abstract

The elements of High Power Electromagnetics (HPE) are Nuclear Electromagnetic Pulse (NEMP), Lightning, and High Power Microwaves. Much of the research in this area falls under the auspices of the Committees on Lightning and EMP Environments and Intentional Noise Sources. In this paper, we survey recent results in HPE, as they apply to these Commission E Committees.

Basic elements of EMP environments from the public domain point of view will be noted. These developments will be put in a historical perspecitive.

Lightning is the next element of HPE. A survey of progress in lightning environments was given at the 1989 U. S. URSI meeting. Updates of recent work will be presented along with a brief reminder of history.

Formal, public treatment of microwave interaction is less well developed. Recent papers by C. E. Baum provide some basics for using EMP concepts for system hardening for microwaves.

Recent Commission E activities, in which elements of HPE were presented, were the EMC-89 Zurich Symposium and the International Commission E Symposium on Planetary and Environmental Electromagnetics. Highlights of those meetings as they apply to HPE will be given.

E1-2
1420

COUPLED TRANSMISSION-LINE MODEL OF PERIODIC ARRAY OF WAVE LAUNCHERS

C. E. Baum
Weapons Laboratory/NTAAB
Air Force Systems Command
Kirtland AFB NM 87117-6008

This paper considers the situation in which the individual wave launchers in an array are long compared to their cross-section dimensions. A two-wire (plus reference) transmission-line model is formulated applicable to symmetrical in-line wave launchers. The flat plates of the launchers are chosen such that a particular form of the characteristic-impedance matrix is realized. This leads to an analytic solution for the early-time propagation on the wavefront. From this one finds the transmission and reflection of the wavefront at the aperture plane.

E1-3
1440

IMPEDANCE CHARACTERIZATION OF AN INCREMENTAL LENGTH OF A PERIODIC ARRAY OF WAVE LAUNCHERS

D.V.Giri

Pro-Tech, 125 University Avenue, Berkeley, CA 94710

Abstract

The concept of distributed sources invokes the uniqueness theorem in electromagnetic (em) theory whereby the fields are known everywhere, if they are specified on a closed surface. Conversely, in synthesizing an em wave, one can attempt to establish the required tangential electric field on boundary surfaces for the desired wave, satisfying the Maxwell's equations. One of many possible ways of configuring the conical wave launchers is the symmetric in-line type. An earlier paper in this session has described and formulated a two-wire (plus reference) transmission-line model for the coupled wave launchers. Such a model is valid for wavelengths large compared to cross sectional dimensions and small compared to launcher lengths.

In this paper, we consider the problem of impedance characterization of an incremental length of a periodic array of symmetric in-line launchers. The transmission line model needs a (2x2) characteristic impedance matrix. Three of the four impedance matrix elements are known analytically and a numerical solution of the Laplace equation is presented for getting the fourth element. This numerical solution also permits one to find all four elements of the characteristic impedance matrix for a given set of geometrical parameters in a cross-section of the unit cell. The numerical solution presented here yield results that agree well with the three known elements of the caharacteristic impedance matrix, thus enhancing our confidence in the computed values for the fourth unknown element. This method solves for the potential distribution for the prescribed set of conductors, electric walls, magnetic walls and assigned potentials on conductors. Once the potential distribution is known, electric fields are numerically found and then , charges on conductors are evaluated using the normal electric field values. From a knowledge of charges and the per-unit-length capacitance matrix, the elements of the characteristic impedance matrix are easily computed.

Results , such as reported here are expected to be useful in arriving at optimal shapes of launcher plates.

E1-4
1500 HEMP COUPLING MODELS TO POWER SYSTEMS: THEORETICAL DEVELOPMENT AND PRACTICAL APPLICATIONS, F.M. Tesche, PO Box 796174, Dallas, TX 75379

An important aspect of the DOE/ORNL HEMP Assessment Program is predicting the voltage and current surges induced in power system components by a high altitude electromagnetic pulse (HEMP) produced by a nuclear burst. For this purpose, a number of calculational models have been developed using transmission line theory as a starting point. Such models include single and multi-wire above-ground lines, buried cables, and shielded cables. These models have been applied to studies of transmission and distribution line (T&D) systems, instrumentation systems, and power system facilities.

This paper will first review the theoretical basis for these models, paying special attention to the relationship between rigorous electromagnetic scattering theory and the approximate transmission line theory. Limits of validity of the transmission line models will be explored, and the impact of its use in power system assessments will be discussed.

The results of applying these transmission line models to selected power system components and facilities will then be discussed. A number of T&D line configurations have been analyzed, and these results will be summarized. A limited amount of experimental field coupling data is available for validating these coupling models, and this will also be discussed.

This work has been sponsored by the Office of Energy, Storage and Distribution of the U.S. Department of Energy, through the Oak Ridge National Laboratory.

E1-5
1540

SOME FEATURES OF WAVEGUIDE/HORN DESIGN

Carl E. Baum
Weapons Laboratory/NTAAB
Air Force Systems Command
Kirtland AFB NM 87117-6008

In transitioning a sinusoidal electromagnetic wave from source to radiating antenna, a conducting waveguide operating in the lowest order H mode is often used. This waveguide can be optimized for its power handling capabilities. As a common rectangular waveguide the $H_{1,0}$ mode has geometric properties which allow E-plane subdivision into some number of rectangular guides. This in turn allows convenient division or recombination of electromagnetic waves. This concept is extended to pyramidal horns which can launch the waves from one or more waveguides. The E-plane subdivision can be used for designing a metallic grating which allows passage of the wave while mechanically supporting a dielectric sheet separating vacuum from gas regions.

E1-6
1600

OPTIMAL POWER HANDLING CAPABILITY FOR PARAMETRIZED UNIFORM WAVEGUIDES

C. S. Kenney
Applied Mathematics Research Group, Research Department
P. L. Overfelt
Physics Division, Research Department
Naval Weapons Center
China Lake, CA 93555-6001

One aim of high power electromagnetics is the transmission of power through a uniform waveguide such that the output at a receiver is maximized. To characterize the waveguide cross section in terms of its power handling capabilities, a dimensionless efficiency factor has been defined (C. E. Baum, Air Force Weapons Lab, Sensor and Simulation Notes, Note 314, 18 November 1988). This factor is a function of only the size and shape of the waveguide cross section. Thus we may optimize the efficiency factor in terms of either waveguide size or fundamental geometry. In this paper, we consider optimization of the power handling capability in terms of the size requirement, assuming that the shape is given. Thus for a given two-dimensional planar domain Ω, which has associated eigenfunctions and eigenvalues satisfying both the Helmholtz equation and Neumann boundary conditions, there is an associated efficiency factor, $\eta = \eta(\Omega)$. If the domain depends on some parameter r (for instance, the width to height ratio of the cross section), then we would like to choose r to maximize $\eta = \eta(r)$.

We find that for waveguides of doubly symmetric cross section (i.e., symmetric about their centers in both x and y), the efficiency factor is a maximum for a given geometry when the second and third lowest eigenvalues are equal. This will be shown for rectangular, rhombic, and elliptic waveguides. A highly convergent method for finding the value of the parameter r, which causes the second and third lowest eigenvalues to be equal for a given geometry will be introduced.

E1-7
1620

SLOW WAVE TRANSMISSION LINE TRANSFORMERS

Albert W. Biggs*
Weapons Laboratory (AFSC)
Kirtland Air Force Base, New Mexico 87117

This study describes the development of a periodic structure which couples a slow wave guide to a fast wave guide. The slow wave guide has periodic square wave corrugations on the guide walls or on the wall of one or both conductors of a two conductor transmission line (i.e., inner or outer conductor of a coaxial line). The slow and fast wave guides have similar spatial configuration (rectangular to rectangular, coaxial to coaxial, etc), but with different characteristic impedances.

Transformer sections in the periodic structures were designed to obtain maximally flat passband responses with binomial coefficients (J. Stone Stone, US Patents 1,643,323 and 1,715,433) and "equal ripple" VSWR responses with Chebyshev polynomial coefficients for minimal VSWR for given bandwidths (Seymour B. Cohn, IRE Trans., MTT-3, 16-21, 1955). The design techniques developed by Cohn were modified to create a variation of phase velocity in the periodic structure with the variation of characteristic impedance of each unit cell.

Examples are presented for periodic structures with 11 Sections (Unit Cells) and 10 Junctions, and with smaller Sections and Junctions decreasing to 2 Sections and 1 Junction for both binomial and Chebyshev cases.

*IPA Grant while at KAFB. TCS from Elec & Comp Engr Dept, University of Alabama in Huntsville, Huntsville, Alabama.

E1-8
1640

EFFECTS OF INITIATION HEIGHT ON LIGHTNING INDUCED ELECTROMAGNETIC FIELDS

Maj. R. L. Gardner, USAFR
Weapons Laboratory (AFSC), Kirtland AFB, NM 87117

Abstract

As a stepped leader nears the ground, an upward going streamer rises to meet it. When the two meet, the return stroke begins, radiating electromagnetic fields. Most of the high frequency emissions of the return stroke are generated at this initiation point; high frequency currents die out in the lossy transmission line formed by the leader channel.

In this paper, a nonlinear nonuniform transmission line model is used to track the currents as they evolve from the initial charged line to the fully developed, upward propagating return stroke current. Each element of the transmission line represents a cross section of the channel. This cross section in turn is modeled by a simple three layer hydrodynamic model of the expanding lossy channel. The diameter of the hot channel is allowed to expand as it is ohmically headed effecting the inductance, capacitance and resistance of the transmission-line element.

These currents then radiate electromagnetic fields, which may be measured at some distance from the lightning strike. It would be useful to be able to remotely sense characteristics of the return stroke. These calculations predict how joining the upward and downward propagating leaders effects the high frequency fields.

Session F-2 1355-Weds. CR1-46
TROPOSPHERIC WIND, WAVES, AND ATTENUATION
Chairman: E.R. Westwater, NOAA/ERL Wave Propagation Laboratory, Boulder, CO 80303

F2-1
1400

SODAR OBSERVATIONS OF ELEVATED TROPOSPHERIC LAYERS

Alan R. Webster and Harvey S. Wong,
Dept. of Electrical Engineering,
The University of Western Ontario,
London, Ontario, CANADA. N6A 5B9.

A microprocessor controlled vertical acoustic sounder (SODAR) has been developed with the objective of providing information on the occurrence and properties of elevated tropospheric layers as these are related to the propagation of radio waves on terrestrial communications links. The use of the microcomputer allows a cost effective way of controlling the basic sodar parameters, such as pulse width, pulse repetition rate and operating frequency, and also allows the storage of the raw return echo data in digital form to facilitate later analysis. 40 MByte cartridge tapes are used to store several weeks of continuously collected (20 second intervals) data, so that the system operates virtually unattended.

Results are presented from several months of operation of the system. Much fine structure is routinely observed some of which is clearly related to atmospheric waves. Here though, the emphasis is placed on the distribution in height of the occurrence of thin elevated layers which might be expected to be influential in the generation of atmospheric multipath propagation. Such distributions, on a monthly basis, are presented for a height range up to 300 m. above local ground.

F2-2
1420

ATTENUATION STATISTICS AT 20.6, 31.65, AND 52.85 GHZ DERIVED FROM A NETWORK OF GROUND-BASED MICROWAVE RADIOMETERS

E. Fionda
Fondazione Ugo Bordoni
190 viale Europa
00144 Rome, Italy

M.J. Falls and E.R. Westwater*
NOAA/ERL/WPL
325 Broadway
Boulder, CO 80302

Next generation communication satellites, such as OLYMPUS and ACTS, will have beacons at 20 and 30 GHz. Currently, there is sparse knowledge of atmospheric attenuation statistics at these frequencies. In particular, attenuation from clouds can play an important role in determining the utility of these new systems. Atmospheric attenuation, and its partitioning into clear and cloudy contributions, can be derived from ground-based radiometric measurements of atmospheric thermal emission. Such radiometers, operated in a long-term unattended mode, are ideal for providing these statistics. From 1985 to 1988, the Wave Propagation Laboratory operated a research network of ground-based, zenith-viewing radiometers in the front range of eastern Colorado. Three of the radiometers were dual-channel water vapor radiometers (WVR) that operated at 20.6 and 31.65 GHz. A fourth radiometer at Stapleton International Airport, Denver, Colorado, has additional channels, including one operating at 52.85 GHz. Using WVR data taken at the Colorado Research Network during 1988, both single-station and two-station attenuation statistics are derived for summer and winter seasons. These statistics exhibit considerable differences between the two periods. In addition, as shown in Fig. 1, Denver attenuation statistics at 20.6, 31.65, and 52.85 GHz are derived for the summer of 1988. Predictability in attenuation between the various channels is also discussed.

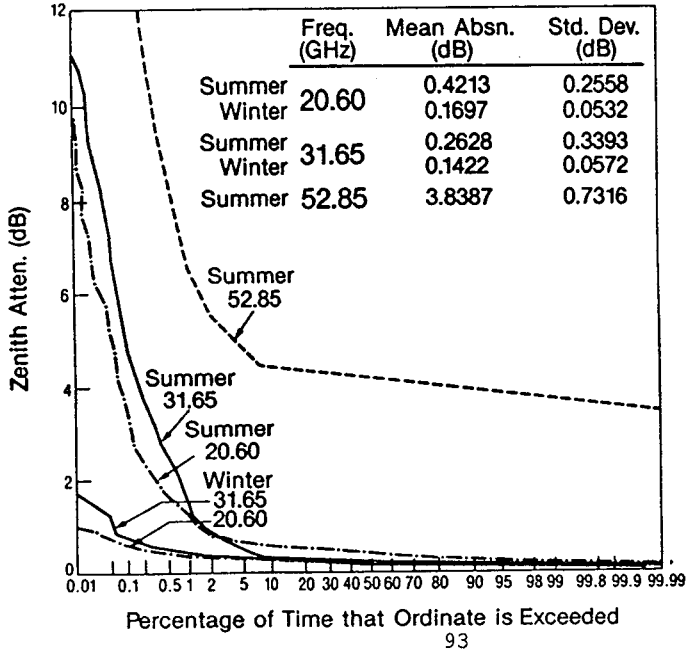

Figure 1.

Radiometrically derived zenith attenuation statistics at Denver, CO 1988.

Jan. 1990 Nat. Radio Sci Meet.

F2-3
1440

DETERMINATION OF THE MEDIUM TEMPERATURE FROM SIMULTANEOUS BEACON AND RADIOMETRIC OBSERVATIONS AT 11.2 GHZ.

W. J. Vogel and G. W. Torrence
Electrical Engineering Research Laboratory
The University of Texas
10100 Burnet Road
Austin, TX 78758-4497

Simultaneous measurements of beacon attenuation and sky temperature have been performed in Austin, Texas since June 1988. The satellite under observation is the INTELSAT F10-VA spacecraft, which is stationed over the Atlantic Ocean and which appears at an elevation angle of 5.8°. Both the right-hand circularly polarized 11.2 GHz beacon and the left-hand circularly polarized radiometer utilize the same 2.4 m aperture conical offset reflector horn antenna.

The data collected during the first year of the experiment have been used to determine an effective physical temperature for the precipitation. The analysis is based on monthly equi-probability values, on the median attenuation measured at a particular sky temperature, as well as on separate atttenuation events, with and without conditioning on the local rainfall rate. The dependence of the results on the method employed is discussed.

F2-4
1500

MICROWAVE-INDUCED ACOUSTIC GRAVITY WAVES IN THE ATMOSPHERE

A.J. Palmer
NOAA/ERL Wave Propagation Laboratory
Boulder, Colorado

In this paper, I examine the physics of generating coherent acoustic-gravity waves in the atmosphere through heating in the beat wave of counter-propagating, dual-frequency microwave beams. I find that detectable acoustic and evanescent gravity-wave signals can be produced with existing c.w. S-band transmitters at a range of a few hundred meters for the acoustic waves and a few tens of meters for the gravity waves. The demonstration of this effect would represent the first coherent, nonlinear interaction of microwave radiation with the atmosphere outside laboratory spatial scales.

The calculations predict that the 7 kHz S-band-induced acoustic wave will be detectable with electronic sensors for both focused and unfocused microwave beams. The induced pressure becomes detectable again in the evanescent gravity-wave frequency range near the so-called characteristic surface-wave frequency for the tight-focused case where the induced velocity of the wave becomes circularly polarized.

The large transverse coherence length of the induced acoustic wave should allow unique acoustic propagation and scintillation experiments to be carried out. Perhaps the most important application involves the induced low-frequency evanescent gravity wave. Unlike the induced acoustic wave, the evanescent gravity wave will not propagate any significant distance from the generation volume without there being a free surface to support the wave. However, the gravity wave's slow phase velocity, together with its polarization and wavelength, will allow the wave to couple to ground-level turbulent eddies. Thus, provided one detects the induced gravity wave within its generation volume, the described method may offer a new opportunity for controlled experimental study of small-scale gravity wave interactions with turbulence.

F2-5
1520

THE OBLIQUE SPACED ANTENNA METHOD FOR MEASURING HORIZONTAL WIND USING ST RADARS

C. H. Liu[1], J. Röttger[2], G. D. Dester[1], S. J. Franke[1], and C.-J. Pan[3]
[1]University of Illinois, Urbana-Champaign
[2]EISCAT Scientific Association, Kiruna, Sweden
[3]National Central University, Chung-Li, Taiwan, ROC

A novel extension of the spaced antenna method for VHF/UHF radar applications is introduced. It is proposed that instead of pointing the spaced antenna beams vertically, an off-vertical oblique configuration could be used. It will be shown that this technique can be used to obtain horizontal wind at independent "points" in the atmosphere without making assumptions about homogeneity or linear variation of the wind fields. To demonstrate the idea of oblique beam spaced antenna technique, we carried out an experiment at the Chung-Li VHF radar in Taiwan on May 13, 1988 with two oblique beams and one vertical beam. Good experimental confirmations are achieved by comparing the results with those derived from the conventional spaced antenna method and the Doppler method. Implications of the proposed technique on measurements of divergence, vorticity, etc. in the atmosphere will be discussed.

Session F-3 1600-Weds. CR1-46
OCEAN AND TERRAIN EFFECTS
Chairman: E.R. Westwater, NOAA/ERL Wave Propagation Laboratory, Boulder, CO 80303

F3-1 1600 FULL-WAVE RADAR SEA ECHO MODELING

F. J. Ryan and F. D. Tappert
Ocean and Atmospheric Sciences Division
Code 541
Naval Ocean Systems Center
San Diego, CA 92152-5000

A radar sea echo model has recently been developed which treats linearly polarized, electromagnetic wave scattering from a rough sea surface in the presence of tropospheric ducting. The method uses full-wave diffraction physics for propagation and a Born approximation for scattering. The model is built around a parabolic electromagnetic (PE) wave equation code and treats the sea surface as a stochastic rough interface via a spectral ocean wave model. The wave propagation/scatter code employs a high-speed, split-step Fourier algorithm to solve the parabolic wave equation. Comparisons between the PE sea echo model and the Georgia Institute of Technology (GIT) clutter model will be presented for C,S and X-band radars under varying sea-state conditions. (Work supported by the Office of Naval Technology)

F3-2
1620

MID-INFRARED REFLECTANCE CHARACTERISTICS OF SELECTED BENCHMARK SOIL SAMPLES

Ram M. Narayanan*, S. E. Green* and D. R. Alexander**
*Dept. of Electrical Engineering, University of Nebraska, Lincoln, Nebraska 68588
**Center for Electro-Optics, University of Nebraska, Lincoln, Nebraska 68588

Active mid-infrared reflectance characteristics of 18 different benchmark soil samples were measured at different angles of incidence at 9.283, 9.569, 10.247 and 10.633 μm wavelengths for both co-polarized and cross-polarized conditions. The measurement set-up consisted of a 100 watt carbon dioxide laser operated at 5 W whose beam was chopped at 2 kHz rate, and directed on the soil sample placed in a petri-dish on a rotating table. The backscattered energy was focused using a 24 cm focal length lens onto a cryostat-cooled HgCdTe detector. A polarizer was used in front of the detector to select the like or the cross-polarized backscatter. The detected signal was amplified in a matched preamplifier followed by a lock-in amplifier prior to recording. Calibration was performed after each measurement using a Labsphere Infra-gold Diffuse Reflectance standard of 94% reflectance. One hundred independent samples were averaged for each measurement to yield a mean reflectance value.

The soil samples were classified according to type, series, mineralogy, location, clay and silt contents, and organic carbon percentage. The selected samples represented wide variability in soil properties. The measurements indicate that certain types of soils have unique reflectance signatures in the 9-11 μm mid-infrared region, which are pronounced at certain incidence angles. For example, an Inceptisol soil type of the Wahiawa series found in Hawaii (Kaolinitic mineralogy, 60% clay, 33% silt, 1.30% organic carbon) shows a peak in the reflectance structure at 9.569 μm compared to the other wavelengths investigated. An analysis of the data indicates that it may be possible to identify certain soil types and their properties using their active mid-infrared reflectance characteristics.

Jan 1990 Nat. Rad. Sci Meeting

F3-3
1640

LMSS APPLIED TO RAILWAYS: A PROPAGATION EXPERIMENT

A. Benarroch, L.Mercader, G. Sastre.
ETSI Telecomunicación
28040 Madrid, Spain

paper read by someone from U. of Madrid

Several LMSS propagation measurements at 1.5 GHz have been performed in the framework of ESA's PROSAT (phase II) program using a locomotive as the mobile platform and the MARECS satellite (A. Benarroch et al. AP-S Proceedings, 815-818, 1989).

The objective if this experiment, whose results will be presented, was to investigate the effect of environment conditions peculiar to railways (tunnels, bridges, stations, cuttings, arches, the electric line) on the received signal.

The measurements took place along stretches of railways through different environments of the North half of Spain, comprising both electrified and non electrified lines.

The cumulative distributions shown in fig. 1 correspond to several of those runs. From them, and from other results obtained from the statistical analysis of the registered data, we conclude:

-The signal is blocked inside tunnels and large stations.
-High cuttings with vegetation may cause deep fades.
-Short, very deep fades are due to bridges.
-Arches cause very short (0.1-0.2 sec.), weak fades.
-No multipath propagation effects have been observed due to the high elevation angle (37°).

of electric lines in electric railways

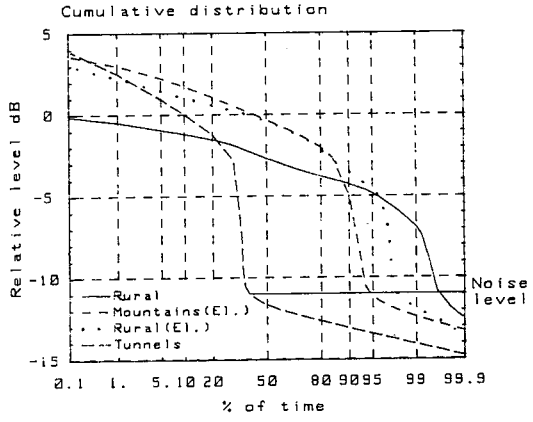

Omnidirectional antenna with 360 sain.

Fig. 1

Session G-2 1335-Weds. CR2-6
CEDAR TECHNIQUES
Chairman: R. Behnke, Upper Atmospheric Facilities, Div. of Atmospheric Sciences, National Science Foundation, Washington, DC 20550

G2-1
1340

AIDA ACT '89: A MULTI-INSTRUMENT CAMPAIGN

Colin O. Hines,
Arecibo Observatory,
Arecibo, PR 00613-0995.

As part of its Arecibo Initiative in Dynamics of the Atmosphere (AIDA), the Arecibo Observatory and its visitors conducted the 720-hour multi-instrument observational campaign AIDA Act '89 in three blocks of time during March - May, 1989. The primary objective was a calibration of two partial-reflection middle-atmosphere radar systems (IDI and SAD, respectively) against other measurements of dynamical activity in the middle atmosphere. A secondary objective was the acquisition of all locally available geophysical data relevant to the region under observation, which lay at roughly 75 - 105 km above the Observatory's HF heating site, where the IDI and SAD were located. (Heights of 10 - 30 km were also under observation by the IDI.)

The IDI and SAD systems are purported by some to yield a measurement of horizontal wind (and vertical wind, in the case of the IDI) in the region from which their partial-reflection returns come. They are purported by others to be potentially subject to contamination, if not to complete confusion, in consequence of atmospheric waves in the same region. Less subject to doubt are the motions revealed by Doppler shifts in incoherent-scatter returns, in airglow emissions, and in radar reflections from meteor trails. These Doppler methods were brought to bear as the means of calibration. Airglow imagers provide a horizontal section, and lidar a vertical section, through the relevant wave fields; they, too, were employed in the campaign as being potentially useful in the interpretation of any discrepancies that may be found between the partial-reflection and the Doppler-determined motions.

The planning and implementation of the campaign will be outlined in this paper, and some initial (and therefore tentative) results will be highlighted.

The campaign was funded primarily by the National Science Foundation, both through its basic support of the Arecibo Observatory (under a cooperative agreement) and through special grants from its CEDAR (Coupling, Energetics and Dynamics of Atmospheric Regions) allocation.

G2-2
1400

THE MESOSPHERE/LOWER THERMOSPHERE RADAR NETWORK AND THE CEDAR PROGRAM

S. K. Avery
Department of Electrical and Computer Engineering
University of Colorado at Boulder
Boulder, CO 80309-0425

Atmospheric radars that probe the neutral atmosphere below 100 km are playing an important role in CEDAR campaigns. These radars operate in the HF-VHF frequency range and consist of wind profilers, spaced antenna radars, and meteor radars. Each type of radar has different capabilities but all provide a measurement of the neutral wind field. In conjuncton with optical instrumentation and incoherent scatter radars, these systems aid in our understanding of the coupling of the troposphere, stratosphere, and mesophere-lower thermosphere.

In this presentation I will discuss the capabilities of these radars and describe some of the CEDAR science that is being addressed.

G2-3
1420

CURRENT AND FUTURE STATUS OF CEDAR FABRY-PEROT INTERFEROMETRY

J.W. Meriwether
Ionospheric Effects Branch
Geophysical Laboratory
GL/LIS
Hanscom AFB, MA 01731-5000

The current status of the CEDAR initiative in Fabry-Perot interferometry exhibits a world-wide network of ground-based automatic stations with the capability of F-region measurements of neutral winds and temperatures with considerable accuracy for conditions of solar maximum. The signal source for these measurements at sites in low and middle latitudes is the night-time 630nm airglow emitted by the dissociative recombination of O_2^+ ions. The altitude of this emission is typically about 1 scale height below h_{max}. Within the high latitudinal regions of the aurora belt and the polar cap, the source signal tends to appear at a lower height, 225 km, through the production of 630nm signal in auroral activity. Procedures have been developed whereby these results are collected in the CEDAR database for use by interested scientists. The technique itself continues to be developed for application to other atmospheric regions and chemical species, most notably that of the geocorona and the mesosphere. Recently, a novel optical technique developed by Prof. P.B. Hays (University of Michigan) has proved to be very successful in enhancing the sensitivity of the instrument by utilizing additional orders of interference. The combination of this optical innovation with the multiplexing gain afforded by a low noise CCD detector provides a net increase of sensitivity of nearly two orders of magnitude. This technology breakthrough will open the door to many new applications in atmospheric science, and first results should be forthcoming within the next two years.

G2-4
1440

Interferometers for the CEDAR Program

P.B.Hays, Professor
Department of Atmospheric, Oceanic and Space Sciences
Space Physics Research Laboratory
University of Michigan
Ann Arbor, Michigan, 48109

The past two decades of investigations by ground based and satellite optical techniques have led to significant advances in our understanding of the upper thermosphere and to a lesser extent the mesosphere. These studies were largely devoted to studies of large-scale (order of thousands of kilometers) features of Earth's thermosphere, the seasonal and latitudinal variations in its dynamics and thermodynamics.

The CEDAR program of the National Science Foundation has as one of its goals the observation of the detailed dynamic structure of the mesosphere and lower thermosphere. This program recognizes the need to develop a new higher sensitivity "Class I" interferometer in order to provide the temporal and spatial coverage needed to improve our knowledge of the smaller scale dynamical phenomena that control the mesosphere and thermosphere.

This paper reviews that present state of high resolution Doppler observations and describes a new Class I instrument being developed by the University of Michigan. The Michigan Class I interferometer utilizes the Circle to Line Interferometer Optical System (CLIO) to convert the circular Fabry-Perot fringes into a linear pattern along the axis of a 45° cone. This linear spectrum has optical integrity for about ten orders and is recorded using a conventional CCD detector. A conservative estimate of the sensitivity gain for this device over the modern S-20 image plane Fabry-Perot Interferometers is a factor of 100, with greater gains possible. The new CLIO FPI clearly will meet the CEDAR objectives for the Class I FPI. With this new instrument the horizontal wind fields can be observed with high temporal resolution. This will allow maps of the winds to be created with horizontal resolution sufficient to compare with the variations that are observed in the intensity of emission features and with the temperature fields that are being determined from rotational development of various emission bands.

G2-5
1520

JOINT RADAR AND OPTICAL REMOTE SENSING OF UPPER ATMOSPHERIC COMPOSITION AND DISTURBANCES

G. G. Sivjee, Professor of Physics
Department of Mathematics and Physical Sciences
Embry-Riddle Aeronautical University
Daytona Beach, FL 32114

Under the CEDAR initiative, the aeronomy community has upgraded both the radar and optical facilities to improve ground-based remote-sensing capabilities for investigations of upper atmospheric compositions and disturbances. The new optical facilities developed under the CEDAR funding include the LIDAR, the imaging spectrometer for multispectral observations of upper atmospheric emissions between 300nm and 900nm, and a multiplexed infra-red Michelson interferometer to extend the coverage beyond 900nm to about 1700nm. The last two optical systems provide measurements of the absolute intensities of atomic lines and molecular band emissions, from which the abundance of the emitters can be determined if the excitation sources are known. The radar measurements provide the electron density and temperature both of which are needed in such calculations. The optical systems also provide the rotational and vibrational distributions of the molecular bands from which the thermodynamics of the emitting region can be determined. Spatial and temporal variations in the abundance and thermodynamics of the upper atmospheric species determined from optical and radar measurements indicate disturbances propagating in the emitting region. Examples of upper atmospheric studies which can be undertaken with the CEDAR facilities include the determination of the thermospheric atomic oxygen density, and its variations, from twilight observations of the O°7320A line emission, gravity wave disturbances in the mesopause as reflected in the modulation of OH brightness and rotational temperature, and nonLTE vibrational distribution of N_2 in the auroral F region.

G2-6
1540

OPTICAL IMAGING AS A REGIONAL IONOSPHERIC DIAGNOSTIC CAPABILITY

Michael Mendillo and Jeffrey Baumgardner
Center for Space Physics
Boston University
725 Commonwealth Avenue
Boston, MA 02215

As part of the National Science Foundation's CEDAR initiative for atmospheric sciences, a new low-light-level imaging capability has been created for use in thermosphere/ionosphere/magnetosphere research. Capable of operating in all-sky (180° field of view) mode, the image-intensified CCD detector obtains images that span $\sim$ 4,000,000 km^2 for typical F-region emissions at 6300 and 7774Å. This spatial coverage, coupled to time resolution in the $\leq$ minute domain, allows for detailed investigations of such auroral and airglow features as, auroral and sun-aligned arcs, sub-auroral SAR arcs, diffuse aurora, and F-region trough, and equatorial plasma depletions. When operated in campaign mode in support of a robust cluster of groundbased and satellite-borne radio and in-situ diagnostics, the all-sky imager sets the context for the unified interpretation of such high resolution line-of-sight measurements. The CEDAR program has played an important role in creating pairs of incoherent scatter radars and all-sky imagers to enhance the scientific yield of upper atmospheric research.

G2-7
1600

A NEW LIDAR TECHNIQUE FOR MEASURING MESOPAUSE SODIUM TEMPERATURES

C.Y. She, H. Latifi, J.R. Yu
Department of Physics
Colorado State University
Fort Collins, CO 80523

Using lidar technique, the measurement of height distributions in sodium density near mesopause has been continually carried out by several research groups. Although it is well known that mesospheric temperature can be determined by a proper measurement of the sodium D_2 fluorescence spectrum, only two attempts have been made. By scanning eight equally-spaced frequencies successively, Gibson et al. (Nature 281, 131, 1979) were able to deduce the temperature near the peak of the sodium layer. By monitoring the frequency of each laser pulse, Fricke and von Zahn (J. Atmo. & Terr. Phys. 47, 499, 1985) were able to obtain a Na temperature profile with 1 km and 10 K uncertainty. Both these groups used tunable pulsed dye laser as the transmitter and did not know the absolute frequency of their laser pulses.

Since the Na lineshape is mathematically known, mesospheric temperature can be determined from the ratio of fluorescence signals at two frequencies. In order to carry out this simple procedure, however, the frequency of the tunable laser transmitter must be known during the measurement. We have proposed the use of a laser system that starts from a stabilized cw single-mode tunable dye laser followed by a pulsed dye amplifier which is in turn pumped by a doubled Yag laser at a rate of 20 Hz. We have shown that the output of this frequency stabilized system can be easily tuned to the narrow peak and crossover resonances of the saturated fluorescence spectrum with a laboratory sodium cell. In collaboration with the researchers (Bills & Gardner) from University of Illinois, the proposed technique and this unique laser system have been used along with a 1.22 m diameter Fresnel lens to measure the mesopause temperature distributions at Fort Collins, CO in August,1989. This paper will discuss the concept and potential of this new lidar technique present a sample of the measurement result.

G2-8
1620

EXPANDED CAPABILITY OF THE SONDRESTROM, GREENLAND INCOHERENT SCATTER RADAR

C. J. Heinselman and R.C. Livingston
SRI International
333 Ravenswood Avenue
Menlo Park, CA 94025

Recent advances in digital electronics have made it possible to significantly enhance incoherent scatter data collection and processing. At Sondrestrom, we have recently upgraded the data collection and on-line processing hardware. Our approach has been to utilize off-the-shelf components and to minimize the specialization of the hardware. We are using board-level processors, fully programmable in C, with direct I/O porting of input data. Use of the direct I/O channel, which is capable of a rate of several megasamples per second, minimizes the requirements of the host CPU; our system consists of a series of AT computers operating on a local area network. The flexibility of the processor programming allows rapid development and testing of data collection and processing modes, for both ionospheric and MST use. Ionospheric data are currently being collected in a lag profile (UNIPROG) format, in parallel with the original Sondrestrom system. Comparisons between the data from the two systems will be used to illustrate the new system capabilities and the advantages of the lag profile method.

G2-9
1640

MOM - A NEW STATE-OF-THE-ART INCOHERENT SCATTER RADAR DATA ACQUISITION AND ANALYSIS SYSTEM AT MILLSTONE HILL

John M. Holt
Atmospheric Sciences Group
MIT Haystack Observatory
Westford, MA 01886

The incoherent scatter radar technique has developed over a twenty five year period into a powerful tool for ionospheric observation and research. These large radar systems are capable of monitoring basic ionospheric parameters through the E and F regions over a large spatial area and with good time resolution. The National Science Foundation provides basic support for a chain of incoherent scatter radar observatories aligned along a magnetic meridian through the east coast of the United States. These stations provide the wide-latitude coverage of ionospheric phenomena appropriate for the studies of large-scale atmospheric coupling which are a part of the CEDAR (Coupling Energetics and Dynamics of Atmospheric Regions) program. The Millstone Hill Incoherent Scatter Radar, operated by the MIT Haystack Observatory, is an integral part of this meridional chain.

The CEDAR program plan calls for upgrading IS radar sites to state-of-the art (Class I) radar instruments to allow the extended operations and the range and temporal resolution necessary for CEDAR objectives to be met. At Millstone Hill three major initiatives have evolved in response to the need to upgrade the facility's capability to meet CEDAR observational requirements. These are MIDAS (Millstone Ionospheric Data Acquisition System), OASIS (Optimal Analysis of Signals from Incoherent Scatter), and MADRIGAL (Millstone Atmospheric Data Retrieval Interactive and Graphical Analysis Library). Together these projects represent a coordinated plan to greatly enhance the scientific utility and flexibility of radar systems. Features include multiple networked receiver chains, digital phase detection and FIR filters, pulse-to-pulse interleaving of transmitter waveforms and frequencies, full treatment of the two-dimensional radar ambiguity function through simultaneous analysis of the entire measured lag-profile matrix, and near real-time storage of the analyzed data in an interactive database.

H2-1
1340

LINEAR CONVERSION: PHASE-SPACE ANALYSIS*

Allan N. Kaufman
Lawrence Berkeley Laboratory
Department of Physics, University of California, Berkeley
Berkeley, CA 94720

Linear conversion occurs when two waves with different polarization (denoted *a*, *b*) have the same frequency ω and wave vector $\mathbf{k}$ at the same position $(\mathbf{x}, t)$ in space-time. When the medium is slowly-varying in four-dimensional space-time, and the coupling between the waves is weak, a finite fraction of wave action-energy-momentum is transferred between the two waves.

The analysis of linear conversion proceeds in two steps, beginning with a Hermitian set of coupled partial differential equations for the N-component wave field. The first step is Friedland's Reduction Algorithm (*L. Friedland and A. N. Kaufman,* Phys. Fluids **30**, 3050, *1987*), a systematic procedure for reducing the set to N=2, while maintaining Hermiticity and conservation of wave action. The second step (*A. N. Kaufman and L. Friedland,* Phys. Lett. **123A**, 387, *1989*) is a metaplectic transformation (*R. G. Littlejohn,* Phys. Reports **138**, 193, *1986*) of wave phase space $(\mathbf{k}, \omega; \mathbf{x}, t)$ in the neighborhood of the intersection of ray *a* with the dispersion surface of wave *b*. This transformation reduces the problem to a simple first-order ordinary differential equation, leading to an analytic expression for the conversion coefficient.

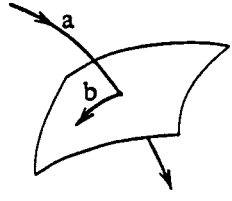

* This work was supported by the U.S. Department of Energy under Contract No. DE-AC03-76SF00098.

H2-2
1420

PARAMETRIC INSTABILITIES IN LASER-PRODUCED PLASMAS*

E. A. Williams
Lawrence Livermore National Laboratory, Livermore, CA 94550

Several parametric processes have been found to be important in the interaction of high intensity ($\gtrsim 10^{14}$ W/cm^2) laser beams with matter, including stimulated Brillouin and Raman scattering and the two plasmon decay instability. In various ways all can be deleterious to the achievement of efficient inertial confinement fusion. After more than a decade of intensive theoretical and experimental study, much has been learned about these processes. The linear theory is well-developed and instability thresholds arising from dissipation and from plasma inhomogeneity have been established. Nonlinear saturation mechanisms have been identified, as have interesting effects from the competition between different instabilities; nevertheless, there remain significant uncertainties in our predictive capability.

* This work was performed under the auspices of the U. S. Department of Energy by the Lawrence Livermore National Laboratory under Contract No. W–7405–Eng–48.

H2-3
1500

PONDEROMOTIVE EFFECTS IN COLLISIONLESS PLASMA

John R. Cary
Department of Astrophysical, Planetary, and Atmospheric Science and Department of Physics
University of Colorado
Boulder, CO 80309-0391

Oscillating electromagnetic forces produce average forces on plasma. To lowest order in the particle velocities, the average force on a particle can be written as the gradient of the *ponderomotive potential.* In this formalism there exists an invariant of the motion: the total ponderomotive energy, which is the sum of kinetic, quiver, and slowly varying electrostatic potential energies. Existence of this invariant simplifies the calculation of ponderomotive equilbria.

The kinetic generalization of the ponderomotive potential is the ponderomotive Hamiltonian [J. R. Cary and A. N. Kaufman, Phys. Fluids **24**, 1238 (1981)]. The ponderomotive Hamiltonian includes the average *velocity-dependent* forces. The ponderomotive Hamiltonian is derived via perturbation theory, in which the lowest-order orbits are those found by neglecting the oscillating fields. That is, the lowest-order orbits are straight lines for unmagnetized plasma, helices for uniform, magnetized plasma, and drift orbits for nonuniform, magnetized plasma.

The ponderomotive Hamiltonian contains, in one function, all of the average particle effects. In addition to the average parallel (to magnetic field) force, it contains the ponderomotive guiding-center drifts and the ponderomotive gyrofrequency shift.

Cary and Kaufman have proven the following theorem: the kernel of the ponderomotive Hamiltonian equals that of the linear susceptibility tensor. Use of this theorem allows one to obtain the ponderomotive Hamiltonian immediately from published formulas for the Vlasov response of a plasma. It also allows one to derive a universal formula for the density depression created by oscillating fields with time-independent amplitudes.

In recent work, we have used adiabatic theory to find the nonlinear generalization of the ponderomotive Hamiltonian. This theory relies on averaging over the orbits that are exact for constant wave amplitude. Such a theory is able to handle resonant particles as well. The trapped and passing particles have different forms for the Hamiltonian. Transitions between the passing and trapped particles are analyzed by separatrix-crossing theory [J. R. Cary, D. F. Escande, J. L. Tennyson, Phys. Rev. A **34**, 4256 (1986); J. R. Cary and R. T. Skodje, Physica D **36**, 287 (1989)].

H2-4
1540

VORTEX STRUCTURES IN MAGNETIZED PLASMAS

W. Horton
Institute for Fusion Studies
The University of Texas at Austin
Austin, Texas 78712

Low frequency convective structures in magnetized plasmas arise from the driving forces of density and temperature gradients (drift waves) and perpendicular electric fields (Kelvin-Helmholtz and current convective instabilities). When the $\mathbf{E} \times \mathbf{B}$ convective nonlinearity is dominant, the system description reduces to pde's with the Jacobian or Poisson bracket nonlinearity $J(\varphi, f) = [\varphi, f] = \mathbf{B} \cdot \nabla\varphi \times \nabla f$ where $\mathbf{E} = -\nabla\varphi(\mathbf{x}, t)$ and f is the density, pressure or charge density. Many examples are found in magnetic confinement systems and in the convective equations for the ionosphere. Slow motion (quasigeostrophic) in rotating fluids obey similar equations and reveal the physical significance of vortex formation, propagation, coalescence and the associated transport.

It is important to recognize that there are two idealized limits for the solution of the convective equations: coherent vortex structures and weakly correlated turbulent fluctuations. For a sufficiently uniform background there are exact, robust dipole vortex solutions that undergo both elastic and inelastic collisions depending on the impact parameter b. The condition for these solitary vortices is that the circulation frequency Ω_E in the vortex exceed the linear wave frequency. At such an amplitude, somewhat above the mixing-length limit, the nonlinearity traps the linear waves forming a long-lived vortex. The presence of sufficient inhomogeneity in the background produces radiation from the vortices leading to their decay.

In contrast when the linear pumping $\gamma_{\mathbf{k}}^{\ell}$ of the system is in the spectral region $S_v(\mathbf{k})\delta(\omega - \mathbf{k}\cdot\mathbf{u})$ of the vortices the solutions change character and are dominated by turbulent fluctuations with $\langle\varphi\varphi\rangle_{\mathbf{k}\omega}$ having a frequency spectrum $(\omega_{\mathbf{k}}^{n\ell}, \nu_{\mathbf{k}}^{n\ell})$ at each $\mathbf{k}$ and power law $I(\mathbf{k}) = \int d\omega \, \langle\varphi\varphi\rangle_{\mathbf{k}\omega} = I_0/k^m$ wavenumber spectrum with $3 \le m \le 8$ for $k > k_1$.

We show examples of these two types of behavior (Horton, *Phys. Fluids* **29**, 1491, 1986) and **B1**, 524, 1989) from the dissipative drift wave system and discuss briefly the relation to the ionosphere convective equations.

H2-5
1640

PHASE SPACE REPRESENTATION FOR ELECTROMAGNETIC WAVES

S.W. McDonald
Berkeley Research Associates
PO Box 241
Berkeley, CA 94701

The propagation of short-wavelength electromagnetic waves in a non-uniform medium is often treated with the eikonal (or geometrical optics) approximation. In the conventional approach, the wave phase and amplitude are evolved along ray trajectories in physical space (or **x**-*space*) generated by the gradient of the local index of refraction. Construction of the wave by this method fails in regions where the ray paths converge or focus; in the vicinity of these *caustics*, the eikonal prescription produces singularities in the wave amplitude.

It is crucial to recognize that the paths of the rays in **x**-space are the *projection* of trajectories in the ray *phase space*; this space consists of both the position **x** *and* the wave vector **k** (the "momentum" conjugate to **x**). The trajectories in this phase space are governed by Hamilton's equations of classical mechanics, with the local dispersion relation $\omega = \Omega(\mathbf{x}, \mathbf{k})$ playing the role of the Hamiltonian. An important feature of these trajectories in phase space is that they do not focus. It would seem natural then, that a representation of the wave defined and constructed in the ray phase space would not suffer the singularity difficulties associated with caustics in **x**-space.

In this paper we shall define a phase space representation (S.W. McDonald, *Physics Reports* **158**, 337, 1988) of an electromagnetic wave field (the local spectral density) based on the Wigner-Weyl correspondence formalism (E.P. Wigner, *Phys. Rev.* **40**, 749, 1932). Using this technique, the exact equation which governs the evolution of the wave in phase space is derived (based on the underlying wave equation in **x**-space). This equation is then treated in the short-wavelength approximation with ordering assumptions consistent with the conventional eikonal method; the result is the wave kinetic equation for the wave action density $J(\mathbf{x}, \mathbf{k}; t)$ (S.W. McDonald and A.N. Kaufman, *Phys. Rev.* **A32**, 1708, 1985). The solution of this equation using the phase space ray trajectories does not encounter singularities, so that the wave on **x**-space (constructed from J by well-defined projection rules) is finite, even in caustic regions. The use of this technique is demonstrated with numerical examples.

H2-6
1720

CAVITON DYNAMICS IN STRONG LANGMUIR TURBULENCE*

Don DuBois, Harvey A. Rose and David Russell
Theoretical Division and Center for Nonlinear Studies**
Los Alamos National Laboratory, Los Alamos, NM, 87545

Recent studies based on long time computer simulations of Langmuir turbulence as described by Zakharov's model will be reviewed. These show that for strong to moderate ion sound damping the turbulent energy is dominantly in nonlinear "caviton" excitations which are localized in space and time. A local caviton model will be presented which accounts for the nucleation-collapse-burnout cycles of individual cavitons as well as their space-time correlations. This model is in detailed agreement with many features of the electron density fluctuation spectra in the ionosphere modified by powerful HF waves as measured by incoherent scatter radar. Recently such observations have verified a prediction of the theory that "free" Langmiur waves are emitted in the caviton collapse process. These observations and theoretical considerations also strongly imply that cavitons in the heated ionosphere, under certain conditions, evolve to states in which they are ordered in space and time. The sensitivity of the high frequency Langmuir field dynamics to the low frequency ion density fluctuations and the related caviton nucleation process will be discussed.

**Research supported by USDOE.

J1-9
1340

THE D.R.A.O. RADIO SCHMIDT TELESCOPE PROPOSAL

The Staff of the Dominion Radio Astrophysical Observatory, National Research Council of Canada, Penticton, B.C., Canada
Presented by T.L. Landecker

There is a scientific need for a telescope which extends the capability of the world's largest single-antenna radio telescopes to higher resolution without significantly sacrificing sensitivity to diffuse emission. An extension of this kind to a fast, sensitive telescope operating at a selection of wavelengths would open up investigations into a wide variety of astrophysical problems. The aperture synthesis technique is the only method capable of delivering the required combination of resolution and sensitivity to fill this need because it allows the collecting area of a telescope and its angular resolution to be independently chosen. In contrast, with single antennas these two factors are inseparably coupled together. Recent advances in the technology of low-noise receivers, optical fibre transmission lines, digital electronics and digital computers allow us for the first time to realistically contemplate the design of an aperture synthesis telescope consisting of a large number of small antennas.

As the basis for discussion, we consider a telescope with the following parameters:

- 100 antennas of diameter 12m in an array about 2 km in extent
- observing capability at 0.4, 1.4/1.6, and 5 GHz, with possible later extension as high as 25 GHz
- continuum and spectral line modes of operation
- full polarimetry capability.

This telescope would be characterized by wide field of view, high sensitivity and excellent dynamic range. Its wide frequency range and high sensitivity would allow mapping of the atomic (HI line), molecular (OH, H_2CO lines), ionized (continuum and recombination line), and relativistic (continuum and polarized continuum) components of the interstellar medium. These attributes would make the telescope widely applicable in galactic and extragalactic astrophysics. The large number of antennas would allow fast imaging for application to solar studies and to variable source work. The large collecting area would make the telescope a powerful VLBI node.

Some typical parameters illustrate these applications. The telescope would be able to map a 1.5 degree field at 21cm wavelength with a continuum sensitivity to extended structure of 57 mK in 1 hour, and would have a sensitivity to unresolved sources of 26 microJy in 1 hour or 0.2 mJy in 1 minute. In a spectral line channel of 10 kHz, sensitivity would be 4K in 1 hour or 1.1K in 12 hours. Resolution would be about 70, 20, and 6 arcseconds at 0.4, 1.5, and 5 GHz.

A Workshop was held in Penticton in October 1989 to discuss the interplay of the scientific objectives and design parameters of the telescope.

J1-10
1400

RECENT ADVANCES IN CRYOGENICALLY-COOLED AMPLIFIERS AND RECEIVERS FOR 1 TO 50 GHZ RANGE

Marian W. Pospieszalski
National Radio Astronomy Observatory*
2015 Ivy Road
Charlottesville, VA 22903

This paper reviews the recent developments in the design, construction and performance of cryogenically coolable, high-electron-mobility transistor (HEMT, MODFET) amplifiers and their application in compact cryogenic receivers for radio astronomy applications.

A simple noise model of a microwave MESFET (MODFET, HEMT) is described (M. W. Pospieszalski, *IEEE Trans. Microwave Theory Tech.*, MTT-37, pp. 1340-1350, 1989) which allows the prediction of noise parameters for a broad frequency range from a single frequency noise parameter measurement. The model is used to study the cryogenic performance of commercially-available and developmental devices in the 1 to 100 GHz range. The state-of-the-art performance and future trends are assessed.

A design technique for low-noise amplifiers using HEMT's is discussed. It is illustrated with the design of amplifiers of moderate (~ 10%) and very wide (octave or more) bandwidth. The specific examples include X-, K_u-, K-, K_a-, and V-band amplifiers as well as a wideband 8 to 18 GHz amplifier.

The construction and performance of a number of receivers built for radio astronomy applications (VLBA, VLA) using state-of-the-art amplifiers and closed-cycle 13 K refrigerators are described (S. Weinreb, M. W. Pospieszalski, R. Norrod, *Proc. 1988 Int. Microwave Symp.*, pp. 945-948, 1988). Examples include an X-band receiver (10.5 K at 8.4 GHz) and a K-band receiver (27 K at 23 GHz), as well as the expected performance of K_a-band and V-band receivers.

---

*The National Radio Astronomy Observatory is operated by Associated Universities, Inc. under Cooperative Agreement with the National Science Foundation.

J1-11
1420

VLBA CONTROL AND MONITOR SYSTEM

B. G. Clark and D. S. Bagri
VLA/NRAO
Socorro, NM 87801-0387

VLBA control and monitor system is required to control the operation of remotely located telescopes and monitor their performance. For this purpose a central control computer located at the Array Operations Center in Socorro, NM, is linked by digital communication links to a small computer at each telescope site. All the equipment at each station is connected to the station computer through a fast serial communication bus. Most of the station equipment is able to interface to the bus through a "Standard interface", developed for this purpose.

The array control computer is a SUN-3 with some functions in a DEC Micro-Vax II computer. Each station computer is a Motorola 68010 microprocessor with a second 68010 used in a dedicated coprocessor configuration to move the serial control/monitor bus intrastation communications. Communication between the central computer and a station computer is (presently) using telephone lines.

The array control computer is used for planning and generating observing requests which are communicated to concerned station computers. In addition, it is used for real time fringe check, and managing monitor data, tape inventory, and maintenance records. A station computer (1) organizes observation request for a new source, (2) sets up the station equipment, (3) controls the antenna, (4) manages the tape system, and (5) acquires the monitor data, checks the equipment performance, flags bad data, and informs (operator) about malfunctioning of any equipment. The monitor data is stored in the station computer and later transferred to the array control computer. In addition, there are a number of user-interface screens, which can be operated from either the central computer or a station computer for on-line display of the monitor data or control of the hardware for debugging/fault finding. The monitor information required for correlated the observed data and post processing of visibility is generated from the monitor data base in the central computer. This paper briefly describes the hardware and an overview of the software.

J1-12 A MODERN RADIO TELESCOPE CONTROL SYSTEM
1440

D. T. Emerson
National Radio Astronomy Observatory
949 N. Cherry Avenue, Campus Building 65
Tucson, Arizona 85721-0655

The control system of the NRAO 12m mm-wave radio telescope at Kitt Peak is being replaced. The new system is extremely modular, both in hardware and software, which leads to reduced development time, easier maintenance and greater versatility. All time-critical operations are performed in satellite micro-processors, controlled by the central control computer, but with minimal coupling between the modules. The key to the new system is the bus network; there are physically separate command, data, time and status buses. Standard interfaces are used wherever possible, to minimize the need for special purpose hardware or software drivers.

The new system is expected to be in operation at the 12m in early 1990. The control system planned for the new Green Bank radio telescope is to be modeled after this new 12m design.

J1-13 HYBRID ANALOG-DIGITAL CORRELATORS
1500

Jon Hagen
National Astronomy & Ionosphere Center
NAIC Lab, 124 Maple Ave
Ithaca, NY 14850

Two designs are presented for correlator elements in which an analog signal is multiplied by a one-bit digital signal. Standard applications for such an element are pulse compression of a phase-coded radar signal where each element decodes one range and autocorrelation spectrometry where the one-bit x analog multiplier produces an undistorted estimate of the correlation function.

A single SPST analog switch provides 4-quadrant multiplication. Present day MOS devices can switch at rates in excess of 10 MHz. It is pointed out that designs based on 1-quadrant or 2-quadrant multipliers acheive very low signal-to-noise ratios.

In the first design, all integration is done in a standard op-amp integrator. The second design replaces the op-amp with a V-to-F converter which acts as a prescaler. Subsequent integration is done in a digital counter. For pulsar or radar observations, a simple circuit using maximal length shift register sequences can provide a multichannel counter for each correlator element.

J1-14
1540

THE HAYSTACK WIDEBAND SPECTROMETER

J. I. Levine, Staff Member
Haystack Observatory
Westford, Mass. 01886

A digital autocorrelation spectrometer is now being constructed at the Haystack Observatory. Signal rates up to 640 megasamples/second will be processed in real time.

The system uses 256 semi-custom gate array chips, contained on 4 multilayer printed circuit modules. Both the gate arrays and the correlator modules were designed at the Netherlands Foundation for Radio Astronomy, Dwingeloo, The Netherlands.

Each of the 4 system modules processes signals at up to 40 megasamples/second and yields a 1024 point autocorrelation function. At higher rates, samples are processed 2,4,8, or 16 at a time (with a corresponding reduction in the number of output points).

Five video and A/D converters supply input to the correlator system. The 5 signal channels are completely independent and can be tuned to different frequency bands, limited only by the digital processing hardware. Numerous signal configurations are possible under software control.

System setup, control, smoothing and transform functions are performed in an off-the-shelf PC/AT type personal computer. A commercial VME to PC bus translator maps the special purpose correlator hardware into the PC's address space and allows control of the spectrometer using standard operating systems and software. An IEEE-488 interface links the spectrometer to the station pointing computer.

The Wideband Spectrometer is scheduled for operations in the first quarter of 1990. It will replace the existing 1024 channel unit, in use since 1974.

J1-15 REAL TIME COHERENT DEDISPERSION OF PULSAR SIGNALS
1600

M.F. Ryba
Department of Physics
Princeton University
Princeton, NJ 08544

The interstellar medium disperses the rapidly varying signals of radio pulsars, introducing a sweep in pulse arrival time that is roughly linear over a small fractional bandwidth (typically 10^{-3}). This sweep in arrival time across a typical bandpass limits timing resolution necessary for high-accuracy timing of pulsars and masks any short time scale phenomena that may be of importance to understanding the emission mechanism. To compensate for this effect, the baseband signal can be sampled and the frequency components delayed appropriately to reconstruct the signal as it was emitted. We have constructed hardware that dedisperses in real time using a CCD transversal filter, and present results obtained using it.

The input signal is mixed to yield baseband in-phase and quadrature components (real and imaginary parts of complex signal) which are then sampled at Nyquist frequency. The CCD then performs a complex convolution with a "chirp" waveform, equivalent to a linear sweep in frequency. The analog convolution is done in a pipeline manner to achieve real time performance. This operation corresponds to the inverse of the impulse response of the interstellar medium. The dedispersed complex signal can then be detected via ordinary means.

J1-16
1620

RFI COUNTERMEASURES

Ivan R. Linscott, and Allen M. Peterson
Center for Radar Astronomy
Stanford University, Stanford, CA 94305
Michael D. Cousins
Geophyics Research Laboratory
SRI International, Menlo Park, CA

The growth of RFI (Radio Frequency Interference), has become so severe that Radio Astronomy is no longer practical on SRI's 150-foot antenna in Stanford, CA. Dissatisfied with this situation we have developed a method to scrub out most RFI and obtain RFI-free bandwidths at L-band. We were led to this method having first surveyed RFI at this site and found that most of the RFI could be classified according to a bandpass filter model, i.e. RFI artifacts in this class were matched using an FIR filter with suitable bandwidth centered on the artifact. This class of RFI can thus be filtered out by processing an initial broadband signal into successively higher frequency resolution bands using a cascade of bandpass filters. Each RFI artifact in this class is then well matched at just one level and only one channel in this cascade, where the artifact is excised. Larger bandwidths are then synthesized from the cleaned, narrowband filter channels. A digital spectrometer implementation of this method, that incorporates VLSI signal processing engines, is expected to support radio frequency bandwidths of up to 100 MHz and practical Radio Astronomy on the 150-foot antenna.

J1-17
1640

INTERFERENCE PERFORMANCE OF A DIGITAL FFT SPECTRAL PROCESSOR

J.R.Fisher, NRAO
Green Bank, WV 24944

Initial measurements with a 1024-channel, 16-bit FFT spectrometer confirm its predicted spectral dynamic range of greater than 45 dB and its ability to handle narrow band signals stronger than the broadband noise power. Input taper functions can be optimized for best trade-off between sensitivity and spectral purity, and two FFT spectra can be offset in time to recover nearly all of the signal loss from input tapering. Real-time signal blanking has proven effective on low duty cycle impulsive noise such as lightning.

This spectrometer has been used for pulsar timing and flux density measurements with time resolutions down to 12.8 microseconds and timing accuracy better than 1 microsecond on millisecond pulsars set by radiometer signal to noise ratio.

Thursday Morning, 4 January, 0830-1200

0830-Thurs. Muenzinger Psychology E050
PLENARY SESSION

1990 URSI STUDENT PRIZE PAPER CONTEST FINALISTS:

ANALYSIS OF GENERALIZED MULTILAYER PRINTED ANTENNAS: Nirod K. Das, 14 Marcus Hall, Dept. of Electrical and Computer Engineering, Univ. of Massachusetts, Amherst, MA 01003

ELECTROMAGNETIC SCATTERING FROM MULTIPLE CYLINDERS USING THE BYMOMENT METHOD: Robert Lee, Electrical and Computer Engineering, Univ. of Arizona, Tucson, AZ 85721

PROPAGATION AND DEPOLARIZATION OF AN ARBITRARILY POLARIZED WAVE OBLIQUELY INCIDENT ON A SLAB OF RANDOM MEDIA: Qinglin Ma, Dept. of Electrical Engineering, Univ. of Washington, Seattle, WA 98195

Thursday Afternoon, 4 January, 1355-1700

Session A-2 1355-Thurs. CR1-42
BROADBAND EM METROLOGY
Chairman: D.F. Wait, Electromagnetic Fields Division, National Institute of Standards and Technology, Boulder, CO

A2-1
1400 THE NIST AUTOMATED NOISE COMPARISON RADIOMETER

J. W. Allen
Electromagnetic Fields Division
National Institute of Standards and Technology
Boulder, Colorado 80303

Development of new microwave systems and technology requires consistent, NIST traceable measurements of noise performance. In order to meet this need, NIST has developed a new family of automated, total power radiometers which incorporate a new advanced, single 6-port ANA, and a modular, radiometer independent software package. This new design, operating with a nominal 100 MHz bandwidth, has an effective input noise temperature of 500 Kelvins, a typical resolution of 30 Kelvins, and decreased sensitivity to vibration as well as to changes in the ambient temperature.

The focus of this presentation will be on the design of this system. Its overall operation and performance, and its flexibility for making through adapter and MMIC measurements.

A2-2 **SENSITIVITY OF MULTI-FREQUENCY RADIOMETERS**
1420 **WITH VARIOUS LOCAL OSCILLATOR DESIGNS**

J.R. Jordan
Wave Propagation Laboratory, NOAA
325 Broadway, R/E/WP5
Boulder, CO 80303

The Wave Propagation Laboratory (WPL) uses multi-frequency radiometers to derive atmospheric temperature and humidity profiles, cloud liquid, precipitable water vapor, and pressure heights. These radiometers are constructed using an automatic-gain-control (AGC) Dicke design (F.O. Guiraud, et al., IEEE Trans. Geosci. Electron., 129-136, 1979) that utilizes two known temperature terminations to maximize long term stability. Due to the high cost of millimeter-wave components, radiometer designs that share hardware by time multiplexing frequencies have been used. These shared mixer designs require a switchable local oscillator (LO) design to select the different operating frequencies. Four techniques have been employed or suggested for the LO in multi-frequency radiometers, both shared and non-shared designs. Each technique degrades the sensitivity relative to a total power radiometer since some portion of the averaging time is not spent viewing the atmosphere.

Separate Oscillators technique utilizes a complete set of hardware for each frequency. The AGC corrected Dicke design views the atmosphere and two terminations one third of the time; therefore, the sensitivity is degraded by the square root of three.

Individually Powered Oscillators allows several frequencies to share a mixer; however, time is required to stabilize each time the frequency is switched. The sensitivity for this design is degraded by the square root of the settling time, plus the time spent viewing the calibration terminations times the number of shared channels.

Switched Oscillators places a switch between the multiple oscillators and the mixer to eliminate the settling time. This improves the above sensitivity to be the square root of the time viewing the calibration terminations times the number of shared channels.

Resonant Cavitys can be used as feedback elements to tune an oscillator to multiple operating frequencies. The sensitivity of this design is degraded by the square root of the switching time plus the time viewing the calibration terminations times the number of shared channels.

Of the four techniques, separate oscillators provides the best sensitivity but suffers from high cost. Individually powered oscillators is the least expensive alternative; however, the long settling times required seriously degrade the sensitivity. Switching between oscillators eliminates the settling time but the added cost of the microwave switches is undesirable. Cavity stabilized oscillators may prove to be an inexpensive alternative but a prototype has not been built and tested.

A2-3
1440

"MINIMAL" BROADBAND RADIOMETER

Sunchana Perera
Electromagnetic Fields Division
National Institute of Standards and Technology
Boulder, Colorado 80303

A new, relatively inexpensive, manual radiometer has been designed at the National Institute of Standards and Technology (NIST). This radiometer has been used to measure unknown noise sources with either primary cryogenic noise standards or calibrated working standards with comparable accuracy.

The radiometer is a total power, heterodyne (double sideband) instrument, relying on a precision waveguide-below-cutoff attenuator for its null-balancing operation. Presently it operates between 2.0 and 12.0 GHz. The frequency range can be easily extended at both ends. Its sensitivity is about 3 K. In order to measure the input mismatches, access to a vector network analyzer is needed. The radiometer is manual: the switching at the input and the attenuator adjustment are done by the operator. The output device is a strip-chart recorder. Software written for a personal computer speeds up data analysis.

Fitting into a standard instrument rack, the radiometer is designed entirely with commercially available components, at a total cost of approximately $20,000 (excluding a local oscillator). This radiometer can play a useful role as a standards laboratory instrument.

A2-4
1520

A DUAL TUNER APPROACH TO ENHANCING THE ACCURACY OF DEVICE NOISE CHARACTERIZATION

William E. Pastori
Maury Microwave Corporation
8610 Helms Avenue
Cucamonga, California 91730

In measurements of the noise parameters of a microwave device, the high output reflection coefficient of a device under test will significantly increase the noise figure of the noise measurement receiver which, in turn, degrades measurement uncertainty. This paper describes a system which uses a second tuner to reduce second stage noise figure and, thus improve measurement uncertainty relative to the more common set-ups and details a simple means of detecting and avoiding test device oscillations due to simultaneous source and load tuning.

A2-5
1540

LOW LOSS ADAPTER MEASUREMENTS

John R. Juroshek
NIST
325 Broadway
Boulder, CO 80302

Measuring the S-parameters of adapters is a difficult problem particularly when those adapters are of mixed connector types such as GPC-7 to 3.5 mm. Network analyzers are usually designed to measure S-parameters for devices with the same connector type. For accurate S-parameter measurements, it is generally desireable to have connectable test ports on the network analyzer so that a thru connection can be made. The thru connection, if available, can be used to establish the zero reference for S_{12}. None of these conditions can be satisfied with most adapter measurements.

This talk describes some of the problems of measuring low loss adapters. Some of the tradeoffs and limitations to making accurate adapter measurements are described. Examples are presented showing adapter measurements that were made at NIST on the dual Six-Port network analyzer. These adapter measurements were used to establish 3.5 mm power standards.

A2-6
1600

IMPROVED TECHNIQUE FOR PERMITTIVITY DETERMINATION USING TRANSMISSION/REFLECTION METHODS

James Baker-Jarvis
National Institute of Standards and Technology
Boulder, Colorado 80303

The transmission/reflection and short-circuit line methods for complex permittivity and permeability determination are examined. Equations for permittivity are developed from first principles. The special case of permittivity measurement is examined in detail. New robust algorithms are presented that eliminate the ill-behaved nature of the commonly-used transmission/reflection procedures at frequencies corresponding to integer multiples of one-half wavelength in the sample. An error analysis is presented which yields estimates of the errors incurred due to the uncertainty in scattering parameters, length measurement and reference-plane position. New equations are presented for determining complex permittivity independent of reference-plane position and sample length.

A2-7
1620

DYNAMIC CALIBRATION OF OSCILLOSCOPES AND WAVEFORM RECORDERS USING PULSE STANDARDS

W.L. Gans
Electromagnetic Fields Division
National Inst. of Standards and Technology
325 Broadway
Boulder, Colorado 80303

Norris S. Nahman
Picosecond Pulse Labs, Inc
P.O. Box 44
Boulder, Colorado 80306

Historically, most users of oscilloscopes calibrated the vertical channel dynamic response by simply measuring the (high) frequency at which the displayed amplitude of a sinewave was reduced by 3 dB compared to the displayed amplitude at some low frequency. Knowing this oscilloscope "bandwidth", however, is not sufficient if one wishes to measure the shape of any non-sinusoidal waveform to within a reasonable accuracy. In order to have some confidence that the pulse waveform shape displayed on the screen is close to the shape of the actual pulse being measured, it is necessary to know the entire transfer function, H(jw), of the vertical channel (or, equivalently, the vertical channel's time domain impulse response.)

In this presentation we will first show some actual measured waveforms obtained from measuring the same pulse on different oscilloscopes and waveform recorders in order to indicate the wide range of (differing) waveform shapes that may be observed. We will then discuss a methodology for calibrating the dynamic response of an oscilloscope or waveform recorder that employs pulse generator standards. This methodology allows one to measure the oscilloscope's vertical channel transfer function, deconvolve its distorting effects, and thus improve the accuracy of the measurement. Equally important, we will also discuss the recently developed tools that now make this methodology possible when the application requires it.

Session B-4 1355-Thurs. CR2-28
EM THEORY II
Chairman: A. Cangellaris, Dept. of Electrical Engineering,
Univ. of Arizona, Tucson, AZ 85721

B4-1
1400

DYADIC GREEN'S FUNCTIONS FOR A CHIRAL SPHERE

Nader Engheta
The Moore School of Electrical Engineering
University of Pennsylvania
Philadelphia, Pennsylvania 19104
and
Marek W. Kowarz
The Institute of Optics
University of Rochester
Rochester, New York 14627

Chirality, which refers to the handedness of an object or a medium, has played an important role in a variety of fields including chemistry, optics, particle physics and mathematics. *Electromagnetic chirality* represents the role of chirality in electromagnetics and is exhibited in a class of materials called chiral materials. Owing to the handed nature of their constituents, these materials themselves possess an intrinsic handedness. For the time harmonic and isotropic case, they are characterized electromagnetically by the set of constitutive relations $\mathbf{D}=\varepsilon_c\mathbf{E}+i\xi_c\mathbf{B}$ and $\mathbf{H}=i\xi_c\mathbf{E}+\mathbf{B}/\mu_c$ where ε_c, μ_c, and ξ_c are, respectively, the permittivity, permeability and chirality admittance of such media. We have shown that electromagnetic waves in these media display two unequal characteristic wavenumbers for the right- and left-circularly polarized (RCP, LCP) eigenmodes. These give rise to a circular birefringence which results in both optical activity and circular dichroism.

In this talk, the dyadic Green's functions for a sphere of finite radius made from an isotropic lossless chiral material are presented and the interaction of radiation emitted by an electromagnetic source with such a sphere is analyzed. Two cases are considered: (1) the source placed at the interior of the chiral sphere and (2) the source located outside the sphere. For both cases, using an exact formulation, the dyadic Green's functions are derived and expressed in terms of the appropriately defined spherical vector wave functions. As an illustrative example, a short electric dipole located at the center of the chiral sphere is studied in detail, and the characteristics of radiated fields and radiation resistance are examined. We show that, in this case, the dipole's radiated fields in the far zone are, in general, elliptically polarized. Furthermore, by choosing the sphere's size and material parameters properly, circular polarization may be obtained. We also demonstrate that the radiation resistance of the dipole depends on the sphere's size and increases monotonically with chirality parameter ξ_c. The motivation behind the present investigation and its potential applications to novel radome designs, spherical lenses for microwave, millimeter-wave and optical regimes, and multipolarized antennas with polarization control are also mentioned.

B4-2
1420

GENERALIZED WKB APPROXIMATION IN CHIRAL STRATIFIED MEDIA

I.V. Lindell, A.H. Sihvola
Electromagnetics Laboratory
Helsinki University of Technology
Otakaari 5A, Espoo SF-02150 FINLAND

The WKB method and its generalization, well known approximate methods for one-dimensional wave propagation and reflection computations in problems involving achiral stratified media, is shown to be extendable to stratified chiral media for waves with normal incidence. The method is based on an expansion in wave fields: certain combinations of the electric and magnetic fields, whose properties are also discussed in the paper. It is seen that for sufficiently slowly varying media, the zeroth-order WKB method gives the propagating field, consisting of two wave fields with two phase velocities, and the first-order WKB method gives the resulting two reflected wave fields.

Applying the present first-order WKB method, an analytic expression for the reflection dyadic due to the stratification is obtained in closed integral form. The method can be further extended for chiral media to what is called the Bremmer series method for achiral media. The present paper applies the following representation of the constitutive equations:

$$\mathbf{D} = \epsilon \mathbf{E} - j\kappa\sqrt{\epsilon_o \mu_o}\mathbf{H},$$

$$\mathbf{B} = \mu \mathbf{H} + j\kappa\sqrt{\epsilon_o \mu_o}\mathbf{E},$$

which has the advantage that the impedances of the wave fields are the same $\eta = \sqrt{\mu/\epsilon}$ as for the corresponding achiral medium. Thus, reflection coefficients turn out to be independent of the chirality parameter κ and the effect of chirality is mainly to change the polarization of the propagating and reflecting wave.

B4-3
1440

GEOMETRICAL OPTICS APPROXIMATION IN CHIRAL MEDIA WITH APPLICATION TO LENS ANTENNAS

I.V. Lindell, A.H. Sihvola, A.J. Viitanen
Electromagnetics Laboratory
Helsinki University of Technology
Otakaari 5A, Espoo SF-02150 FINLAND

Wave propagation in inhomogeneous chiral media is considered by decomposing the electromagnetic fields in two *wave fields*, which do not couple energy to one another in homogeneous chiral media. When the inhomogeneity is slow enough, the coupling between the wave fields can be neglected, which leads to simple geometrical optics equations with distinct rays for the two wave fields. With the additional assumption of small chirality, it can be seen that the effect of the chirality to the paths of the two geometrical optics rays is negligeable and they actually coincide. Thus, the main effect of chirality is to add a different phase shift to the two wave fields, which is seen as a change of polarization of the total geometrical optics field. This can be used in advantage to correct the polarization rotation due to the curvature of the rays and, thus, obtain an extra parameter in the design of lens antennas. Because it is the integral of the chirality parameter that affects the polarization rotation, the chirality can be distributed in infinitely many ways along the rays.

In the present study, an analysis is made to correct the cross polarization of radially inhomogeneous lens antennas for a dipole as the feed element. The method is applied to Maxwell's and Luneburg's lenses resulting in different examples of distributions for the chirality function. For example, for the Maxwell lens a distribution function is obtained with a simple analytic expression but a singularity at the feed point and another one with no singularity but a more complicated analytic expression. Also, the polarization of the Eaton lens can be corrected through a suitable chirality distribution in the lens.

B4-4
1500

COMPLEX EIGENFREQUENCIES OF DISPERSIVE DIELECTRIC CYLINDERS AND THE RELATIONSHIP TO SURFACE WAVES

Douglas J. Taylor and Herbert Überall
Department of Physics
The Catholic University of America
Washington, D.C. 20064

ABSTRACT

The complex electromagnetic eigenfrequencies for dielectric cylinders are found by numerically searching for poles in the series solution coefficients for infinite dielectric cylinders. A physical interpretation of the resonances in terms of surface waves has been developed to understand the phenomena. Phase velocities of these surface waves are computed from the real portions of the complex resonance frequency. The effect of a physically realizable dielectric dispersion, using simple models obeying Kramers-Kronig relations, on the complex resonances and the surface wave phase velocities is studied. The asymptotic properties of the complex resonances, in terms of large frequency and mode order, are mathematically derived and the asymptotic values of surface wave phase velocities are shown to agree with numerical results and intuition. The extension of these results for isotropic dielectric materials to cylindrically symmetric anisotropic materials having dielectric permittivities,

$$\epsilon_\rho = \epsilon_1$$

$$\epsilon_\phi = \epsilon_z = \epsilon_2$$

is discussed.

Jan 1990 Nat. Radio Science Meet.

B4-5
1520

DUAL-SHAPED OFFSET SYNTHESIS USING PARAMETER OPTIMIZATION OF THE SOLUTIONS TO THE FIRST ORDER GEOMETRICAL OPTICS PARTIAL DIFFERENTIAL EQUATIONS*

K. Shogen & R. Mittra
University of Illinois
Urbana, IL 61801

V. Galindo-Israel & W. Imbriale
JPL, California Institute of Technology
Pasadena, CA 91109

When integrating the geometrical optics derived non-linear partial differential equations (PDE's) for offset dual-shaped reflector synthesis from a prescribed outer projected perimeter *inwards*, it was found earlier that computational problems do arise in the central region of the reflectors. It was also found that these computational problems can be largely bypassed if the integration of the PDE's is started from a prescribed *inner* rim and integrated *outward*. In this case, however, a circular, or otherwise prescribed, *outer* rim is not guaranteed. In addition, a new parameter of the PDE's is introduced, the radius, ρ_0, of the inner projected rim of the main reflector when the inner value of $\theta = \theta_0$ for the subreflector is prescribed. This parameter exists in addition to other initial parameters of the dual reflector system.

A poorly selected inner radius parameter ρ_0, or other poorly selected initial parameters can preclude the obtaining of useful solutions to the first-order PDE's by the methods discussed earlier. Two complementary methods for choosing the parameter ρ_0 and other parameters will be discussed.

The first method utilizes the initial values found from an approximate solution to the PDE's. A second method utilizes an optimization algorithm which searches for the parameters of the PDE's which minimize a prescribed object function. Such an object function may measure the deviation of the projected outer perimeter from circular (or some other desired shape). Alternatively, a minimum cross-pol distribution in the aperture (optimum mapping function) may be chosen as the object function.

An offset dual-shaped Cassegrainian type high gain antenna is synthesized to illustrate the first method described above. The second method of optimization is illustrated by synthesizing a Gregorian low noise/high gain offset dual-shaped reflector antenna. One parameter (ρ_0), two parameter (ρ_0 and a parameter A_ψ describing the arbitrary initial function ψ_{ϕ_0}), and three parameter (ρ_0, A_ψ, and Ω-tilt angle of subreflector) optimizations are illustrated.

*The listing order of the authors is arbitrary.

B4-6
1540

CONVERGENCE OF OPEN PORT CURRENTS IN THE MODIFIED DIAKOPTIC THEORY

David F. Taylor and Chalmers M. Butler
Department of Electrical and Computer Engineering
Clemson University, Clemson, SC 29634-0915

The utility of the modified diakoptic theory for the analysis of curved thin-wire antennas has been demonstrated [*Proc.*, 1989 URSI EMT Symposium, Stockholm, pp. 349-401, August, 1989]. For antennas of this type the first order approximation of open-port currents yields satisfactory results. In some cases involving thicker wires, however, this approximation is not sufficient.

For this reason, a systematic calculation of higher order open-port currents has been devised for improved approximation. The first order diakoptic current is calculated as outlined in the above reference, and then this current is treated as an independent source exciting a secondary current on each of the wire segments in the structure. The sum total of induced currents calculated in this manner apparently converges to the "true" open-port current on the structure, thus allowing the approximation error to be made arbitrarily small.

After each iteration of this process, the choice of whether or not to perform an additional step must be made. Ideally, the decision should be made on the basis of some measure of the accuracy of the total approximate open-port current and not on the relationship between two successive approximations. To that end, an error criterion ratio, $|\mathbf{E}_{tan}/\mathbf{E}_{normal}|$ (due to the total calculated current), is determined. This ratio is zero for the "correct" current on the diakopted wire structure. The actual value of the error is significant. If a particular accuracy of solution is desired, an approximate upper limit on this ratio can be determined.

Use of this error ratio as an indicator of the accuracy of approximate open-port current distribution has been tested for a range of values of the ratio. The approximate open-port current distribution is then used to determine an open-port impedance matrix from which the currents on the antenna (at the open-port locations) can be calculated. The error in the final antenna currents calculated from the diakoptic theory depends on the error ratio used in computation of the approximate open-port currents, not on the geometry of the antenna. Results are demonstrated for a number of examples.

B4-7
1600

A PRELIMINARY INVESTIGATION INTO THE EXTENSION OF LS-DECOMPOSITION TO ACCOUNT FOR A CONDUCTING HALF-SPACE

T. L. Simpson
Electrical and Computer Engineering Dept.
University of South Carolina, Columbia, SC 29208

R. C. Robertson
Electrical and Computer Engineering Dept., Code 62RC
Naval Postgraduate School, Monterey, CA 93943

The procedure referred to as LS-decomposition has been shown to be an effective method for efficiently computing the elements of the impedance matrix when antenna structures are evaluated using moment method techniques (Simpson, Logan, and Rockway, URSI Abstracts, 356, June, 1988). In addition, antenna terminal impedance is easily obtained as a byproduct of LS-decomposition. In LS-decomposition the impedance matrix is expressed as

$$[Z] = j\omega[L] + \frac{1}{j\omega}[S] + \omega^2[Z_r] \tag{1}$$

where $[L]$ is an inductance matrix, $[S]$ is an elastance matrix, and $[Z_r]$ is the residual matrix. The inductance and elastance matrices are real and independent of frequency, and in the quasi-static limit the residual matrix is a real, frequency independent matrix.

In this paper the extension of LS-decompostion to take into account the effect of an infinite conducting half-space will be examined. This extension will allow the efficient evaluation of antenna structures operating in the proximity of the earth and the sea at low frequencies. In this preliminary study, a vertical dipole above a conducting half-space will be considered. For this case, the quasi-static Green's function is

$$G(\vec{r}|\vec{r}') \approx \frac{1}{4\pi}\left(\frac{e^{-j\beta R_1}}{R_1} + \frac{e^{-j\beta R_2}}{R_2} - j2\omega\epsilon_0\frac{1}{\sigma R_2}\right) \tag{2}$$

where $R_1 = \sqrt{(x-x')^2 + (y-y')^2 + (z \mp d)^2}$, d is the source point elevation, $\beta = \omega\sqrt{\mu_0\epsilon_0}$, and σ is the conductivity of the conducting half-space. This approximate Green's function is exact in the limit as $\omega \to 0$.

Numerical results are obtained over a band of frequencies and compared to results obtained by other techniques.

B4-8
1620

ELECTROMAGNETIC RESPONSE OF TWO CROSSING, INFINITELY LONG, THIN WIRES.

J. L. Young
J. R. Wait
Electromagnetics Laboratory
ECE, Building 104
University of Arizona
Tucson, AZ 85721, USA

The electromagnetic response of two infinitely long, mutually perpendicular, thin wires will be considered. By applying Fourier spectral transform techniques, we derive a set of coupled integral equations for the general case when the wires are over a lossy half space; the unknowns are the spectral currents flowing on each wire. The equations are given in terms of self and mutual impedance functions and generalized source functions.

Two methods are employed to determine the spectral current functions. The first relies on collocation moment method techniques; the second, employs the method of multiple scatterers such that the zeroth order, first order and higher order terms are considered. We show explicitly that the two methods yield the same results for the leading terms. In either case, once the spectral current functions are determined, we may obtain the spatial currents flowing on each wire by applying fast Fourier transform algorithms.

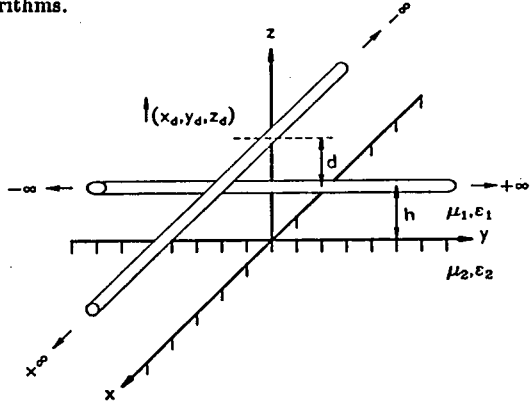

B4-9
1640

ASYMPTOTIC EXPANSION OF EIGENMODE-EXPANSION PARAMETERS IN THE COMPLEX-FREQUENCY PLANE

C. E. Baum
Weapons Laboratory/NTAAB
Air Force Systems Command
Kirtland AFB NM 87117-6008

This paper extends the analysis of the eigenmode-expansion-method (EEM) parameters to their asymptotic forms in the left and right s-planes. The geometric properties of the object of interest are dominant in these asymptotic forms. The minimum circumscribing sphere gives an optimal choice of coordinate center for best convergence properties over all angles of incidence.

B4-10
1700

IDENTIFICATION OF PARAMETERS DESCRIBING A CONDUCTOR-BACKED DIELECTRIC SLAB

H.N. Tran
Division 1265
Sandia National Laboratories
P.O. Box 5800
Albuquerque, NM 87185, USA

D.G. Dudley
Electromagnetics Laboratory
ECE, Building 104
University of Arizona
Tucson, AZ 85721, USA

In this parametric inverse problem, we consider a lossless dielectric slab excited by a transient plane wave. The scattered electric field from the slab is presented in the ray-optic and the complex-resonance forms. Our interest is to extract the complex-resonances of the system in order to identify the parameters that describe the scatterer. We review the signal processing procedure and the identification procedure employed to identify the poles of the system. We investigate the effect of noise on identification and determine the maximum amount of noise one can impose on the system. In addition, we study the effect of data truncation on our identification procedure. We also discuss the parameters that dictate the minimum record required for successful identification. Finally, we demonstrate some similarities in effect of noise and truncation on our identification process.

Session BA-1 1355-Thurs. CR0-30
ANTENNAS
Chairman: W.L. Stutzman, Bradley Dept. of Electrical Engineering, Virginia Polytechnic Institute and State Univ., Blacksburg, VA 24061

BA1-1
1400

FEASIBILITY STUDY OF A SYNTHESIS PROCEDURE FOR ARRAY FEEDS TO IMPROVE RADIATION PERFORMANCE OF LARGE DISTORTED REFLECTOR ANTENNAS

W. L. Stutzman, Professor
W. T. Smith, Graduate Student
Bradley Department of Electrical Engineering
VPI & SU
Blacksburg, VA 24061-0111

Surface errors on parabolic reflector antennas degrade the overall performance of the antenna. They cause amplitude and phase errors in the aperture field which lower the gain, raise the side lobes, and fill in the nulls. These are major problems in large space reflector antenna systems. For example, future multiple beam antenna systems requiring spatial isolation to allow frequency reuse could be rendered useless if high side lobes are present.

Space antenna structures are difficult to build. They must maintain a nearly perfect parabolic shape in a harsh environment while remaining lightweight. The restrictions on the structure become more severe as science and technology requirements demand electrically large antennas. Mechanically, there are technologies for building antennas with adaptive surfaces that can compensate for many of the larger distortions caused by thermal and gravitational forces. However, as the frequency and size of the reflectors increase, the subtle surface errors become significant and degrade the overall radiation pattern. It is for this reason that another method must be used to further improve the radiation pattern.

Electromagnetic compensation for surface errors in large space reflector antennas has been the topic of several research studies. Most of these studies try to correct the focal plane fields of the reflector near the focal point and, hence, compensate for the distortions of the overall radiation pattern. The compensation is implemented by weighting the elements of an array feed. In most of the studies, a precise knowledge of the reflector surface is required (surface shape and the first and second derivatives).

An alternative approach to electromagnetic compensation is presented in this study. The proposed technique uses pattern synthesis to compensate for the surface errors. It differs from previous methods in two major respects. The previous studies used a global algorithm that tries to correct the entire focal plane field near the focal point and modify the entire radiation pattern. The pattern synthesis approach uses a localized algorithm in which pattern corrections are directed specifically towards portions of the pattern requiring improvement. The second major difference is that the pattern synthesis technique does not require knowledge of the reflector surface, but instead uses radiation pattern data to perform the compensation.

BA1-2
1420

IRIS-EXCITED SHUNT SLOTS IN RECTANGULAR WAVEGUIDE *

Winifred Ellen Kummer
Hughes Aircraft Co., Radar Systems Group
PO Box 92426, Mail Station R2/10G24
Los Angeles, CA 90009

This paper describes theoretical and experimental results for iris-excited shunt slots located along the centerline of the broad wall in rectangular waveguide. This type of coupling design has the advantage of eliminating the grating lobes caused by offset radiating slots in planar arrays. When the iris-excited shunt slot is used in waveguide coupling applications, it minimizes unwanted coupling between the feed slot and radiating slot.

The iris-excited shunt slot consists of a centered longitudinal slot excited by a thin inductive iris. The element is used as a radiating slot, and as a shunt-series coupling slot. The theoretical model treats both the zero thickness slot and the finite thickness slot.

The theoretical approach uses integral equations for the fields scattered by the currents on the iris and the electric field in the aperture of the slot. The scattering parameters are obtained by the method of moments.

A comparison with measurements performed at X-band concludes the paper. Good agreement is obtained, both for the radiating slot and the shunt-series coupling slot.

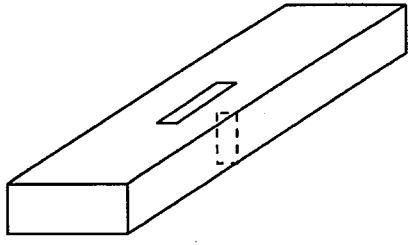

* This work was performed as a graduate research project at U.C.L.A. under the direction of Professor Robert S. Elliott.

BA1-3
1440

NUMERICAL EXPERIMENTATION OF SLOTTED MICROSTRIP ANTENNAS

Dave
D. I. Wu and D. C. Chang
Department of Electrical and Computer Engineering
University of Colorado
Boulder, CO 80309

Although slotted antennas have been in use for many years, much of the existing knowledge about them stems primarily from experimentation. Since relying on experiments to study innovative antenna ideas is generally impractical, numerical modeling provides an attractive alternative. When done accurately, numerical modeling can be a very powerful tool for providing basic knowledge about the physical behavior of a complex structure.

In this paper, we will use a general 2D integral equation/moment method solver for microstrip structures to examine the the behavior of a slotted antenna. The algorithm is based on a mixed potential integral equation approach using 2D rectangular pulses as the expansion and the testing functions (B. Brim and D. Chang, *National Radio Science Meeting, Meeting Digest*, p. 164, 1987, and p. 8, 1988, Boulder, CO). By modifying the source of excitation in the original algorithm to a normally-incident plane wave, we can do numerical experimentation on various microstrip antennas. Construction and gridding of an antenna geometry are done graphically. This allows for arbitrary placement of slots as well as non-uniform gridding. By using smaller-size cells adaptively, charge concentration near the slot can be characterized accurately.

The emphasis of this paper will be on antennas loaded with a long, narrow slot. Modulating an optical carrier using the induced E-field in the slot region is one application of this type of antenna. Thus, our goal is to maximize the strengh of the E-field in the slot region. To do so, we will purposely choose the slot length in such a way that in the freqency range of interest, both slot resonance and patch resonance are possible. The interactions between the two finite structures, namely the slot and the patch, and the effect of their individual resonances on the induced E-field will be examined. Parametric study on the variation of the maximum E-field across the slot as a function of slot locations will be presented. We will also explore the use of multiple slots to generate E-fields that are 90° out of phase, which is critical in achieving a single-side-band modulation of the optical carrier.

Cancelled

BA1-4 1500 ARRAY ERROR EFFECTS IN ADAPTIVE BEAMFORMING

Hans Steyskal
Electromagnetic Sciences Directorate
Rome Air Development Center
Hanscom Air Force Base, MA 01731

"In the adaptive antenna literature, signal-to-interference-plus-noise ratio (SINR) is widely accepted as a valid measure of output signal quality..." (N. Jablon, IEEE Trans. AP-34, Aug. 1986). However, this measure ignores the quality of the adapted antenna pattern, which also is of interest in many practical cases. This paper therefore focuses on the patterns, that result from adaptive beamforming algorithms, and how they are affected by array tolerance errors.

Two algorithms are considered: SINR maximization (S. Appelbaum, IEEE Trans. AP-24, Sept. 1976) and constrained power minimization (J. Capon et al, Proc. IEEE, 55, Feb. 1967, O. Frost, Proc. IEEE, 60, Aug. 1972). For an ideal array the criteria lead to the same adapted pattern, which has a well maintained pattern structure and deep nulls in the interference directions. In the presence of tolerance errors, however, we find that the two criteria differ drastically. Whereas the former is quite tolerant, the latter is extremely sensitive to errors and frequently leads to surprisingly large pattern degradation.

Contrary to the case of conventional arrays, where errors tend to fill in pattern nulls, the adaptive pattern nulls are remarkably stable and instead the main beam is spoiled. Thus the tolerances, i. e. a second order effect, can lead to a first order effect on the pattern. This is a consequence of the nonlinear processing involved in adaptive beamforming.

Jan 1990 Nat Radio Sci Meet

BA1-5
1520

ACCURATE ANALYSIS OF ELLIPTICAL HYBRID-MODE HORN ANTENNAS

Erik Lier and Sembiam Rengarajan*
Electrical Engineering Department
University of California, Los Angeles, CA 90024-1594
*Department of Electrical and Computer Engineering
California State University, Northridge, CA 91330

Elliptical hybrid-mode horns may be applied as a feed in elliptical reflector antennas for high aperture efficiency and low cross-polarization. Elliptical corrugated horns have high production costs and have a limited cross-polar bandwidth (≈ 10%). Recently experimental work on the dielectrically filled elliptical horn (E. Lier, C. Stoffels, "Recent advances on elliptical beamshape horns", *Proc. 1989 IEEE AP-S/URSI Int. Symp.*, San Jose, USA, June 1989, pp. 1431-1434) shows that potentially large cross-polar bandwidths (> 30%) can be realized.

The purpose of this paper is to present initial computer results on the propagation behavior and cross-polar performance based on the accurate cylindrical waveguide model of the elliptical dielectric horn (S. Rengarajan, J. E. Lewis, "Dielectric loaded waveguides", *IEEE TRANS. Microwave Theory Techn.*, vol. MTT-28, no. 10, pp. 1085-1089, Oct. 1980). The convergence with respect to the number of terms in the fundamental hybrid-mode will be discussed, as well as the propagation constants of the odd and even modes. Radiation pattern of this horn is computed by assuming that the aperture field distribution is the same as that of the dominant odd and even modes. Cross polar characteristics of the elliptical hybrid-mode horn computed from this theory will also be discussed.

Mathieu functions involved

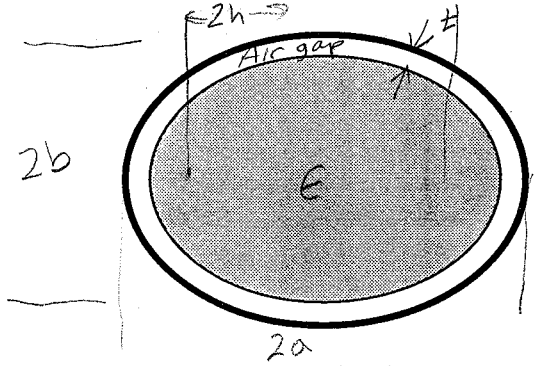

Illustration of partly filled dielectric (dielcore) waveguide

A. Love built an elliptical corrugated horn for an elliptical reflector

Jan 1990 Nat. Radio Sci. Meeting

BA1-6
1540

LOW SIDELOBE EDGE TAPERS FOR ARRAYS

Christopher McCormack
DFEE
USAF Academy, CO 80840
Randy L. Haupt
DFEE
USAF Academy, CO 80840

Criterion: peak SLL
optimized based on a
cost function. Powell's
method

Low sidelobe array synthesis is possible by tapering the current distribution at only a few edge elements rather than at every element in the array. Such an array is easier to build and test because the center elements (center subarrays) are uniformly weighted. The figures below show the current taper and resulting far field pattern of a 16 element equally spaced array with 8 inner elements uniformly weighted and 4 outer elements nonuniformly weighted. We calculate the edge amplitude weights using constrained minimization.

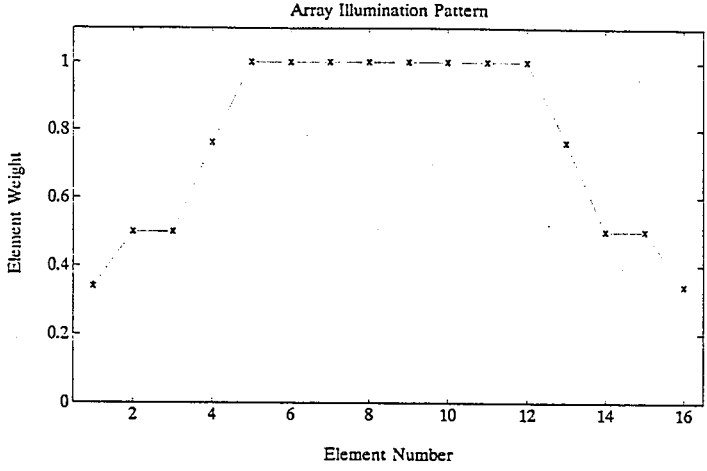

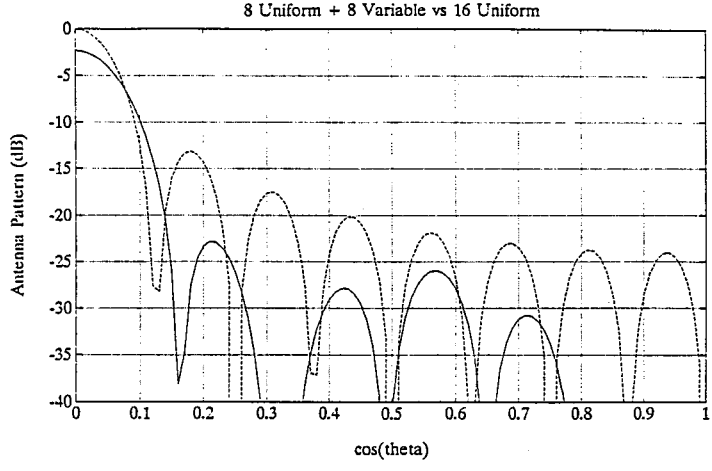

Jan 1990 Nat. Radio Sci. Meeting

BA1-7
1600

BEAM SQUINT DETERMINATION IN PARABOLIC ANTENNAS WITH CIRCULARLY POLARIZED FEEDS

Dah-Weih Duan and Yahya Rahmat-Samii
Department of Electrical Engineering
University of California, Los Angeles
Los Angeles, CA 90024-1594

Beam squint phenomenon is an important design issue for modern reflector antennas because it can affect the antenna pointing performances. Squint was previously observed in offset parabolic reflectors with an on-focus circularly polarized feed. The same phenomenon, however, also happens in the situation where the circularly-polarized feed is offset from the focus no matter whether the reflector is symmetric or offset. This is not an unusual situation in multiple beam applications.

The purpose of this paper is to characterize the squint phenomenon in these offset-feed configurations and present a formula which predicts squint angles accurately in all configurations where squint could possibly be observed in parabolic reflector antennas with circularly polarized feeds. These configurations are

1. offset reflector with on-focus feed,
2. symmetric reflector with offset feed,
3. offset reflector with offset feed.

In deriving this formula, geometrical optics (GO) is used to construct the field over the antenna aperture. The phase shift caused by the reflection from the reflector, which is responsible for the squint phenomenon, is derived. The aperture field integration which gives the radiation field of the antenna is then manipulated by a procedure involving change of variables (Adatia and Rudge, Elec. Lett., 11(21):513-515, 1975) to give the formula being discussed. In this formula, squint angles are determined by the angle between the incident beam and the radiated beam as well as reflector focal length in terms of wavelength. Computer simulations have been performed with a program based on the physical optics method to identify the actual squint angles with the complete diffraction analysis. The accuracy of this formula is justified for all cases of practical interest.

BA1-8
1620

A MODIFIED DIAKOPTIC THEORY ANALYSIS OF A TOP-LOADED ANTENNA

David F. Taylor and Chalmers M. Butler
Department of Electrical and Computer Engineering
Clemson University, Clemson, SC 29634-0915

For the top-loaded monopole above a ground plane, we present the results of measurements and diakoptic theory analysis, as well as results of a method of moments analysis for comparison. The diakoptic analysis of the top-loaded antenna is performed by introducing several open ports into the antenna structure, determining the approximate open-port current distribution on the resulting structure, and determining an open-port impedance matrix which is solved for the port currents of the antenna subject to specified port voltages. With the ports introduced in the diakotic procedure shorted and the source voltage applied at the original input port, one recovers the original antenna structure. The approximate open-port currents are determined using an iterative technique. Three important phenomena are noted when the open-port locations are varied. First, as expected, the accuracy of the solution is a function of the number of iterations used when determining the approximate open-port currents on the diakopted structure. Second, if the approximate open-port currents are accurate, the results obtained by the diakoptic analysis are very accurate (compared to the measured input impedance of the antenna and the results of the method of moments analysis). Third, it is shown that the number of iterations required for an accurate solution depends strongly on port location and is much larger for some open-port locations than for others. Data are presented for several top-load configurations and port combinations.

Cancelled

BA1-9
1640

ANALYSIS OF THE DUAL FREQUENCY MICROSTRIP ANTENNA BY SEGMENTATION METHOD

T. N. Chang and J. C. Fang
Department of Electrical Engineering
Tatung Institute of Technology
40 Chung-Shan North Road, 3rd Sec.
Taipei, Taiwan

The segmentation method and cavity model have been used to analyze a loaded microstrip antenna. The load itself has been modeled as a two port device. Five segments were used to represent the antenna which contains a pin diode. We were able to evaluate the electric field distribution underneath the patch and at the periphery of the antenna structure. This permits calculation of the radiation pattern using equivalent magnetic currents. The input impedance is also calculable. Agreement between theory and experiment is very good. The method presented is applicable to arbitrarily shaped loaded microstrip antennas.

BA1-10
1700

MICROSTRIP ANTENNA ARRAYS FOR SIDE LOOKING AIRBORNE RADARS

Albert W. Biggs*
Electrical and Computer Engineering Department
University of Alabama in Huntsville
Huntsville, Alabama 35899, USA

A method for design of microstrip antenna elements in antenna arrays is described. It combines the magnetic source and input impedance formulations to give an approximate design method having simplicity and high precision.

This method is applicable for microstrip antenna configurations ranging from rectangular, square, and rhombic, to circular and elliptical. A rectangular or square configuration is described for circular polarization, while rectangular configurations are available for dual frequency antennas.

Results of analytical studies provide antenna patterns in terms of magnetic current distributions. These magnetic current distributions are developed on the basis of feed point and physical configuration. Input impedances are uniquely formulated from transmission line modes.

*With an Intergovernmental Personnel Act (IPA) Grant at the Weapons Laboratory/AWPB, Kirtland AFB, New Mexico 87117-6008. TCS from Electrical Engineering Department, University of Alabama in Huntsville, Alabama 35899.

D3-1
1400

MICROWAVE INTEGRATED OPTICAL TRANSDUCER FOR OPTICAL READOUT OF PATCH ANTENNAS

Walter Charczenko, Holger Klotz, and
Alan Mickelson
Dept. of Electrical and Computer Engineering
University of Colorado, Campus Box 425
Boulder, CO 80309-0425

In many phased array antenna systems, it is possible to replace coaxial cable and microstrip feedlines with optical fibers. This will result in a reduction on size and weight of the system along with an increase in the bandwidth. Optical fiber will also make the transmission system immune from EMI (Electromagnetic Interference) and EMP (Electromagnetic Pulse).

Presently signals from antennas are transduced onto fiber optic links by RF intensity modulating semiconductor lasers either through current injection or using an external modulator. Intensity modulation necessitates the need for long lengths of fiber wrapped around PZT rings in order to achieve time delay. An integrated optical single side band modulator can be used as a transducer or local oscillator. Single side band encoding of the microwave signal onto the optical carrier can bring about the use of coherent optical techniques using other integrated optical elements to perform time delay, phase shifting, mixing, and direction of arrival operations.

The microwave optical interaction on electro-optic substrates can be modelled using coupled mode theory. The depth of modulation of an optical carrier directly from a patch antenna is shown from numerical simulations and experimental measurements to be too small in order to be practical in present day ($LiNbO_3$, $LiTaO_3$, GaAs) substrates. Therefore in order to reduce the amount of amplification necessary, a coplanar waveguide resonant electrode structure is required. At the conference numerical simulations and experimental measurements on patch antenna and resonant electrode integrated optical modulators will be presented.

D3-2
1420

OPTICALLY IMPLEMENTED BUTLER MATRICES FOR MICROWAVE PROCESSING

Paul J. Matthews, Marc R. Surette and Alan R. Mickelson
University of Colorado at Boulder
Department of Electrical and Computer Engineering
Boulder, CO 80309-0425

A Butler matrix performs an operation which is closely related to a Fast Fourier Transform (FFT). The radar application of this is that a Butler matrix takes a linear phase taper and transforms it to a signal in a single channel and vice versa. In a practical radar, targets will always be in the far field and therefore appear as linear tapers. In the past, Butler matrices were implemented with discrete microwave components. Microstrip implementations were impractical because Butler matrices required the crossing of waveguides. Optically implemented Butler matrices are not constrained by this problem because optical waveguides can be crossed without interfering. Optical Butler matrices can be monolithically fabricated from arrays of passive optical 3 dB directional couplers and phase shifters. An optically implemented Butler matrix constructed of these passive devices would also be immune to EMP and EMI effects as well as being light weight, low loss and rugged.

The feasibility of optically implemented Butler matrices for radar applications depends upon the ability to accurately and repeatably fabricate passive optical 3 dB directional couplers. Directional couplers may be readily fabricated in $LiNbO_3$ using the two-step proton exchange/anneal technique (P.G. Suchoski, T. Findakly and F.J. Leonberger, Optics Lett. 13(11), 1050, 1988). Using this technique, a step index waveguide is first formed by immersing a suitably masked $LiNbO_3$ crystal in a benzoic acid bath. The resultant waveguide is subsequently annealed at an elevated temperature to produce a graded index profile. This second annealing step gives an extra degree of freedom in the waveguide fabrication and can thus be used to tailor a passive directional coupler until highly accurate 3 dB splitting is obtained. This procedure of slow annealing has enabled us to repeatably and accurately fabricate passive optical 3 dB directional couplers in $LiNbO_3$ which may be used in optically implemented Butler matrices.

D3-3
1440

NUMERICAL SIMULATION OF THE LIGHT AMPLIFYING OPTICAL SWITCH

R. E. Owens
Department of Electrical and Computer Engineering
Clemson University, Clemson, SC 29634-0915
S. A. Feld and C. W. Wilmsen
NSF ERC for Optoelectronic Computing Systems
Department of Electrical Engineering
Colorado State University, Fort Collins, CO 80523

We present a numerical simulation of a light amplifying optical switch (LAOS) which is a promising device for applications in optical computing. The device consists of a vertically- integrated InP/InGaAs heterojunction phototransistor (HPT) and InGaAs/InP light-emitting diode (LED) grown epitaxially on an InP substrate. This structure is similar to the optically-bistable device with light amplification reproted earlier (A. Sasaki, S. Metavikul, M. Itoh, and Y. Takeda, IEEE Trans. Electron Devices, ED-31, 805-811, 1984).

The simulation solves the semiconductor equations including the effects of optical carrier generation using a one dimensional finite differences technique (J.E. Sutherland and J.R. Hauser, IEEE Trans. Electron Devices, ED-24, 4, 363-372, 1977). We present steady-state results which yield insight regarding the operation ofthe device. In particular, the conditions for optical bistability and the sensitivity of the optical gain to base width and doping are examined. In order to verify the simulation the results are compared to experimentally obtained I- V characteristics for the HPT and LED which are used to fabricate the device.

D3-4
1520

MODELING OF PHOTO-CONDUCTIVE SWITCHES

K. Connolly, R. Joshi*, S. El-Ghazaly and
R. Grondin
Center for Solid State Electronics Research
Arizona State University
Tempe, Arizona 85287-6206

*Dept. of Electrical and Computer Engineering
Old Dominion University
Northfolk, Virginia 23529

Ultrafast electrical waveforms can be generated and characterized using lasers and the electro-optic sampling technique. Rise times in the sub-picosecond range have already been achieved (D. Auston, IEEE J. Quantum Electronics, QE-19, 639, 1983). One of the structures used by several workers involves a gap in a microstrip structure fabricated on a semi-insulating GaAs (K. Meyer *et al.*, in *Picosecond Electronics and Optoelectronics*, Springer-Verlag, Berlin, 1985). The photoconductive switch is turned on by illuminating the gap with a laser pulse. Other laser pulses are used to electro-optically sample the electrical waveform as it propagates on the microstrip-line. We have developed a theoretical approach to model the transient behavior of this switch by incorporating an ensemble Monte-Carlo technique in a three dimensional time-domain solution of Maxwell's equations using the finite difference scheme (Y. Lu *et al.*, 6th International Hot Electron Conf., Scottsdale, 1989). In this approach we avoid many simplifying assumptions commonly made.

In this paper, we will discuss the main features of the model and how Maxwell's equation solution and the ensemble Monte-Carlo technique are linked together. Some of the preliminary results will also be presented.

D3-5 1540 MEASUREMENTS OF PARASITIC COUPLING IN MICROSTRIP CIRCUITS USING ELECTRO-OPTIC SAMPLING

Dag R. Hjelme, Alan R. Mickelson, Cole Howard, and John Dunn
Department of Electrical and Computer Engineering
University of Colorado
Boulder, CO 80309-0425

Parasitic coupling, the unintentional coupling between adjacent circuit elements, is a problem that will become increasingly important as the packing density of MMICs (Monolithic Microwave Integrated Circuits) increases. The parasitic coupling is essentially a small quantity, thus represent a challenging measurement problem. In standard network analyzer measurements, these small coupling effects could easily be masked by inaccuracies in the de-embedding process or the limited dynamical range.

The electro-optic sampling technique, with its potentially large dynamical range , non-invasivenes and the possibility to define reference planes anywhere on the circuit, is a well suited technique with which to study these weak coupling effects.

Here we report on the measurement of parasitic coupling among canonical microstrip geometries, using electro-optic sampling. Aluminum microstrip lines are fabricated on $LiTaO_3$ electrooptic substrates. Mounted in a test fixture, the circuits can be excited in the 2-18 GHz range and probed using subpicosecond pulses from a dyelaser. Using this technique, we measure both scattering parameters and potential distributions and how they are affected by parasitic coupling.

D3-6
1600

OBSERVATIONS OF QUANTUM SEPARATRIX CROSSING IN OPTICAL WAVEGUIDES

Alan Rolf Mickelson and Indra P. Januar
Dept. of Electrical and Computer Engineering
University of Colorado, Campus Box 425
Boulder, CO 80309

Petre Rusu and John R. Cary
Physics Department, Box 390
University of Colorado
Boulder, CO 80309

In the nearly four decades since Lorentz first demonstrated to us that reasonably simple, deterministic, nonlinear differential equations can give rise to extremely complex and unpredictable behavior, it has been shown that such "chaos" arises from practically all classical physical systems which can exhibit any appreciable nonlinearity. However, as is well known, the world is actually quantum mechanical and not classical at all, so the question arises as to how chaos may appear in quantum mechanical systems. As quantum mechanical systems do not have line-like phase space trajectories, but rather smeared out (uncertain) paths, it is not at all clear how, for example, homoclinic tangles, which require intricate infinitesimal interleavings, will pass over to the quantum case, if they pass over at all. Clearly, the place to start looking for quantum chaos is in those problems where there are so many states that one can begin to ignore uncertainty. This is where the quantum and classical pictures overlap, and analogies become clear.

A prime example of an "almost" classical system is that of a potential with many bound states. Thus in an adiabatically varying double well potential, classical trajectories that cross the separatrix are chaotic. This leads to diffusion of the adiabatic invariant. In the quantum mechanical bound state problem, by adiabatically expanding the wells without changing the separatrix region, it is possible to "move" a bound state from a height above the separatrix, through the separatrix and into the two welled region. Theory has shown that quantum effects can eliminate the chaos observed in the classical problem. The problem addressed here is that of experimentally verifying these effects.

As is well known, the Schroedinger equation for any potential problem is formally identical to the paraxial wave equation for a waveguide, if t is replaced with z and the potential replaced with the index distribution. Further modification of the axial index distribution with increasing longitudinal coordinate is formally equivalent to adiabatic modification of the quantum mechanical potential. This is fully in line with the fact that Maxwell's equations are the quantum mechanical equations of motion for a single photon. Indeed, tapered waveguides were fabricated and prism coupling experiments performed on the resulting waveguides. These experiments showed good qualitative agreement with the theory of quantum separatrix crossing. Quantitative results will be presented at the conference.

Session E-2 1355-Thurs. CR1-9
NATURAL AND MANMADE NOISE AND SPECTRUM MANAGEMENT
Chairman: E.K. Smith, NASA Propagation Information Center, Dept. of Electrical Engineering, Univ. of Colorado, Boulder, CO 80309

E2-1
1400

REVIEW OF NATURAL AND MAN-MADE RADIO NOISE PROGRESS 1986-1989

David B. Sailors
Ocean and Atmospheric Sciences Division
Naval Ocean Systems Center
San Diego, Ca 92152-5000

The progress in natural and man-made noise investigations from 1986 to 1989 is reviewed. Most but not all natural noise investigations have been made at frequencies below the HF band. Herman et al.(Radio Sci.,21 25-46,1986) describe the measurement and statistical analysis of wideband MF atmospheric radio noise. Results presented include the temporal structure of atmospheric noise, the distribution and time variation of the measured average noise power, and comparisons with predictions by the CCIR. The impact on bandwidth and system performance is presented by Giordano et al.(Radio Sci.,21,203-222,1986). Stanford University(Fraser-Smith,A.C.,NATO AGARD Conference Proc. 420,4A, 1987) is operating a global network of eight computer-controlled receiving systems for the measurement of electromagnetic noise in the 10-32,000 Hz frequency band. The digital data are being used primarily for statistical studies of the global distribution of ELF/VLF noise. Field and Warber(NATO AGARD Conference Proc. 420,3,1987) addressed the role of horizontal lighting strokes in producing transverse-electric(TE) LF atmospheric noise. Turtle et al.(Radio Sci.,24,325-339,1989) presented measurements of both TE and TM LF atmospheric noise aboard a free-floating balloon at altitudes up to 20 km. La Belle(J.Atmos. Terr. Phys.,51,197-211, 1089) reported radio noise of auroral origin from 1968-1988.

Although much of the man-made radio noise efforts have been concerned about spectrum occupancy at HF, Hagn(NATO AGARD Conference. Proc. 420,5, 1987) discussed what the scientific community knew and did not known about man-made radio noise. Measurement of man-made radio noise was also discussed. An experiment to measure spectral occupancy at HF has been undertaken by Gott(NATO AGARD Conference Proc. 420,7,1987) since the sunspot maximum of 1982. The aim was to provide data which may be used to advise HF operators on typical occupancy they may encounter. Hagn et al. (IEEE Trans. Broadcasting,34,1988) reported measurements of spectrum occupancy and signal levels made at four locations in the United States and at two locations in Europe. The paper presented some initial results comparing spectrum-occupancy and signal-level data between CONUS and Europe.

E2-2
1420

ELF/VLF RADIO NOISE MEASUREMENTS IN GREENLAND DURING A PCA EVENT

A.C. Fraser-Smith and P.R. McGill
STAR Laboratory, Stanford University,
Stanford, California 94305
J.P. Turtle
Rome Air Development Center, Hanscom Air Force Base,
Massachusetts 01731

We report simultaneous measurements of ELF/VLF radio noise at two locations in Greenland (Thule and Sondrestromfjord) around the time of a moderately large polar cap absorption (PCA) event that started on 12 August 1989. Thule is close to the center of the polar cap and thus the ELF/VLF noise signals reaching it are particularly exposed to the ionospheric effects of a PCA, whereas the ELF/VLF noise signals at Sondrestromfjord, which is located close to the inner edge of the auroral zone, should be less affected. These general expectations are supported by the results of our measurements, which show some major changes in the Thule noise statistics during the PCA but only smaller changes at Sondrestromfjord. The changes depend markedly on the frequency of the noise signals. At Thule, for frequencies in the approximate range 250 Hz to 1.5 kHz, there is an increase in the rms noise amplitudes and a filling-in, or loss, of the minimums in the diurnal variation during the 2-3 days following the start of the PCA. The increase can amount to as much as 10-15 dB. For frequencies in the range 30 - 41 kHz there is a similar, but weaker, increase in the rms noise amplitudes. For most other frequencies in the range 10 Hz to 41 kHz that are covered by the measurements there is little change in the noise statistics. However, in the range 4 - 10 kHz there is a marked decline in the rms noise amplitudes in the 24 hours following the start of the PCA, after which there is a rapid recovery to the undisturbed levels. At Sondrestromfjord the most marked change appears to be the suppression of the diurnal variation in the 2-3 days following the start of the PCA.

E2-3 1440 VLF RADIO NOISE IN THE ARCTIC, Francis J. Kelly, Naval Research Laboratory, Code 4183, Washington, DC 20375-5000

The atmospheric radio noise measurements at Spitzbergen, Svalbard, during 1985 and 1986 are reviewed and summarized. Comparisons with theoretical models of atmospheric noise are displayed. Noise was measured from 15 kHz to 80 kHz. Signal level observations at Spitzbergen are also given.

E2-4 Paper Deleted
1500

E2-5 RECENT ADVANCES IN COMMUNICATING IN THE PRESENCE OF NON-
1540 GAUSSIAN NOISE, A. D. Spaulding, Department of Commerce, NTIA/ITS, 325 Broadway, Boulder, Co 80303, 303-497-5201

Since the normally assumed white Gaussian interference is the most destructive in terms of minimizing channel capacity, substantial improvement can usually be realized if the real world interference environment (non-Gaussian) is properly taken into account. Also, "normal" receivers optimized for Gaussian noise are generally extremely suboptimum in the real-world interference environment. Over the past decade, a substantial body of effort has taken place in developing adaptive signal detectors and estimators, both parametric and nonparametric, for the real non-Gaussian world, usually stressing "small" signal detection.

It is the purpose of this short presentation to briefly review current efforts and results in this area. These generally are in two areas: (1) Continued theoretical threshold signal detection (and estimation) development, including simultaneous space-time signal processing in vector EMI fields, considering cases of space and/or time non-independence; (2) Testing and continued development of detectors, based on time independent interference samples, using actual interference samples rather than samples generated from various theoretical EMI mathematical models. Illustrative examples will be given in both areas.

E2-6
1600

NEW SYSTEM CONCEPTS FOR DIRECTIONAL MEASUREMENT OF ATMOSPHERIC NOISE, Richard L. Johnson and Gina E. Miner, Electromagnetics Division, Southwest Research Institute, San Antonio, Texas 78228

Radio direction finding techniques have been used for a number of years in research activities designed to locate sources of electrical emissions embedded in thunderstorm cells. One of the more difficult problems encountered in that work is the occurrence of large errors caused by wave interference effects. The errors are generally due to simultaneous electromagnetic signals radiated from multiple sources within the storm. Three primary approaches have been used to overcome wave interference effects: (1) high-speed data sampling, (2) waveform recognition and (3) wavefront planarity testing.

An advanced spectral estimation technology has emerged during the past decade which provides the capability to achieve wavefield decomposition with more realistic antenna array configurations than was possible with earlier techniques. Using limited array apertures, new superresolution methods permit one to determine the angle of arrival for each signal present in a multicomponent wavefield.

Among the new generation of spectral estimation techniques, the ESPRIT eigen based method was selected for study in our work. The algorithm provides a closed form solution and does not require a calibration of the antenna array. We have developed three important extensions to the algorithm described in the literature: (1) a generalized method has been implemented to do multisignal phase ambiguity resolution across array apertures greater than one wavelength, (2) the ESPRIT technique has been extended to the multidimensional case of azimuth and elevation, and (3) a bearing quality indicator based on the measured data is used to assess the validity of the angle of arrival estimate. Projected system performance applying these concepts is presented using computer simulated data which evaluates detection probability, false alarm rate and failure to alarm rate.

E2-7
1620

NATURAL RADIO NOISE ABOVE 50 MHZ A REPORT BY THE WORKING GROUP

Ernest K. Smith
NASA Propagation Information Center
Department of Electrical Engineering
University of Colorado
Boulder, Colorado 80309

This talk will describe the present status and future needs of CCIR Report 720 "Radio Emission From Natural Sources Above About 50 MHz". Over the past years URSI has responded to CCIR's request to improve and update this text and has made significant contributions, particularly in the area of galactic noise maps. Present needs include

- computer representation of the galactic noise maps and of the charts of emision noise from the clear atmosphere
- of of charts or codes of emission from clouds on a worldwide statistical basis and
- of improved representation of the brightness temperature of land surfaces as a function of frequency, soil type and angle of incidence.

Session E-3 1640-Thurs. CR1-9
SPECTRUM MANAGEMENT
Chairman: R.D. Parlow, NTIA Office of Spectrum Management,
U.S. Dept. of Commerce, Washington, DC 20230

E3-1
1640 SPECTRUM MANAGEMENT--FUTURE DIRECTIONS, Richard D. Parlow, Associate Administrator, National Telecommunications and Information Administration, 14th & Constitution N.W., Washington, D.C. 20230

This fall, NTIA is undertaking a complete review of current policies and processes for management of the radio spectrum in the United States. No comprehensive review of U.S. spectrum use and management has occurred for almost a generation. Yet, demands on this resource continue to expand exponentially and we see no end in sight.

Even with advances in technologies such as fiber optics which may free spectrum resources for other needs, or the introduction of spectrum efficient modulations will not, in the conventional sense, meet our future needs. In light of the economic value of the radio spectrum, economic forces as a tool in managing this resource deserve consideration.

The goals of this year long review will include affording maximum opportunity for existing and new services; ensuring that U.S. national defense, law enforcement and other essential Government service requirements are met; ensuring that international frequency management accommodates U.S. interests; and providing U.S. spectrum users and innovators ready access to the resource.

One of our first actions will be to issue a Notice of Inquiry (NOI) to request public comment on specific economic, technical, and regulatory issues to be studied concerning U.S. spectrum policy. This is all part of an overall effort to have extensive consultations with the private sector, the FCC, Government spectrum users, and the Congress. The status of the spectrum review and other related matters will be discussed.

E3-2
1700 HF ISSUES FOR THE 1992 WORLD ADMINISTRATIVE RADIO CONFERENCE, David J. Cohen, National Telecommunications and Information Administration, 179 Admiral Cochrane Drive, Annapolis, Maryland 21401

A World Administrative Radio Conference (WARC) to deal with Frequency Allocations in certain parts of the spectrum is scheduled to convene in 1992. One of the parts of the spectrum to be considered is the HF Spectrum. The impetus for including HF in this 1992 Conference is Recommendation 511 of the 1987 HF Broadcasting WARC (HFBC-87) which requested that a future WARC consider the possibility of extending the HF spectrum allocated exclusively to the broadcasting service with the aim of future planning of that spectrum for broadcasting.

A synopsis will be given of past international HF allocation actions (WARC 79) and current U.S. management of the HF spectrum. The HF technical and other issues of importance to the 1992 conference will be discussed. One issue of significant interest is the possible effects of reallocation on other HF services, such as fixed and mobile.

G3-1
1400

GROUP PATHS AND DISPERSION COEFFICIENTS OF PULSED RADIO SIGNALS REFLECTED FROM PLANE AND SPHERICAL MODEL IONOSPHERES

Ikmo Park and K. C. Yeh
Wave Propagation Laboratory
Department of Electrical and Computer Engineering
University of Illinois at Urbana-Champaign
1406 W. Green St., Urbana, IL 61801

When pulsed electromagnetic signals are propagated through a stratified, inhomogeneous, isotropic ionosphere, their forms are distorted because of dispersion. To the first order approximation, this dispersion distortion is determined by the dispersion coefficient ϕ'', the second derivative of the phase with respect to the angular frequency. Using the linear and parabolic electron density distributions as functions of height, analytic expressions of the group path and dispersion coefficient are obtained for the plane earth-ionosphere geometry. A very slight modificaton is made in the linear and parabolic electron density distributions to derive analytic expressions of the group path and the dispersion coefficient for the spherical earth-ionosphere geometry. The results obtained under the plane and spherical earth-ionosphere geometries are compared. In an attempt to simplify the analysis, the secant law applicable to the plane geometry is modified for application to spherical geometry. In this regard, a correction factor can be introduced. This correction factor is computed and a dispersion coefficient in terms of a correction factor is derived using a modified secant law and the geometry of a spherical earth-ionosphere. All calculations are made under conditions which neglect the earth's magnetic field, absorption, and irregularities. The results show the dependence of dispersion coefficient on propagation geometry and ionospheric model parameters.

G3-2 1420 *TOWARD AN OPTIMUM RECEIVING ARRAY AND PULSE-SET FOR THE DYNASONDE.*

by M L V Pitteway, Brunel University, Uxbridge, UB8 3PH, and
J W Wright, British Antarctic Survey, Cambridge, CB3 0ET *

ABSTRACT

The accuracy and efficiency with which radio echo parameters may be estimated by a modern digital ionosonde depends less upon the specific hardware design and performance (provided these attain certain minimal and easily achieved standards) than upon the software-designed strategies of pulse-set design and receiving antenna layout. The initial problem, worthy of solution in real time for economic reasons, is to identify bona-fide echoes as such, and to reject false signals. A method of coincidence detection works well for this purpose, itself requiring intercomparison among the echoes from a small number of transmitted pulses. The second problem is parameterization, at present not attempted in real time. All echo parameters, except the pulse amplitude and time of arrival, are determined by phase angle differences, themselves obtained necessarily modulo 360^0, from high resolution complex amplitude data. Each parameter is therefore subject to aliasing ambiguities which must be anticipated in each strategy, and minimized. The aliasing problem exists in parallel to, and rather independently of, the problem of extracting the principal phase dependent parameters (three components of echo-location, Doppler, polarization rotation, and an average phase angle) in terms of the measured complex amplitudes. The latter problem is conveniently expressed as a least squares minimization, provided that more than six independent phase measurements are available. An analysis of several pulse-set and antenna layouts is presented, including two which have been used extensively with the Trömso Dynasonde (of the Max Planck Institute Heating program) and in EISCAT comparisons. Our preferred layout consists of six receiving dipoles arrayed in threes along the 141m diagonals of a square, at distances in proportion to 0,2,3 from the north and west antennas. With well determined phases, this array combines the aliasing invulnerability (below 8 MHz) of the 47m baseline with most of the echo-location resolution of the 141m baseline. We discuss the effects of phase measurements noise to degrade this performance.

* Now at 1915 Spruce Avenue, Longmont Colorado 80501.

G3-3
1440

COMPARISON OF VHF DOPPLER BEAM SWINGING AND SPACED ANTENNA OBSERVATIONS WITH THE MU RADAR: FIRST RESULTS

J.S. Van Baelen*, T. Tsuda**, A.D. Richmond*, S.K. Avery***, S. Kato**, S. Fukao** and M. Yamamoto**
*High Altitude Observatory
National Center for Atmospheric Research
P.O. Box 3000
Boulder, CO 80307
**Radio Atmospheric Science Center
Kyoto University, Japan
***Department of Electrical and Computer Engineering and CIRES
University of Colorado at Boulder
Boulder, CO 80309-0425

Using the MU radar (34°51'North, 136°06'East), we designed an experiment to perform a comparison between wind measurements obtained by two different techniques: Doppler Beam Swinging (DBS) and Spaced Antenna (SA). The SA data are analysed by full correlation analysis (FCA) to extract the apparent and true velocities. Eventhough the results of the two techniques agree generally well, subtle differences are observed. A critical review of the possible sources of discrepancy arising from each technique is then attempted.

G3-4
1520

THE INSTRUMENTATION FOR METEOR ECHO DETECTION AND COLLECTION

J.P. Avery, M.J Leary, T.A. Valentic, and R.L. Obert
Department of Electrical and Computer Engineering and CIRES
University of Colorado at Boulder
Boulder, CO 80309-0425

The meteor echo detection and collection (MEDAC) system is designed to work in parallel with stratosphere-troposphere (ST) and mesosphere-stratosphere-troposphere (MST) radar systems. The MEDAC system relies on scatter from ionization trails left by meteorites in the 70 to 110 km region to measure wind velocity. By using a non-turbulent scattering mechanism, the MEDAC system is capable of complementing the standard ST and MST systems; specifically by providing mesospheric measurements on ST radars, and night-time coverage on MST radars.

The interface between the radar and the MEDAC system is designed for minimal impact on the radar system. The changes to radar operating procedures may be more problematical; these will be discussed. The instrumentation for MEDAC has undergone an evolutionary development process from the proof of concept device to the current "production" systems. This talk will describe the process, with emphasis on the current design.

Advanced technologies may be employed in future systems. These directions will be discussed.

G3-5
1540

EXTRACTION OF ATMOSPHERIC TIDES FROM METEOR ECHO DATA

S.E. Palo and S.K. Avery
Department of Electrical and Computer Engineering
University of Colorado at Boulder
Boulder, CO 80309-0425

The data from the Meteor Echo Detection and Collection System (MEDAC) is a non-uniform sampling of the continuous wind field in the atmosphere. In order to analyze the wind fields we need to determine the wave parameters from the non-uniform time series.

The estimation technique of wave parameters can be divided into two classes: the parameterized class where the wave frequency is assumed and the class where the frequency is estimated. The two classes of estimators will be discussed along with the estimation techniques currently being used on the MEDAC system.

G3-6
1600

WIND MEASUREMENTS USING MEDAC

T.A. Valentic, S.E. Palo, S.Y. Su*, J.P. Avery, and S.K. Avery
Department of Electrical and Computer Engineering
University of Colorado at Boulder
Boulder, CO 80309-0425
*National Central University
Chung-Li, Taiwan, ROC

This talk will describe the results obtained with the Meteor Echo Detection and Collection (MEDAC) system. These include horizontal wind profiles and meteor echo collection statistics from the 80 km to 100 km region. A comparison of mean winds and tides from Christmas Island (2°N, 158°W), Chung-Li, Taiwan (23°N, 120°E), and Platteville, Colorado (40°N, 104°W) will be made.

Session GH-1 1355-Thurs. CR1-46
IONOSPHERIC MODIFICATION
Chairman: L.M. Duncan, Dept. of Physics and Astronomy, Clemson Univ., Clemson, SC 29634

GH1-1 1400 **IONOSPHERIC MODIFICATION EFFECTS OF MODULATED PUMP WAVES**

Lewis M. Duncan
Dept. of Physics and Astronomy
Clemson University, Clemson, SC 29634-1911

This presentation describes Arecibo incoherent scatter radar observations of HF-enhanced plasma line response to pump wave modulation. In particular, the depth and shape of plasma wave response to a variety of modulation schemes is measured, and observed to differ substantially from that predicted for a simple model of pump wave amplitude variation around a fixed instability threshold. In addition, the method by which the modulation is produced also is observed to have significant influence over the long-term behavior of the enhanced plasma waves, and maintenance of conditions associated with the ionospheric pre-conditioning phenomenon. Sinusoidal and square pulse amplitude modulations of the pump wave at frequencies from less than 1 Hz to greater than 10 kHz are used to isolate plasma effects excited by ponderomotive (fast) and thermal (slow) driving forces. Interpretation of the recent observations will be discussed in terms of current phenomenological issues in ionospheric modification.

GH1-2
1420 HIGH POWER RADIOWAVE HEATING OF A CONVECTING IONOSPHERE*

M.J. Keskinen and P. Bernhardt
Space Plasma Branch
Plasma Physics Division
Naval Research Laboratory
Washington, DC 20375-5000

An analytical study of large scale, late time aspects of high power radiowave heating of a convecting ionosphere is made. Convection produced by both gravity and neutral thermospheric winds in included. Simple models for high power HF propagation in convecting and steepening plasma density depletions are formulated. Growth rates for the generalized thermal self-focusing instability in the presence of convection and steepening are computed. The results of this study are compared with observations.

* Work supported by ONR.

GH1-3
1440

TEMPORAL EVOLUTION OF HF-ENHANCED PLASMA LINES

S.P. Kuo
Weber Research Institute, Polytechnic University
Farmingdale, New York 11735
F.T. Djuth
Space Sciences Laboratory, The Aerospace Corporation
Los Angeles, California 90009
M.C. Lee
Plasma Fusion Center
Massachusetts Institute of Technology
Cambridge, Massachusetts 02139

The HF-enhanced plasma lines observed in the Arecibo heating experiments are referred to be the radar returns at frequencies near the sum and difference of the radar frequency and the HF heater frequency. These enhanced spectral lines are attributed to the backscatter of radar signal by those of excited plasma waves located in a specific altitude interval so that their wavevectors can match the backscattering condition. A nonlinear theory is developed to describe the temporal evolution of those specified plasma waves which in turn leads to the evolution of observed HF-enhanced plasma lines (HFPLs). Both phenomena of intensity overshoot and expansion of originated altitude interval in time are described. The theoretical results agree very well with the observation. The theoretical results also show that the degree of overshoot of HFPLs depends on the magnetic dip angle of the observational site. Only those of plasma waves propagating in certain bands of spectral angle about the geometrical field will exhibit overshoot in time. The overshoot band around the dip angle of Arecibo is wider than that of Tromsø, and no overshoot band exists around the dip angle of Boulder.

GH1-4
1520

INTENSITY MODULATION OF HF HEATER-INDUCED PLASMA LINES

S.P. Kuo
Weber Research Institute, Polytechnic University
Farmingdale, New York 11735
M.C. Lee
Plasma Fusion Center
Massachusetts Institute of Technology
Cambridge, Massachusetts 02139

The Arecibo HF heater is normally composed of two separate sets of antenna array, transmitting waves vertically at the same frequency and polarization. However, when these two sets of antenna array radiate at slightly different frequencies, the intensities of HF heater-induced plasma lines (HFPLs) can be drastically modulated. In recent Duncan et al's experiments, the 100% intensity modulation of HFPLs was seen to persist even when the secondary set of antenna array radiated at a few percents of the power transmitted by the primary set of antenna array. We offer an explanation and show that there exists a minimum power P_{min}, which can be roughly estimated from $P_{th}[(E_0/E_{th})-1]^2$ where E_{th} and P_{th} are the threshold field and threshold power of the parametric decay instability, respectively, E_0 is the field intensity of heater wave. If the secondary set of antenna array radiates at a power lower than P_{min}, the 100% intensity modulation of HFPLs will not be observed. The functional dependence of P_{min} on the difference frequency of the two sets of antenna array is also predicted for future experiments to corroborate.

GH1-5 1540 VLF HEATING OF THE LOWER IONOSPHERE, Umran S. Inan, Space, Telecommunications and Radioscience Laboratory, Stanford University, Stanford, CA 94305

Data from a recent ground-based controlled wave-injection experiment indicates that the plasma temperature in the nighttime lower ionosphere (80-90 km altitude) overhead a powerful (300 kW radiated power) VLF (28.5 kHz) transmitter is increased by as much as 30-50% due to the absorption of the radiowave power in the plasma. The effect was first observed in data acquired during 0335-0350 UT on 7 May 1989 when specialized keying formats (3s ON/2sOFF) were transmitted using the NAU transmitter in Aquadilla, Puerto Rico, operating at 28.5 kHz. The heating effect was detected as synchronized amplitude change on a 24.0 kHz signal from the NAA transmitter located in Cutler, Maine observed at Palmer Station (PA), Antarctica, with the NAA-PA great circle path passing within 50 km of the NAU transmitter in Aquadilla. The observed effect is attributed to a modification of the collision frequency in the lower ionosphere as a result of the wave power absorbed at altitudes of 80-90 km, near the ionospheric reflection height for VLF waves. Calculations of wave absorption coefficient and expected power levels indicate that absorption of the whistler-mode (ordinary) wave energy at a lateral distance of 100km from the transmitter can lead to a 60% enhancement in the collision frequency at 85km altitude. The wave electric field intensities in the heated region for the 28.5 kHz transmitter are of order 20 mV/m. Since ionospheric electric field transients of up to 50 mV/m are observed in association with lighting, the result indicates that lightning discharges may also cause detectable modification of the lower ionosphere.

Session J-2 1335-Thurs. CR2-26
GENERAL SESSION
Chairman: R.F. Jurgens, Jet Propulsion Laboratory, Pasadena, CA 91109
SOLAR RADIO ASTRONOMY DURING MAX 91
Organizers: K.R. Lang and R.F. Willson, Jr., Dept. of Physics, Tufts Univ., Medford, MA 02155

J2-1
1340

1400 MHZ OBSERVATIONS OF SOLAR FLARE ON JUNE 20, 1989

T. A. Kucera, G. A. Dulk, T. S. Bastian, and L. A. Belkora
Dept. of Astrophysical, Planetary and Atmospheric Sciences
University of Colorado at Boulder
Boulder, CO 80309-0391

As part of the June Max '91 campaign we observed the solar flare starting at about 1500 UT June 20, 1989 at 1400 MHz with the VLA. This flare is of special interest because it was associated with a coronal mass ejection. Ejected matter from this event has been detected at both 35 GHz and 169 MHz. We were in a scanning mode going over seven different pointings in the face of the sun so that every 25 min we got a snapshot of the North-West limb where the flare occurred, imaging out to a radius of 1.5 $R_\odot$. To increase our dynamic range we used frequency synthesis, a technique which involves taking data at several frequencies so as to increase uv coverage. Shortly after the flare we recorded an image of the sun with the Arecibo telescope. We will present our results from the radio imaging and also an EUV image of the sun taken the same day.

This research was supported by NASA's Solar Terrestrial Theory and Solar Heliospheric Programs under grants NAGW-91 and NSG-7287 and National Science Foundation grant ATM 87-19371 to the University of Colorado, Boulder.

J2-2
1400

RADIO MICROBURSTS AT METER-DECAMETER WAVELENGTHS

G. Thejappa, N. Gopalswamy and M.R. Kundu
Astronomy Program
University of Maryland, College Park, MD 20742

We study the characteristics of microbursts using a large data base obtained with the multifrequency radioheliograph of the Clark Lake Radio Observatory. Most of the new observations were made during July 29, 1985 to August 2, 1985; we also include for statistical studies the microburst data used in our earlier studies. We perform a statistical analysis of many characteristics such as frequency drift, source size and brightness temperature and compare them with the properties of normal type III bursts. We investigate the coronal structures and surface activities associated with some of the events. We find that (i) the brightness temperature is in the range 6×10^5 K to 6×10^7 K; (ii) the drift rate of the microbursts is slightly smaller than that of normal type III bursts, implying electron beams with speeds ~ 0.2 c.

We explore various theoretical interpretations of the observed low brightness temperatures. The low beam speed implies that induced scattering of the Langmuir waves on the ions may not play any role in stabilizing the beam-plasma instability. The inhomogeneous character of the leading edge of the beam and collisions may restore the two-stream instability following quasilinear relaxation. Such beams can explain brightness temperatures ~ 10^7 K. Alternatively, spontaneous emission of Langmuir waves in the absence of the two-stream instability can also explain the low brightness temperatures.

J2-3
1420

HIGH SPATIAL RESOLUTION OBSERVATIONS OF SOLAR FLARES AT 3.3 MM WAVELENGTH

M.R. Kundu, S.M. White, N. Gopalswamy
Astronomy Program
University of Maryland, College Park, MD 20742
and
J.H. Bieging
University of California, Berkeley, California

During the upcoming solar maximum (Max'91) we plan to use the BIMA (Berkeley-Illinois-Maryland Millimeter Array) for imaging solar flares at millimeter wavelengths in a quasi-dedicated mode and study high energy aspects of the flare phenomenon. We also plan to use a dedicated single dish telescope for patrol observations of the Sun.

We have used the presently available Hat Creek array in March, 1989 to observe the major flare-producing active region AR 5395 at 3.3 mm. For most of the observing period (March 12-18, 1989) only two elements of the interferometer were available, with a spacing corresponding to 1 arcsec spatial resolution. This is smaller than the expected size of many solar burst sources. The available time resolution was only 10 seconds. Numerous bursts were seen during the observing peirod. Among the striking results from these data are the presence of much flux at 1 arcsec scales at 87 GHz, rise times of less than 10 seconds at millimeter wavelengths, and time delays of the millimeter relative to the microwave bursts and the hard X-rays in several (but not all) cases. On several occasions three baselines were available, and the data reveal striking asymmeteries of up to a factor of 10 in flux in different directions. We believe that many of our bursts were over-resolved. We interpret much of the temporal spikiness to be due to "spatial noise", i.e. the presence of numerous variable structures at the 1 arcsec scale which combine in the interferometer beam. We do not believe we are detectng the total flux in these bursts. Nonetheless, this interpretation provides important information about burst development and spatial structure. This interpretation is confirmed by OVRO data: the phase measured at OVRO during a flare which showed spikiness at Hat Creek was highly variable, indicating shifts in the effective source centroid even at microwave frequencies.

J2-4
1440

UPLINK RADIO OCCULTATION: WAVE OF THE FUTURE?

G.L. Tyler, V.R. Eshleman, D.P. Hinson, I. Linscott,
E.A. Marouf, A.M. Peterson, R.A. Simpson

Center for Radar Astronomy
Stanford University
Stanford, CA 94305-4055

For almost a quarter century, radio occultation and bistatic-radar techniques have played a leading role in probing atmospheres, ionospheres, rings, and surfaces of the solar system planets and three of their major satellites. Information regarding these targets is obtained from observation of the perturbations in the amplitude, phase, and power spectrum of highly coherent sinusoidal signals transmitted from a spacecraft flying by the target and received on the ground. This "downlink" configuration was dictated by the need to record on the ground the massive volume of data usually collected (e.g., 10^{11} bits in about 10^3 s at Saturn) for later "off-line" processing. A typical 10 - 20 W spacecraft transmitted power limits achievable SNR at the distance of Saturn, for example, to about 50 dB in 1 Hz bandwidth. Potential future occultation and bistatic-scattering experiments could significantly benefit from a 30 - 40 dB SNR increase if conducted in "uplink" configuration, where 20 - 200 kW of power is typically available for transmission, at the expense of required onboard signal processing capability for data conditioning and compression. A spacecraft-receiving subsystem that meets power, weight, and data throughput constraints is well within today's available flight- qualified technology.

Technical feasibility is demonstrated through detailed conceptual design of a "Radio Science Receiver System," to be proposed for Cassini, an orbiting spacecraft planned to investigate Saturn, its rings and satellites during the years 2002 - 2006. We estimate, for example, that Cassini uplink radio occultation and bistatic-scattering could map both tenuous and thick regions of Saturn's rings with better than 100 m resolution and yield direct particle size distribution over 10 cm - 10 m radius range, a quantum leap over the Voyager spacecraft capabilities. The increased SNR also enables deeper probing of Saturn's atmosphere, possibly to levels below the ammonia cloud base, and also enable detailed dynamical studies of the small scale turbulence and wave structures in the atmospheres of Saturn and Titan. Furthermore, sensitive bistatic-radar observations could provide a wealth of information about Titan's surface state, small scale structure, and reflectivity. While Cassini is an obvious immediate beneficiary, an uplink configuration opens the door for other inventive applications such as scattering and propagation studies of comet nucleii, the unusual surfaces of the Galilean satellites, and the polar caps of Mars, among others.

J2-5 GOLDSTONE SOLAR SYSTEM RADAR SIGNAL PROCESSING
1520

E. H. Satorius, R. F. Jurgens, C. R. Franck, S. D. Howard,
L. Robinett, P. Jennex, S. Morris and D. Hills
Jet Propulsion Laboratory, MS 238-420
4800 Oak Grove Drive
Pasadena, California 91109

A high speed data acquisition system for the Goldstone Solar System Radar (GSSR) has been developed for processing echoes from planets, moons and asteroids (L. J. Deutsch, R. F. Jurgens and S. S. Brokl, The Telecommunications and Data Acquisition Progress Report 42-77, pp.87-96, Jet Propulsion Laboratory, Pasadena, CA 1984). For range-doppler mapping applications, the system utilizes a binary phase-coded (BPC) transmitted waveform and the received echoes are demodulated and correlated with a replica of the transmitted BPC waveform. A simplified block diagram showing the primary data processing path is depicted below.

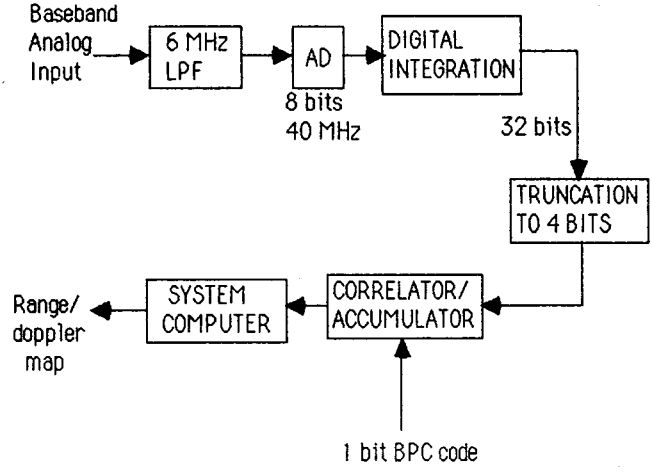

In this paper, we present an overview of the operation of this system focussing on nominal parameters that are utilized for the primary solar observations (Mars, Venus, Mercury, etc.). In addition, we summarize the results of an extensive, computer-aided performance analysis which has been carried out to quantify system dynamic range and processing gain. The results of this analysis not only provide an assessment of anticipated data quality for the various solar observations, but also provide useful guidelines for choosing GSSR data acquisition system parameters to enhance performance in future observations.

J2-6
1540

MODEL FOR 12.6cm WAVELENGTH RADAR BACKSCATTER FROM MARS

T. W. Thompson
Jet Propulsion Laboratory
California Institute of Technology
Pasadena, CA 91109
and
H. J. Moore
United States Geological Survey
Menlo Park, CA 94025

We have developed a model for both polarized (OC) and depolarized (SC) radar backscatter from Mars at 12.6-cm wavelength. Our model (1) matches the variations in total radar cross sections with longitude observed by Goldstone in 1986 along 7° S and (2) yields spectra that generally agree with the observed spectra.

In our model, Mars's surface is divided into radar map units that are based on geologic map units. These radar map units are further subdivided using thermal inertias. Depolarized-echo strengths for plains units vary as $A\cos(\theta)$ (where θ is the incidence angle and A is a backscatter intensity assigned to the radar map units on a degree-by-degree basis). Depolarized-echo strengths for volcanic units vary as $A\cos^2(\theta)$. Polarized-diffuse echo strengths vary as $3A\cos(\theta)$ for the plains units and as $A\cos^2(\theta)$ for the volcanic units. Quasi-specular echoes were computed using Hagfors' scattering law for angles of incidence out to 30°. Echo strengths (normal reflectivities) and root-mean-square slopes (the C parameter) were assigned to the units by trial and error. Coarse-scale topography is not included in the model.

Like the observations, model total-polarized (OC) cross sections vary with longitude as a two-cycle curve with maxima near 30° and 240° w. and minima near 130° and 330° W.; and model total-depolarized (SC) cross sections vary with longitude as a one-cylcle curve with a maximum near 135° W. and a minimum near 330° W.

J2-7 1600 RADIO PANEL OF AASC DISCUSSION: Chairman: K.I. Kellermann, NRAO, Edgemont Rd., Charlottesville, VA 22903

Session J-2 (cont.) 1930-Thurs. CR2-26
RADIO PANEL OF AASC DISCUSSION (cont.)
Chairman: K.I. Kellermann, NRAO, Edgemont Rd., Charlottesville, VA 22903

J2-8 RADIO PANEL OF AASC DISCUSSION
1930

Session AB-1 0835-Fri. CR1-46
MICROWAVE METROLOGY
Chairman: M. Kanda, Electromagnetic Fields Division, National Institute of Standards and Technology, Boulder, CO 80303

AB1-1
0840

MULTIGRID ANALYSIS OF FOUR-POINT-PROBE MEASUREMENTS OF TAPERED RESISTIVE SHEETS

Sue E. Haupt
National Center for Atmospheric Research
Boulder, CO 80307

Randy L. Haupt
DFEE
USAF Academy, CO 80840

Tapered resistive sheets can be attached to perfectly conducting bodies to modify their scattering patterns. A tapered resistive sheet consists of a fabric impregnated with carbon or a thin dielectric sheet coated with a thin metal film. Some applications require accurate measurement of the resistivity to achieve the desired scattering performance. One method to measure the resistivity is the four-point-probe. Four-point-probe measurements assume the probes are in the center of a constant resistive sheet. Measuring the resistivity of a tapered resistive sheet violates both assumptions: (1) the resistivity is not constant, and (2) the probes must be moved close to the edge to measure the resistive taper.

We numerically modeled the tapered resistive sheet/four-point-probe measurement system to determine the effects of tapering the resistivity of the sheet and moving the probes away from the center of the sheet. The equation for the voltage on a tapered resistive sheet is given by

$$-\nabla \cdot G(x,y) \nabla V(x,y) = 0$$

Relaxation is an appropriate method to solve this elliptic equation. However, relaxation leads to errors in the large-scale components of the solution. Application on grids of various resolutions in a systematic manner ameliorates this problem.

More specifically, we use a multigrid approach, beginning with the two-dimensional version of the MUDPACK system of multigrid solvers. This system readily allows specification of a nonconstant resistivity. However, this is not a straightforward application since the current injected by the four-point-probe introduces right-hand side singularities. We account for this by imposing interior boundary points that must be maintained on all levels of grid.

AB1-2
0900

WAFER-LEVEL MMIC MEASUREMENTS AT NIST

Roger Marks
Microwave Metrology Group, 723.01
National Institute of Standards and Technology
325 Broadway
Boulder, CO 80303

The NIST program to support on-wafer S-parameter measurements is concerned with the development of calibration techniques as well as physical standards. The focus is on TRL-based methods using transmission lines as standards. NIST is particularly interested in variations on the TRL theme in which redundant measurements are used to improve calibration accuracy. The concepts of the method, as well as preliminary simulated and measured results, will be presented.

AB1-3
0920

DEVELOPMENT OF ON-WAFER STANDARDS AT NIST

D. F. Williams, National Institute of Standards and Technology
325 Broadway Dept. 723.01
Boulder, CO 80303

The National Institute of Standards and Technology, in conjunction with an industrial consortium, has begun a program to develop standards and calibration services for microwave wafer level probing systems. Impedance standards are being designed to support wafer level S-parameter measurements from 1 to 40 GHz. Preliminary work is being done to develop a wafer level noise calibration service. The philosophy and scope of the effort will be discussed.

AB1-4
0940

RADIATION PROPERTIES OF PIGTAIL-TERMINATED COAXIAL TRANSMISSION LINES

Hassan A. N. Hejase
Department of Electrical Engineering
University of Kentucky
Lexington, Kentucky 40506-0046

Pigtail connections play a crucial role in radiation and shielding effectiveness. The inner conductor of the transmission line shown in Figure is excited by a delta-gap voltage generator on one end and terminates by an impedance load Z on the other end. The outer conductor or shield (assumed perfect) may be grounded through pigtails or left floating. Assuming thin-wire approximation, and using image theory and network analysis, the line could be modeled as a thin-wire antenna. The well-tested "WIRES" code is then used to compute the antenna radiation properties and shielding effectiveness. Computations are performed in the RF frequency range (30-1000 MHz). Pigtails on either or both ends of the line are treated as well as the floating-shield case (reference case). The effect of varying pigtail length and load terminations will be discussed.

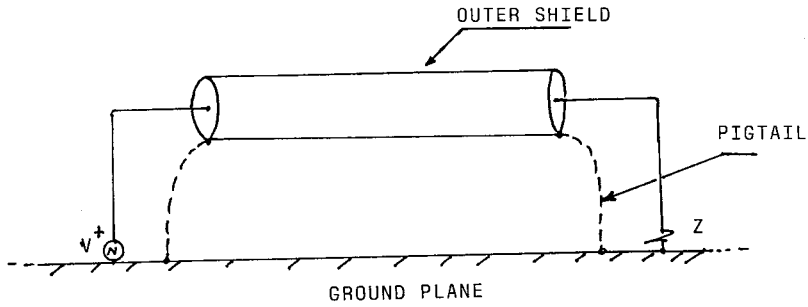

AB1-5
1020

OPTIMIZING LOW-FREQUENCY PERFORMANCE OF PYRAMID ABSORBERS USING BACKING LAYERS

Hugh Gibbons
Electromagnetics Laboratory
Dept. of Electrical and Computer Engineering
Campus Box 425
University of Colorado
Boulder, Colorado 80309

Present-generation anechoic chambers exhibit excellent broadband suppression of reflected waves in the microwave region using pyramidal (cone) absorbers. The very small reflections from pyramidal absorbers result from the fact that incident microwaves reflect several times from the cones before finally being reflected back away from the absorbers; since a fraction of the incident wave is absorbed at each bounce, the waves are very much depleted by the time they reflect back from an array of absorbers.

For lower-frequency waves, however, the case is very different. These waves have skin depths and wavelengths which exceed the spacing between the cones. As a result, the incident waves see the absorbers as a material having averaged or effective permittivity and conductivity which differ from those of air or "pure" absorber. The incident wave penetrates into the absorber material, which in the tapered region is effectively uniaxially inhomogeneous and anisotropic. It is therefore possible to approximate fields in the tapered region as plane waves propagating in an inhomogeneous medium, and to characterize the absorber array as a nonuniform transmission-line segment.

In order to extend the usefulness of microwave anechoic chambers to lower frequencies, we propose the use of an array of pyramid-absorbers as the topmost of a stack of absorbing layers. The different materials used in constructing the backing layers are intended to cause a low-Q resonance in the absorbing material, producing increased absorption of the incident wave at low frequencies without affecting higher frequency performance. The optimal design process which will be presented minimizes selected objective functions of the normal reflection coefficients at VHF frequencies where improvement upon current anechoic chambers is desired.

AB1-6 1040 ONE-WAY MILLIMETER WAVE RADOME TRANSMISSION LOSS MEASUREMENTS

Albert W. Biggs* and Peter L. Romine
University of Alabama in Huntsville
Huntsville, Alabama 35899, USA

This paper presents results of a measurement program for obtaining the one-way millimeter wave transmission loss through ablative radomes. Millimeter wave transmission loss was measured experimentally in the Systems Evaluation Test Chamber (SETC) at Redstone Arsenal, Alabama. Two different radome configurations were evaluated at the SETC. One had a metal cone attached to the tip of the radome, and the other had a small circular aperture (no cone).

One radome was measured with and without the nose cone, so that three sets of measurements were made. Results were plotted with a computer aided design program, with loss in decibels (dB) for the vertical scale and the azimuth and elevation angles in degrees for the horizontal scales.

One computer program, PROGRAM DATA, reads millimeter power measurements and writes them into the specified disk file. The other computer programs, PROGRAM LOSS, reads radome test data from PROGRAM DATA and converts it to dB and writes azimuth and elevation dB's to standard output. Both computer programs were written in "C" language. In three dimensional loss plot, the higher loss is identified at the 0° azimuth and 0° elevation angles.

*On an IPA Grant with WL/Kirtland AFB, New Mexico, 87117.

AB1-7
1100

SMALL ANGLE BISTATIC SCATTERING MEASUREMENT RESULTS USING NEAR-FIELD METROLOGY

M.A. Dinallo
BDM International
1801 Randolph Road, SE
Albuquerque, New Mexico 87106

Based upon a two-probe scanning metrology, near-field bistatic scattering measurements were acquired for a sphere (R.B. Rogers et.al., "Near-field Bistatic RCS Measurements," BDM/ABQ-88-0996-TR, RADC-TR Final Technical Report, March 1989.). The purpose of this experiment was to demonstrate the viability of using near-field metrology (D.M. Kerns, "Plane-Wave Scattering Matrix Theory of Antennas and Antenna-Antenna Interactions, NBS Memo 162, June 1981) for determining a scatterer's far-field RCS (M.A. Dinallo, "Extension of Plane-Wave Scattering-Matrix Theory of Antenna-Antenna Interactions to Three Antennas: A Near-Field Radar Cross-Section Concept," Proceedings Antenna Applications Symposium, University of Illinois, September 1984). The measured bistatic near-field was probe and background corrected, spatially filtered, and used to calculate the scattered far-field angular spectrum of the sphere. Comparisons were made to the theoretical E and H plane spectrums and within the spatial "domain-of-validity" agreement varied from fair to excellent. These results support the idea that a scatterer's far-field RCS can be determined based upon near-field metrology. The data comparisons will be presented along with a description of the instrumentation and spatial filtering used.

Session B-5 0835-Fri. CR2-28
NUMERICAL METHODS
Chairman: S. Rengarajan, Dept. of Electrical and Computer Engineering, California State Univ., Northridge, CA 91330

B5-1
0840

NUMERICAL ANALYSIS OF ERRORS ARISING IN THE FINITE ELEMENT SOLUTION OF ELECTROMAGNETICS PROBLEMS

L.J. Bahrmasel
R.A. Whitaker
McDonnell Douglas Research Laboratories
P. O. Box 516
St. Louis, MO 63166

We present a systematic study of errors arising in the finite element solution of electromagnetics problems characterized by a one or two-dimensional scalar Helmholtz equation with either Neumann or second order Bayliss-Turkel boundary conditions. Linear, quadratic, and higher order polynomial basis functions have been used. Let h be the maximum of the diameters among all the elements in the mesh and let p be the degree of the polynomial bases. Then the approximation theory and error analysis associated with the finite element method show that under reasonable hypotheses, the L_2-norm of the error is of the order h^{p+1} and that the matrix condition number is of the order h^{-2}. Moreover, if h is decreased too much, substantial errors may appear in the matrix elements, especially when analytical quadratures are used. For even moderately small values of h, standard results from the perturbation analysis of linear equations show that the judicious use of double-precision arithmetic in parts of the algorithm may be necessary to obtain results that are at best single-precision accurate. Our computed results are compared with these theoretical observations. While some of these observations are well known in the FEM community, the effect of complex-valued solutions and "non-standard" boundary conditions on error bounds and conditions numbers has not been adequately documented.

In addition, we make some observations on questions regarding the placement of the artificial boundary and non-physical reflections from the boundary (A.F. Peterson et al, PIERS, 1989).

B5-2
0900

A NOVEL IMPLICIT TIME-STEPPING CONJUGATE GRADIENT SCHEME FOR COMPUTING TRANSIENT ELECTROMAGNETIC FIELDS ON A METALLIC ENCLOSURE

Sina Barkeshli, Harold A. Sabbagh and Denis J. Radecki
Sabbagh Associates, Inc.
4639 Morningside Drive
Bloomington, Indiana 47401

A novel conjugate gradient scheme is developed for a three dimensional model of transient electromagnetic field coupling into a metallic enclosure (cavity). The model is based on the H-field boundary integral equation, and a finite element technique and utilizes an implicit time-stepping algorithm.

In the classical "explicit" time-stepping algorithm, the present values of the unknown tangential magnetic fields on the surface of the cavity, i.e., the surface currents, are found in terms of the calculated values in the past and the present value of the incident field. In this scheme there is no need for solving any system of linear equations. However, the main draw back of this algorithm is that the time stepping interval = Δt, must be less than (ρ_{ij}/c_0), where ρ_{ij} is the *minimum* spatial sampling interval, and c_0 is the speed of light. In addition, due to the accumulation of computing round off errors, and other phenomena, spurious oscillations occur during the "late time" of time stepping. These disadvantages are somewhat alleviated by an implicit time-stepping algorithm. In this algorithm an arbitrary time increment, Δt, can be used, but it requires the solution of a vector-matrix equation, $\mathcal{R}\mathbf{A} = \mathbf{Y}$, at each time step, where $\mathcal{R}$ is a known dyadic vector-matrix operator, $\mathbf{A}$ is the unknown column vector, and $\mathbf{Y}$ stands for the right-hand side. A novel conjugate gradient algorithm based on this system of vector-matrix equations is developed. The novelty of the algorithm is two-fold: First, the adjoint operator of $\mathcal{R}$ has been derived from the concept of the generalized quadratic form, which is required for the conjugate gradient scheme; second, because the size of the problem is exceedingly large, and in addition, we are dealing with an ill-conditioned operator, the global-to-local coordinate transformation is utilized in order to solve the operator equation over the two dimensional surface of the enclosure, rather than a three dimensional global coordinate system. This procedure not only provides a 33% (1/3) reduction of the size of the original system of equations, but also accelerates the rate of convergence.

Analytical development of this novel implicit time-stepping algorithm, along with some numerical results will be presented.

B5-3
0920

A Multizone, Time-Domain RCS Method with Gridding Based on Material Properties

Vijaya Shankar, Alireza Mohammadian, William F. Hall
Rockwell International Science Center
Michael Schuh
NASA Ames Research Center

Prediction of RCS for arbitrarily shaped layered objects requires a grid system that properly represents the geometry and the varying material properties in a manner that allows application of different boundary conditions, such as that on a perfectly conducting surface, across a material interface, across thin lossy coatings and resistive sheets. Since the speed of propagation is material dependent $\left(c = \frac{1}{\sqrt{\epsilon\mu}}\right)$, the grid resolution in each layer needs to be tailored based on the local material properties. A multizone frame is developed, where each zone of material layer is allowed to have its own grid and the transfer of information from one zone to another zone is done preserving appropriate material interface boundary conditions.

Results are presented for a variety of layered two and three dimensional cases to illustrate the power and the flexibility of this multizone approach.

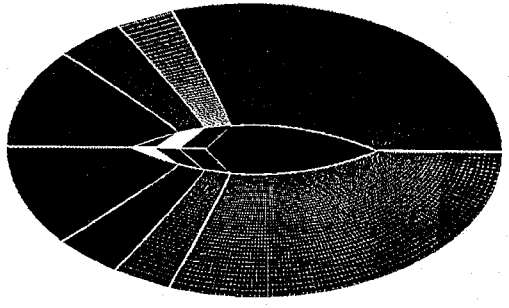

Multizone grid for a layered ogive

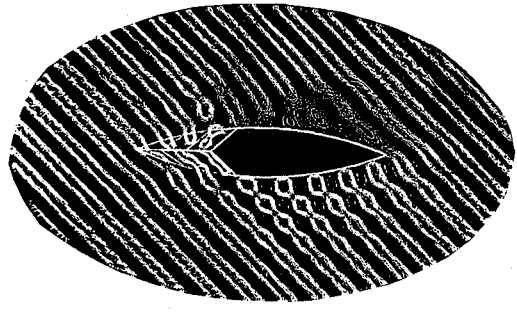

Instantaneous total field

B5-4
0940 **EFFICIENT COMPUTATION OF SOMMERFELD-TYPE INTEGRALS ARISING IN SCATTERING FROM A MULTI-LAYERED DIELECTRIC SLAB**

R. A. Whitaker
McDonnell Douglas Research Laboratories
P.O. Box 516
St. Louis, MO 63166

We present an efficient algorithm for the evaluation of Sommerfeld-type integrals that arise in a collocation solution for integral equations associated with an integral equation formulation for antennas and scatterers penetrating a multi-layered dielectric slab. Because of the presence of layered media, the computation of the elements of the moment matrix requires the numerical computation of Sommerfeld-type integrals appearing in the Green's function for the slab. The matrix is dense, so large numbers of these integrals must be computed. The potential errors in the solution of the linear system depend on the accuracy of the matrix elements. Hence, both efficiency and control of accuracy are desirable.

Adaptive quadrature schemes allow for reasonable control of accuracy, but often involve substantial cost due to large numbers of integrand evaluations. Indeed, the cost of integrand evaluations is the primary contributor to the overall cost of the quadratures. In the problem at hand, the Green's function for the slab is defined in a piecewise continuous manner and the computation of the Green's function in any one layer requires the recovery of the Green's function in all of the other layers. Hence the evaluation of the integrands is expensive and therefore, a "one at a time" approach to the computation of the integrals is wasteful. An alternative approach is the use of a quadrature algorithm for vector-valued functions. In addition, the integrands require the evaluation of elementary transcendental functions which are vectorizable on machines with Cray-like architecture. Thus, we should exploit potential vectorization.

We have developed a quadrature algorithm based on the design philosophy of QUADPACK (Piessens, et al.). Our adaptive algorithm uses Gauss-Kronrod quadrature formulae and allows for vector-valued functions, control of accuracy, and the vectorization of the vector-valued function evaluations. The results of computational experiments will be presented.

B5-5
1000

SOLVING THE RESONANCE PROBLEM IN ELECTROMAGNETIC SCATTERING COMPUTATION[1]

W.D. Murphy†, V. Rokhlin*, and M. S. Vassiliou†
(alphabetical)
†Rockwell International Science Center, 1049 Camino Dos Rios, Thousand Oaks, CA 91360
*Dept. of Computer Science, Yale University, New Haven CT 06520

The "resonance problem" considered here is that at certain values of the wavenumber k, the second-kind integral equation for solving scattering problems can become extremely ill-conditioned. This affects both the accuracy and speed of numerical solutions. The convergence of iterative methods in particular is adversely affected by large condition numbers. We consider the second-kind integral equation, derived using double-layer potentials, for TM scattering from a conductor. We solve an exterior Dirichlet problem. It has nonunique solutions for values of k at which the corresponding homogeneous interior Neumann problem has a nontrivial solution. These values of k are the resonant wavenumbers.

Numerically, we discretize the integral directly using quadrature formulas (Nystrom's method). We employ fourth-order convergent quadrature formulas which handle the logarithmic singularities in the problem (Murphy, Rokhlin, and Vassiliou, *Electron Lett.* 25, 643, 1989). We tested the solution procedure at resonant k's for circular and elliptical scatterers (roots of derivatives, respectively, of Bessel functions and modified Mathieu functions). We found very large condition numbers for the discrete matrices (up to $O(10^7)$), generally leading to poor solutions.

We apply two approaches to alleviate the resonance problem. The first is to use a different integral equation, based on both single and double-layer potentials, analogous to the combined-field equation (CFIE). This leads to low condition numbers, and good solutions, at resonant k.. The second method is to use the original second-kind integral equation, introduce a small imaginary part in k, and extrapolate back to the real axis. Solutions obtained by the two methods are in excellent agreement.

By solving the resonance problem, we ensure that fast and accurate solutions are obtainable at any arbitrary wavenumber.

[1]*This work was partially supported by Air Force Office of Scientific Research Contract Number F49620-89-C-0048*

B5-6
1020

THE FAST MULTIPOLE METHOD (FMM) FOR ELECTROMAGNETIC SCATTERING PROBLEMS[1]

W.D. Murphy†, V. Rokhlin*, and M. S. Vassiliou†
(alphabetical)
†Rockwell International Science Center, 1049 Camino Dos Rios, Thousand Oaks, CA 91360
*Dept. of Computer Science, Yale University, New Haven CT 06520

The Fast Multipole Method (FMM) was developed by Rokhlin (*J. Comp. Phys.* 60, 187-207, 1985; *Yale Univ. Research Report* YALEU/DCS/RR-440, 1985) to reduce the computation time required for solving scattering problems modeled in the form of integral equations. When such integral equations are discretized, a full dense linear system of size n x n results. If direct methods such as Gaussian Elimination are used to solve the system, $O(n^3)$ arithmetic operations are needed. If indirect methods such as Generalized Conjugate Residual (GCR) are employed, $O(n^2)$ arithmetic operations are needed for each iteration. Rokhlin has shown that the operation count may be reduced to $O(n \log n)$per iteration, by using the structure of the Green's function and the fact that only an approximation to the matrix product is needed. The algorithm is analogous to the evaluation of the field created by a charge and dipole distribution (hence the name "Fast Multipole Method"). The actual implementation thus far uses a simpler algorithm which achieves $O(n^{4/3})$, although $O(n \log n)$ is achievable theoretically. For moderately large problems ($n \approx 20000$), the two algorithms yield similar CPU times, although for very large problems, implementing the full $O(n \log n)$ algorithm is desirable.

Originally, Rokhlin's work was for acoustic scattering problems where a fluid scatterer is embedded in a two-dimensional fluid space. This mathematical problem is formulated as a coupled system of integral equations between the interior and exterior problems. Rokhlin extended these ideas also to two and three-dimensional potential theory (Laplace's equation) where even faster computations are possible (O(n) operations).

We review some of these results, and extend their application to the area of electromagnetic scattering. Initial results with the $O(n^{4/3})$ algorithm have been obtained for TM scattering from arbitrarily shaped two-dimensional closed conductors. The FMM, combined with fourth-order convergent quadrature formulas in Nystrom's method (Murphy, Rokhlin and Vassiliou, *Electronics Letters* 25, 543-644, 1989) represents a very fast and accurate method to solve electromagnetic scattering problems from electrically large objects.

[1]*This work was partially supported by Air Force Office of Scientific Research Contract Number F49620-89-C-0048*

B5-7
1040

DIRECT TREATMENT OF THE EFIE WITH HALF THE COMPUTATION

Francis X. Canning
Rockwell International Science Center
1049 Camino Dos Rios
Thousand Oaks, CA 91360

The Electric Field Integral Equation (EFIE), whether it is used for either polarization in two dimensions or is used in three dimensions, involves a complex symmetric operator. Whenever the same testing and basis functions are used, the resulting moment method equation is also complex symmetric (and also non-Hermitian). Stable methods exist which directly solve this matrix with roughly half the storage and execution time as required for the non-symmetric case. Apparently these methods are not widely known and the resulting advantage in storage and execution time of the EFIE (when a direct solution is used) over other methods (such as the MFIE and CFIE) seems not to be widely appreciated.

Direct solutions of moment method problems usually are accomplished in terms of the LU decomposition of the matrix "Z." As is well known, this decomposition method is unstable, unless atleast partial pivoting is used. The only form of partial pivoting that preserves symmetry involves interchanging the rows and columns at the same time and in the same way. Unfortunately, this cannot remove small (or zero) elements from the diagonal, so the resulting method is unstable. However, there are two stable methods. One method involves factoring Z into two conjugate triangular matrices, and a third nonsymmetric tridiagonal matrix. Another, the diagonal pivoting method, is even included in Linpack (see CSPFA, CSPSL, CSIFA, CSISL, ...). Both of these methods require, to leading order, storage for $N^2/2$ complex numbers and $N^3/6$ complex multiplications and additions. This is exactly half of the requirement for the nonsymmetric case. More details and some references are given in F.X. Canning, Direct Solution of the EFIE with Half the Computation, submitted to IEEE Trans. on AP.

Methods for finding the condition number of Z and also for correcting scattered fields for the effects of interior resonances have previously been described. We show that these calculations can also be done using the faster decompositions given above, so they again take a negligible additional execution time and storage.

We have described a method for halving the computer resources with *no loss in accuracy* for direct solution of the moment method equations when Z is symmetric. It is hoped that by drawing attention to this little known fact, many existing Galerkin EFIE codes might be converted to run at half the cost. In addition, conversion to a symmetric formulation might be considered for existing nonsymmetric EFIE computer codes.

B5-8
1100

ORTHOGONAL BASIS FUNCTIONS THAT GENERATE A SPARSE MOMENT METHOD MATRIX

Francis X. Canning
Rockwell Science Center
1049 Camino Dos Rios
Thousand Oaks, CA 91360

In the past, integral equation based calculations of electromagnetic scattering and radiation (e.g. moment method calculations) have required a full N by N matrix when there are N unknowns. In this paper, novel basis and testing functions are presented for which all but of order N of these matrix elements are so small that they may be approximated by zero. Details of this **impedance matrix localization** technique are given in F.X. Canning, "Reducing Moment Method Storage from Order N^2 to Order N," Electronics Letters, Sept. 14, 1989 and F.X. Canning, "Transformations that Produce a Sparse Moment Method Matrix," submitted to IEEE Trans. on Antennas and Propagation.

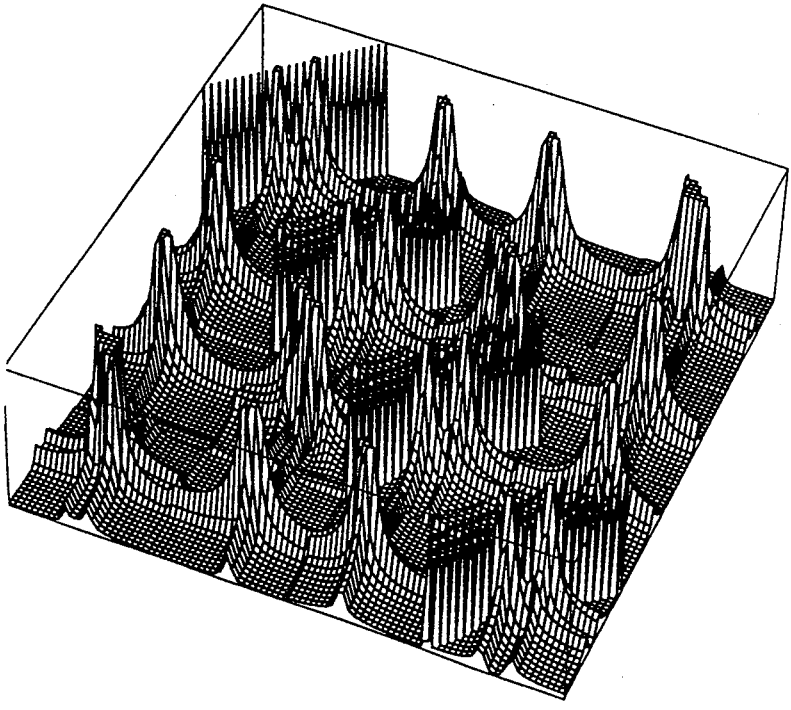

3D PLOT OF THE MAGNITUDES OF THE RESULTING MATRIX ELEMENTS

B5-9
1120

APPLYING GENERALIZED MATRIX INVERSES IN COMPUTATIONAL ELECTROMAGNETICS PROBLEMS

M. Thorburn, V.K.Tripathi
Electrical & Computer Engineering Dept.
Oregon State University
Corvallis, Oregon 97331-3202

Electromagnetics problems, resulting from the analysis of antennas, scattering, or microwave integrated circuits, often require the formulation and solution of large linear systems of equations. Typically the systems are formulated so that they are non-singular and can be solved using traditional matrix inversion.

A Generalized Matrix Inverse (GMI) [Penrose, Proc. Cambridge Phil. Soc., 51] can be defined to give a generalized solution to systems that might otherwise either not have a solution or not have a unique solution. Traditionally GMI's have been used in problems such as electromagnetic geophysical inversion [Frank & Balanis, IEEE-GRS, vol.27, #3, 1989] and in many areas of data assimilation. Recently GMI's were used in an analysis of discontinuities in MIC's for one port and in-line two port problems that where overdetermined [Chen & Gao, IEEE-MTT, vol.37, #3, 1989] and in a procedure to improve moment-method predictions with measurements [Stach, ACES Symposium 1989].

This paper will begin with a study on the use of the GMI for a variety of simple canonical electromagnetic problems in antennas, scattering, and microwave circuits for both underdetermined and overdetermined cases. Comparison with known solutions will be made and interpretation of the results will be given. The paper will conclude with a presentation on the application of GMI's to a family of general microstrip discontinuity problems of importance in printed circuit and microstrip antenna design.

B5-10
1140

SOME IMPROVEMENTS TO THE FDTD METHOD FOR CALCULATING RCS OF PERFECTLY CONDUCTING TARGETS

By

C. M. Furse, S. P. Mathur and O. P. Gandhi
Department of Electrical Engineering
University of Utah, MEB 3280
Salt Lake City, Utah 84112

ABSTRACT

The finite-difference time-domain (FDTD) method has been used extensively to calculate scattering and absorption from both dielectric objects and perfectly conducting objects. Several improvements to the FDTD method for calculation of RCS of perfectly conducting targets are presented in this paper. The use of sinusoidal and pulsed FDTD excitations are compared to determine an efficient method of finding the frequency response of targets. Maximum cell size, minimum number of external cells, and a new method to eliminate field storage in the shielded internal volume of perfect conductors are discussed to minimize the large computer storage requirements of FDTD. The dc offset in the magnetic fields around highly conductive objects is observed and removed by post-processing to achieve convergence of RCS calculations. RCS calculations using FDTD method in two dimensions are presented for both square and circular infinite cylinders, illuminated by both TE and TM polarized plane waves. RCS of a metal cube in three dimensions is also presented. Good agreement between FDTD calculations and theoretical values is achieved for all cases, and parameters necessary to achieve this agreement are examined.

C1-1
0840

Subspace Methods for Real Time Adaptive Beamforming

Michael P. Clark **Richard A. Roberts**

Department of Electrical and Computer Engineering

University of Colorado at Boulder

Abstract

Adaptive beamformers which construct their weight vectors using direct inversion of the array covariance matrix have many desirable characteristics. However, due to finite resources, matrix inversion may constitute an intractable computational problem. We consider a rank-one eigenvalue update procedure for tracking the covariance matrix. When subspace methods are employed with the update procedure, computation is dramatically reduced and real time beamforming becomes practical.

C1-2
0900

EIGENSPACE SPATIAL-SPECTRUM ESTIMATION WITH MULTIPLE BEAM ANTENNAS, K.M. Buckley, M. Hoffman, and X. L. Xu, Department of Electrical Engineering, University of Minnesota

Eigenspace based azimuth/elevation-spectrum estimation with a continuous aperture MBA is investigated, assuming small fractional bandwidths centered in the GHz frequency range. Mayhan and Niro have considered this problem previously, concentrating on systems considerations, using as an example the MUltiple SIgnal Classification (MUSIC) spatial-spectrum estimator. This presentation focuses on the selection of an eigenspace azimuth/elevation-spectrum estimator. We consider performance issues such as spectrum estimator dependent source ambiguity, resolution thresholds, location estimate variance and false source detections.

For a planar MBA array, eigenspace estimators which compute a azimuth/elevation spectrum by projecting antenna/feed vectors (on the array manifold) onto only a single vector in the estimated noise-only subspace exhibit source ambiguity. This ambiguity is manifested as annular ring peaks in the azimuth/elevation spectrum. It results because generally, for planar arrays, the orthogonal complement of any vector in the noise-only subspace will be orthogonal to all antenna/feed vectors on a continuous line trace on the 2-dimensional array manifold. This ambiguity limits the number of spectrum estimators which can be applied to MBA's. There are two basic approaches to eigenspace spatial-spectrum estimators that can be used with MBA's to provide *unambiguous* source azimuth/elevation estimates. These are the MUSIC approach, and the First prINcipal vEctorS (FINES) approach recently developed by Buckley and Xu. Both MUSIC and FINES suppress false peaks. Azimuth/elevation estimates derived from FINES have variance comparable to that of MUSIC. We recommend FINES because it provides higher resolution.

C1-3
0920

Analysis of Sampled-Aperture Radar Data Using the Method of Multiple Windows

by:

Simon Haykin, David Thomson, Tasos Drosopoulos, and Vytas Kezys

---

ABSTRACT

In this paper we briefly review the low-angle tracking radar problem, and describe a sampled-aperture radar system for an experimental study of this problem. The system consists of a 32-element array antenna that incorporates dual-frequency transmission, with one frequency fixed and the other one adjustable. Provision is also made for the use of dual polarization on transmit. Experimental data have been collected with this system at a site on Lake Huron, Ontario. Part of this data base has been analyzed using Thomson's method of multiple windows. The paper will present the results of this power spectrum analysis, highlighting the characteristics of diffuse multipath, and the effects of frequency diversity and polarization.

C1-4
0940

RANK REDUCTION AND ORDER SELECTION FOR INVERSE PROBLEMS

A. Thorpe and L. Scharf, Dept. of Electrical and Computer Engineering, University of Colorado, Boulder, CO 80309-0425

There are two types of problems in the theory of least squares: parameter estimation and signal extraction. Parameter estimation is called "inversion" and signal extraction is called "filtering." In this paper we present a unified theory of rank reduction and order selection for solving over-determined and under-determined versions of these problems. We present results of numerical experiments conducted on synthetic time series.

C1-5
1020

A CEPSTRUM BASED TECHNIQUE FOR THE DECONVOLUTION OF TDR SIGNALS

Abdelhak Bennia and Sedki M. Riad
Bradley Department of Electrical Engineering
Virginia Polytechnic Institute and State University
Blacksburg, VA 24061

The impulse response of an unknown system is recovered from time domain reflectometry data by implementing a method based on the homomorphic deconvolution theory. The separation process of the convolved signals is achieved through the combination of the cepstrum technique and conventional signal processing procedures such as noise filtration. The method is possible due to the nature of time domain reflectometry signals being studied.

Some experimental results are presented to illustrate the application of the technique to time domain reflectometry deconvolution problems.

C1-6
1040

THIRD ORDER PHASE LOCKED LOOP: CHARACTERIZATION AND PARAMETERS

José Manuel Riera Salís, Luis Mercader del Río
Dpto. SSR, ETSIT Telecomunicación, 28040 MADRID (Spain)

It is well known (W.C.Lindsey,Synchronization Systems...,Prentice-Hall,1972) that optimum tracking of a frequency ramp requires a third order Phase Locked Loop. Apart from this fact, only a few other aspects about third order loops appear in the technical literature. Nevertheless, third order PLL could be very useful in some new applications, namely mobile communications.

In this paper we will present a new set of parameters developed to describe third order loop behaviour. Noise bandwidth (BL), transient processes and optimality are related to these parameters (ω_n,ζ,γ), which acquire a clear physical meaning. The theory is based on the well-known second order loop theory, so that it may be easily understood by design engineers who are used to it.

As an example, in the figure we plot several constant bandwidth curves versus the above mentioned parameters.

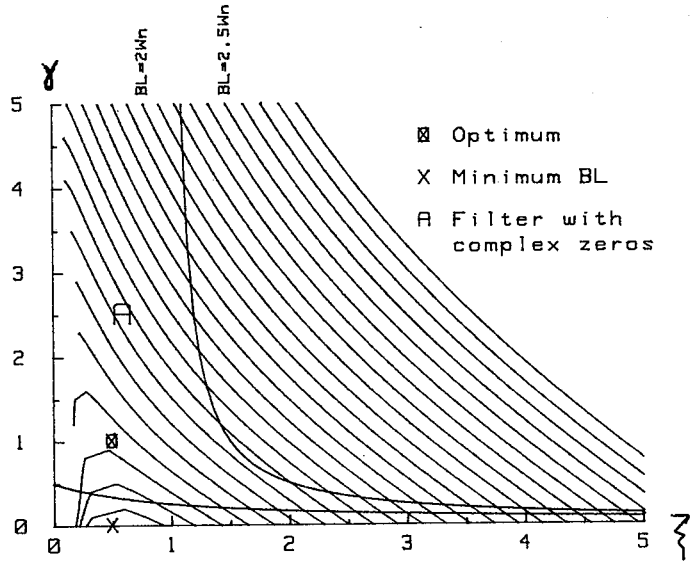

Session D-4 0835-Fri. CR1-40
MICROSTRIP STRUCTURES
Chairman: J.W. Mink, Army Research Office

D4-1
0840

EFFICIENT CALCULATION OF PARASITIC COUPLING EFFECTS ON MICROSTRIP S-PARAMETERS

Kent J. Larson
Department of Electrical and Computer Engineering
University of Colorado at Boulder
Boulder, CO 80309-0425

On a local microstrip network, the parasitic coupling of adjacent microstrip lines may often produce undesirable effects on S-Parameter measurements. This effect increases as the parasitic line approaches the microstrip line of interest. This is exemplified by the undesirable effects induced at either the input of an active device (such as a high gain amplifier) or on a highly resonant circuit (such as a filter).

The purpose of this work is to derive a general approach toward dealing with parasitic effects on MMIC circuits when the parasitic problem involves "loose" coupling. The approach is to first solves for the network's S-Parameter values disregarding all parasitic effects. This is accomplished using currently available software packages. The unperturbed S-Parameters are then used to solve for voltages and currents everywhere in the local network. Through analysis of the induced vector magnetic potential, dependent voltage sources are developed which ultimately are reincorporated into the original network for reanalysis by the commercial software package. The resulting S-Parameters give first order perturbed results demonstrating the effect of the parasitic line. The geometry of this method is simple to construct, and it is anticipated this approach will be more computationally efficient that full wave integral equation methods. The method also takes advantage of utilizing commercially available software packages.

The talk will discuss a specific case of the approach, that of a linear half-wave resonator placed near a transmission line. For this parasitic resonator example, both theoretical and experimental results will be given.

D4-2
0900

BINOMIAL AND CHEBYSHEV TRANSFORMERS FOR DIELECTRIC AND MICROSTRIP LINES

Albert W. Biggs* and Robert T. Kinasewitz**
*Electrical and Computer Engineering Department
University of Alabama in Huntsville
Huntsville, AL 35899
**Armament R & D Center
Picatinny Arsenal, New Jersey 07806

This paper describes the design of binomial and Chebyshev transformers for microstrip lines (R.M. Knox, IEEE Trans. MTT-24, 806-814, 1976), strip dielectric waveguides (T.T. Fong and S.-W. Lee, IEEE Trans. MTT-22, 776-783, 1974), inverted strip dielectric guides (T. Itoh, IEEE Trans. MTT-24, 821-827, 1976), image waveguides and "insular" guides (R.M. Knox and P.P. Toulios, Proc. Nat'l. Elec. Conf., Chicago, 489-492, 1974), insulated image guides (W.V. McLevige, T. Itoh, and R.Mittra, IEEE Trans. MTT-23, 788-794, 1975), slot lines (S.B. Cohn, IEEE Trans. MTT-17, 768-778, 1969), double-layer slot lines (N. Samardzija and T. Itoh, IEEE Trans. MTT-24, 768-778, quasi-planar transmission lines such as coplanar guides, conductor backed coplanar guides, coplanar strips, suspended stripline, inverted stripline, microslab guides, and finlines (T. Itoh, IEEE Trans. MTT-37, 275-280, 1989).

Transformer sections or unit cells in the transformer were designed to obtain maximally flat passband responses with binomial coefficients (J. Stone Stone, U.S. Patents 1,643,323 and 1,715,433) and "equal ripple" VSWR response with Chebyshev polynomial coefficients, where minima VSWR are achieved with a given bandwidth (or maxima bandwidth with a given VSWR).

An example is developed with microstrip lines. The characteristic impedances can be found with three models (H.A. Wheeler, IEEE Trans. MTT, MTT-13, 171-185, 1965; M. Schneider, BSTJ, 48, 1421-1444, 1969; E.O.Hammerstad, Proc. European Microwave Conf., Hamburg, Germany, 268-272, 1975). Tabulations were made with characteristic impedances for different copper clad dielectric sheet thicknesses, relative dielectric constants, and ratios of stripline width to sheet thickness.

*With an Intergovernmental Personnel Act (IPA) Grant at the Weapons Laboratory/AWPB, Kirtland AFB, New Mexico 87117-6008. TCS from Electrical Engineering Department, University of Alabama in Huntsville, Huntsville, Alabama 35899.

D4-3
0920

ENTIRE-DOMAIN BASIS ANALYSIS OF COUPLED MICROSTRIP TRANSMISSION LINES

C.-H. Lee and J. S. Bagby*
Department of Electrical Engineering
University of Texas at Arlington
Arlington, TX 76019
Y. Yuan and D. P. Nyquist
Department of Electrical Engineering
Michigan State University
East Lansing, MI 48824

A full-wave spectral-domain integral equation formulation is used to analyze coupled microstrip transmission lines. A Method of Moments solution is implemented utilizing entire-domain basis functions which incorporate appropriate edge conditions for transverse and longitudinal current components, allowing for closed-form evaluation of spatial integrals.

In contrast with earlier subdomain basis solutions, greatly improved accuracy is obtained using far fewer terms. Numerical results in the form of dispersion curves and current distributions are presented for several modes, and are compared with the results of other techniques.

D4-4
0940

PROPAGATION REGIMES ON INTEGRATED MICROSTRIP TRANSMISSION LINES

J. S. Bagby* and C.-H. Lee
Department of Electrical Engineering
University of Texas at Arlington
Arlington, TX 76019
D. P. Nyquist and Y. Yuan
Department of Electrical Engineering
Michigan State University
East Lansing, MI 48824

There has recently been a resurgence of interest in the propagation characteristics of open microstrip transmission lines. This is due to the discovery of new propagation regimes for higher-order modes on the lines.

In contrast to the dominant EH_0 mode on microstrip transmission lines, three distinct propagation regimes for higher-order modes exist on open integrated transmission lines. In this paper a powerful new integral equation formulation is used to analyze propagation in all three regimes for integrated microstrip transmission lines.

This formulation provides a clear physical picture of the different propagation regimes based on the location of poles and branch points in the complex spectral variable plane. The intgral equation is discretized via the Method of Moments, where entire-domain basis functions incorporating suitable edge behavior are utilized to provide accurate results with relatively few terms. Numerical results obtained are compared with the results of other workers, and good agreement is observed.

D4-5
1000

CONVERGENCE OF THE NUMERICAL SOLUTION FOR A MICROSTRIP JUNCTION BASED UPON A TRIANGULAR CELL EXPANSION

J. X. Zheng and David C. Chang, MIMICAD Center
Department of Electrical and Computer Engineering
University of Colorado,
Boulder, Colorado 80309-425

In numerical modeling of microstrip junction discontinuities, it is often necessary to solve appropriate integral equations for the vector current distribution over a surface having a non-rectangular geometry. Dividing the surface of interest into triangular cells and replacing both the x- and y-component of the current distribution by a linear approximation, had been proposed as a viable alternative to the more typical scheme of using rectangular cells of varying size to match the portion of boundary having a non-rectangular shape. Such a scheme has a direct analogy in the finite element method. Orientation and shape of these cells do not seem to have a strong bearing to the convergence of this solution process.

We have implemented such a scheme for solving current distribution on a microstrip structure. We obtain first a formulation which only two scalar Green functions of electric and magnetic type. They are evaluated numerically, after extracting the the singular or the 1/R term. The results are then fit into a polynomial in R in a least-square manner. The moment integrals associated with each term in the polynomial, including the 1/R, are then evaluated analytically.

Different orientations and shapes were investigated and compared with bench marks obtained earlier for a rectangular microstrip of arbitrary width. We first included only the x-component for the case of narrower width, since experimental results suggest that the y-component indeed can be ignored in that case. All schemes of trian-gulation exhibit convergence when enough number of cells are used; however, the manner they approach convergence differ greatly from one to another. On the other hand, no visible convergence is observed when we include both x- and y-component, unless a substantially larger number of cells are used. Plausible explanations to this peculiar behavior will be offered in this work.

D4-6
1020

MICROSTRIP CONDUCTOR LOSS CALCULATIONS USING THE LEWIN/VAINSHTEIN METHOD

Edward L. Barsotti, Edward F. Kuester, and
John M. Dunn
MIMICAD Center
Department of Electrical Engineering
University of Colorado at Boulder
Boulder, CO 80309-0425

Recently, Lewin (*IEEE Trans. Micr. Theory Tech.*, vol. 32, pp. 717-719, 1984) and Vainshtein (*Sov. Tech. Phys. Lett.*, vol. 12, no. 6, pp. 298-299, 1986) have independently developed a perturbation method of calculating the strip portion of the conductor loss of a nonzero-thickness microstrip using integrations of the currents from the limiting case of a quasi-TEM zero-thickness strip. The ground plane loss contribution is typically small in a microstrip environment, so the strip contribution forms the major part of the total conductor loss. The edge singularity is avoided by stopping the integration just short of the edge by an amount determined by the local geometry near the nonzero-thickness edge. Actual implementation of this method may be difficult, since division of the zero-thickness current onto the top and bottom surfaces of the strip can be difficult in planar lines, particularly in microstrip.

An examination of the derivation and implementation of the Lewin/Vainshtein method will be done here. The results from this method will be compared with other published loss results which use the surface impedance boundary condition, including the commonly accepted results of Pucel et al. (*IEEE Trans. Micr. Theory Tech.*, vol. 16, pp. 342-350, 1968; corrected in *IEEE Trans. Micr. Theory Tech.*, vol. 16, p. 1064, 1968) and Schneider (*Bell System Technical Journal*, vol. 48, no. 5, pp. 1421-1444, 1969).

D4-7
1040

EFFICIENT ANALYSIS OF PLANAR SINGLE AND DOUBLE LAYERED MICROSTRIP GEOMETRIES USING ASYMPTOTIC CLOSED FORM MICROSTRIP SURFACE GREEN'S FUNCTIONS

Sina Barkeshli
Sabbagh Associates, Inc.
4639 Morningside Drive
Bloomington, Indiana 47401

Newly developed closed form asymptotic representations of the grounded single (substrate) and double (substrate/superstrate) layered slab Green's functions can be very efficiently applied to solve planar microstrip configurations. These asymptotic Green's functions remain accurate even for very small lateral separations of source and observation points (e.g., a few tenth of the free space wavelengths); for observation points in the vicinity of the source, a modified form of the Sommerfeld integral is used. It is noted that the conventional Sommerfeld integral as well as the plane wave spectral (PWS) representations of the single layered as well as double layered Green's functions converge very slowly when the source and field points are laterally separated and both are located in the same interface.

Various quantities of interest for single and double layered geometries such as the input impedance and the current distribution of a finite length, center-fed strip doipole in substrate and substrate/superstrate configurations will be presented. The numerical efficiencies of these newly developed Green's functions will be discussed.

D4-8
1100

SPURIOUS RADIATION FROM MICROSTRIP BENDS AND Y-JUNCTIONS WITH ARBITRARY ANGLES

M. D. Abouzahra
Massachusetts Institute of Technology
Lincoln Laboratory
Lexington, MA 02173
R. Pavelle
Computer Algebra Associates
23 Berkshire Drive
Winchester, MA 01890

All discontinuities and transitions in microstrip lines radiate either by intention or spuriously. Estimates of the power radiated from various microstrip discontinuities, such as right-angle corner, open circuit, short circuit, matched and unmatched terminations, Y-junction, and matched symmetrical T-branch, were first reported by Lewin [Proc. Inst. Elec. Eng., 117, Part C, pp 163-170, Sept. 1960]. More accurate estimates of the power radiated from open circuit and short circuit microstrip discontinuities, as well as from a mismatched termination, were reported later by Abouzahra and Lewin [IEEE Trans. Microwave Theory Tech., Vol. 27, pp 722-723, Aug. 1979 and Vol. 29, pp 666-668, July 1981].

In this paper, the far-field Poynting vector method, which was originally described by Lewin and later extended by Abouzahra and Lewin, is used to derive closed form expressions for the power radiating from microstrip bends and Y-junctions with arbitrary angles. This paper also explains how computer algebra (MACSYMA) is used to derive the closed-form expressions. The derivation of these expressions is sufficiently laborious that manual derivation would have been very difficult or almost impossible.

This work was sponsored by the Department of the Air Force. The views expressed are those of the authors and do not reflect the official policy or position of the U. S. Government.

D4-9
1120

INTEGRAL-OPERATOR ANALYSIS OF LEAKY MICROSTRIP MODES--SPECTRAL EVALUATION OF RELEVANT KERNELS

J. M. Grimm* and D. P. Nyquist
Department of Electrical Engineering
Michigan State University, E. Lansing MI 48824
J. S. Bagby
Department of Electrical Engineering
University of Texas at Arlington, Arlington TX 76019

Over the past few years, the phenomena associated with the bound guided-wave modes of the microstrip transmission line have been investigated thoroughly. Since the bound discrete modes are relatively well understood, efforts here are focused on the analysis of the discrete leaky-wave modes of microstrip transmission lines.

Analysis of these leaky modes can be accomplished by the application of a well-known electric field integral equation, namely

$$\hat{t}\cdot(k_c^2+\nabla\nabla\cdot)\int_C \bar{\bar{g}}(\vec{\rho}\mid\vec{\rho}\,';\zeta_k)\cdot\vec{k}(\vec{\rho}\,')\,d\ell' = 0 \quad \text{... for all } \vec{\rho}\in C$$

where $\bar{\bar{g}}$ is the Hertzian potential Green's dyad for the background region, $\vec{k}$ is the current of the microstrip mode with eigenzeta ζ_k, and C is the cross-sectional contour of the microstrip surface. The components comprising the Green's dyad are inverse Fourier transforms on spectral variable ξ, and assume the form of Sommerfeld integrals. These dyadic components possess, in the transform plane, singularities that correspond to the background structure surface wave modes, and zeros in the transformed wavenumbers that necessitate branch cuts to determine proper Riemann surfaces. For convergence of the dyadic components in the leaky wave regime, a priori knowledge of the exact inversion contour is needed.

The migration paths and characteristics of the transform plane poles and branch points will discussed. An alternative technique, utilizing the entire complex transform plane, will be applied to the evaluation of the Green's dyadic for microstrip leaky-wave modes. This technique has the advantage of not requiring a priori knowledge of the inversion contour, and also having a simple physical analogy. Comparisons with real-line integration techniques will also be made.

D4-10
1140

ANALYSIS OF DISPERSION CHARACTERISTICS AND LEAKAGE PROPERTIES OF MICROSTRIP TRANSMISSION LINES

Yi Yuan and Dennis P. Nyquist
Department of Electrical Engineering
Michigan State University
East Lansing, Michigan 48824

Dispersion and leakage characteristics of microstrip transmission lines are of considerable importance and practical interest due to the extensive use of the microstrip configuration in micro/mm-wave integrated circuits. At high frequencies, accurate evaluation of dispersion and leakage characteristics are essential to the analysis of wave propagation and device interactions in microstrip circuits. Previous study revealed that leaky modes reside in a "radiation region" where higher order modes are below cutoff [Oliner, 1986].

In this paper, we present a rigorous full-wave integral equation analysis of dispersion characteristics and leakage properties of microstrip transmission lines. This EFIE description is based on an electric dyadic Green's function for layered IC environments. The complete propagation-mode spectrum of microstrip line is identified from a singularity expansion of its currents. An excitation and coupling theory is developed. Radiation and surface-mode leakage properties are studied via complex analysis. Particular attention is given to pole and branch point singularities of the Sommerfeld integrals implicated in the Green's function. It is found that the poles and the branch points migrate when the discrete modes enter into the leaky regime. In that region, complex contour integration must be utilized instead of the conventional real axis inverse transformation. The proper integration contour in the complex plane is determined and justified. From this analysis the leaky-mode characteristics of microstrip line are deduced naturally and consistently.

Numerical implementation for the microstrip line is developed. The EFIE's for isolated and coupled microstrip lines are solved by Galerkin's moment method with Chebyshev polynomial basis functions. Dispersion characteristics, leakage properties and current distributions are obtained and are compared with other available published data.

Session G-4 0855-Fri. CR2-6
HIGH LATITUDE EFFECTS
Chairman: H. Soicher, U.S. Army Communications, Electronics Command, Ft. Monmouth, NJ

G4-1
0900

FIRST RESULTS FROM THE DIGISONDE AT SONDRESTROM

J. Buchau,[1] G. Crowley,[2] and B. W. Reinisch[2]

[1]Geophysics Laboratory, Hanscom Air Force Base, Bedford, MA 01731

[2]University of Lowell Center for Atmospheric Research (ULCAR), 450 Aiken Street, Lowell, MA 01854

The Digisonde is an advanced ionospheric sounder developed at ULCAR. It is an exciting new tool for obtaining important ionospheric information. Like a conventional ionosonde, the Digisonde yields vertical electron density profiles. The antenna arrangement and sophisticated data processing system also permits plasma drift velocities to be derived from the ionospheric reflections.

In June 1989, a Digisonde system was installed at Sondrestrom, Greenland (67°N, 50°W), colocated with the incoherent scatter radar. Electron density profiles and drift data under different conditions will be presented: both are extremely high quality. The drifts can generally be interpreted in terms of a two cell convection pattern.

G4-2
0920

IMF CONTROLLED VARIATIONS IN THE CONVECTION FLOW DIRECTION NEAR THE CORRECTED GEOMAGNETIC POLE

P S Cannon[1,2], B W Reinisch[1], J Buchau[3], G Crowley[1], and R Lepping[4]

[1]University of Lowell Center for Atmospheric Research, 450 Aiken Street, Lowell, Massachusetts 01854, USA.

[2]Permanent Address - Applied Ionospheric Physics Laboratory, Flight Management Department, Royal Aerospace Establishment, Farnborough, Hampshire GU14 6TD, UK.

[3]Geophysics Laboratory, Hanscom Air Force Base, Bedford, Massachusetts 01731, USA.

[4]Goddard Space Flight Center, Greenbelt, Maryland 20771, USA.

The F-region ionospheric plasma convection direction at Qaanaaq, near the corrected geomagnetic pole, has been measured using a Digisonde 256 ionosonde. Data from 1986, 87, and 88 have been selected when stable Bz north or Bz south interplanetary magnetic field (IMF) conditions obtained for 30 minutes previous to the convection measurement. The IMF was measured by the IMP8 spacecraft. Several hundred convection direction measurements have been selected and examined for consistency of flow direction as a function of all components of the IMF field strength. Preliminary analyses indicate that when Bz is negative the strength of the IMF By component strongly controls the convection flow direction. Regression analyses will be presented quantifying the variations of flow direction with IMF component field strength.

G4-3
0940

A COMPARISON OF PLASMA DENSITIES BY EISCAT AND THE DYNASONDE FROM AURORAL ALTITUDES: EVIDENCE OF INTENSE STRUCTURE

J. W. Wright*, P. N. Collis**, T. S. Virdi***
British Antarctic Survey, Cambridge, U. K.
* now at: 1915 Spruce Ave. Longmont, Colo. 80501
** EISCAT Scientific Association, S-98128 Kiruna Sweden
***University College of Wales,Aberystwyth SY233BZ

Under conditions of moderately-energetic particle precipitation typical or the equatorward side or the auroral oval, plasma densities obtained from routine analysis of EISCAT Common Program data are often a factor or 2 to 5 smaller than those suggested by co-located Dynasonde ionograms. We consider the reasons for this disagreement, and in particular we reject the implications of diffractive and multiply-refractive scatter as alternatives to the usual plasma-frequency interpretation of ionogram echoes. We examine the effects of the (5-minute and shorter) temporal averaging applied to the EISCAT data and conclude that together with the evidently small size (perhaps as little as 20 km) and high velocity of these structures, this accounts for much, if not all, of the disagreement. We point out the significance of the higher plasma densities in the 110-150 km height range for estimates of Joule and particle heating.

G4-4
1000

PLASMA STRUCTURING IN THE POLAR CAP

S. Basu
Geophysics Laboratory (LIS)
Hanscom AFB, MA 01731, USA
Sunanda Basu
Institute for Space Research
Boston College
Newton Center, MA 02159, USA

Satellite in-situ measurements of density and electric field and propagation experiments providing scintillation, total electron content and drift data are utilized to investigate the manner in which ionospheric plasma becomes structured within the polar cap. It is found that under IMF B_Z southward conditions, large scale ionization patches which are convected through the dayside cusp into the polar cap get continually structured. The structuring occurs through the ExB gradient drift instability process which operates through an interaction between the anti-sunward plasma convection in the neutral rest frame and large scale plasma density gradients that exist at the edges of the ionization patches. It is shown that with the increase of solar activity the strength of the irregularities integrated through the ionosphere is greatly increased. Under the IMF B_Z northward conditions, the plasma structuring occurs around the polar cap arcs in the presence of inhomogeneous electric field or disordered plasma convection. In that case, the irregularity generation is caused by the competing processes of non-linear Kelvin-Helmholtz instability driven by sheared plasma flows and the gradient drift instability process which operates in the presence of ordered dawn to dusk motion of arc structures. The integrated strength of this class of irregularities also exhibits marked increase with increasing solar activity presumably because the ambient plasma density over the polar cap is enhanced.

G4-5 1040 IONOSPHERIC IRREGULARITY MORPHOLOGY NORTHWEST OF COLLEGE, ALASKA NEAR SUNSPOT MAXIMUM

R. D. Hunsucker, D. Prichard and B. S. Delana (Geophysical Institute, University of Alaska Fairbanks, Fairbanks, AK 99775-0800)

An ULCAR Digisonde 256 has been modified to permit it to be used as an oblique HF backscatter sounder in addition to functioning as a digital ionosonde. Since late 1988 until the present time the sounder makes 8 soundings per hour; 4 vertical incidence and 4 backscatter. The oblique soundings are made in support of the proposed Alaskan OTH radar through the USAF Geophysics Lab at Hanscom AFB, Massachusetts.

Diurnal and geomagnetic-storm-time behavior of groundscatter and "auroral clutter" echoes is illustrated. During the late fall and winter of 1988 groundscatter and backscatter from large ionospheric irregularities were present ~ 57% and 46% of the time respectively, on an azimuth of 290°. The behavior of other "clutter" type echoes and correlation with various geophysical parameters is also discussed, as well as HF backscatter signatures during the great geomagnetic storm of March 1989.

G4-6
1100

ATMOSPHERIC GRAVITY WAVE (AGW) SOURCES AND PROPAGATION OBSERVATIONS: EVENTS ON APRIL 15, 1989 AT SØNDRE STRØMFJORD

R. D. Hunsucker and Ning Jing (Both at: Geophysical Institute and Department of Physics, University of Alaska Fairbanks, Fairbanks, AK 99775-0800)
L. J. Lanzerotti and C. G. Maclennon (Both at: AT & T Bell Laboratories, Murray Hill, J 07974)

Two large, energetic ionospheric events occurred at 1515 UT and 1610 UT on April 15, 1989 at Søndre Strømfjord. Using measurements from the incoherent scatter radar and a simultaneously-operating magnetometer, we obtained data describing Joule heating, electric fields, current densities, ion velocities, and Pedersen and Hall conductivities in the ionospheric E-region. We calculated the Lorentz force effects (J x B) and found that the *y* and *z* components of the Lorentz force (northward and upward) versus time are very similar to the Joule heating versus time for three different antenna positions during the events. Using theories developed by Chimonas and Hines, Testud, and Francis, we calculated the ratio of the contributions of the Lorentz force and Joule heating for the generation of AGWs. For most of the interval studied, Joule heating was dominant. An interesting observation is that the ratio of *L/J* is lowest during the maxima of the two events. Simultaneous ionospheric irregularity data acquired with the Goose Bay HF Radar were also analyzed.

G4-7
1120

A HIGH THRUPUT INTERFERENCE-RESISTANT HF/MBC SYSTEM FOR HIGH LATITUDE LINKS

A. K, Gupta
SIGCOM COMPANY
10 Wheeler Road
Westborough, MA 01581

In this paper,we propose a channel adaptive high thruput interference resistant combined HF/MBC system employing novel techniques to counter time-varying path losses,doppler spread and multipath spread of a high latitude link.Some of the techniques employed are coded MFSK signalling (A. K. Gupta and J. R. Herman,National Radio Science Meeting,Boulder,CO. 1988),multichannel diversity,frequency management techniques such as frequency hopping and frequency stepping.Further processing gain in noise reduction can be obtained by this author proposed high suppression adaptive filtering(A. K. Gupta,National Radio Science Meeting,San Jose, Calif.,June 1989).A complete block diagram of this system is given in Fig. 1.

A channel adaptive high thruput MBC(meteorburst communication) system and measurement of channel parameters such as multipath spread was first proposed by this author in 1979(A. K. Gupta and M. D. Grossi, Proc. of IES conf.,Crystal city,VA,April 1981,A. K. Gupta,National Radio Science Meeting,Houston,TX,May 1983).The system required that the data rate be made constant over the trail life-time despite time-barying path losses,doppler spread and multipath spread.Dr. E. J. Baghdady proposed the capacity calculations and identification of factors affecting capacity be examined. He also suggested the use of his on-line signal to noise ratio monitoring technique to maintain a constant data rate over the trail life-time. The channel probing and meteor ststistics calculations were proposed by Dr. M. D. Grossi.An ideal high thruput system will incorporate a recently proposed modified Rician model(A. K. Gupta and J. R. Herman,National Radio Science Meeting,Syracuse, NY,june 1988; A. K. Gupta and J. R. Herman,'MBC Engineering Design Handbook', GTE report,Dec. 1987) in a multimedia multichannel system incorporating HF/MBC systems.

A discussion of an adaptive high data rate jam resistant HF system for high quality information transmission ,including digital voice as in mteteorburst real-time system,through time-varying channel conditions in single-hop ionospheric path in mid-latitude or in transauroral belt is given inreferences(A. K. Gupta,IEEE Int. AP Symposium and URSI meeting, Syracuse,NY,June 1988;A. K. Gupta and M. D. Grossi,AFGL-TR-79-0236,june, 1980;A. K. Gupta and M. D. Grossi,Proc. of IES Conf. ,Crystal city,VA, April 1981).

FIG. 1

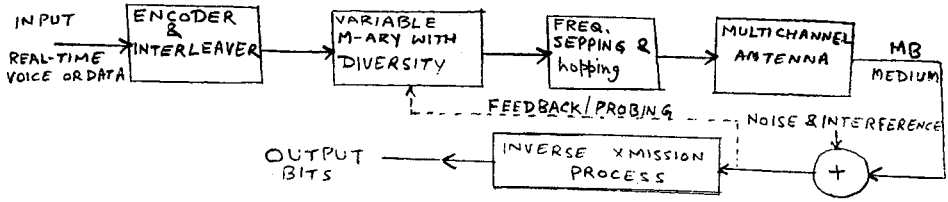

Session H-3 0855-Fri. CR0-30
ACTIVE EXPERIMENTS OF WAVE INJECTION FROM THE ACTIVE SATELLITE
Chairman: W.W.L. Taylor, TRW, Redondo Beach, CA

H3-1
0900 HIGH-POWER VLF WAVE INJECTIONS IN THE ACTIVE PROGRAM, R.W. Fredricks, RAM Technical Services, Thousand Oaks, CA

The ACTIVE program of the USSR involves an international scientific effort in both Eastern- and Western-block nations. The 10 kW VLF transmitter aboard the Soviet-built main satellite transmits signals near 10 kHz from selected portions of its orbit (roughly 500 km x 2500 km at 82.6 degrees inclination with 116 minute period). A Czech-built subsatellite carries EM-field and particle diagnostics to measure responses-at-a-distance to these active VLF wave injections. In this paper, results of transmissions and their implications with regard to whistler-mode propagation and wave-particle distribution interactions will be presented. Future wave-injection experiments planned during the life of the ACTIVE program will be discussed.

Work reported herein was funded by NASA through TRW Space & Defense, Redondo Beach, CA, as part of the Waves in Space Plasmas (WISP) project.

H3-2
0920 ACTIVE: A MULTINATIONAL PLASMA WAVE EXPERIMENT, William W.L. Taylor, TRW, Redondo Beach, CA

On September 28, 1989, the USSR launched their space plasma wave laboratory, ACTIVE, to do the first high power plasma wave transmission and propagation experiments in space. ACTIVE consists of the two satellites, a transmitter spacecraft and receiver spacecraft, in a 500 by 2500 km altitude orbit, inclined 83^{o}, and associated ground stations. The transmitter will deliver 5 kW to a 20 m diameter loop antenna at eight frequencies between 9.0 and 10.2 kHz. Both spacecraft have extensive diagnostic instrumentation. The scientific objectives include antenna characteristics, propagation, wave-particle interactions, and nonlinear effects. ACTIVE has been planned under the leadership of IKI, who also provided the transmitter satellite, in Moscow with cooperating scientists from Czechoslovakia providing the receiver subsatellite. Scientists from Bulgaria, Cuba, GDR, Hungary, Poland, U.S., Canada, Japan, Brazil, Finland, and England are also participating. The U.S. Team hopes to fully participate in planning, data gathering (from satellites and ground stations), and data analysis. The participants have agreed to fully share their data. ACTIVE promises to be a very valuable project for plasma physics and for international scientific cooperation.

H3-3
0940

INPUT IMPEDANCE OF A SMALL LOOP ANTENNA AT VLF FREQUENCIES IN THE LOW ALTITUDE MAGNETOSPHERE, T.F. Bell, Space Telecommunications and Radioscience Lab, Stanford University, Stanford, CA 94305

One of the principle problems involved in the design of a VLF transmitter for *in situ* operation in the magnetosphere is the matching of the reactive input impedance of the radiating antenna so that significant power can be delivered to the antenna. In the case of a dipole antenna, the reactive impedance can be very large compared to the resistive portion and the impedance can be a strong function of the ambient plasma parameters as well as the characteristics of the plasma sheath which surrounds the antenna. Thus the tuning of such a variable reactance antenna is a major problem. On the other hand it has been believed that a loop antenna whose size is much smaller than typical whistler mode wavelengths at VLF ($\sim$1 km) does not present as serious a problem in so far as tuning is concerned since it is known that a loop antenna with constant current couples only weakly to the plasma and does not possess a significant plasma sheath. In the present work we examine the radiation characteristics of small loop antennas in the magnetosphere and show that the major portion of the energy is radiated into quasi electrostatic whistler mode waves with wave normals near the resonance cone angle. We show that the wavelengths of these radiated quasi-electrostatic waves can be as small as 20 m. The production of radiation at these wavelengths implies that the current distribution around the loop antenna may also show variation with this scale. With this thought in mind we calculate the input impedance of a small loop antenna in the magnetosphere with a weakly non uniform current distribution. We show that small variations in the current distribution can lead to significant changes in both the reactance and resistive portions of the input impedance. For 10% current variation, the radiation resistance can increase by as much as two orders of magnitude, while the reactive increases by a somewhat smaller factor. We conclude that the assumption of uniform current distribution along a small loop antenna in the magnetosphere is not generally warranted and that significant coupling may commonly exist between the loop antenna and the magnetospheric plasma. We apply our results to the AKTIVNY experiment and show how this effect could lead to increased radiation from the AKTIVNY loop antenna.

H3-4
1000

GYRORESONANT PITCH ANGLE SCATTERING BY QUASI-ELECTROSTATIC WHISTLER MODE WAVES INJECTED FROM SATELLITE BASED VLF TRANSMITTER, U.S. Inan and T.F. Bell, Space, Telecommunications and Radioscience Laboratory, Stanford University, Stanford, CA 94305

A new formulation of gyroresonant pitch angle scattering by obliquely propagating whistler-mode waves is applied to the case of VLF waves injected from the AKTIVNY transmitter. Results indicate that the diffusion coefficient for waves propagating within a few degrees of the resonance cone can be up to 10-100 times larger than that for longitudinally propagating waves. Since the gyroresonant electron energy corresponding to the quasi-electrostatic waves is also lower, it appears as if two distinct populations of electrons can be expected to be precipitated. For 10 kHz waves at L=2.3 near the geomagnetic equator, waves at low wave normal angles interact with 50keV electrons whereas the quasi-electrostatic waves interact with electrons of 0.2-1.0 keV energy. If the radiation from the AKTIVNY transmitter excites whistler-mode waves over a broad range in wave normal space, one would expect the associated electron precipitation fluxes to peak near 50 keV and <1 keV electron energy.

H3-5
1020

3-D RAY TRACING SIMULATIONS OF VLF WAVES EXCITED BY A SOURCE IN THE MAGNETOSPHERE, V.S. Sonwalkar, U.S. Inan, and T.F. Bell, Space Telecommunications and Radioscience Lab, Stanford University, Stanford, CA 94305

We present 3-D ray tracing simulations of very low frequency waves excited by a source in the magnetosphere. The computer code incorporates a 3 dimensional magnetospheric density model with plasmapause. The model used for the study has the plasmapause at L=4.2, fairly representative of the magnetosphere under moderate geomagnetic activity. The equatorial electron densities used in the model agree well with those obtained by the whistler method and in situ satellite measurements. The source of the waves is assumed to be located at altitudes between 500 and 2500 km, at geomagnetic latitudes between 0° and 70°, and at 0° geomagnetic longitude. The source is assumed to radiate at a fixed frequency of 10 kHz. We study (1) the accessibility of different regions of the magnetosphere to the waves as a function of the source location, (2) the expected wave normal directions and electric and magnetic field intensities per radiated watt, assuming that the source radiates uniformly within the allowed propagation resonance cone, and that there is no damping or amplification of the waves, (3) the effect of the plasmapause in trapping and guiding the waves to low altitudes and to the ground. The results are discussed in the context of the wave injection experiments from the ACTIVNY satellite and their observations on the DE 1 and EXOS D satellites and at a number of ground stations in the western hemisphere.

Session H-4 1040-Fri. CR0-30
ELECTRODYNAMIC TETHERS AND TETHERED ARRAYS
Chairman: R.M. Bevensee, Lawrence Livermore Laboratory, Mail Station L-156, P.O. Box 5504, Livermore, CA 94550

H4-1
1040

ESTIMATES OF RADIATED POWER FROM THE TETHERED SATELLITE SYSTEM

Denis J. Donohue, K.J. Harker*, P.M. Banks
Space, Telecommunications and Radioscience Laboratory
Stanford University, Stanford CA 94305-4055

In their 1986 paper, Barnett and Olbert (A. Barnett and S. Olbert, Journal of Geophysical Research, 91, 10117-10135, 1986) developed a formalism for calculating the radiated electromagnetic fields from a passive electrodynamic tether orbiting in earth's ionosphere. By estimating the passive current level flowing in the tether, Barnett and Olbert derived approximate closed form expressions for the radiation impedance from such a tether. In the present work we have extended the formalism of Barnett and Olbert to produce calculations of the spectral density of tether radiation while treating the passive dc current level as an unknown. In addition, we have made detailed calculations using the appropriate system dimensions for the upcoming TSS-1 experiment. By treating only the actual tether and ignoring current flow in the sub-satellite or wake effects of the space shuttle, we find a significant amount of broadband wave energy to be radiated into the whistler mode, above the lower hybrid frequency of the plasma. In addition, we find the effect of decreasing wire radius (holding the total current constant) is to increase both the bandwidth and total radiated power.

In the presentation we will discuss limitations of the theory along with recent attempts to introduce finite temperature effects and to model the conducting sub-satellite. Most importantly, we will emphasize consequences of the theory for the upcoming TSS-1 experiment, including the effect of a high radiation impedance on current collection capability and the detectibility of predicted wave emissions.

* Dr. Harker is now at SRI International, Menlo Park, CA 94025

H4-2
1100

PLASMA WAVE TURBULENCE GENERATED AROUND LARGE SPACE STRUCTURES WITH AND WITHOUT ELECTRON BEAM INJECTIONS.

T. Neubert, B. E. Gilchrist, A. C. Fraser-Smith, P. R. Williamson, and P. M. Banks
STAR Laboratory, Stanford University, Stanford, CA 94305-4055
S. Sasaki
Institute for Space and Astronautical Sciences, Tokyo 153, Japan
W. J. Raitt
Center for Atmospheric and Space Sciences, Utah State University, Logan, UT 84322-4405

We report on observations of plasma wave turbulence generated during active perturbation sequences of the Charge-2 sounding rocket experiment. The payload was divided into two sections, a Mother and a Daughter, which were electrically connected by an insulated, conducting tether. Shortly after launch, the two platforms were separated, drifting apart in a direction perpendicular to the velocity vector and to the direction of the ambient magnetic field. The maximum separation distance was 426 m, which was reached at the end of the flight.

The Mother carried an electron beam accelerator (1 keV, 0-46 mA) and a high voltage (HV) bias system (0-460 V), biasing the Mother negative relative to the Daughter. The operation of the HV bias system simulated the electrodynamics of large orbiting space structures like TSS-1. The Daughter carried wave receivers (600 Hz to 10 MHz) connected to electric dipole antennas and a tether current monitor.

Strong, broad-band ELF/VLF turbulence was generated both during electron beam emissions and when the HV bias was applied between the two payloads. Turbulence in the HF range was only observed during electron beam emissions. At low beam currents, the HF spectrum peaked at frequencies slightly above the electron gyrofrequency. At higher beam currents, the overall spectral intensity increased and the spectral shape became broad-band with the intensity proportional to about $f^{-1.5}$. Both ELF/VLF and HF turbulence were quenched by neutral gas/thruster emissions from the Mother payload. At such times, the HF spectrum returned to the peaked form, observed at low beam currents. The observations are compared with earlier reported observations and related to discussions of Beam Plasma Discharge in space experiments and of wave generation by return current electrons.

H4-3
1120

PRINCIPLES OF VLF ANTENNA ARRAY DESIGN IN MAGNETIZED PLASMAS

H. C. Han[+], J. A. Kong[+], T. M. Habashy[*], and M.D. Grossi[§]

[+]Department of Electrical Engineering and Computer Science
Massachusetts Institute of Technology
Cambridge, MA 02139

[*]Schlumberger-Doll Research
Ridgefield, CT 06877-4108

[§]Harvard-Smithsonian Center for Astrophysics
Cambridge, MA 02138

The study of electromagnetic radiation from sources in the ionospheric plasmas has received much attention in the research on the satellite-borne antennas. For many years, special attention has been given to the radiation in the very low frequency (VLF) band due to its applications in the down-link communication systems. Intensive efforts had been placed by many authors on the investigation on the single element radiation, both theoretically and experimentally. However, limited by its low radiation efficiency, the utility of a practically sized single VLF radiator could highly depend upon the focusing effects characterized by the inflection points on the k-surface associated with the medium. In recent years, the construction of a large space-based antenna array has been made feasible during the progress of the spacecraft technology. With a properly phased large VLF linear or planar array, a narrow beam width and consequently a high directivity can then be achieved.

In this paper, we study the far field pattern of a VLF phased array located in a magnetized plasma. We discuss the general principles of antenna array design in the anisotropic media. Special attention is drawn to the two-dimension planar array allowed to rotate with respect to an axis perpendicular to the plane of the array, and the main beam of which is kept in the same direction as that of the geomagnetic field line during the rotation. We also discuss the applicability of the principle of pattern multiplication as well as the effects of different types of radiating elements for different k-surface geometries.

H4-4
1140

MONITORING FROM SPACE THE E.M. EMISSIONS OF A TETHER BY MEANS OF AN AUTONOMOUS ORBITING ROBOT

Mario D. Grossi
Harvard-Smithsonian Center for Astrophysics
Cambridge, Massachusetts 02138

The experimental verification of the ability of an electrodynamic tether in Earth orbit to genetate and radiate e.m. waves from ULF to HF, is an important undertaking of tether science and engineering. In particular, the detection of e.m. waves below the ion cyclotron frequency would open the possiblity for tether use in special radio communications at ULF and ELF.

A "phantom loop" model of tether radiation at ULF, based on "remote" closure in the ionosphere of the tether current, supports the expectation that radiation in this frequency band will be substantial, while the opposite is held true by the believers in "local" current closure.

The launching in Earth orbit by NASA and ASI of tether systems of the TSS class, scheduled for the early and mid '90s, is a good opportunity, in principle, for the resolution of this conflict.This is so, provided that the received signal is large enough to be above noise, based on the allegedly optimistic predictions of the "phantom loop" model. A probative experiment, as long as the tether current is kept low for safety reasons, can be conducted by flying a receiving satellite at distances from a fraction of a kilometer up to hundreds of kilometers from the tether system.

An autonomous space robot called SPIDER, presently under development by the Italian Space Agency(ASI), can be used for the above purpose. This robot can be maneuvered to move at various distances and to acquire several positions with respect to the tether, with the objective of carrying out a measurement campaign capable of saying a conclusive word on the issue whether the tether's current closure is "remote" or "local", and whether or not electrodynamic tethers will ever be able to perform as effective antennas usable in radio engineering applications of practical importance.

The paper illustrates the SPIDER vehicle , its performance as an orbiting body, its maneuverability, its instrumentation payload and the scientific and engineering value of associating it with experimentation conducted on the radiation capabilities of electrodynamic tethers.

Session JE-1 0855-Fri. CR2-26
INTERFERENCE IN RADIO ASTRONOMY
Chairman: T.E. Gergely, Division of Astronomical Sciences,
National Science Foundation, Washington, DC 20550

JE1-1
0900

DIURNAL VARIATIONS OF UNINTENTIONAL MANMADE VHF AND UHF RF NOISE: SURVEYED FROM A LIGHT AIRCRAFT

M. C. Cudak, G. W. Swenson, Jr.
Department of Electrical and Computer Engineering
University of Illinois at Urbana-Champaign
Urbana, Illinois 61801
and
W. W. Cochran
Illinois Natural History Survey
Champaign, Illinois 61820

Since July of 1989, a study of unintentional broadband manmade noise has been in progress over a set of small towns in Illinois. The small towns are surveyed on three frequencies --148 MHz, 22 MHz, and 412 MHz-- simultaneously from a small aircraft equipped with a set of downward looking antennas. The noise flux from towns with populations larger than 25,000 is presented as brightness temperatures. To date, the peak brightness temperatures have ranged from 6100 Kelvins at 148 MHz to only 570 Kelvins at 412 MHz. Furthermore, there appears to be considerable diurnal variation ranging from 6100 Kelvins at 6:00 PM (CDST) to 2900 Kelvins at midnight (CDST).

The standard route adopted for this study was originally surveyed in August, September, and December of 1972 (G. W. Swenson, Jr., W. W. Cochran, Science, 181, 543-545, 1973). The records of 1972 are compared to recent records for indications of long term variations.

JE1-2
0920

INTERFERENCE TO RADIO ASTRONOMY FROM SATELLITE TRANSMITTERS OPERATING IN ADJACENT BANDS

W. K. Klemperer
Electromagnetic Fields Division
National Institute of Standards and Technology
Boulder, Colorado 80303-3328

There has been an unfortunate proliferation in the number of satellites (operating in radio bands between 1.2 and 2.7 GHz) causing interference to radioastronomy. The usual protection from ground-based transmitters which terrain-shielding can provide is ineffective in most cases. The spread-spectrum technique utilized by navigation satellites of the GPS and GLONASS systems is particularly troublesome. Considerable progress has been made in the design of lightweight, efficient filters for use on satellites. There are also new and better band-pass and band-reject filters which can be used to some advantage at radio observatories. The degree of protection from adjacent band interference which can now be achieved by various cooperative schemes will be discussed. However, the costs of behavior modification for satellites are not trivial: in addition to the usual weight and reliability penalties there are also significant reductions in channel capacity.

JE1-3
0940

RFI SITE SURVEYS IN THE BAND 1.0 GHZ -> 10.4 GHZ

Edward T. Olsen, Earl B. Jackson, and S. Gulkis
169-506
Jet Propulsion Laboratory
4800 Oak Grove Drive
Pasadena, CA 91109

In support of the NASA SETI program, JPL has started to conduct an omni-directional, low-sensitivity, coarse-resolution RFI survey of selected radio observatory sites (1) to assess the site RFI environment and (2) to test the utility of such a survey to predict the RFI environment which will be experienced by SETI prototypes on the main beam. To date, measurements have been made at DSS 13 in Goldstone, CA and Arecibo in Puerto Rico. Planned sites for future observations over the next two years include Algonquin Radio Observatory in Ontario, Canada, OSU Radio Observatory in Columbus, Ohio, OVRO in Big Pine, CA, Meudon Observatory in France, NRAO in Green Bank, West Virginia, and Tidbinbilla in Australia.

The JPL Radio Spectrum Surveillance System (RSSS) is a computer controlled, single channel scanning spectrometer with programmable resolution, bandwidth, sweep frequency range, integration time, and threshold. It is a stand alone system capable of unattended operation with its own antenna, front-end amplifiers, spectrum analyzer, data recorder and controlling computer. A noise diode at the front end provides a calibrated reference signal from which the detected signal levels can be deduced. The antenna can be (1) a 60° included angle inverted discone or (2) a 1-meter paraboloid. In the latter case, the azimuth of an observation is under control as well.

The standard operational strategy employes the inverted discone and sweeps the RF band between 1.0 GHz and 10.4 GHz repeatedly at 10 kHz resolution, $\beta \cdot \tau = 5$, and a threshold 10 dB above the local noise floor. The sensitivity achieved by this strategy is $\approx$ -120 dBm and the 9.4 GHz band is swept at $\approx$ 50 minute intervals. Events whose detected power exceeds the threshold are written to disks which are returned to JPL for analysis in a relational database. The database contains time-tagged power, frequency and (if appropriate) azimuth of detected events.

The database is analyzed to determine (1) the time variability of RFI activity, (2) the distribution of incident power of detected events, (3) the probability that a frequency will be obscured by RFI, (4) the fraction of the RF band obscured as a function of detected power and (5) a catalog of the RF occupancy as a function of maximum detected power and duty cycle.

A surprising amount of RFI has been detected at Arecibo in the radio astronomy protected bands (1420 MHz -> 1427 MHz and 1660 MHz -> 1670 MHz). Repeated observation of the RF band yields valuable statistical data on the duty cycle and spectral signature of transmitters, even those which are not often active.

JE1-4
1000

SHOWDOWN IN WEST TEXAS

Patrick C. Crane
National Radio Astronomy Observatory
Post Office Box O
Socorro, New Mexico 87801-0387

West Texas has been the site of a showdown between radio astronomers and the United States Customs Service. This conflict is an example of the problems that radio astronomy will face as other radio services make greater utilization of transmitters mounted on aircraft, balloons, and satellites. In this instance the conflict appears to have been resolved to the satisfaction of both parties.

The conflict arose when the Customs Service decided to locate an aerostat (a balloon-mounted radar) near Marfa, Texas to track aircraft flying in the vicinity of the border between the United States and Mexico. The site chosen by the Customs Service is only 42 km from the Fort Davis antenna of the Very Long Baseline Array (VLBA) radio telescope being constructed by the National Radio Astronomy Observatory. Because the operating altitude of the aerostat is 10,000 feet above ground level, there is no terrain shielding and the aerostat and the VLBA antenna are line of sight. The aerostat, now operational, operates in the government radiolocation allocation 1215-1400 MHz and potentially will interfere with operations of the VLBA antenna (after it becomes operational in February 1990) in the band 1350-1750 MHz, including the famous "protected" band 1400-1427 MHz.

Peaceful coexistence has required addressing several concerns of the radio astronomers - the possibility of the transmitted signal damaging or overloading the receiver and the possibility of radio-frequency interference from the out-of-band emissions from the transmitter - without seriously limiting the capabilities of the aerostat. This will be achieved through modifications to the aerostat and the VLBA receiver, operational restrictions on both the aerostat and the VLBA antenna, and coordination between the two parties.

JE1-5
1040

MONITORING INTERFERENCE NEAR THE 408 MHZ RADIO ASTRONOMY BAND: TECHNIQUES, STRATEGIES AND RESULTS

T.L. Landecker[1], P.E. Dewdney[1], D.N. Romalo[2], G.H. Hovey[1], D. Lam[3]

[1] Dominion Radio Astrophysical Observatory, National Research Council of Canada, Penticton, British Columbia, Canada

[2] Electrical Engineering Department, University of British Columbia, Vancouver, British Columbia, Canada

[3] Electrical Engineering Department, University of Alberta, Edmonton, Alberta, Canada

The spectrum near the 408MHz radio astronomy band is being monitored for radio interference with a system based on a real-time Fast Fourier Transform (FFT) spectrum analyzer. Direction of arrival, frequency, intensity, and time of occurrence are recorded under microcomputer control. A sensitive receiver can be connected to any one of eight directional antennas to establish direction of arrival. The FFT spectrum analyzer has a real time bandwidth of 0.5 MHz. Total frequency coverage of 20 MHz is obtained by stepping the local oscillator frequency. Examples will be presented of interfering signals originating within the observatory and beyond it, and the emission spectrum of digital and computer equipment will be discussed.

JE1-6
1100

IMPROVED INTERFERENCE PROTECTION AT ARECIBO

Michael M. Davis
National Astronomy & Ionosphere Center
P.O. Box 995
Arecibo, Puerto Rico 00613

The Gregorian Upgrading of the Arecibo 1000 foot diameter radio/radar telescope will include significant new interference protection. At present the line feeds used to illuminate the reflector and correct for spherical aberration have little or no protection from interference. They are suspended some 435 feet above the reflector, with a nearly unblocked view of the horizon. Recent quantitative measurements of the interference levels at the Observatory indicate a relatively high occurrence probability for manmade interference, especially at L-Band (E. Olsen, private communication). At present only the low sidelobe response of the line feeds protects sensitive observations from these interfering signals.

The Gregorian offset subreflector system which will replace the short wavelength line feeds consists of a 65-foot secondary, 35-foot tertiary, and a set of standard scalar horn feeds. It is essential that these be placed in a protective enclosure to reduce wind loading on the structure. This space frame enclosure, which will be covered with aluminum panels, serves also to protect the subreflectors and feed from interference. Radiation will have access to the feed only through the opening at the bottom of the space frame. Care is being taken in the design to ensure the absence of scattering paths for interference. In particular, there is no blockage of any ray paths in the optical design of the system, other than the unavoidable shadowing of the reflector by the support platform.

JE1-7
1120

AN ATTEMPT TO CHARACTERIZE RFI AT ARECIBO FOR FUTURE SETI OBSERVATIONS

J.C. Tarter, P. Backus, D.K. Cullers
SETI Institute
2035 Landings Drive
Mt. View, CA 94043

S. Gulkis, E.T. Olsen, E.B. Jackson
Jet Propulsion Lab
4800 Oak Grove Drive
Pasadena, CA 91109

J. Dreher
NASA Ames Research Center
MS 229-8
Moffett Field, CA 94035

D. Werthimer, W. Herrick
University of California at Berkeley
Space Sciences Lab
Berkeley, CA 94720

In June/July 1989 SETI scientists from JPL, The SETI Institute, and UC Berkeley conducted an extensive series of observations to characterize the interference environment at Arecibo Observatory. Four different instrument systems were operated simultaneously to provide coarse and fine frequency resolutions at sensitivities comparable to the main beam and the antenna sidelobes.

The JPL Radio Spectrum Surveillance System (RSSS) was initially mounted high on the support triangle at Arecibo in order to get a clear view of the horizon. Prior to the start of the scheduled telescope observations, it scanned the 410 MHz RF band covered by the line feeds at 1 kHz resolution using its own receivers and omni-horizon discone antenna. "Quiet" as well as "noisy" regions inside and outside of the protected radio astronomy bands were selected on the basis of this precursor survey for comparative studies with the narrowband systems. Simultaneous observations were then carried out with the narrowband systems in spot bands at 1 kHz and 100 Hz, utilizing both the RSSS receivers and discone and the Arecibo receivers and main beam.

The narrowband systems employed were (1) Arecibo's own 2048 channel auto correlator, operated at 68 Hz or 1.2 kHz resolution, (2) MCSA 1.0, a first generation prototype SETI spectrum analyzer developed by Stanford University, and (3) SERENDIP 2.0, developed by UC Berkeley.

MCSA 1.0 produces 74,000 channels of 1/2 Hz resolution data every 2 seconds and is controlled by a VAX 11/750 host with a SUN/3 for graphical display and diagnostics. Although it can sample the input data stream and create the spectra continuously, limited I/O bandwidth and disk capacity result in only 15 kHz of the unthresholded data being recorded for 6 minutes before the observations are interrupted to write to tape.

To increase the instantaneous bandwidth sampled at high resolution, the UC Berkeley SERENDIP 2.0 system was upgraded with a fast read/write optical disk and "borrowed" for these observations. This system can provide 65,536 channels of 1 Hz resolution and in its normal mode of operation only a few of these channels exceeding some threshold are recorded to disk. With the increased disk storage capacity, it was possible to store all 65K channels in 2.62 seconds. Although this device then undersampled the data in time, it complemented the data from the MCSA 1.0 which undersampled the data in frequency.

The telescope was driven over a full range of azimuth and elevation angles while recording data simultaneously with the four systems. Over a one week period about 5 gigabytes of data were recorded for comparison.

The RSSS then performed a 3-week survey of the 1.0 GHz to 10.4 GHz band at 10 kHz resolution. Finally, the RSSS was moved to progressively lower stations, and data were taken over the frequency ranges 1280 MHz to 1450 MHz and 1600 MHz to 1730 MHz utilizing the RSSS receivers and discone antenna. The RSSS automatically recorded to disk any detected event that exceeded a pre-set threshold, and the recorded data were later analyzed at JPL.

In addition to characterizing the interference at the site from the point of view of radio astronomy, we also wished to learn how or whether data from the low sensitivity and coarse resolution RSSS can be used to predict the interference to be experienced by a high resolution spectrometer attached to a high gain antenna. The results of this study and some preliminary results from similar work scheduled to be completed at Algonquin Observatory and the Ohio State University Radio Observatory will be presented.

JE1-8
1140

THE 1992 WORLD ADMINISTRATIVE RADIO CONFERENCE

T. E. Gergely
Division of Astronomical Sciences
National Science Foundation
1800 G Street, N.W.
Washington, D.C. 20550

The International Telecommunication Union (ITU) convened a World Administrative Radio Conference (WARC) for 1992. The Conference has been charged with allocating spectrum to satisfy the requirements of new services, such as High Frequency Broadcasting, Direct Sound Broadcasting, and Mobile Satellite, and with facilitating the bringing into existence of others, such as High Definition Television. Allocations for these services may affect the 3-30 MHz, 0.5-3.0 GHz, and 11.7-23.0 GHz frequency ranges, approximately. In addition, the Conference may define new space services and allocate spectrum to them, in frequency bands above 20 GHz. The possible impact of these developments on radio astronomy, and the preparations required by the radio astronomy community for the Conference, are going to be discussed.

Poster Paper THE GREEN BANK RFI ENVIRONMENT

Wesley A. Sizemore
National Radio Astronomy Observatory
P. O. Box 2
Green Bank, West Virginia 24944

A poster-paper is presented showing spectral plots of selected frequency bands below 2 GHz depicting the current RFI environment at the National Radio Astronomy Observatory facility at Green Bank, West Virginia. Spectral plots of current RFI events in radio astronomy bands and information on the National Radio Quiet Zone will also be displayed.

Session B-6 1335-Fri. CR2-28
THEORY AND NUMERICAL METHODS
Chairman: W.R. Stone, 1446 Vista Claridad, La Jolla, CA 92037

B6-1
1340 **ALTERNATIVE REPRESENTATION OF TIME-DEPENDENT FIELDS**

R.K.Ritt
Department of Mathematics
Illinois State University
Normal, IL, 61761

It is well known that for a large class of scattering and propagation problems, in which there is a time dependent source, s(t), and a field u(t), for which u(0) = 0, the field can be written as a convolution:

$$u(t) = \exp(At) * s(t).$$

If exp(At) is represented by the Laplace inversion integral, acting on the Laplace transform $(s - A)^{-1}$, this representation can be used to obtain asymptotic (large t) representation as a series of damped oscillations.

An alternative representation for exp(At) is the spectral integral:

$\int_{-\infty}^{\infty} \exp(irt)\, P(dr)$, in which P(dr) is the projection valued measure which resolvesthe operator -iA.

We use this representation to obtain asymptotic representation of u(t) for small t, and give physical interpretations of the terms of the expansion.

B6-2
1400

CALCULATION OF THE INDUCED EDDY CURRENTS IN A CONDUCTING MEDIUM USING THE METHOD OF IMAGES

Dominique Durand and A. Stewart Ferguson
Applied Neural Control Laboratory
Department of Biomedical Engineering
Case Western Reserve University
Cleveland, OH., 44106 U.S.A

Magnetic stimulation can used to achieve non-invasive excitation of neural tissue in both the peripheral and the central nervous system. Although this is a potentially important technique for non-invasive stimulation of the nervous system, the mechanisms underlying this type of stimulation are unknown and in particular, the spatial distribution of the current density induced by the imposed magnetic fields is not understood.

The coil is located perpendicular to the surface of the non-homogenous medium. The solution to Maxwell Maxwell's equations in this case is:

$$\mathbf{J}_{Total}=\mathbf{J}_{Source}+\mathbf{J}_{Ohmic}$$

$\mathbf{J}_{Source}$ is the source generating the currents: $-d\mathbf{A}/dt$ where $\mathbf{A}$ is the magnetic vector potential. $\mathbf{A}$ is defined by:

$$\mathbf{B}=\nabla \times \mathbf{A}$$

$\mathbf{J}_{Ohmic}$ is the ohmic current generated by the sources. Since the total current must be divergence free, then:

$$\nabla \cdot \mathbf{J}_{Total} = \nabla \cdot \mathbf{J}_{Source} + \nabla \cdot \mathbf{J}_{Ohmic} = 0$$

Therefore:

$$\nabla \cdot \mathbf{J}_{Ohmic} = -\nabla \cdot (-d\mathbf{A}/dt) = d(\nabla \cdot \mathbf{A})/dt$$

The solution of this Poisson equation is known in an homogenous medium and is given by:

$$\mathbf{J}_{Ohmic} = \frac{1}{4\pi\sigma}\int \frac{\frac{-d(\nabla \cdot \mathbf{A})}{dt}}{R^2} dv$$

The theory of images was then used in order to replace the inhomogeneous medium by a homogeneous one. The perpendicular component of $\mathbf{J}_{Total}$ at the interface is then zero and the current density can be evaluated by first calculating the magnetic vector potential $\mathbf{A}$ and its divergence using the elliptic function formulation, then solving numerically the volume integral for $\mathbf{J}_{Ohmic}$ and adding the component $\mathbf{J}_{Source}$. Since the divergence of the vector potential is zero everywhere in space except at the surface discontinuity, the volume integral is replaced by a surface integral thereby considerably simplifying the solution. The results show that the current density vector is no longer contained within a plane parallel to the coil but has components in all three directions.

B6-3
1420

A COMPARATIVE STUDY OF HIGH FREQUENCY DIFFRACTION ANALYSIS TECHNIQUES FOR CIRCULAR DISCS WITH DIPOLE FEEDS

Dah-Weih Duan, Yahya Rahmat-Samii, and John Mahon
Department of Electrical Engineering
University of California, Los Angeles
Los Angeles, CA 90024-1594

Efficient and accurate high frequency diffraction analysis techniques have been of great interest for many years because of their importance for a wide range of applications. The purpose of this paper is to study the behavior of the solutions obtained by eight diffraction analysis techniques including (1) physical optics, (2) Mitzner's incremental length diffraction coefficients, (3) Michaeli's equivalent edge currents, (4) Ando's modified physical theory of diffraction, (5) geometric theory of diffraction (GTD), (6) uniform geometrical theory of diffraction (UTD), (7) uniform asymptotic theory (UAT), and (8) the method of moments for a canonical system consisting of a flat conducting circular disc and a forwardly radiating dipole feed. Methods (2), (3), and (4) are modifications of Ufimtsev's physical theory of diffraction (PTD).

Methods (2) to (6) are summarized for half plane diffraction in forms which are convenient both for comparison and calculation. The moment method solutions are treated as exact so that the correctness of other solutions can be examined. Important features of the far field radiation patterns resulted from these methods are examined for cases with different disc sizes and different frequencies. Features of particular interest are the performances at reflection boundaries, caustics, and near $\theta = 90°$, as well as the prediction for cross-polarization fields, side lobe levels, and nulls.

Mitzner's and Michaeli's methods give identical solutions for this disc-dipole system. Compared with the moment method solutions, they correct the PO solutions in an efficient manner and provide the most accurate solutions for all observation angles. While other techniques suffer from different difficulties when the sizes or complexity of the scatterers are increased, Mitzner's and Michaeli's methods seem promising for future applications because of their accuracy, efficiency, and ease in programming.

B6-4
1440

DERIVATION OF GENERALIZED TRANSITION/BOUNDARY CONDITIONS FOR PLANAR MULTIPLE LAYER STRUCTURES

M.A. Ricoy and J.L. Volakis
Radiation Laboratory
Department of Electrical Engineering and Computer Science
The University of Michigan
Ann Arbor, Michigan 48109-2122

Infinite order generalized impedance boundary conditions (GIBCs) and generalized sheet transition conditions (GSTCs) for planar multilayer configurations are developed via the Taylor series expansion method. The conditions are derived in a matrix product form where each matrix corresponds to a specific layer. An overall composite boundary/transition condition is obtained by making finite order approximations to the elements of each matrix for the cases of "low contrast" and "high contrast" material layers. The accuracy of the truncated boundary conditions is examined by comparing their implied reflection and transmission coefficients with the corresponding exact coefficients. Design curves are also given which relate the maximum order of the conditions required to stimulate a coating or layer of specific thickness and contrast. Expressions are then derived for the reflection and transmission coefficients of the GIBC/GSTC sheets and these are compared to exact coefficients to demonstrate the validity of the derived GIBCs/GSTCs.

B6-5
1500

OBTAINING HIGH ACCURACY IN FINITE ELEMENT SCATTERING PROBLEMS USING AN ABSORBING BOUNDARY CONDITION

J. W. Parker
M/S 198-136A
Electronics and Control Division
Jet Propulsion Laboratory,
California Institute of Technology
Pasadena, California, USA 91109

Use of an absorbing boundary condition for terminating a finite element domain for electromagnetic scattering problems raises the crucial question: how much error is incurred? Past theoretical work has focused on the error strictly due to the absorbing boundary condition representing a truncation of an asymptotic approximation in powers of the radial distance, implying improvement when the absorbing boundary is placed farther from the object; this implication is often not verified in numerical studies. Our work with a two-dimensional scalar finite element model reveals that much confusion has resulted from failure to separate several sources of error: deviations from an ideal object shape, deviations from an ideal absorbing boundary shape, mesh density, and polynomial order of the basis functions, as well as the absorbing boundary condition approximation. We demonstrate that sufficient care in each of these areas can produce computed fields of virtually any desired accuracy. In particular, we show that with quadratic basis functions, node densities of about 600 per square wavelength, a second-order Bayliss-Turkel boundary condition imposed on a circle at a distance of about one half wavelength from a dielectric cylinder (with a relative dielectric of 2.56 and cylinder radius a such that ka=1) one obtains far field agreement with an analytic solution to about one part in 10^5 relative to the maximum far-field magnitude. In order to obtain merely moderate accuracy, the most important requirement is the use of quadratic basis functions and isoparametric elements. We show that when this is done with sufficient node density to accurately model the curvature in the scattering object and the absorbing boundary, the computed field accuracy is well-behaved with respect to the distance from the object to the absorbing boundary; that is, accuracy improves when this distance is increased.

B6-6
1520

MAGNETIC DIPOLE EXCITATION OF AN INSULATED CONDUCTOR OF FINITE LENGTH

David A. Hill
Electromagnetic Fields Division
National Institute of Standards and Technology
Boulder, CO 80303

The excitation of currents on underground conductors is important in many applications. Power lines and rails in tunnels can enhance transmission for mine communications, and electromagnetic probing of the earth can be influenced by the presence of cables or pipes (J.R. Wait and K.R. Umashankar, Pure and Appl. Geophys., 117, 711-742, 1978). Most work on dipole excitation of conductors has treated infinitely long conductors (D.A. Hill, IEEE Trans. Geosci. Rem. Sens., GE-26, 720-725, 1988). This idealization allows a spatial Fourier transform formulation that simplifies the calculation of the current distribution and the scattered fields, but does not consider the effects of end reflections.

In this paper our model consists of an insulated conductor of finite length in a homogeneous, lossy earth excited by a vertical magnetic dipole. The insulated conductor has an arbitrary terminating impedance at each end. The theory of excitation of such a conductor by an external field has been developed previously (R.W.P. King, IEEE Trans. Antennas Propagat., AP-24, 327-330, 1976), and it involves an integration of the incident axial electric field over the length of the conductor. For a magnetic dipole source the incident electric field is nonuniform, and we perform the integration numerically.

Numerical results for the current distribution and the scattered fields have been generated to illustrate the effects of frequency, conductor length, terminating impedances, and dipole location. For open circuit terminations, the length of the conductor should be at least a half wavelength to be an effective scatterer. This condition dictates a minimum frequency for applications involving detection of conductors. In most cases the current distribution shows standing waves as a result of end reflections, but for long conductors the current distribution approaches previous results for infinitely long conductors.

B6-7
1540

SURFACE WAVES OF A STRIP GRATING ON A GROUNDED DIELECTRIC SLAB.

Fethi H. Bellamine and Edward F. Kuester
Electromagnetics Laboratory
Department of Electrical and Computer Engineering
Campus Box 425
University of Colorado
Boulder, CO 80309

Surface waves propagating on a periodically grated or corrugated surface have been of interest for many years in the study of leaky-waves and travelling wave antennas, travelling wave amplifiers, band-pass filters and transmission lines at microwave and millimeter wave frequencies.

Many authors have studied the properties of surface waves propagating along a metal grating on the surface of a grounded dielectric slab. But, in their work they restrict the direction of propagation to be perpendicular to or nearly parallel to the strips of the grating, and some have made additional restrictive assumptions about the parameters. In this presentation, a new method using equivalent boundary conditions is applied to address the problem of propagation of surface waves in an arbitrary direction to describe the effect of the strip grating.

In the second part of the presentation, resonance frequencies of a one dimensional periodic array of identical, equally spaced, thin metallic strips located on the surface of a grounded dielectric substrate are evaluated for different slot widths and for arbitrary strip directions. These results may have application to the design of slotted microstrip patch antenna.

B6-8
1600

ANALYSIS OF DISCONTINUITIES IN PLANAR DIELECTRIC WAVEGUIDES: A RECURSIVE NUMERICAL MODE MATCHING METHOD

Qing-Huo Liu and Weng Cho Chew
Electromagnetics Laboratory
Department of Electrical and Computer Engineering
University of Illinois
Urbana, IL 61801

The numerical mode matching method has been formulated before for the analysis of multiregion, vertically stratified media. It has been applied to the areas of microwave sensing and complex dielectric waveguide systems. In this paper, we propose an more effective algorithm, which is called the recursive numerical mode matching method, to analyze the discontinuity problems in planar dielectric waveguides. The new recursive numerical mode matching method is different from the previous numerical mode matching method in that it is based on an add-on algorithm. This makes the analysis of multiregion, vertically stratified media much more effective, because it requires much less amount of computer memory and computation time. With this algorithm, the required computer memory is independent of the number of regions in the problem, and the computation time is linearly proportional to the number of regions. Therefore, this method is particularly suitable for the analysis of planar waveguide discontinuities and waveguide bends. With this method, we can analyze many large problems which are impractical with finite element method. Various problems of the planar dielectric waveguide discontinuities are solved to demonstrate the usage of the recursive numerical mode matching method.

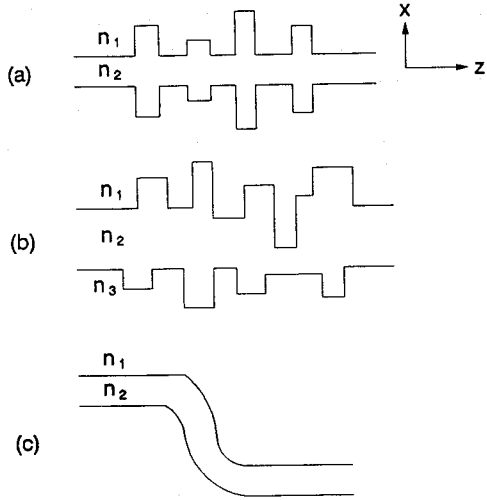

B6-9
1620

ANALYSIS OF MULTI-RECTANGULAR DIELECTRIC WAVEGUIDES BY NUMERICAL MODE MATCHING METHOD

Qing-Huo Liu and Weng Cho Chew
Electromagnetics Laboratory
Department of Electrical and Computer Engineering
University of Illinois
Urbana, IL 61801

In this paper, a hybrid method for the analysis of the propagation characteristics of various rectangular waveguides is proposed based on the recent development of the numerical mode matching method for multiregion, vertically stratified media. Unlike the conventional two-dimensional finite element method which is widely used for the analysis of dielectric waveguide problems, the numerical mode matching method proposed in the paper uses the propagation properties of the waves on the cross section of the waveguides to convert the two-dimensional problem into a few one-dimensional problems. These one-dimensional problems are then solved with the one-dimensional finite element method to find the eigenvalues and eigenmodes of arbitrary layered media, resulting in a great saving of the number of unknowns needed. This novel analysis method has been implemented numerically for analyzing arbitrary structures of rectangular dielectric waveguides. The comparison of the results with those available in literature are favorable. With the numerical results for various waveguide structures, the method is demonstrated to be efficient and capable of solving very complex structures such as coupled rib waveguides and coupled channel waveguides.

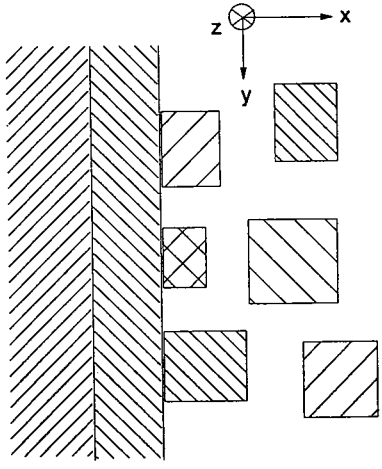

B6-10
1640 SIMULATION OF EM RADIATION FROM ANTENNA ELEMENTS AND ARRAYS USING CFD-BASED FVTD METHOD

A. H. Mohammadian, V. Shankar, and W. F. Hall
Rockwell International Science Center
P. O. Box 1085
Thousand Oaks, CA 91358

The computational fluid dynamics (CFD)-based approach to solve Maxwell's equations known as finite-volume time-domain (FVTD) method which was introduce about two years ago (V. Shankar and W. F. Hall, Proc. of URSI Meeting, Jan. 1988) has come a long way and has reached a very sophisticated level of maturity (V. Shankar, W. F. Hall, and A. H. Mohammadian, AIAA-89-1987). At present, the the code developed on this method is capable of computing the near field and RCS of arbitrary objects with any degree of geometrical and material sophistication both internally and externally. The code has multizone capability and can handle unequal grid lines in neighboring zones. It is also equipped with advanced pre-processors for geometry description and grid generation, as well as post-processors using color graphics and animation for presentation of the outputs.

This paper will discuss the application of FVTD method to radiation problems and presents some preliminary results in 2-D for radiation from the open end of a parallel-plate waveguide, a horn, arrays of parallel-plate waveguides (including binomial arrays), and a reflector antenna. In these simulations part of the feed structure is included in the computational domain so that the higher order modes that are excited in the transition region are accurately taken into account. The radiation patterns and aperture fields will be compared against the traditional physical optics approximations and in some cases the exact results (parallel-plate waveguide only).

Session C-2 1355-Fri. CR1-9
NONPARAMETRIC SPECTRUM ANALYSIS
Chairman: D.J. Thomson, AT&T Bell Laboratories, Murray Hill, NJ 07974

C2-1
1400 OPTIMAL SIMULTANEOUS ESTIMATION/DETECTION OF UNKNOWN SPECTRAL COMPONENTS, Alfred O. Hero, Dept. EECS, Univ. of Michigan, Ann Arbor, MI 48109

The simultaneous estimation and detection problem arises in cases where estimation of signal parameters is of interest but signal presence is not certain. For example, in a version of the passive array direction finding problem source bearings are to be estimated from the MUSIC spectrum but the number of source signals is unknown. Previous approaches to this kind of problem have been based on ad hoc techniques of decoupled estimation/detection, e.g. find the number of sources using AIC or some other criterion and then estimate the source parameters. In this talk we will present a unified approach to this problem based on an optimal estimation strategy which simultaneously guarantees a given level of detection performance. Specifically, we derive an estimator/detector which is a min-max optimal estimation rule among those rules which are constrained to have a false alarm probability less than or equal to a prespecified level o. We illustrate this procedure for examples of multi-compenent spectral estimation and ambiguity function processing with nuisance parameter uncertainty and we compare its performance to sub-optimal decoupled/detection techniques.

C2-2 1420 QUADRATIC INVERSE THEORY FOR NON-STATIONARY TIME SERIES,

David J. Thomson, AT & T Bell Laboratories, Murray Hill, N.J. 07974

When estimating spectra and related functions from data it is commonly assumed that the observations are a sample from a stationary process. Here we examine the problems of detecting narrow-band non-stationarity in short data samples and the influence of such non-stationarity on the variance of spectrum estimates. We decompose the covariance matrix of the eigencoefficients used in multiple-window spectrum estimation methods (Proc.IEEE 70, pp 1055-96, 1982) into a series of known basis matrices with scalar coefficients. For a given bandwidth and sample size, we describe simultaneous orthogonal expansions for both the *power (time)* function and for the eigencoefficient covariance matrix. The limiting power basis functions are eigenfunctions of a narrow band $sinc^2$ kernel while the corresponding basis matrices are trace-orthogonal so that the observable non-stationary is described by a series of quadratic forms.

C2-3 1440 **Estimation of the Spectra of Unequally-Spaced Data**

Craig Lindberg , Mathematical Sciences Research Center, AT&T Bell Labs, Murray Hill, NJ 07974.

It is not uncommon to encounter data sets consisting of measurements at irregularly-spaced temporal or spatial locations, such as records collected by arrays, astronomical observations, and data sets with missing values. Noninterpolating, nonparametric techniques suitable for the estimation of the harmonic and continuous parts of spectra are presented. These methods involve solutions to a Slepian-Landau-Pollak concentration problem with novel features.

C2-4 1500 MAXIMUM LIKELIHOOD AND MAXIMUM ENTROPY SPECTRUM ESTIMATES DERIVED FROM MULTI-WINDOW POWER ESTIMATES: L. Du and L. Scharf, Dept. of Electrical Engineering and Computer Engineering, Univ. of Colorado, Boulder, CO 80309

C2-5 1520 TITLE TO BE ANNOUNCED: K.S. Lii, Univ. of California, Berkeley, CA

Session D-5 1335-Fri. CR1-40
WAVEGUIDES FOR HIGH FREQUENCY APPLICATIONS
Chairman: K.C. Gupta, Dept. of Electrical and Computer Engineering, Univ. of Colorado, Boulder, CO 80309

D5-1
1340 RADIATION LOSSES FROM SINGLE STEPS IN LOSSLESS DIELECTRIC SLABS

Albert W. Biggs*
University of Alabama in Huntsville
Huntsville, Alabama 35899, USA

Radiation or mode conversion losses from single steps in lossless dielectric slab waveguides are presented. Cladding above and below the guiding slab may have the same or different refractive indices.

Formulation of even and odd guided TE/TM modes are presented for slab guides. The guided modes are evaluated from appropriate wave equations in the guidingslabs and the surrounding cladding regions, producing both propagating fields inside the slab and attenuating or evanescent waves in the outside cladding. Graphical solutions of the eigenvalue equations for different modes are presented.

Corresponding TE/TM radiation modes were formulated in cladding regions. Guided modes are a finite set, while radiation modes are a continuum. Dirac Delta functions were found in some of the integrands while evaluating integral equations for radiation modes in slab claddings. Although Dirac Delta functions introduce singular behavior, their presence made calculations physically meaningful.

The radiation losses for a single step are found with incident guided modes on the step, with reflected guided and and radiation modes before the step, and with transmitted guided and forward scattered radiation modes before and after the step. Radiation losses are obtained with orthogonality relationships between guided/radiation modes and continuity of tangential fields at the step boundary. Slab configurations include rising or descending steps at the top/bottom of the slab.

*On an IPA Grant with WL/Kirtland AFB, New Mexico 87117.

D5-2
1400

OPTICAL SURFACE WAVES, TE MODES, AND TM MODES FROM SOURCES IN DIELECTRIC SLABS

Albert W. Biggs*
Electrical and Computer Engineering Department
University of Alabama in Huntsville
Huntsville, Alabama 35899, USA

Optical surface waves, TE modal, and TM modal expressions are developed for a three layer medium. Space and ground waves are also included. The three layer medium consists of an upper layer of air above a two layered dielectric slab. The lower layer may be conducting soil, sea water, or a perfectly conducting ground plane. A horizontal electric dipole is the source. The composite media may also be a cladding dielectric layer above a guiding dielectric layer, with a dielectric cladding substrate below the guiding layer.

Boundary conditions and Fourier transforms are applied to the Hertz vector potential wave equations in the upper guiding dielectric layer and in the air above. Integral expressions for the horizontal components of the Hertz vector potential are found for each layer.

*With an Intergovernmental Personnel Act (IPA) Grant at the Weapons Laboratory/AWPB, Kirtland AFB, New Mexico 87117-6008. TCS from Electrical Engineering Department, University of Alabama in Huntsville, Alabama 35899.

D5-3 1420 **A COMPARISON OF TWO NUMERICAL TECHNIQUES FOR PLANAR OPTICAL WAVEGUIDES OF ARBITRARY REFRACTIVE INDEX**

Yinggang Tu[1], I.C. Goyal[2] and R. L. Gallawa

National Institute of Standards and Technology
Electromagnetic Technology Division
Boulder, CO. 80303-3328

In this paper we determine the eigenfunctions and eigenvalues for optical waveguides having nonuniform refractive index profiles in the transverse direction using two recent techniques. In one technique, we solve the scalar wave equation by expanding the fields in a Fourier series (C.H. Henry and B.H. Verbeek, IEEE J. Lightwave Technology, 7, 308-313, 1989). The expansion is then used to develop matrix equations that result when the waveguide is approximated by a series of rectangular elements of constant refractive index. Far from the core region, artificial boundaries are imposed to require that the fields vanish at those boundaries. The propagation constant and field distribution are then found by solving the eigenvalue and eigenfunction problems.

Comparison is made with a newly developed technique that allows an approximate solution to second order linear differential equations of the type encountered in mathematical physics in general and optical waveguides in particular. The technique is reminiscent of the WKB method but the new method holds even at the turning points, where the WKB method fails. Whereas the WKB method yields exact results if the refractive index is constant, our method is exact under slightly more general conditions. This new method, based on the use of Airy functions, gives very good results for both the eigenfunctions and the eigenvalues.

The talk will discuss both techniques and give numerical results for several refractive index profiles of current interest in optical communications. In one case, we will use a profile that has an exact solution. That will allow a meaningful comparison between the exact solution and the two numerical techniques.

[1] Visiting Scholar on leave from National Institute of Metrology, Bejing, People's Republic of China

[2] Visiting Scholar on leave from the Indian Institute of Technology, Physics Department, New Delhi, India

D5-4 1440 A NUMERICAL METHOD FOR WAVE PROPAGATION IN A NONUNIFORM OPTICAL WAVEGUIDE

Yinggang Tu[1], John Gary[2], I. C. Goyal[3] and R.L. Gallawa
National Institute of Standards and Technology
Electromagnetic Technology Division
Boulder, CO 80303-3328

We propose an efficient numerical method to solve for the electromagnetic fields propagating in an optical waveguide that is nonuniform in the direction of propagation (z-direction) as well as in the transverse direction. In this method, the electromagnetic field is first expanded in terms of the Hermite-Gaussian basis functions (A. Sharma and S. Banerjee, Optics Lett., 14, 96-98, 1989). The scalar Helmhotz equation is then converted into matrix equations using the orthogonal collocation method. The incident field is sampled at the collocation points as the initial condition. Axial propagation is then determined by solving the matrix equations numerically, using the Runga-Kutta method.

This method has some advantages over the commonly used beam propagation method (BPM method). In the BPM method, the numerical computation time may become significant if the beam propagates a fairly long distance, while the computation time for this proposed method is relatively small. In addition, only a few terms (compared with the number required with BPM) are needed in the expansion to achieve the same accuracy.

The method relies on the knowledge of the field at the input to the nonuniform waveguide. The required CPU time and the accuracy achieved depend on the choice of a "scaling factor" that appears in the argument of the Hermite-Gauss basis function. This will be illustrated and discussed in the numerical examples that will be presented in the talk. Comparison with other methods will be made.

[1] Visiting Scholar on leave from National Institute of Metrology, Bejing, People's Republic of China

[2] Scientific Computing Division, National Institute of Standards and Technology.

[3] Visiting Scholar on leave from the Indian Institute of Technology, Physics Department, New Delhi, India

D5-5
1500

SURFACE-WAVE SCATTERING BY DIELECTRIC INHOMOGENEITIES ALONG OPTICAL FIBER WAVEGUIDE

Paul F. Havala, BELLCORE, Red Bank, NJ 07701
Dennis P. Nyquist*, Dept. of Elect. Engrg.
Michigan State University, East Lansing, MI 48824

The scattering (reflection, transmission, and radiation) of guided surface waves by dielectric inhomogeneities (obstacles) along a circular dielectric-fiber waveguide is studied by a full-wave integral-operator formulation. An electric-field integral equation (EFIE) for the unknown field in the discontinuity region is based upon an electric dyadic Green's function for currents immersed in the optical-fiber environment. Numerical solutions to the EFIE lead to the induced field in the discontinuity region, in terms of which the scattered waves are determined. Radiated power is finally quantified using a power balance argument.

A circular dielectric fiber of radius "a" is described by refractive index profile $n_f(\rho)$; a step-index fiber is characterized by $n_f=n_g$ in guiding region $\rho<a$ and $n_f=n_s$ in surround region $\rho>a$. An incident surface wave $\vec{E}^i$ is assumed to propagate along the fiber and impinge upon the dielectric obstacle. If that discontinuity has index $n_d(\vec{r})$ in region V, then it results in excess polarization current $\vec{J}_{eq} = j\omega\delta n^2(\vec{r})\varepsilon_0\vec{E}$ there, where $\delta n^2(\vec{r}) = n_d^2(\vec{r})-n_f^2(\rho)$; that induced current subsequently maintains scattered field $\vec{E}^s$. The total field is consequently $\vec{E} = \vec{E}^i + \vec{E}^s$, and expressing $\vec{E}^s$ excited by $\vec{J}_{eq}$ in terms of electric Green's dyad $\overline{\overline{G}}^e$ leads to the scalar component EFIE's

$$E_\alpha(\vec{r}) - j\omega\varepsilon_0 \sum_\beta \int_{V'} G^e_{\alpha\beta}(\vec{r}\,|\,\vec{r}\,')\delta n^2(\vec{r}\,')E_\beta(\vec{r}\,')\,dv' = E^i_\alpha(\vec{r}) \quad \text{... for } \vec{r}\in V \text{ and } \alpha,\beta = \rho,\theta,z.$$

Components $G^e_{\alpha\beta}$ of the electric Green's dyad are obtained by complex analysis as singularity expansions in the complex spatial-frequency (propagation-constant) plane; the result is an expansion in the discrete and continuous components of the propagation-mode spectrum. The latter representation is convenient, and believed to be new. Subsequent to solving the EFIE's for the induced field, the scattered waves excited by the excess polarization current are determined by again exploiting the electric Green's dyad.

Independent systems of EFIE's are obtained for each circular harmonic of order n in the incident surface-wave field. A Galerkin's moment-method solution is implemented for the induced field in the obstacle, using a Dini series to represent its radial dependence and pulse basis functions to express its axial variation. Induced field distributions, scattering coefficients, and radiated power are quantified for obstacles along strongly and weakly guiding fibers. Extensive numerical results are obtained.

D5-6
1520

CALCULATION OF TRANSMISSION LINE PARAMETERS AND ELECTRIC FIELD DISTRIBUTION OF COPLANAR ELECTRODES ON LAYERED DIELECTRIC SUBSTRATES

P. Weitzman, J. M. Dunn and A. R. Mickelson
Department of Electrical and Computer Engineering
University of Colorado
Campus Box 425
Boulder, CO 80309-0425

A numerical technique for calculating the electric field distribution and capacitance of coplanar strip electrodes place on top of a layered dielectric substrate is presented. A Green's function for the potential due to a point charge in the plane of the electrodes is found using Fourier transform techniques. The charge distribution on the electrodes is calculated by solving an integral equation. The static capacitance is calculated by integrating the charge distribution. The electric field at any point in the substrate can be found by integrating the charge distribution times the Green's function.

Approximations are made to speed up the calculations of fields and capacitance with minimal effect on accuracy. The results obtained by this numerical technique are compared to results obtained by other methods and to experimental data.

D5-7
1540 **THE ANALYSIS OF FINLINES IN CIRCULAR WAVEGUIDE HOUSINGS BY THE METHOD OF LINES**

M. Thorburn, A. Biswas, V.K. Tripathi
Electrical & Computer Engineering Dept.
Oregon State University
Corvallis, Oregon 97331-3202

Finlines in circular waveguide housings, as an alternative transmission media, can be used for millimeter wave propagation. It has advantages similar to that of finlines in rectangular housing and can be easily excited by the electric fields of the dominant TE_{11} mode of the circular guide. This type of transmission line has a broad band of single mode propagation and was reported in 1955 in a paper concerning an ultra-bandwidth finline coupler [Robertson, Proc. IRE, vol.43, #6]. Only recently, the application of the finite element method to a family of general finline structures has been reported [Eswarappa, Costache, & Hoefer, IEEE-MTT, vol.37, #2, 1989] with results for the dispersion characteristics of such structures.

This paper begins by modifying the method of lines [Schulz & Pregla, Radio Science, vol.16, 1981; Thorburn & Tripathi, Natl. Radio Science Mtng, 1988] for applications to general finline structures in a circular-cylindrical geometry. The fields are written in terms of z-directed Hertzian potentials and a system of partial differential equations results which is then solved with relative ease for structures with surfaces of constant radius or constant polar angle. The paper concludes by calculating the cutoff frequencies, dispersion characteristics and characteristic impedances of a class of finlines in circular waveguide housing for the dominant and higher order modes.

D5-8
1600

NUMERICAL MODELING OF PLANAR CIRCUITS WITH PSEUDO MESHES

David C. Chang and J. X. Zheng
MIMICAD Center & Department of Electrical and Computer Engineering, University of Colorado, Boulder, Colorado 80309-425

Numerical modeling of planar circuits typically involves finding an efficiently algorithm for a set of two-dimensional vector integral equations over a planar surface or surfaces of finite dimensions. In the case of microstrip, the unknown is the current distribution on the metal surface, while in the case of co-planar waveguides and slotlines, the unknown is the aperture electric field, or the magnetic current distribution located in the interface. The guided wave structures are typically rectangular in nature, with exception perhaps at the corners or other localized discontinuities where they often are triangular rather than rectangular in shape. For this reason, many of the existing algorithms formulated either in the spectral domain or in the spatial domain, for rectangular structures are not particularly effective nor efficient.

Dividing up the surfaces into triangular cells and using a linear approximation of current distribution within each cell is an obvious choice for this kind of structures. However, the triangulation not only can not take advantage of the rectangular nature of the structure over a majority portion of the structure under consideration, it also tends to create superficial ripples in the current and charge distributions from cell to cell. As a result, its convergence sometimes is notoriously slow as shown in a companion paper. What we need, then, is a scheme which takes advantage of the geometry of the structure and which, at the same time, satisfies our physical intuition of current flow.

In this paper, we shall describe a particular choice of basis functions based upon a linear approximation of the unknown currents over either a rectangular or a triangular cell. Instead of requiring both the normal and the tangential components of current distribution to be continuous across a cell boundary, we only require the normal component to be continuous. Physically the scheme can be represented topologically by an equivalent set of wire meshes, and subjected to the same type of constraints as a wire mesh at the boundaries. Such an interpretation has an added advantage in helping us to determine cell shape and cell orientation according to our physical intuition. It also allows us to impose the boundary conditions at the edges of a structure most directly. Numerical results obtained for a chamfered right-angle microstrip corner will be included in the presentation.

D5-9
1620

A NEW METHOD FOR COMPUTING THE IMPEDANCE ELEMENTS FOR PLANAR STRUCTURES (USING TRIANGULAR BASIS FUNCTIONS)

S. L. Dvorak, Dept. of Elect. and Comp. Eng.
University of Arizona, Tucson, AZ 85721
E. F. Kuester, Dept. of Elect. and Comp. Eng.
University of Colorado — Campus Box 425
Boulder, CO 80309

Application of Galerkin's method to planar MMIC circuits or antenna structures results in an impedance matrix which must be computed. The impedance elements can be represented in two forms. The spatial domain representation involves a four-dimensional (4-d) integration of a 1-d Sommerfeld integral (ie., the Green's function for the structure). The integrand of this 1-d Sommerfeld integral contains elementary transcendental functions and Bessel functions of the first kind. A number of authors have demonstrated that the well known properties of the Bessel function can be used to develop an asymptotic extraction technique (AET) for the 1-d Sommerfeld integrals.

The impedance elements can also be represented as 2-d Sommerfeld integrals in the spectral domain. In [S. Dvorak and E. Kuester, **Scientific Report No. 94**, (EM Lab., Dept. of Elec. and Comp. Eng., Univ. of CO, Boulder, 1989)], the angular integral, in the polar representation of the 2-d Sommerfeld integral, is rewritten in terms of a finite number of incomplete Lipschitz-Hankel integrals (ILHI's). Therefore, the impedance elements can be represented in the spectral domain in a form that is similar to that of the 1-d Sommerfeld integral; however, the integrand now contains ILHI's along with Bessel functions. It turns out that the ILHI's can be represented in terms of a series of Bessel functions. It is also demonstrated in that report that expressing the 2-d Sommerfeld integrals in this form allows for the development of an AET which is similar to the AET used for the 1-d Sommerfeld integrals.

All of the work in the report cited above is based on the choice of piecewise sinusoidal (PWS) basis functions. In this presentation, we will discuss the modifications that are necessary for the case of triangular basis functions. Actually, a number of simplifications occur for this case. We will apply this technique to the analysis of a printed strip dipole antenna in a layered medium. Comparisons will be made for the efficiency of the PWS and triangular basis functions.

D5-10
1640

TE WAVE EXCITATION AND SCATTERING BY OBSTACLES IN SURROUND OF ASYMMETRIC PLANAR DIELECTRIC WAVEGUIDE

Boutheina Kzadri*, Dennis.P.Nyquist
Department of Electrical Engineering
Michigan State University
East Lansing, Michigan 48824

Excitation of TE waves along an asymmetric planar dielectric waveguide is studied. The layered substrate/film/cover environment, typical of integrated circuits for millimeter and optical wavelengths provides such a planar guiding structure. Surface waves are excited when the film-layer guiding region has positive index contrast relative to its surround. An electric Green's function (believed new) is constructed for the TE field maintained in the cover layer by currents immersed in that region. Using a direct complex analysis approach, the Green's function is expanded in the discrete and continuous propagation spectrum components for the asymmetric planar waveguide. The electric Green's function is exploited to study scattering of TE surface waves by dielectric obstacles in the film layer.

An x-invariant TE field, having only an x component, is excited by the similar component of current. Spectral analysis in the axial transform domain leads to

$$E_x(y,z) = \int_{LCS} G(y \mid y';z-z')\, J_x(y',z')\, dy'dz'$$

where LCS designates the longitudinal cross section of the source region and the Green's function is represented by 1-D spectral integral. Subsequent to complex transform plane analysis, $G(y \mid y';z-z')$ is decomposed into the superposition of a discrete surface wave, arising from pole singularities, and a radiative component arising from integrations about substrate/cover branch cuts. If a dielectric discontinuity having index contrast $\delta n^2 = n_d^2(y,z) - n_f^2$ is immersed in the cover layer, an excess polarization current is excited and maintains a scattered field. This current is proportional to the product of the induced field and the refractive index contrast. Within the obstacle the total field $\vec{E} = \vec{E}^i + \vec{E}^s$ consists of the impressed field of an incident wave augmented by the scattered field. Rearranging leads to the EFIE

$$E_x(y,z) - j\omega\varepsilon_0 \int_{LCS} \delta n^2(y',z')\, G(y \mid y';z-z') E_x(y,z)\, dy'dz' = E_x^i(y,z)$$

Numerical solutions to the EFIE lead to the induced field within the obstacle from which scattering coefficients are calculated. Extensive numerical results for various obstacle configurations will be presented. An attempt to present some experimental results will be done.

Jan 1990 Nat. Radio Sci. Meeting

Session J-3 1335-Fri. CR2-26
MILLIMETER AND SUB-MILLIMETER-WAVE TECHNIQUES
Chairman: R. Blundell, Smithsonian Astrophysical Observatory,
60 Garden St., Cambridge, MA 02138

J3-1
1340

INTEGRATED SYSTEMS MANUFACTURE OF ERROR COMPENSATING SUBREFLECTOR FOR NRAO 12-M RADIO TELESCOPE

Charles E. Mayer
Department of Electrical Engineering
University of Alaska Fairbanks
Fairbanks, AK 99775-0660

John H. Davis and Heinrich D. Foltz
Department of Electrical and Computer Engineering
The Univerity of Texas at Austin
Austin, TX 78712

The aperture efficiency and beam shape of the National Radio Astronomy Observatory 12-m antenna was imporved by designing and installing a surface error compensating secondary reflector. The secondary reflector compensates for surface errors on the primary reflector by adjusting the ray path lengths so that they are of constant length as they travel through the optical system of the 12-m antenna. The primary surface errors were measured holographically using the LES-8 satellite at 38 GHz. The necessary ray path adjustments were then calculated from these data and the subreflector was subsequently machined.

The program was remarkable in several respects. First, the frequency of the holographic measurement was 38 GHz while the frequency of primary use of the radio telescope is from 200 to 360 GHz. Thus, a very high precision measurement was necessary at 38 GHz so that extrapolation to frequencies above 200 GHz was possible. Second, the program required very many distinct tasks--receiver buliding, satellite coordination and tracking, data collection, data analysis, subreflector design and analysis, subreflector machining, and subreflector installation and testing.

This presentation reports on the seamless integration of many of the above tasks into a single design and manufacturing system. The input to the system was the raw far field antenna pattern and the output of the system was a machined error compensated subreflector. The cascaded tasks of the system were connected by a bit stream through 4 computers and a high precision numerical mill. Several computer aided design techniques and automated manufacturing techniques were incorporated to streamline the procedure.

J3-2
1400

MECHANICALLY TUNABLE GUNN OSCILLATORS

J. E. Carlstrom and R. L. Plambeck
Radio Astronomy Laboratory
University of California
Berkeley, CA 94720

We describe continuing work on wideband, mechanically tunable second harmonic Gunn oscillators of the design described by Carlstrom, Plambeck, and Thornton (1985, *IEEE-MTT*, **33**, 610). The oscillator frequency is set by adjusting the length of a coaxial cavity which is coupled to a rectangular waveguide. Only harmonics of the fundamental frequency are coupled out through the waveguide, which is chosen to have a cutoff frequency above the resonant frequency of the cavity. The output power at the second harmonic is optimized by adjusting a waveguide backshort. Fractional bandwidths of 50% have been achieved. The frequency is electronically tuned over few hundred MHz by varying the bias voltage. The oscillator is phase locked by exploiting the bias tuning. Oscillators of this design have been used as local oscillators for low-noise receivers operating over the 70 – 115 GHz atmospheric window for several years, and more recently with frequency multipliers to provide LO power at higher frequencies.

Improvements to the mechanical design have led to smoother tuning, broader bandwidths, and higher output powers. Recent work has concentrated on high power InP oscillators to drive frequency multipliers for observations up to 492 GHz. We have obtained output powers greater than 100 mW over a 15 GHz bandwidth, and greater than 50 mW over a 25 GHz bandwidth, centered at 82 GHz.

J3-3 1420

BEAM-FORMING PLANAR ARRAY S.I.S. MIXERS AND MULTIPLIERS

H.D. Foltz, J.H. Davis, and S. Laycock
Electrical Engineering Research Laboratory
University of Texas at Austin 78712

Preliminary results will be presented on beam-forming structures formed from parallel superconducting strips on a quartz substrate. The strips are periodically interrupted with series pairs of SIS junctions. The resulting array can be modeled as a wire polarizing grid with a nonlinear equivalent wire impedance, and could act as a mixer or frequency multiplier. This structure has the advantage that it directly forms a beam without the need for a horn or other antenna, and can be made easily as part of the SIS fabrication process.

When used as a mixer, the array is illuminated with signal and local oscillator beams, while the intermediate frequency signal and d.c. bias are coupled through the edges of the array. For operation as a frequency multiplier, the array is illuminated with a pumping beam at the fundamental frequency and reflects a beam at the second or third harmonic. Although the SIS junctions are very low level devices (nanowatt power levels at the harmonic frequencies), large numbers of junctions can be integrated into the structure, so that the full array produces sufficient power for use as a local oscillator for SIS mixers.

The array has a beam efficiency on the order of 80% when uniformly illuminated. The niobium-trilayer junctions which we intend to use should be useful to at least 500 GHz, and computer simulations with typical IV curves show a frequency multiplier conversion of 15% when doubling in the submillimeter range.

Jan 1990 Nat. Radio Sci. Meeting

J3-4
1440

PLANAR ANTENNA STRUCTURES FOR SIS RECEIVERS

T.H. Büttgenbach, T. G. Phillips
California Institute of Technology
Pasadena, CA
R. E. Miller
AT & T Bell labs
Murray Hill, NJ
T. L. Rose
University of Cologne
Federal Republic of Germany

A quasioptical heterodyne receiver based on a Pb alloy superconductor-insulator-super-conductor (SIS) tunnel junction mixer for submillimeter astronomy has been developed. Performance of this receiver from 115 to 76 GHz will be discussed as compared to theoretical limits. Several planar antennas (Bow Tie, log-periodic and logarithmic spiral antennas) have been investigated. Room temperature beam pattern measurements using low frequency scale models and high frequency Bi microbolometers, and their impact on receiver coupling efficiencies to the Caltech Submillimeter Observatory telescope will be presented.

Cancelled

J3-5 1500 ANTARCTIC SUBMILLIMETER TELESCOPE REMOTE OBSERVATORY: J. Bally and A.A. Stark, Radio Physics Research Dept., Bell Labs, Holmdel, NJ 07733

J3-6
1540

MILLIMETER WAVELENGTH SIS RECEIVERS

John Payne
National Radio Astronomy Observatory
2015 Ivy Road
Charlottesville, VA 22903

This paper describes an SIS receiver for millimeter wavelengths based on a closed-cycle refrigerator system operating at 4.2 K. The complete receiver consists of a number of small inserts, each insert covering a portion of the frequency range from 70-360 GHz. At the present time, inserts have been developed for the frequency ranges 70-90 GHz, 90-115 GHz and 200-240 GHz. A dewar has been developed to hold eight such inserts. An optical switch on top of the dewar selects pairs of inserts, one for each polarization. A double sideband receiver noise temperature of 19.1 K at 100 GHz has been measured using this system.

J3-7 1600 HETERODYNE SHOTTKY MIXERS AT 300 GHz: A.L. Betz, Space Science Lab, Univ. of California, Berkeley, CA 94720

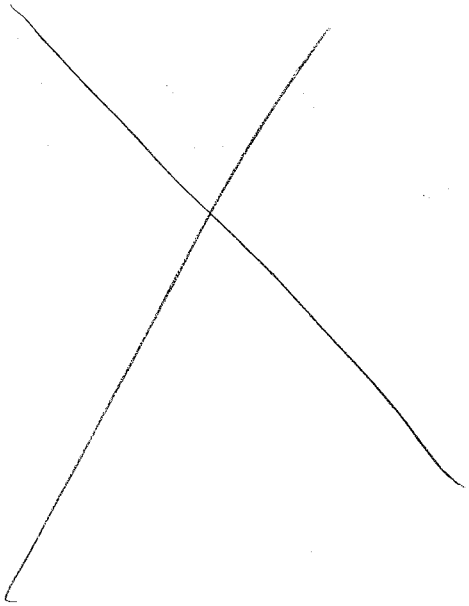

J3-8
1620

THE SUBMILLIMETER TELESCOPE (SMT) PROJECT

Robert N. Martin
Stewart Observatory
University of Arizona
Tucson, AZ 85721
602-621-4031
Jaap W. M. Baars
Max-Planck-Institut für Radioastronomie
Auf dem Hügel 69
D-53 Bonn 1
West Germany
011-49-228-5251

Submillimeter astronomy represents, perhaps, the last wavelength frontier of radio astronomy. This spectral region promises rich rewards in astrophysical terms but has so far remained largely unexplored mainly for technical reasons. To exploit the potential of submillimeter astronomy, the Stewart Observatory of the University of Arizona and the Max-Planck-Institut für Radio Astronomie, West Germany have collaborated on the construction and operation of a dedicated submillimeter facility. The Submillimeter Telescope (SMT) will be located at an altitude of 3180 meters (10.425 feet) on Emerald Peak (Mt. Graham) 75 miles northeast of Tucson in southern Arizona. The instrument is an alt-azimuth mounted f/13.8 Cassegrain homology telescope with two Nasmyth and bent Cassegrain foci. It will have diffraction limited performance at a wavelength of 300μm rms.

An important feature of the SMT is construction of the primary and secondary reflectors out of aluminum-carbon fiber reinforced plastic (CFRP) face sheet sandwich panels and the reflector backup structure and secondary support out of CFRP structural elements. This modern technology provides both a means for reaching the required precision of the SMT for both night and day operation (basically because of the law coefficient of thermal expansion and high strength-to-weight ratio of CFRP) and a potential route for the realization of lightweight telescopes of even greater accuracy in the future. The SMT will be the highest accuracy radio telescope ever built (at least a factor of 2 more accurate then existing telescopes). In addition, the SMT will be the first 10m class submillimeter telescope with a surface more accurate than $\lambda/12$ at the important 350 λm wavelength atmospheric window.

In this paper we will briefly discuss (1) the structural design, including dynamical measurements of the completed reflector structure, (2) the use of CFRP technology in the design, (3) the technology involved in replicating 6μm rms panels from pryex molds, (4) the novel corotating enclosure for the facility, and (5) the planned measurementation. The current state of the construction of this facility will be summarized.

J3-9 1640 WAVEGUIDE RECEIVERS ABOVE 500 GHz: E.C. Sutton, Space Sciences Lab, Univ. of California, Berkeley, CA 94720

Steve Clifford, Head of VPL (Tech Corelon Little's place)

INDEX

Condensed Technical Program

THURSDAY, 4 JANUARY (cont.)

1355-1640		
E-2	NATURAL AND MANMADE NOISE AND SPECTRUM MANAGEMENT	CR1-9
1355-1700		
A-2	BROADBAND EM METROLOGY	CR1-42
B-4	EM THEORY II	CR2-28
BA-1	ANTENNAS	CR0-30
D-3	OPTOELECTRONIC TECHNIQUES	CR1-40
G-3	METHODS AND METEORS	CR2-6
GH-1	IONOSPHERIC MODIFICATION	CR1-46
1440-1700		
J-2	RECENT ADVANCES IN RADAR ASTRONOMY	CR2-26
1640-1700		
E-3	SPECTRUM MANAGEMENT	CR1-9
1700-1800		
Commission B Business Meeting		CR2-28
Commission C Business Meeting		CR1-9
Commission G Business Meeting		CR2-6
1930		
J-2	RADIO PANEL OF AASC DISCUSSION (cont.)	CR2-26

FRIDAY, 5 JANUARY

0835-1200		
AB-1	MICROWAVE METROLOGY	CR1-46
B-5	NUMERICAL METHODS	CR2-28
C-1	ARRAY PROCESSING AND INVERSE PROBLEMS	CR1-9
D-4	MICROSTRIP STRUCTURES	CR1-40
0855-1040		
H-3	ACTIVE EXPERIMENTS OF WAVE INJECTION FROM THE ACTIVE SATELLITE	CR0-30
0855-1200		
G-4	HIGH LATITUDE EFFECTS	CR2-6
JE-1	INTERFERENCE IN RADIO ASTRONOMY	CR2-26
1040-1200		
H-4	ELECTRODYNAMIC TETHERS AND TETHERED ARRAYS	CR0-30
1335-1700		
B-6	THEORY AND NUMERICAL METHODS	CR2-28
D-5	WAVEGUIDES FOR HIGH FREQUENCY APPLICATIONS	CR1-40
J-3	MILLIMETER AND SUBMILLIMETER WAVE TECHNIQUES	CR2-26
1355-1700		
C-2	NONPARAMETRIC SPECTRUM ANALYSIS	CR1-9

IGARSS

91 Finland
92 Dallas (F)
93 Japan or China
94 Los Angeles (F?)

Atmosphere by radar in tropics
Brazil 1990 ??

17-20 August 1992 EM Theory Symp Sydney Australia

Comm B

92 Chicago
93 Michigan